The University of Nottingham

School of the Built Environment

Institute of Architecture

Ventilation Characteristics of Buildings Incorporating Different Configurations of Curved Roofs and Wind Catchers

(With Reference to Human Thermal Comfort)

Omar S. M. Asfour

B.Sc., M.Arch. (Architecture)

Thesis submitted to the University of Nottingham for the degree of Doctor of Philosophy

Nottingham, United Kingdom

September 2006

ABSTRACT

This study investigates the effect of utilising different configurations of curved roofs and wind catchers on natural ventilation performance of buildings. It compares airflow rates and internal airflow velocity and distribution, before and after, employing domed and vaulted roofs for wind-induced natural ventilation and, thus, thermal comfort improvement. This also includes the role of integrating different wind-catcher systems into the investigated curved roofs. A review of the related background studies and literature has revealed the architectural importance of these elements, and their potential for natural ventilation and passive cooling in hot climates, with particular reference to the Middle East. A review of the different natural ventilation prediction methods has also exposed the challenge associated with air infiltration modelling and understanding.

Computational Fluid Dynamics (CFD) simulation, using Fluent 5.5 software, has been used as a main research tool. The code used has been validated based on a comparison between airflow rate estimated using Fluent 5.5 software, and airflow rate estimated using the Network mathematical model. This ensures the reliability of the natural ventilation performance assessment carried out. A parametric approach has been adopted to establish a systematic comparison between the effects of the different geometrical and climatic parameters considered, with a reasonable variety that fit the study limits. This included a summarised thermal comfort assessment, implementing the Tropical Summer Index (TSI), developed by Sharma and Ali (1986).

The comparison showed that the use of the curved roofs and wind catchers for natural ventilation leads to a significant improvement in natural ventilation of the indoor space, presented as a reformation of internal airflow paths, and a reduction of the area of the still-air zone by about 20%. This increases the average indoor velocity, and improves thermal comfort conditions inside the building, depending on the outdoor climatic conditions. This has been found to be more critical under less favourable wind conditions, as in the case of deep-plan buildings. The results obtained in this study have been used to formulate design guidelines, which progress the understanding of airflow behaviour inside and around buildings incorporating different combinations of curved roofs and wind catchers. This is a new contribution to the research efforts carried out in the field of sustainable architectural design.

RESEARCH PAPERS

The following papers have been submitted for publication as a direct result of this research:

Asfour, O. S., and Gadi, M. B. A Comparison between CFD and Network Models for Predicting Wind-Driven Ventilation in Buildings. Paper communicated to Building and Environment, 2006.

Asfour, O. S., and Gadi, M. B. Using CFD to Investigate Ventilation Characteristics of Dome as a Wind-Inducing Device in Buildings. Paper communicated to the International Journal of Green Energy, 2006.

Asfour, O. S., and Gadi, M. B. Using CFD to Investigate Ventilation Characteristics of Vault as a Wind-Inducing Device in Buildings. Paper communicated to Building and Environment, 2006.

Asfour, O. S., and Gadi, M. B. Effect of Integrating Wind Catchers with Curved Roofs on Natural Ventilation Performance in Buildings. Paper communicated to Architectural Engineering and Design Management, 2006.

Asfour, O. S., and Gadi, M. B. Effect of Utilising Curved Roofs and Wind Catchers for Natural Ventilation on Human Thermal Comfort. Paper communicated to Architectural Engineering and Design Management, 2006.

ACKNOWLEDGMENT

Praise and thanks to Allah, who has provided me with the aid and assistance to complete this work

Before I start to acknowledge the people who helped in the completion of this work, I would like to express my gratitude to my father, who was the first person in guiding me to the path of knowledge. He would have wished to have seen the completion of this work, but, unfortunately, passed away before this was possible.

Indeed many people have encouraged me to complete this work. In particular, I am grateful to my supervisor Dr. Mohamed B. Gadi for his invaluable support. I would also like to thank the school of the Built Environment and the International Office at the University of Nottingham for their partial funding of this study.

I would like to extend my gratitude and sincere appreciation to my family at home, Palestine, especially my mother, for their support and patience during the course of this study. To them and all others who, in their own way, contributed to the completion of this research work: Thank you from my heart.

LIST OF CONTENTS

LIST OF FIGURES

FIGURES OF CHAPTER 1

FIGURES OF CHAPTER 2

FIGURES OF CHAPTER 3

FIGURES OF CHAPTER 4

FIGURES OF CHAPTER 5

FIGURES OF CHAPTER 6

FIGURES OF CHAPTER 7

FIGURES OF CHAPTER 8

FIGURES OF CHAPTER 9

LIST OF TABLES

TABLES OF CHAPTER 2

TABLES OF CHAPTER 3

TABLES OF CHAPTER 5

TABLES OF CHAPTER 6

TABLES OF CHAPTER 7

TABLES OF CHAPTER 8

TABLES OF CHAPTER 9

TABLES OF CHAPTER 10

ABBREVIATIONS

CAD	Computer Aided Design.
CFD	Computational Fluid Dynamics.
Dc	Dome with closed apertures.
Do	Dome with opened apertures.
PPD	Percentage of People Dissatisfied.
PMV	Predicted Mean Vote.
TSI	Tropical Summer Index.
T	Tower, wind catcher.
Vc	Vault with closed apertures.
Vo	Vault with opened apertures.

NOMENCLATURE

A_n	area of an opening (m^2).
A_{eff}	effective area of an opening (m^2).
B	breadth of a building (m).
C	heat exchange by convection (W).
C_p	static wind pressure coefficient.
C_d	discharge coefficient for a window.
E	heat loss by evaporation (W).
g	acceleration due to gravity (m/s^2).
H	height of a building (m).
h	difference in height between two points (m).
K	heat exchange by conduction (W).
k	turbulent kinetic energy (W).
L	turbulence length scale (m).
M	metabolic rate (W).
MRT	mean radiant temperature (°C).
P_d	dynamic pressure (Pa).
P_s	static pressure (Pa).
P_w	wind pressure (Pa).
Q_n	airflow rate (kg/s, l/s, m^3/s).
R	heat exchange by radiation (W).
R_o	flow resistance of an opening (Pa.m^{-3}.s).
RES	heat loss by respiration (W).
RH	air relative humidity.
R_n	Reynolds number.
S	heat storage in the body (W).
T_{db}	dry-bulb temperature (°C).
$T_{\rm i}$	internal air temperature (°C).
$T_{\rm r}$	reference or outdoor air temperature.
T_{wb}	wet-bulb temperature (°C).
V	time-mean wind speed (m/s).
V_r	time-mean reference wind speed (m/s).
V_i	internal wind speed, at datum point (m/s).
V_t	instantaneous wind speed (m/s).
v_t	wind speed fluctuating component (m/s).
W	mechanical work (W).

Greek

α	wind angle.
ΔP	pressure difference across an opening (Pa).
ρ	air density (kg/m^3).
ε	dissipation rate of turbulent kinetic energy.

CHAPTER 1 : INTRODUCTION

1.1 Background

Since the industrial revolution, dramatic changes have occurred in the world of architectural design. The architect has stepped away from simple vernacular designs towards a design, which is characterised by being heavily energy consuming, in terms of construction and operation. For example, it is estimated that 50% of all resources consumed across our planet are used in construction (Edwards and Hyett, 2001). Large amount of this energy consumption is spent on the operation and control of buildings indoor environment, which is heavily dependent on mechanical systems in many types of buildings and in different ranges. This has resulted in an extensive consumption of unsustainable energy resources, like fossil fuels, which affect the quality of our built environment.

As the population of the world increases, dependence on these unsustainable energy resources is no longer sufficient nor reliable. Researchers today, and for many decades, have faced the challenge of introducing solutions that increase buildings dependency on natural and sustainable resources of energy. One of these challenges is to secure thermal comfort within the indoor environment of buildings relying on passive means and systems. Amongst these passive systems is ventilation provision in terms of air quantity and quality. It is an old problem, yet addressed by many innovative solutions. One of these is the straightforward and easy-to-use application of natural ventilation strategy.

Natural ventilation as a design strategy in domestic and non-domestic buildings has attracted the attention of designers and researchers. Many books and theses have been introduced to help designers implement it effectively. This includes many fields of development and innovation, and for different climates and regions. In particular, this research focuses on the potential improvement of wind-driven natural ventilation performance, as a ventilation strategy in hot climates, with reference to the Middle East. The issue that has been addressed, in the context of improving natural ventilation use in buildings, is the reinvention of the use of the curved roofs and wind catchers as wind-inducing devices in buildings. This study investigates many ideas regarding the utilisation of domed and vaulted roofs, in addition to the integration of different wind-catcher systems. Computational Fluid Dynamics (CFD) three-dimensional simulation has been used as a main research tool. Many sides of this study are discussed in the following sections, including its aims, objectives, methodology, and a brief presentation of the thesis format.

1.2 Research aims

Many studies have been carried out in the last few decades to reduce energy consumption, including the application of natural ventilation in buildings. These sincere efforts have inspired this study and increased the interest to contribute to the relevant knowledge acquired up to date. One of the methods implemented in this regard is to re-introduce the use of existing architectural elements as wind inducing and passive cooling devices in buildings. Amongst these elements are the traditional architectural elements, which have considerable importance and symbolism. This is due to their historical and cultural significance. However, they are not always effectively utilised to serve the needs of contemporary design sustainability.

Thus, the aim of this study is to investigate the role of the curved roofs and wind catchers in improving wind-induced ventilation, and thus human thermal comfort in buildings. This has been carried out using CFD three-dimensional simulation, and a parametric methodology. In addition, this study aims to contribute to the methods of energy saving in order to increase public awareness of environmental issues and to encourage further use of architecturally sustainable strategies.

1.3 Research objectives

Given the aims of this research project, it is possible to state its main objectives, as follows:

- To improve the understanding of wind-induced natural ventilation behaviour utilising curved roofs and wind catchers.
- To propose some design ideas that are expected to improve this performance.
- To assess human thermal comfort before and after implementing these ideas.
- To analyse research findings in a way that provides some design guidelines for architects, in order to give these findings more value.
- To develop and expand the use of CFD as a research tool in the field of sustainable architectural design.

1.4 Research methodology

This study has been carried out in two main stages: the literature review, and the empirical, or modelling, study. This is illustrated in the following two sections:

1.4.1 Literature review

This review aims to outline, in a summarised manner, many aspects that are related to this natural ventilation study. This may be divided into two main parts:

- A review of natural ventilation usage in buildings (Chapters 2 and 3).
- A review of the architecture of the targeted elements and their utilisation for natural ventilation (Chapter 4).

The first part has been covered in two chapters. The first chapter highlights some of the aspects that are related to natural ventilation in general. This includes: the natural ventilation concept, its relationship with thermal comfort, its objectives, advantages, driving forces, and strategies. The second chapter reviews some of the common methods used in predicting wind-induced natural ventilation in buildings. This has facilitated choosing an appropriate prediction model for the empirical study, which is CFD simulation.

The second part of the literature review aims to link and project the knowledge acquired in the first part on the targeted architectural elements, namely curved roofs and wind catchers. Demonstrating the architectural role of these elements has highlighted the need to reinvent their use and relationship. Thus, to serve the study interest in natural ventilation, the potential for wind-induced natural ventilation in buildings incorporating domed and vaulted roofs, in addition to wind catchers has been reviewed. This includes an analysis of the factors that affect the application of natural ventilation utilising these elements, and several related background studies.

1.4.2 Modelling study

Prior to the modelling study, it was necessary to ensure the reliability of the CFD code that will be implemented. Thus, a validation study was carried out, as will be discussed in Section 1.4.3. This study has shown the reliability of the code and encouraged further use of it in the modelling study. In order to carry out the modelling study, an analytical approach was adopted. This means that the targeted architectural elements were analysed individually in order to demonstrate their role in natural ventilation. This included analysis to determine the effect of domed roofs, and then the effect of vaulted roofs. After that, these elements were simulated in different combinations. This included the integration of curved roofs with different wind-catcher systems. In order to investigate the effect of any specific factor on natural ventilation performance, it has been assumed that other factors are fixed.

In order to establish a systematic and more comprehensive approach to the study, natural ventilation performance of the above-mentioned targeted elements has been investigated through a parametric approach, which has been facilitated by the implementation of CFD code. As these parameters are numerous and interacting, many of them have been assumed fixed, while others have been varied. After that, and through the analysis of the data obtained, it is possible to observe the effect of these factors and produce relevant practical recommendations. In order to facilitate the analysis of the results, different aspects of natural ventilation performance have been discussed separately, although it is believed that there is some interaction between them. Thus, natural ventilation performance of the different building elements has been discussed separately. This includes airflow rate through roof and wall openings, in addition to airflow distribution in the interior space.

A. Airflow rate provision

This accounts for the quantity of air that enters the building. In many related studies, especially those done in wind tunnels, wind pressure coefficient is used as an indicator of the induced airflow rate through the building. This depends on the fact that higher positive values of this coefficient mean higher static pressure of the wind and, thus, higher airflow rate and vice versa. In the case of CFD studies, including this study, it is possible and easier to obtain numerical data of airflow rate through building openings, and also velocity magnitudes inside and around the building. This has been used towards the end of the study in assessing human thermal comfort conditions, utilising the Tropical Summer Index (TSI), which has been developed by Sharma and Ali (1986).

B. Airflow distribution

This accounts for the uniformity of airflow distribution in the occupied level of the internal space of the building. Many studies such as Shao *et al.* (1993) and Yaghobi (1991) have evaluated this parameter descriptively utilising visualization techniques. However, an additional numerical criterion has been developed in this study. This has helped to estimate the area of different velocity zones in the internal occupied space of the building, as a percentage of the area of the plan, utilising contours of velocity magnitude and the AutoCAD software. This method gives good understanding of internal airflow behaviour and distribution, which numerically illustrates the performance of the natural ventilation system, before and after the suggested improvements.

1.5 Outline of the thesis

This study consists of ten chapters. The first (present) chapter aims to introduce the scope of the study and outline its main aspects. The remaining nine chapters are divided into two main parts: the literature review (Chapters 2 to 4), and the modelling study (Chapters 5 to 10). These chapters are illustrated in Figure 1.1. The context of these chapters is summarised below:

In Chapter 2, general aspects of natural ventilation in buildings have been reviewed. This includes:

- The natural ventilation concept and its advantage, compared to mechanical ventilation strategy.
- Its objectives, driving forces, and strategies.
- The relationship between natural ventilation and human thermal comfort.
- Comparison between its advantages and disadvantages.

Given that wind-induced natural ventilation in hot climates is the main focus of this study, Chapter 3 has reviewed some of the techniques and methods used in predicting wind-induced natural ventilation. This review includes:

- Factors affecting wind pressure on buildings.
- The empirical, Network, wind tunnel, and CFD models.
- Discussion of the advantages and disadvantages of each method.
- More details of the use of CFD, namely Fluent 5 software.

After illustrating many concepts and applications related to natural ventilation in buildings, Chapter 4 aims to introduce the targeted architectural elements in this study and their role in natural ventilation. These elements are the curved roofs and wind catchers. This chapter introduces the unique architectural relationship between these elements, and the possibility of taking advantage of this relationship in improving their use for natural ventilation. After that, the factors that affect this use have been introduced. Urban factors have been illustrated briefly, and then the architectural ones related to the dome, vault and tower. This has been followed by:

- A presentation of historical background regarding the use of these elements for natural ventilation.
- The mechanism of utilising them for natural ventilation.
- Some relevant background studies.

The remaining chapters serve the empirical study. Before starting the modelling study, it was necessary to validate the selected CFD code, which was Fluent 5.5. As this study has no access to laboratory testing facilities, this has been achieved by comparing Fluent 5.5 software results to the ones obtained using the Network mathematical model. Results showed good agreement and encouraged further use of the code. Chapters 6 and 7 investigate the effect of domed and vaulted roofs on wind-induced natural ventilation performance in buildings. At the beginning of Chapter 6, the involved climatic parameters have been presented. However, the geometrical parameters are explained at the beginning of each chapter individually. Chapters 6 and seven investigate parametric studies that compare different building configurations and different wind velocities and directions, before and after utilising the openings of these roofs for natural ventilation. Results have been analysed in terms of airflow rate provision and internal airflow distribution. Results showed that these elements assist to increase airflow rate in the building, but does not guarantee an improved internal airflow distribution.

Thus, Chapter 8 discusses the potential of different systems of wind catchers for improving internal airflow distribution. This has been demonstrated by integrating the wind catcher with domed or vaulted roofs in order to provide or suck air at the leeward zone of the building. The same assessment criteria have been implemented and the results have been compared with those obtained in the previous two chapters. Chapter 9 assesses in a summarised manner the studied system in terms of thermal comfort performance. Fluent 5.5 software has been used to estimate the average internal air velocity in the occupied level of the building, which has been equally divided into nine zones. The Tropical Summer Index (TSI) has been used to assess thermal comfort by observing the change in the percentage of people feeling thermally comfortable as a response to the change in internal air velocity. In general, results showed the advantage of the studied ventilation system in improving natural ventilation performance, in terms of airflow rates, internal airflow distribution, and human thermal comfort.

After the completion of the empirical chapters, conclusions and recommendations have been presented. This includes presentation of design guidelines related to natural ventilation use in buildings, and areas that require future research. Thesis structure is summarised in the Figure 1.1.

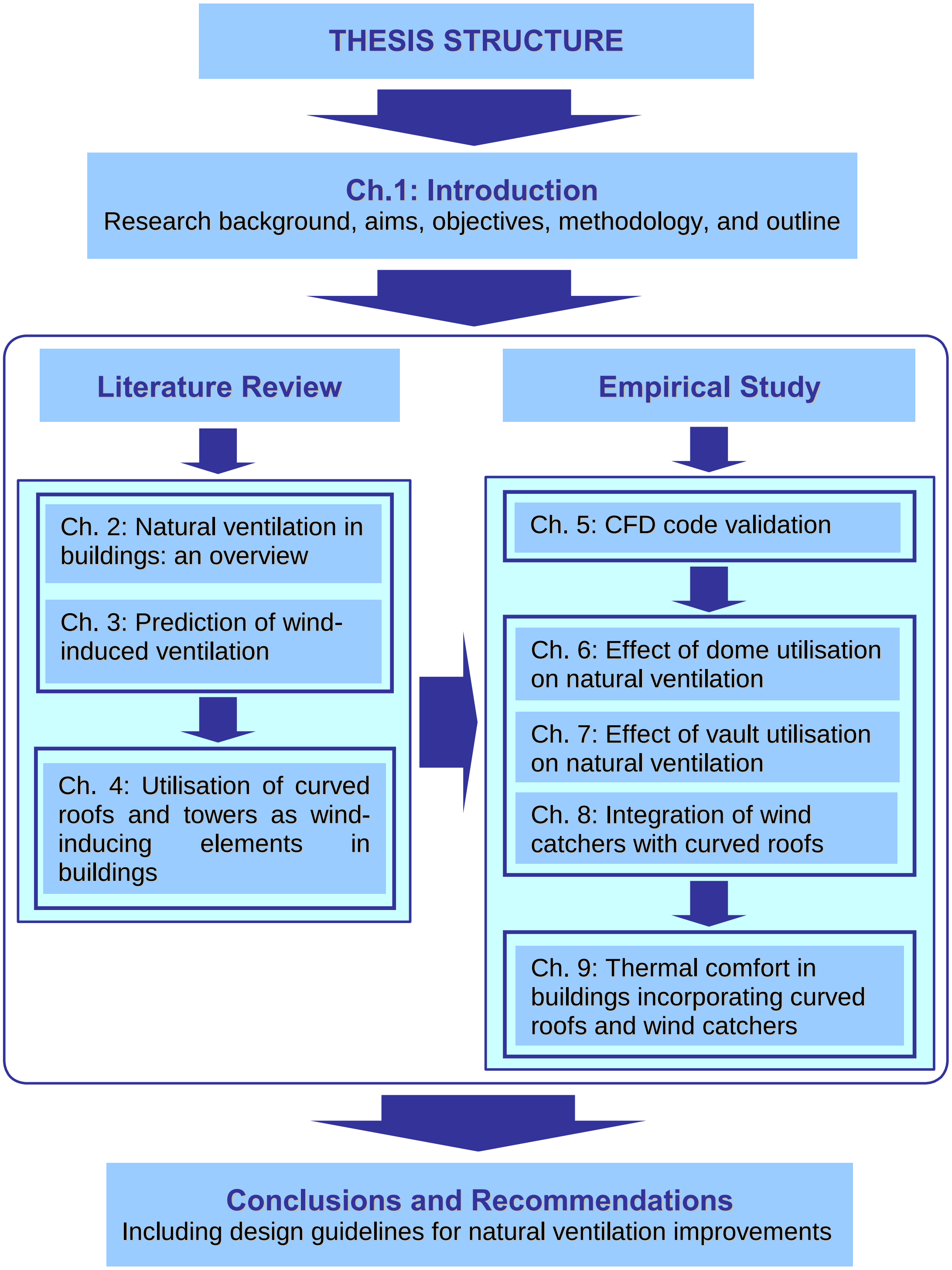

Figure 1.1: Structure of the thesis

CHAPTER 2 : NATURAL VENTILATION IN BUILDINGS: AN OVERVIEW

Introduction

This chapter aims to introduce the study with a summarised presentation of natural ventilation applications in buildings. It defines the concept of natural ventilation in buildings, and compares natural and mechanical ventilation strategies. Then it presents some aspects of natural ventilation utilisation of buildings, which include: its objectives, driving forces, strategies, and role for passive cooling.

It then demonstrates the relationship between natural ventilation and human thermal comfort. This includes: the concept of human thermal comfort, its personal and environmental factors, in addition to an overview on the related heat transfer mechanisms. Then, it highlights the role of natural ventilation in improving thermal comfort conditions. This chapter concludes by comparing the advantages and disadvantages of natural ventilation utilisation in buildings.

2.1 Concept of natural ventilation in buildings

Ventilation in any building can be one of two kinds (Liddament, 1996):

2.1.1 Purpose-provided ventilation

This is defined as “the process by which clean air, normally outdoor air, is intentionally provided to a space and stale air is removed” (Liddament, 1996, p.1). This process can be accomplished by a natural, mechanical, or hybrid system. Natural ventilation is defined as “the air flow resulting from the designed provision of specified apertures such as openable windows, ventilators, shafts, etc. and can usually be controlled to some extent by the occupant” (CIBSE, 1988, p.A4.1).

2.1.2 Infiltration

Infiltration term is used to describe the uncontrolled air movement to and from buildings. This air movement occurs naturally through cracks, gaps, and porous materials used in building facades.

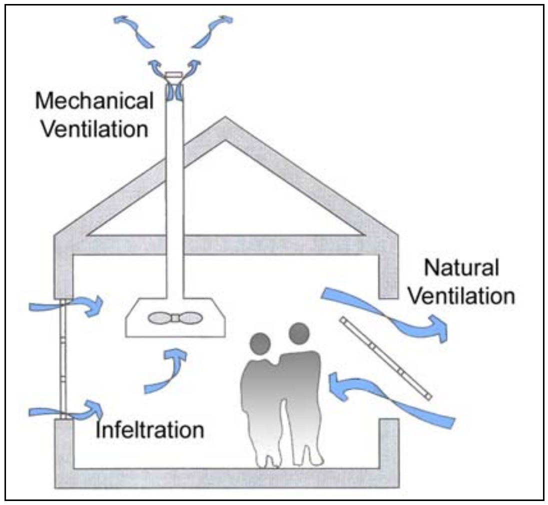

Figure 2.1: Ventilation is a combination of infiltration, and purpose-provided ventilation by natural or mechanical means

Source: (BICEPS module, 1997).

2.2 Mechanical Ventilation

Although this study focuses on natural ventilation, it is useful to have a summarised idea about mechanical ventilation. This helps rationalising the advantages and disadvantages of each strategy, as will be discussed in Section 2.7. Mechanical ventilation relies on a mechanically generated power to drive airflow, instead of the natural driving forces. According to CIBSE (1997), mechanical ventilation strategy is divided into many kinds:

2.2.1 Mechanical Extract

In this system, a fan is used to extract air out of the space. Accordingly, the generated suction forces drive the outdoor air into the space through the purpose-provided openings.

2.2.2 Mechanical Supply

In this system, a fan is used to supply air into the space, where pressure difference forces the air to leave the space through some purpose-provided openings.

2.2.3 Mechanical Balanced Ventilation

Here, both supply and extract networks are incorporated into the space to provide filtered air and extract the ‘old’ one. It is possible that a proportion of the indoor air is re-circulated and mixed with the incoming outdoor air.

2.3 Why natural ventilation?

In the early stage of any design process, it is crucial to evaluate the feasibility of the use of natural ventilation strategy. The most important criterion in this regard is to deliver the required amount of air in the required time and place, with a minimal environmental impact. According to CIBSE (1997), evaluation of advantages and disadvantages of any HVAC system is governed by many factors, like:

- Robustness: the possibility of any failure should be considered.
- System cost: this includes: capital, operation, and maintenance costs.
- User’s preference: this includes thermal comfort, quality of the indoor environment, and system control.

2.3.1 Natural ventilation advantages

Natural ventilation utilisation in buildings, compared to the mechanical ventilation, has many advantages. This includes:

- It is fossil fuel free. This has no direct negative environmental impact, like air pollution, global warming, etc.
- It requires less construction and operation cost, and minimum maintenance.
- It is reliable and easy-to-use in many types of buildings, like residential and office buildings. The potential for personal control of the environment increases users satisfaction and productivity (Energy efficiency Best Practice Programme, 1998).

2.3.2 Natural ventilation use disadvantages

Despite of the above-mentioned advantages of natural ventilation, it still has some disadvantages:

- Wind has a random nature in both direction and magnitude. This means that securing stable indoor environment depending totally on natural ventilation is not in possible, compared to the steady conditions of mechanical ventilation.
- Utilising natural ventilation in some building types seems to be impractical, especially those of deep plans, or those requiring high control level of indoor environment, like hospital buildings.
- Natural ventilation utilisation has many consequent issues, like: building security, safety, including the event of fire, and reliable control.

2.3.3 Balance between advantages and disadvantages

It is crucial in the early stage of the design process to balance between advantages and disadvantages of natural ventilation utilisation, considering the conditions of each individual project. Thus, it is difficult to state an absolute rule. However, and from an environmental point of view, the use of natural ventilation should be promoted wherever possible and feasible. In the last few decades, mechanical ventilation has been heavily used in buildings. This has caused a rapid increase in energy consumption in these buildings.

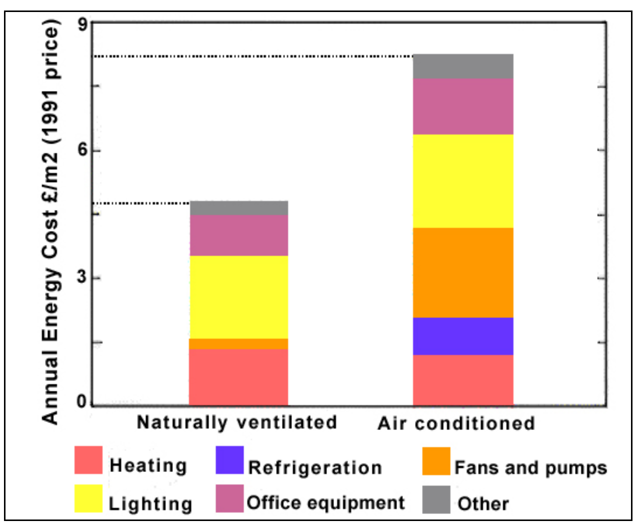

Figure 2.2: Comparison between the annual energy costs of naturally ventilated and air conditioned buildings

Source: (Energy Efficiency Best Practice Programme, 1998)

Mechanical ventilation is an energy-intensive process. In average, naturally ventilated buildings are 40% less in operation energy cost when compared to mechanically ventilated buildings (CIBSE, 1997). This in fact has attracted the attention of many researchers since many years. The worldwide concern has increased regarding many associated environmental impacts, like: global warming, pollution, and shortage of the fossil fuel itself. As a result, the concept of 'energy-efficient design' has developed the architectural design priorities. This design strategy aims to "provide thermal comfort and acceptable indoor air quality with the minimum use of energy" (CIBSE, 1998, p.6-1).

Thus, the concern has turned back again to find a solution in natural ventilation in order to make it more effective and reliable. Many studies have been carried out to make the use of natural ventilation in buildings more efficient, and reduce the use of mechanical plants (Liddament, 1996). This includes many aspects, like:

- Producing natural ventilation design guidelines for different types of buildings.
- Improving the detailed design of architectural elements that can be utilised for natural ventilation.
- Utilisation of hybrid ventilation systems, wherever the use of natural ventilation as a sole strategy is impractical. These systems integrate natural ventilation with mechanical energy-efficient plants.

2.4 Objectives of natural ventilation in buildings

Ventilation of buildings is important for health and comfort requirements at all building types. The following diagram illustrates the main objectives of natural ventilation utilisation in buildings.

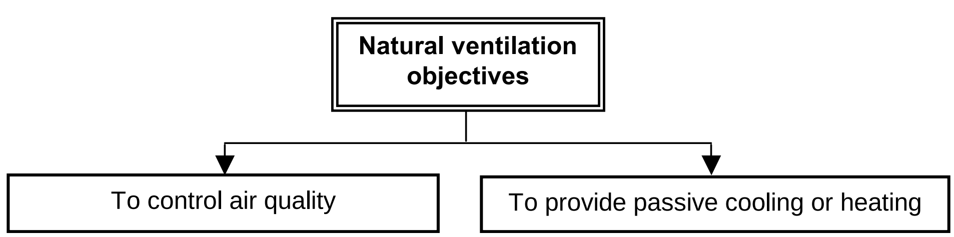

Figure 2.3: Design objectives of natural ventilation

2.4.1 Natural ventilation for indoor air quality

Indoor Air Quality (IAQ) is an important side of natural ventilation application in buildings. In general, natural ventilation improves IAQ through three mechanisms:

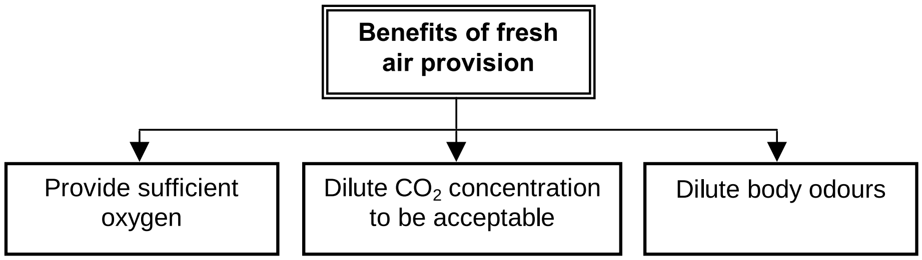

Figure 2.4: Benefits of fresh air provision

Source: (BRE, 1994). Reproduced by the author

It is important to note that little ventilation may result in a poor IAQ, while excessive ventilation may cause undesired draughts. Ultimately, ventilation rate should be sufficient to maintain both IAQ and thermal comfort requirements. In summer, sufficient oxygen is normally provided through windows. In winter, according to BRE (1994), background ventilation is required in a minimum rate of 400 mm^2/ m^2 of multi-cell building floor area. This can be achieved by using trickle ventilation. In addition, natural ventilation protects the environment from the harmful gases. One of the most common gaseous pollutants is Carbon Dioxide, CO_2.

Table 2.1: Limits of some internal gaseous pollutants in buildings

Source: (BICEPS module, 1997)

Pollutants	Source	Levels (ppm)	Limits (ppm)
Carbon Dioxide	People, combustion	320 to 2500	5000 ppm
Oxides of Nitrogen	Combustion, cooking, smoking	0.5 to 0.3	---
Carbon Monoxide	Combustion, cooking.	3 to 17	35 ppm

The effect of CO_2 concentration on human being varies from deep respiration to immediate death. Thus, it is important to predict the expected CO^2 concentration due to building occupants, equipments, external sources, etc, and insure that the upper allowed limit is not exceeded. The amount of CO_2 in air is usually expressed in percent, or in parts per million (ppm). Many solutions have been introduced to control this concentration, like CO^2 concentration sensors. When CO^2 concentration reaches a predefined level, these sensors automatically operate natural ventilation, like opening windows or roof vents, to replace the stale air with fresh one.

2.4.2 Natural ventilation for passive cooling

Passive cooling is defined as “processes of heat dissipation that will occur naturally, that is without the mediation of mechanical components or energy inputs” (Goulding *et al*, 1992, p.91). Many passive cooling techniques are available. Their implementation depends on the local conditions and design limitations. One of these techniques is natural ventilation. Figure 2.5 categorises and summarises some of these techniques.

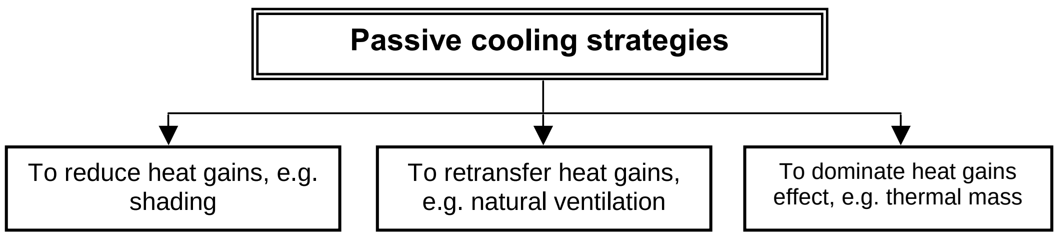

Figure 2.5: Natural ventilation is one of the passive cooling strategies

Source: (Zöld, no date). Reproduced by the author

Natural ventilation, as a passive cooling strategy, is used to cool down indoor air, building structure, and building occupants. This can be achieved via many techniques. Some of them can be found in Section 2.6. The role of natural ventilation in passive cooling is highly affected by the local climatic conditions. For example:

- In summer: if the outdoor air temperature is less than the indoor one, airflow through a building removes internal heat gains and increase human thermal comfort. If the outdoor air temperature is higher than the indoor one, it is possible to reduce air temperature by some techniques, like night-time ventilation, explained in Section 2.6, and underground cooling. In hot arid regions, natural ventilation works effectively when integrated with an evaporative cooling method.
- If both outdoor and indoor air temperatures are equal, natural ventilation still important to supply fresh air and increase occupants comfort.
- In winter, a minimum ventilation, or infiltration, rate is required to maintain an acceptable indoor air quality.

2.5 Natural ventilation driving forces

Natural ventilation relies on natural driving forces. These forces are either the stack effect, due to the difference in air temperature, or the wind effect, due to the difference in air pressure. These two driving forces are discussed below:

2.5.1 Wind effect

In wind-induced or wind-driven ventilation, air passes through a building due to pressure difference generated between its inlets and outlets. When wind reaches the windward face of a building, a high-pressure zone formulates there. This pressure pushes air inside, around, and over this building. Accordingly, a negative pressure zone occurs on the literal and leeward sides.

This results in air movement from the higher-pressure zone to the lower one, which is known as the wind effect. Wind-induced ventilation is more effective in hot climates, when compared with stack-induced one. This is because of the low temperature difference between indoor and outdoor temperatures (Chow, 2004). Wind-driven ventilation depends on many factors. These factors are discussed in details in Section 3.1 of Chapter 3.

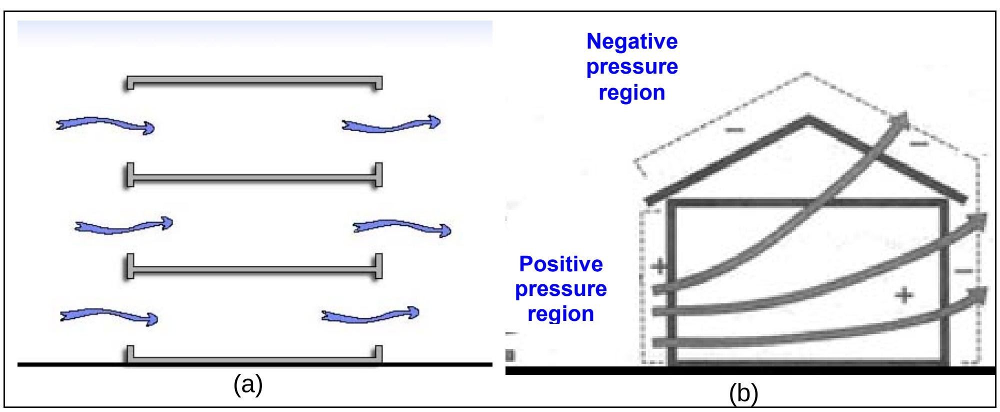

Figure 2.6: Wind-induced natural ventilation

Source: a: (BRE, 1994), b: (Liddament, 1996).

2.5.2 Stack effect

This kind of ventilation is known as the temperature-induced or buoyancy-induced ventilation. It occurs as a result of the difference between indoor and outdoor air temperatures. Warmer air has less density. Thus, and due to density stratification, this air rises to leave the building through the high-level openings, and the cooler outdoor air replaces it through building inlets or by infiltration. This is dependant on the stack height and temperature difference.

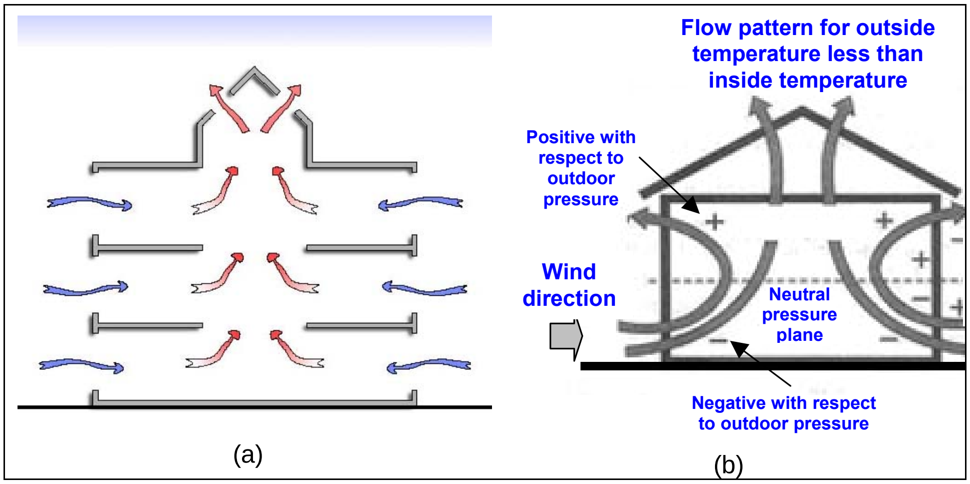

Figure 2.7: Temperature-induced natural ventilation

Source: a: (BRE, 1994), b: (Liddament, 1996).

2.5.3 Combined stack and wind effect

In some climatic conditions, both wind and stack driving forces have an effective role in ventilation. So, combining them is useful strategy for thermal comfort improvement. It is important in this case to avoid any possible adverse effect of this combination, e.g. when they drive airflow in opposite directions.

2.6 Natural ventilation strategies

It is possible to implement natural ventilation in buildings in different systems. Each system has its own advantages and limitations of applicability, due to the local climatic conditions and design requirements. This section presents a summary about some of these systems. Further details can be found in the relevant references, like: CIBSE (1997), and Liddament (1996).

2.6.1 Wind-induced ventilation

This strategy depends mainly on pressure difference between inlets and outlets as a driving force. It includes (CIBSE, 1997):

A. Single-sided ventilation

Single-sided ventilation, as illustrated in Figure 2.8, operates by openings located in one side of the building. It is effective up to a maximum depth equals to the double of a space height.

B. Cross ventilation

Cross ventilation is more effective than single-sided ventilation strategy. It is used to create airflow paths between building inlets and outlets, which passes through the occupied level of the building. Cross ventilation is effective up to a maximum depth equals to five times the height of the room. It can be driven by wind effect, like the case of using wall openings, or by stack effect, like the case of using atrium ventilation, where the resulting flow path is vertical.

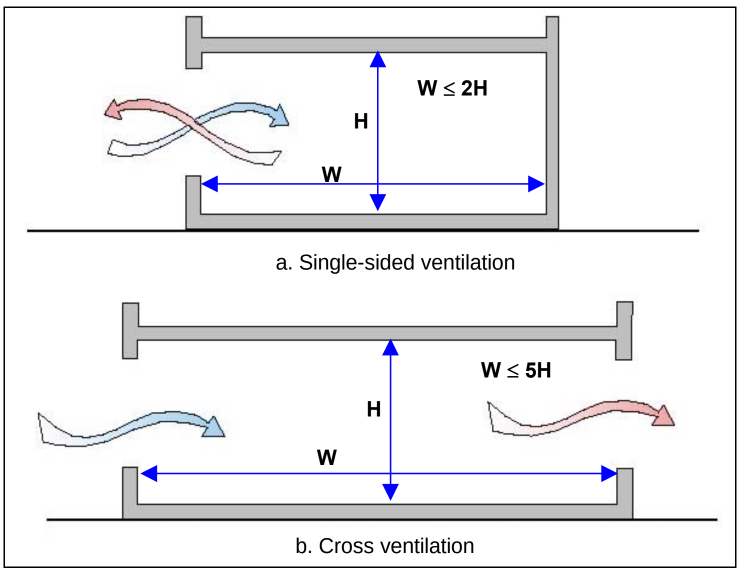

Figure 2.8: Single-sided and cross ventilation strategies

Source: (CIBSE, 1997).

It is also important to plan good distribution of openings. Openings located at opposite walls are more effective for cross ventilation, compared to those located at adjacent walls. Also, vertical position of the inlet should be in relation with the occupied level of the space. Generally, low inlet is recommended for cooling and high outlet is recommended for stack ventilation.

The minimum window area should be about 5% of floor area, with the use of tickle ventilation to secure the minimum flow rate (Smith, 2001). In any case, window area should be enough to meet the required ventilation rate, which varies depending on the building use. For example, and according to CIBSE (1988, p.A1-9), the recommended airflow rate for open-plan offices is 8 l/s per person. Table 2.2 illustrates the three possible probabilities of inlet and outlet area.

Table 2.2: Possibilities of inlet and outlet opening area

Source: (Moore, 1993)

Illustration (A_i =inlet area, A_o=outlet area)	Observation	Design target
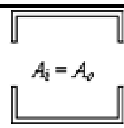 $A_i = A_o$	Maximum air change created	Building cooling
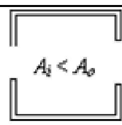 $A_i < A_o$	Maximum interior air speed	Users cooling
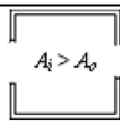 $A_i > A_o$	Air speed reduced inside, and accelerated outside.	Outdoor spaces cooling.

2.6.2 Solar-induced ventilation

This strategy depends mainly on temperature difference between inlets and outlets as a driving force. It includes:

A. Solar Chimney

The main components of the solar chimney are illustrated below. Solar chimney can be integrated in vertical elements of buildings, like: stairwells and elevator shafts, chimneys, etc. Its design includes a black metal absorber installed behind its front. This is insulated from the internal space by the means of air cavity and thermal insulation. Heated air in this cavity rises and leaves through the top opening. Thus, cooler fresh air, provided by wall openings, is induced inside the space. This air circulation is accelerated when prevailing wind currents passes over the chimney. Solar chimney can also be utilised for heating in winter. This can be achieved by modifying openings arrangement, so that the heated air in the cavity is admitted inside the space, as illustrated below.

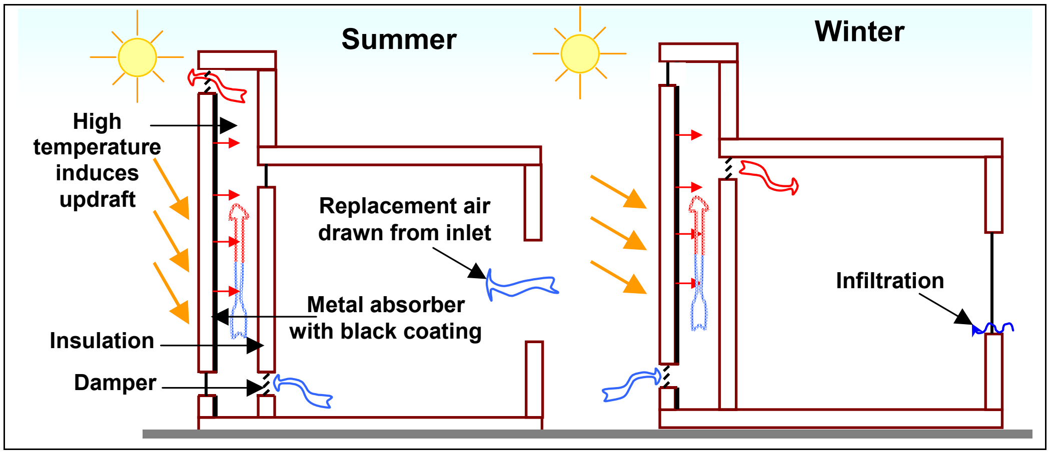

Figure 2.9: Solar chimney

B. Trombe wall

The main components of the Trombe wall are illustrated below. Its operation concept is similar to that of solar chimney, but using different building materials with different thermal properties. Trombe wall can be utilised effectively for heating in winter by utilising solar radiation during daytime. During night, and depending on the thermal properties of the wall located beyond the glazing panels, heat stored in the wall is released, which heats up the space.

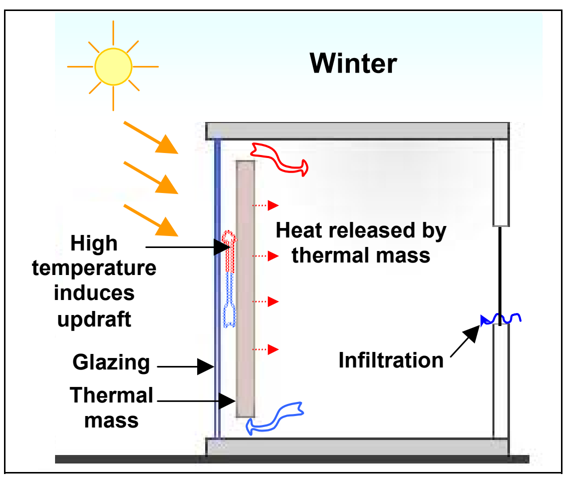

Figure 2.10: Trombe wall

C. Atrium ventilation

Atrium building is simply is a glass-covered courtyard, towards which all internal spaces are oriented. This architectural configuration is widely used in public buildings, like offices. Airflow is induced from the different building spaces towards the atrium by stack effect. Air then rises to the top of the atrium, where outlets are placed. In this case, the atrium should be extended above the roof by several meters to increase stack height for the upper floor. The difference between atrium and solar chimney is that atrium function as a central space for circulation and social gathering. This makes it an attractive ventilation strategy in public buildings.

D. Double façades

Double facades are used to induce air through a cavity located between glass panels in the outer skin of the building. This is implemented for the whole façade instead of a separated vertical element, like Tromb wall or the solar chimney. Air in the cavity is heated up and driven inside the building by stack effect, with or without the use of fans. In summer, hot air leaves the cavity through the outer layer openings. The application of other ventilation strategies including night ventilation is possible, depending on the type and orientation of the double skin façade.

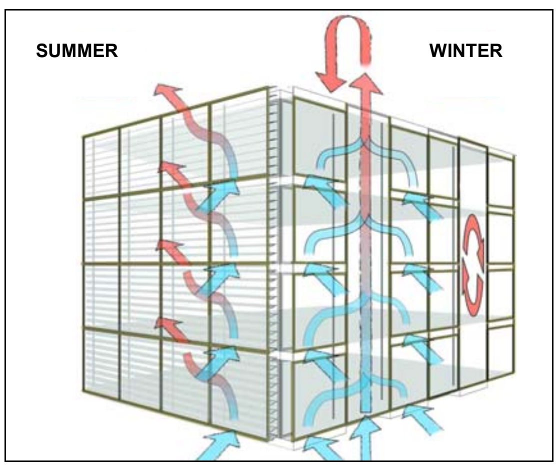

Figure 2.11: Double façade

Source: (Lund Institute of Technology, 2004. Available online: http://www2.ebd.lth.se/avd%20ebd/main/personal/Harris)

2.6.3 Night ventilation

This strategy relies mainly on the thermal properties of building materials, which are used as a thermal sink. The low temperature of night airflow cools down building envelope, when this airflow passes over it. At morning, this envelope absorbs heat gains, released due to solar radiation and building operation. Thus, efficiency of night-time ventilation, as a passive cooling technique, depends on two factors:

- Difference between the outdoor and indoor air temperature.
- Thermal characteristics of the building materials used.

According to CIBSE (1997), some issues should be considered when applying this strategy, like:

- Appropriate building material selection, with sufficient contact surface area between them and air.
- Security of the building.
- Temperature control to avoid over-cooling.

2.6.4 Mixed natural ventilation strategy

Different natural ventilation systems can be combined in one building. This gives the designer a wider margin to deal with each single space according to its requirements. As an example, simple combination between cross-ventilation, for an open plan office area, and single-sided ventilation, for cellular office rooms, is illustrated below:

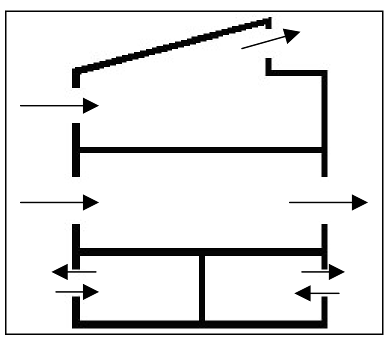

Figure 2.12: Example on combined-ventilation strategy

2.6.5 Mechanically-assisted strategy

In some cases, natural ventilation is insufficient to secure an acceptable level of human thermal comfort. It is possible to overcome this problem by integrating some mechanical devices, like fans, to assist the use of natural ventilation. In mechanically ventilated buildings, this strategy is useful to reduce energy consumption. This requires an assessment of the local climate conditions, in addition to an effective control strategy. Some examples of the application of this strategy are:

- The use of fans at the top of solar chimney to help air extract, when driving stack is not enough to achieve the required air change rate.
- The use of mechanical ventilation for some spaces located in the centre of deep-plan buildings.
- The use of mechanical supply when quality of the outdoor air is unacceptable.

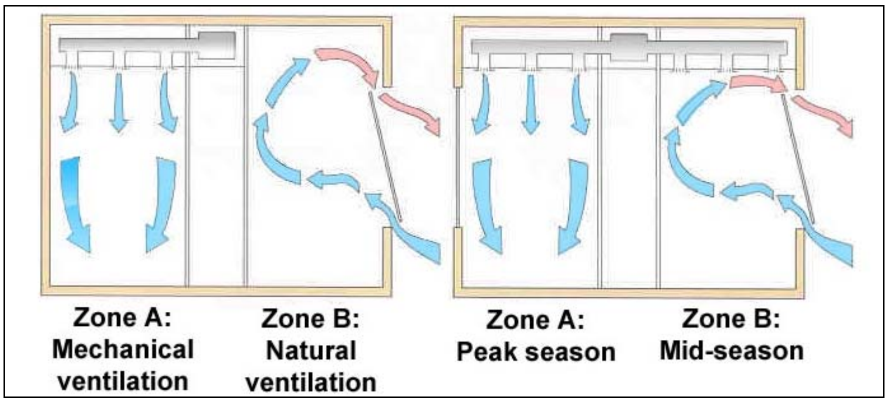

Figure 2.13: Examples of hybrid ventilation

Source: (Energy Efficiency Best Practice Programme, 1998).

2.6.6 Criteria of natural ventilation strategy selection

Depending on local climatic conditions and building design requirements, it is possible to choose an appropriate natural ventilation strategy. These factors are illustrated below:

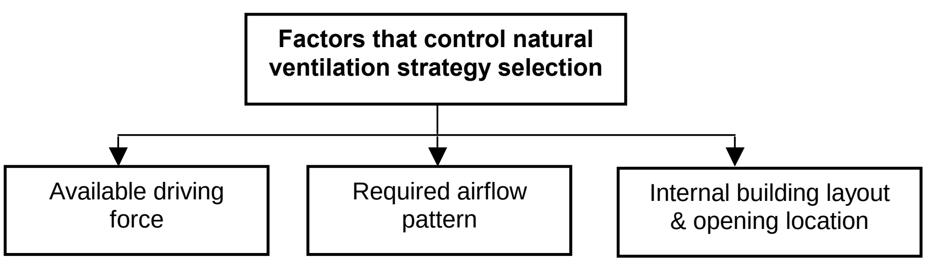

Figure 2.14: Factors that control selection of natural ventilation strategy

Local climatic data analysis helps specifying the dominant ventilation driving force. Assessment of the resulting airflow pattern is mainly qualitative, and mainly depends on the requirements of building operation and users. For example, some related aspects are: direction of airflow paths from the inlets towards the outlets, maximum airflow speed, airflow behaviour in the case of fire, etc. The last factor, illustrated above, is related to the layout of the plan, and the location of the openings.

2.7 Natural ventilation and thermal comfort

This section presents an overview on human thermal comfort in buildings, and the role of natural ventilation in this regard.

2.7.1 Human thermal comfort definition

There are many definitions of thermal comfort. This is because thermal comfort is dependant on many parameters, which are sometime difficult to measure, and depend on personal preferences. For example, this is clear in ASHRAE Fundamentals (1997) (see: Santamouris and Asimakopoulos, 1996, p.129), which defines human thermal comfort as “the conditions in which a person would prefer neither warmer nor cooler surroundings”. The same point is also clear in the definition given in the British Standards (BSI, 2005, p. 10), which states that thermal comfort is “that condition of mind which expresses satisfaction with the thermal environment”.

Furthermore, thermal comfort control is more difficult in naturally ventilated buildings, duo to the instability in the climatic conditions. This is not the case in air-conditioned buildings. Despite this difficulty, many models have been developed for thermal comfort assessment. To understand the assessment criteria, it is crucial to demonstrate the parameters that affect human thermal comfort, and the related heat transfer mechanisms.

2.7.2 Thermal comfort personal factors

These factors are related to human beings, like age, sex, and activity. As indicated by Santamouris & Asimakopoulos (1996), the most important factors are:

A. Occupant activity:

Metabolic rate of human body is in relation with its activity. For example, a person doing a heavy activity requires more cooling, and vice versa. This parameter estimates the amount of energy produced per square metre of body surface area of human beings. It is measured in metabolic or *met* unit, which is “the metabolic rate of a seated person when relaxing, i.e. 58 W/m^2” (Goulding *et al.*, 1992, p.60).

Table 2.3: Typical heat emission of human body against its activity

Source: (Goulding *et al.*, 1992). Summarised by the author

Activity	W/m^2	*met*
Sleeping	40	0.7
Seated	60	1.0
Walking	150	2.6
Exercise	175-235	3.0-4.0

B. Occupant clothing

Clothing can be considered as a bodily thermal insulation. The unit of this insulation is *clo*, which is equivalent to an insulation of 0.155 m^2 K/W obtained by a winter business suit. Table 2.4 illustrates thermal insulation of different clothing categories. Similarly to the previous factor, clothing affect heat transfer rate between the body and the ambient environment.

Table 2.4: Clothing values for thermal comfort calculations

Source: (Goulding *et al.*, 1992). Summarised by the author

Clothing	m^2 K/W	*clo*
Nude	0	0
Light summer ensemble	0.08	0.5
Typical indoor winter ensemble	0.16	1.0
Heavy business suit	0.23	1.5

2.7.3. Thermal comfort environmental factors

There are many environmental factors that affect thermal comfort, as shown in Figure 2.15. A summary on each factor is given below. The role of these factors in the bodily heat transfer mechanisms and, therefore, human thermal comfort is explained in Sections 2.7.4 and 2.7.5.

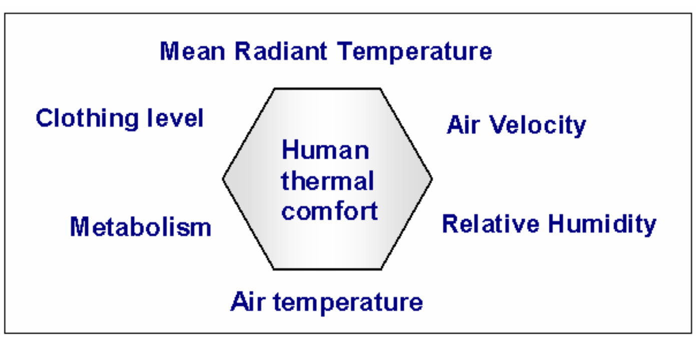

Figure 2.15: Primary factors affecting human thermal comfort

A. Dry-Bulb Temperature, T_{db}

T_{db}, or air temperature as usually named, is the ambient air temperature measured by a thermometer freely exposed to heat radiation in the air. It is called so because it is measured with a standard thermometer whose bulb is not wet. This is to avoid any effect of evaporative heat transfer, which is considered in the Wet-Bulb Temperature, T_{wb}. It is usually measured in degrees Celsius (°C) or degrees Farenheight (°F).

B. Mean Radiant Temperature, MRT

Objects in the space affect human thermal comfort, even if they are not in a direct contact with the human body. This is considered by the environmental factor of MRT. These objects absorb or emit heat, depending on their thermal properties and temperature difference between them and the surrounding air. Thus, MRT refers to the average temperature of surrounding surfaces, which is nearly the same of ambient air temperature in the normal cases (Moore, 1993).

MRT is measured using globe thermometer, which is a normal dry bulb thermometer encased in a 150 mm diameter matt-black copper sphere which has absorptivity approaching that of the skin. When surrounding objects are warmer than the average skin temperature, MRT should be positive, and vice versa. It is important to note that MRT is independent of ambient air temperature. For example, if the body is exposed to the sun it will be more comfortable even at lower air temperatures.

C. Relative Humidity, RH

Humidity refers to the amount of moisture vapour in a specific volume of warm air. This amount of vapour, under any dry bulb temperature, is known as the absolute humidity, and is measured in g/kg. Maximum possible amount is known as dew point. Relative humidity (RH), therefore, is the ratio between the absolute humidity to this maximum amount, expressed as a percentage. Relative humidity is measured using hygrometers.

D. Air Velocity

Air movement can be natural or mechanical. It is measured using anemometers, normally in metres per second. More details about this environmental factor are given in Section 3.1.1 in Chapter 3.

2.7.4 Bodily heat transfer mechanisms

Any building can be described as a "set of various systems coupled together" (Allard & Alvarez, 1998, p.30). Amongst these systems are the heat transfer mechanisms. According to Marsh (1998a), physiologists found that absorptivity and emissivity of human skin is considered high, compared to other known substances. This means that human body is highly responsive to any changes in the ambient temperature.

To understand the effect of natural ventilation, as a passive cooling technique, on human thermal comfort, it is essential to explain how human body gives off heat by the skin surface and respiration. This is because any passive cooling technique that utilises natural ventilation has in its heart the implementation of heat transfer mechanisms. Bodily heat transfer mechanisms can be divided into four mechanisms (Moore, 1993):

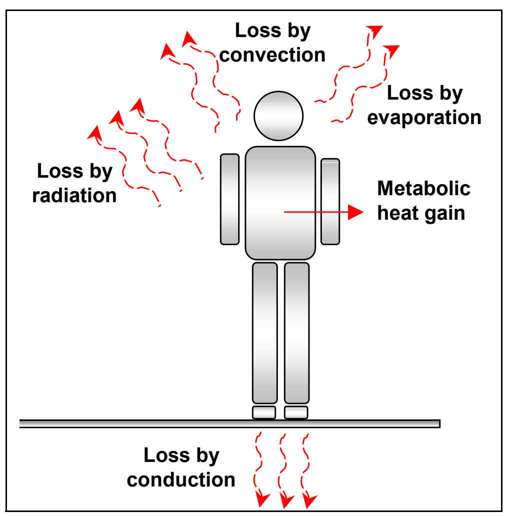

Figure 2.16: Bodily heat transfer mechanisms

Source: (Moore, 1993). Reproduced by the author

A. Convection

Heat energy here is transferred through fluids by the physical movement of particles, e.g. movement caused by buoyancy effect. Convective heat transfer rate is in proportion with temperature difference between skin and ambient air. It is also in proportion with air speed. This means that skin loses heat by convection when cold air passes over it. Also, additional convection occurs due to breathing as cool air is drawn into the body.

B. Radiation

Heat energy here is transferred by electromagnetic waves. This occurs when surface atoms of any material emit thermal energy as electromagnetic waves in the infrared range of wavelength. Radiation rate is dependent on material properties and temperature. Human skin loses heat by radiation depending on the MRT value of surrounding objects. This is also dependant on the distance between these objects and the human body.

C. Evaporation

When skin temperature increases, due to the increase of ambient temperature or activity level, it becomes difficult for the body to maintain its heat balance depending only on convection and radiation. In this case, evaporation of sweat encourages more heat transfer between skin and ambient air, causing skin to cool down. This mechanism is in inverse proportion to relative humidity of the ambient air. This means that in 100% RH, no moisture absorption occurs in the air, and hence no evaporation. Evaporation also is in proportion to the ambient air velocity.

D. Conduction

Heat energy here is transferred through materials without molecules movement. This mechanism occurs in both solid materials and fluids. Heat here is transferred directly between adjacent molecules in a time duration, which depends on material properties. This mechanism is less important than the above-mentioned ones in terms of thermal comfort determination. It occurs when human body is in a direct contact with another material, which has effective thermal capacity and conductivity, like ground tiles for instance.

2.7.5 Effect of natural ventilation on thermal comfort environmental factors

As mentioned before, one of the main objectives of natural ventilation is to encourage heat transfer between human body and its ambient environment. The effect of natural ventilation on the environmental factors related to human thermal comfort is highlighted below:

A. Effect of air velocity on air temperature

It is recommended to reduce air velocity in winter in order to maintain the required air temperature for thermal comfort. In summer, and when outdoor air temperature is less than the indoor temperature, increasing air velocity by natural ventilation encourages bodily heat loss by convection, which reduces the ambient air temperature. This increases convective heat transfer between skin and ambient air, as cooler air replaces the warmer one, which is closer to the skin.

If the outdoor temperature is already higher than upper recommended limit for thermal comfort, then the use of thermal mass and night ventilation, as explained in Section 3.6.3, are useful strategies to improve thermal comfort conditions by both convection and radiation. The above-mentioned two scenarios are true in the case of hot arid climate. In the case of hot humid climate, high air velocities help enhancing evaporative heat transfer over skin surface. This is because drier ambient air replaces the saturated air near the skin. In all cases, air velocity should be kept below its allowed upper limit. Table 2.5 gives some indications in this regard:

Table 2.5: Internal air speed classification in buildings

Source: (Marsh, 1998a)

Airflow description	Airflow velocity		Airflow description	Airflow velocity	
	m/s	km/h		m/s	km/h
Still	0.0	0.0	Hair and Papers Move	1.0	4.0
Not Noticeable	0.1	0.4	Noticeably Draughty	1.4	5.0
Barely Noticeable	0.3	1.0	Unpleasant Breeze	1.7	6.0
Pleasant Breeze	0.5	1.8	Gusting Breeze	2.0+	6.5+
Light Breeze	0.7	2.5	---	---	---

B. Effect of air velocity on MRT

MRT is a very important factor that determines human thermal comfort. In winter, increasing MRT can compensate the low value of air temperature. In summer, and for passive cooling, increasing air velocity helps removing the undesired heat emitted by the ambient surfaces. Thus, these surfaces are cooled down by convection. When MRT becomes less than skin temperature, these surfaces act as thermal sinks. This can be enhanced by implementing night-time ventilation, provided that outdoor temperature is low enough.

C. Effect of air velocity on RH

Relative humidity is usually recommended to be between 40% and 70%. Values outside this range result in the climate being humid or arid, in addition to being hot. According to ASHRAE, (see: Goulding *et al.*, 1992), when air temperature is more that 30°C, the effect of RH on thermal comfort becomes more pronounced. In high relative humidity, increasing air movement effectively encourages bodily heat transfer by evaporation.

2.7.5 Thermal comfort assessment

Thermal comfort prediction is not an easy task, due to the number of interacting factors, including personal preferences. However, many models have been developed. In fact, explaining these models is out of the scope of this study, as the main objective here is to give a summarised background. One of these models is the Tropical Summer Index (TSI), which has been implemented in Chapter 9, and explained in Section 9.2 of Chapter 9.

Another example is the work of Penwarden (1973), depicted in the following graph. This graph shows the relationship between thermal comfort conditions of a person in different air temperatures, wind speeds, in addition to clothing levels. Calculations of the heat balance between a person and his surroundings show that it is possible to achieve thermal comfort in higher air temperature when wind velocity increases, especially in the case of low wind velocity. It also shows a comparison between thermal comfort conditions in sunny and shaded places. For example, moving from a sunny place and still air (less than 0.5 m/s) to a shaded place and a high wind speed of 5 m/s would require an increase of 13°C in air temperature to keep thermal comfort.

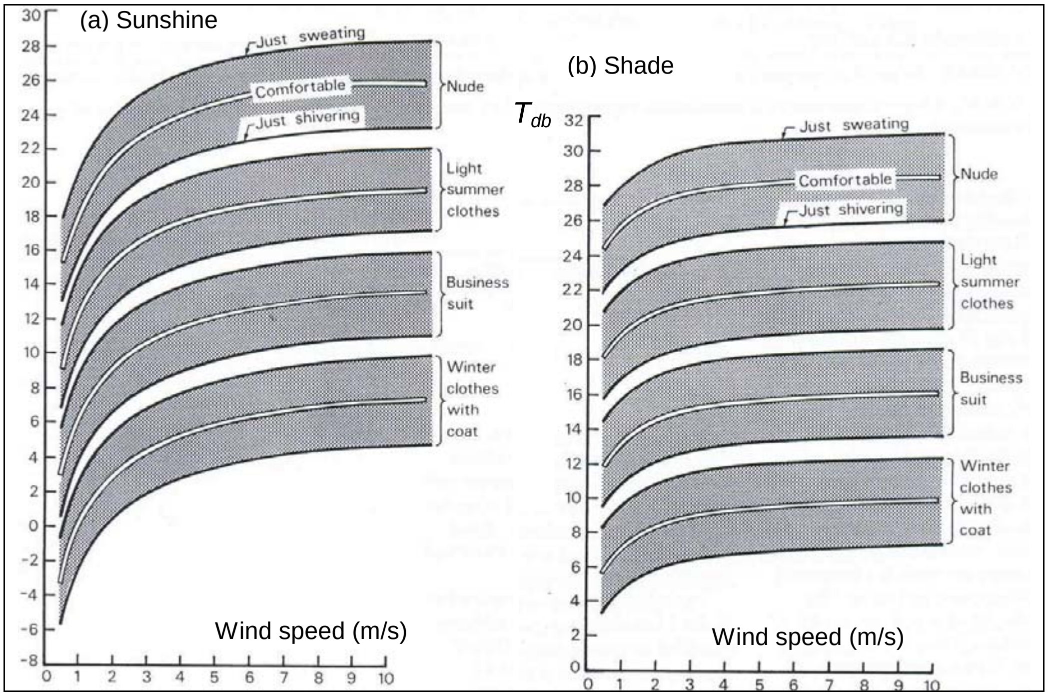

Figure 2.17: Thermal comfort conditions for a strolling person in different wind velocities and clothing conditions

Source: (Penwarden and Wise, 1975)

As explained by Awbi (2003), the well-known Fanger's model, developed in 1970, is the most comprehensive model for thermal comfort assessment up to date. Marsh (1998a) mentioned that this model has been adopted as an ISO standard. Fanger's steady-state energy balance model applies the heat balance equation, in addition to other empirical equations and different assumptions. This equation is:

$$S = M + W + R + C + K - E - RES \qquad \textbf{(2.1)}$$

Where: S = heat storage in the body, M = metabolic rate, W = mechanical work, R = heat exchange by radiation, C = heat exchange by convection, K = heat exchange by conduction, E = heat loss by evaporation, and RES = heat loss by respiration (all units are in W).

This equation is derived depending on the Law of Energy Conservation. It balances the rate of bodily metabolic and activity heat production to the heat loss by different mechanisms. To describe thermal sensation when human body is not in thermal equilibrium, Fanger's model estimates what is known as the Predicted Mean Vote.

PMV index contains many categories to describe mean thermal sensation of a large group of people. This scale is recommended by ISO to be between –0.5 and 0.5.

Table 2.6: Fanger's PMV index

Source: (Santamouris & Asimakopoulos, 1996)

Thermal description	PMV
Hot / cold	±3
Warm / cool	±2
Slightly warm / cool	±1
Neutral	0

It is also possible to use PMV calculators to investigate the effect of the different thermal comfort factors. An example is given below. Knowing the PMV, the Predicted Percentage of Dissatisfied people (PPD) can be determined as well. PPD increases as PMV moves up or down from 0, which is the neutral value. The maximum value of PPD is 100% and the minimum value is 5%, as it is impossible practically to satisfy all building users.

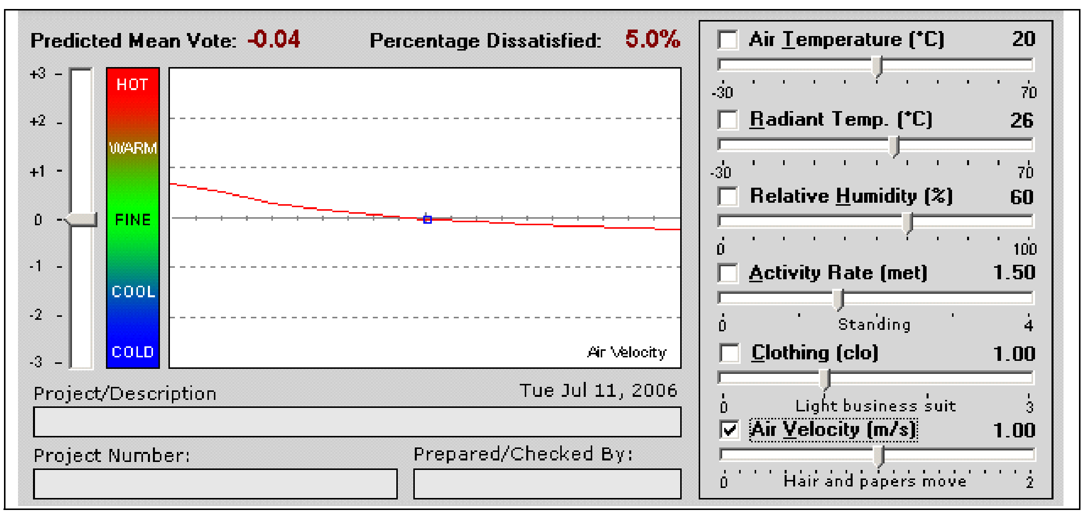

Figure 2.18: An Interactive PMV Calculator

Source: (Marsh, 2006. Available online: http://www.squ1.com/downloads)

2.8 Conclusions

Natural ventilation utilisation in buildings requires understanding of many relevant aspects, like: its driving forces, and strategies. Natural ventilation strategy is of a great environmental advantage, compared to the mechanical ventilation strategy. This has encouraged a further investigation of natural ventilation implementation in buildings, considering its main objectives of providing buildings with the required air quality and quantity.

A review of human thermal comfort revealed that natural ventilation has a high potential for improving thermal comfort in hot climates. Increasing airflow rate, or velocity, up to the required level is a desired parameter in this case. This means that wind effect is more effective in inducing airflow in buildings in hot climates. Generally, maximizing airflow rate encourages bodily heat transfer mechanisms, mainly by convection and evaporation. Therefore, Chapter 3 will investigate the prediction of wind-induced natural ventilation. This will be carried out in a way that serves the need of a numerical analysis in the reported empirical study.

CHAPTER 3 : PREDICTION OF WIND-INDUCED NATURAL VENTILATION

Introduction

This chapter discusses the prediction of wind-induced natural ventilation, which is an essential part of the empirical study. This has been introduced by an overview on the factors that affect wind pressure in buildings, which is the main driving force in the case of wind-induced natural ventilation. This includes a discussion of the effect of mean wind speed, pressure coefficient, and air density on wind pressure. After that, this chapter presents some of the common methods that have been used in natural ventilation prediction in buildings. This includes the empirical models, wind tunnel, Network mathematical model, and CFD.

This is followed by a discussion of the advantages and disadvantages of each method in order to choose an appropriate one for this study. Given that CFD is the prediction method that is implemented; more details have been presented on the relevant CFD software, which is Fluent 5.5. This includes a summary of the relevant applications, like: mesh generation, turbulence model, boundary conditions, and output types.

3.1 Background: factors affecting wind pressure on buildings

Before demonstrating some of the methods used in predicting wind-induced ventilation, it is useful to present a summarised background on wind pressure on buildings. A brief introduction on wind as a driving force of natural ventilation can be found in Section 2.5.1. When wind blows on a building, it creates positive and negative pressure fields around it. Wind pressure on building surfaces is a result of air pressure modified by a coefficient that considers the effect of building shape, surroundings, and wind direction. This pressure coefficient will be discussed later on in this section. In general, the following expression is commonly used to estimate the time average pressure acting at any point on the surface of a building. In other words, it estimates the contribution of wind, in excess to the ambient air pressure, to air pressure difference across an exterior opening, at any defined point on the building:

$$P_w = 0.5\, C_p\, \rho V^2 \qquad \textbf{(3.1)}$$

Where P_w is wind pressure (Pa), C_p is static pressure coefficient, ρ is reference air density (kg/m^3), V is time-mean wind speed at datum level (m/s). It is clear from this equation that wind pressure mainly depends on air speed and density. Other factors, like building shape and wind direction, are considered in the wind pressure coefficient. More details about these factors are given below:

3.1.1 Mean wind speed

Wind velocity is defined as "a constantly varying vector quantity described by its speed and direction" (Goulding *et al.*, 1992, p.32). If its speed is expressed in m/s, air pressure in equation 3.1 will be expressed in kg/m/s^2, i.e. N/m^2 or Pascal (Pa). Wind speed is recorded and averaged in meteorological stations for a defined period of time. Wind velocity at any point in this record can be estimated from:

$$V_{(t)} = V + v_{(t)} \qquad \textbf{(3.2)}$$

Where $V_{(t)}$ is the instantaneous wind speed, V is the time-mean value, and $v_{(t)}$ is the fluctuating component. By integrating $V_{(t)}$ over a known period of time, V can be estimated (Awbi, 2003).

One of the important wind characteristics is that its behaviour varies along what is known as the 'atmospheric boundary layer'. This term defines air layer, which is close to the ground, in which airflow is affected by terrain properties. Its depth varies from less than 100 m up to 2 km, depending on the climate and terrain properties (Goulding *et al.*, 1992). Because of the frictional drag forces of the earth surface, wind speed at ground level is much lower than the higher free stream speed (Schriever, 1976). A more built up terrain results in a lower speed near the ground.

In wind modelling, it is important to consider wind velocity profile along the height of the problem domain. However, it is a common practice in building applications to neglect the effect of thermal stratification on wind velocity (Allard and Alvarez, 1998). Meteorological data usually give mean wind speed at open area and height of 10m. It is necessary to correct this value before using wind-modelling studies. To do so, the following simple expression is commonly used:

$$V / V_r = cH^a \qquad \textbf{(3.3)}$$

Where V_r is time-mean reference wind speed 'obtained from meteorological data' (m s^{-1}); H is the height of the building; c is parameter relating wind speed to terrain nature, and a is an exponent relating wind speed to the height above the ground. These two factors are given below.

Table 3.1: Terrain factors for equation 3.3

Source: (CIBSE, 1988)

Terrain	*c*	*a*
Open flat country	0.68	0.17
Country with scattered wind breaks	0.52	0.20
Urban	0.35	0.25
City	0.21	0.33

Generally, wind speed is much lower in the 'city' terrain when compared with the open country one. In some cases, wind speed at building height in city centres may be only about the third of the free stream, or reference, wind speed. Also, wind speed in urban canyons, like a street, can only be 10-30% of the free-stream wind speed (Athienitis and Santamouris, 2002).

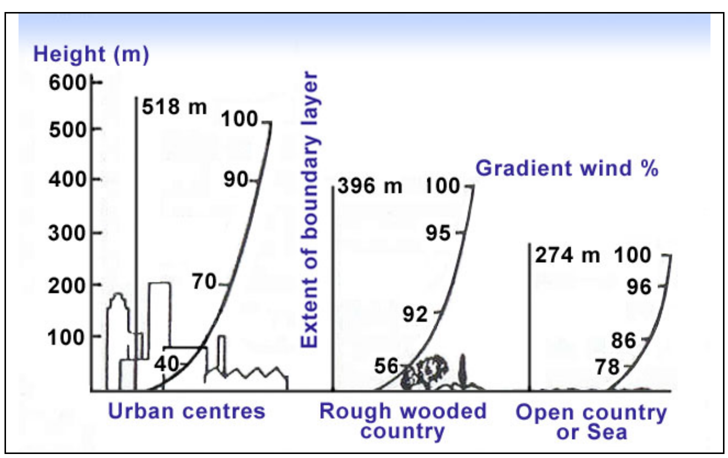

Figure 3.1: Mean wind velocity profiles for different types of terrain

Source: (Bain *et al.*, 1971). Reproduced by the author.

This means that ventilation potential varies in different urban locations. Therefore, careful planning of the site is important to ensure an effective natural ventilation design. Air velocity has also a direct effect on airflow behaviour. Normally, airflow is described as 'laminar' or 'turbulent'. In laminar airflow, change in flow direction, caused by obstructing surfaces, is gradual. This results in smooth and consistent airflow direction with uniform speed. In turbulent airflow, the situation is the opposite, since movement of individual particles is completely random. Change in the flow direction, caused by obstructing surfaces, results here in discontinuous airflow direction with greatly change in speed (Moore, 1993).

Mathematically, specification of airflow as laminar or turbulent is dependant on Reynolds Number. Reynolds Number for a fluid is "the ratio of inertia forces to viscous forces" (Wikipedia, 2006a). Airflow is likely to be laminar at low Reynolds Number, approximately up to 2,000 for flow within a pipe, where the inertia forces are not too large with respect to the fluid viscosity. This is of course affected by the urban roughness explained above. Generally, wind at wall level in urban areas is extremely turbulent (Sachs, 1978). Turbulent flows are less desired than smooth ones. In case of extreme wind speeds, turbulent flows can cause some safety hazards.

3.1.2 Pressure coefficient

Pressure coefficient, C_p, is used to correct the value of air pressure acting on building envelope taking in account the effect of building shape and surroundings, and wind direction. If pressure at the point for which C_p is calculated is higher than the pressure of the free stream, then C_p is positive and vice versa. C_p is positive on the windward due to the impact of the wind and its deflection on the windward surface. It is negative on the leeward due to boundary layer separation from the surfaces at sharp edges joining the roof and the windward wall (Awbi, 2003).

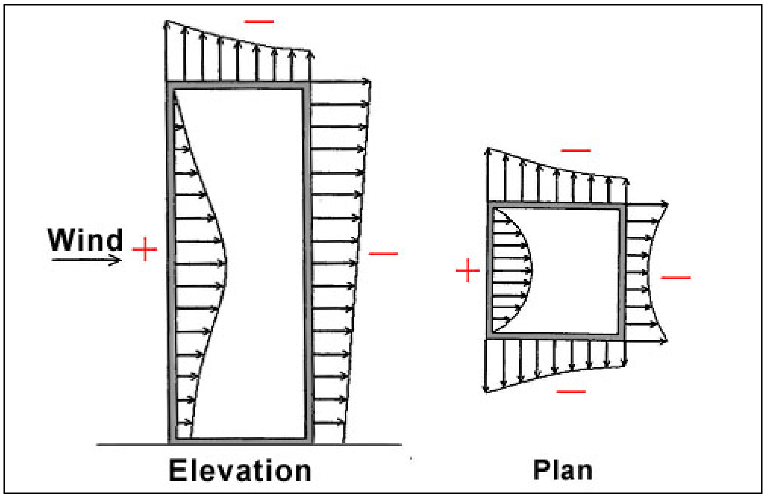

Figure 3.2: Wind pressure distribution on a flat-roof building

Source: (Awbi, 2003).

It is a common practice in research that pressure coefficient is measured in wind tunnels, as will be explained in Section 3.2.2. This method gives accurate data of wind pressure distribution. It also simulates airflow patterns around buildings using smoke technique, combined with photography. It is also possible to obtain pressure coefficient value using CFD modelling or using some especially developed computer programs. Bala'zs developed a software package called CPBANK containing a set of C_p data files for different predefined building geometries and exposures (Allard and Alvarez, 1998). It is also possible to find C_p data for typical building geometries in some standards, like British Standards Institution (BSI, 1991), and Air Infiltration and Ventilation Centre (Liddament, 1986).

Table 3.2: Surface averaged pressure coefficients of square buildings surrounded by buildings of equal height, with a height up to three storeys

Source: (Liddament, 1986). Reproduced by the author

Surface	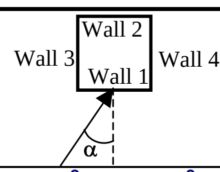							
	0°	45°	90°	135°	180°	225°	270°	315°
Wall 1	0.2	0.05	-0.25	-0.3	-0.25	-0.3	-0.25	-0.05
Wall 2	-0.25	-0.3	-0.25	0.05	0.2	0.05	-0.25	-0.3
Wall 3	-0.25	0.05	0.2	0.05	-0.25	-0.3	-0.25	-0.3
Wall 4	-0.25	-0.3	-0.25	-0.3	-0.25	0.05	0.2	0.05

3.1.3 Air density

The last parameter that affects wind pressure is air density. Air density varies between about 1.1 kg/m^3 and 1.3 kg/m^3. The approximate density of air under the following properties: 20^oC, 1013.25 mbar pressure, and 50% relative humidity is 1.2 kg/m^3. This is known as the standard or typical air density (National Physical Laboratory, 2002). So, air density is dependent on air properties of temperature, humidity and pressure. For wind-induced natural ventilation in hot climate zones, indoor and outdoor air have no significant difference in their properties. It is possible therefore to assume in airflow rate calculations that air densities of inflow and outflow are nearly the same (Bahadori and Haghighat, 1985).

3.2 Prediction methods of wind-induced natural ventilation

Natural ventilation prediction is not an easy task. This is because of the complexity of its driving forces, since many parameters interact simultaneously. To overcome this problem, many methods have been developed. These methods vary in terms of accuracy, complexity, and cost. It is important to choose the appropriate method according to the project nature and budget. In fact, explanation of these methods is out of the scope of this study. However, it is useful here to demonstrate some commonly used methods. According to Liddament (1996), these methods can be divided into two main parts:

- Measurements methods: this includes many methods, like: tracer gas, pressurization, component air-tightness, flow visualisation using smoke, wind tunnels, etc. Some of these methods are full-scale ones, like tracer gas methods, and some of them are done on scaled models, like wind tunnel tests.
- Calculation methods: this includes: simplified theoretical models, Network models, Computational Fluid Dynamics (CFD), etc. Majority of these models are nowadays computer-aided, like CFD method.

3.2.1 Empirical models

These models consist of general and simplified formulas for airflow prediction. They are practical, within their limits, for airflow estimation. However, the assumptions they are based on affect their accuracy. These models are mentioned in many ventilation references, like ASHRAE (1997), and CIBSE (1988). They help designers estimate the gross airflow rate due to wind effect, temperature effect, or both of them. This requires the knowledge of the total free opening area, reference wind velocity, discharge coefficient, and pressure coefficients across the building in the case of cross ventilation. Discharge coefficient is used to correct the real free window area to its effective area, as will be discussed in Section 3.2.3. Pressure coefficient data for such problems can be obtained from the standard data, as explained in the Section 3.1.2. An example of these empirical formulas is illustrated in Table 3.3. In fact, these models are useful for single-cell enclosures, since they ignore the internal partitions. More detailed models are usually used in the prediction of airflow rate in more complicated cases, as discussed in the following sections.

Table 3.3: Empirical formula for cross ventilation rate due to wind

Source: (CIBSE, 1988).

Wind-driven ventilation strategy	Schematic	Formula
Cross ventilation	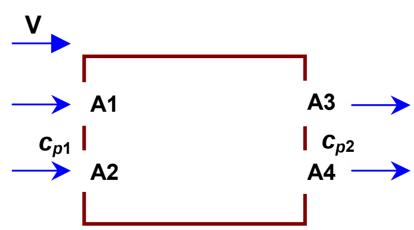	$Q_n = C_d A_n V (\Delta Cp)^{1/2}$ $\frac{1}{A_n^2} = \frac{1}{(A_1 + A_2)^2} + \frac{1}{(A_3 + A_4)^2}$ Q_n is airflow rate (m^3/s), A_n is the total free windows area (m^2), C_d is the discharge coefficient, and C_p is the pressure coefficient.

3.2.2 Wind tunnel

The wind tunnel technique is a common prediction method of natural ventilation. It is usually used to measure wind pressure distribution in buildings, presented by wind pressure coefficients, and therefore the performance of wind-driven ventilation. There are different types of wind tunnels. They are usually divided into two main parts: the high-speed and the low-speed wind tunnels. For natural ventilation studies in buildings, the second type is used, where the influence of air compressibility is negligible. Some types of wind tunnel have a combined smoke and photography facility for airflow visualization.

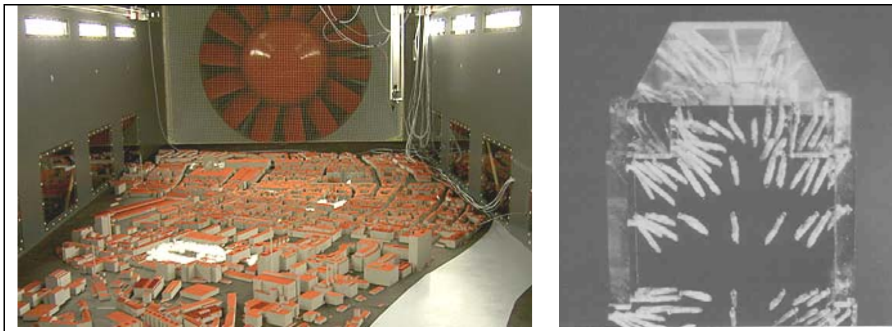

(a) (b)

Figure 3.3: Wind tunnel test, showing pressure taps on the building model

Source: a: (University of Basel, 2001. Available online: http://pages.unibas.ch/geo/mcr/Projects/BUBBLE/textpages/md_windtunnel.en.htm), b: (Liddament, 1996)

In wind tunnel tests, a scaled model of the tested building is constructed and placed on a turntable inside the tunnel, in order to consider wind direction. Then, pressure sensor taps are installed at selected points on the building, especially its openings. Pressure of the free stream wind is also measured. The obtained pressure coefficient values can then be used at mathematical natural ventilation prediction models. Reference wind speed is usually considered to be wind velocity of the free stream. It is obtained using wind tunnel adaptable fan. Also, cubic blocks are used to simulate terrain roughness. Although this method is common and useful in both ventilation design and research, it is considered to be costly and time consuming, especially for parametric studies. Also, it deals with external airflows around buildings, and does not give detailed outputs for airflow inside them.

3.2.3 Network model

This model simulates airflow paths in naturally ventilated buildings by a flow network. This network is represented by group of nodes, simulating the openings, and group of lines, simulating flow paths. Figure 3.4 shows the network of a square room with four openings. The advantage of this model is that it has more flexibility than the empirical models in considering more complicated building configurations. Therefore, it is possible to divide natural ventilation system into parts and study airflow driving force between these different parts, which leads to airflow rate estimation. It is intended to use this model in the validation study in Chapter 5. Therefore, more details about it are given below.

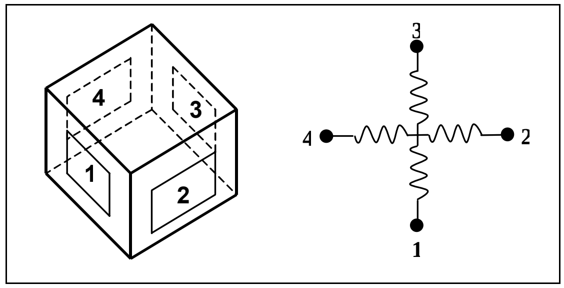

Figure 3.4: Flow network for a simple room

Assuming a building with N zones, a number of N equations should be established in the Network model. Each equation is dependant on the previous one. According to the Law of Mass Conservation, the summation of mass flows should be zero. Application of the same concept in each opening, or node, will result in a set of non-linear equations that should be solved iteratively (Santamouris, 1998). In the case of wind-induced natural ventilation, the knowledge of internal and external pressure coefficients at each opening is required to solve these equations for pressure difference across each opening. These coefficients can be obtained experimentally or from the standard pressure coefficients data, as explained in Section 3.1.2. A number of computerized Network models are also available, such as AIOLOS software, which has been developed by Allard (see: Athienitis and Santamouris, 2002).

Generally, airflow rate is in proportion to pressure difference across the opening, and in inverse proportion to any airflow resistance at any opening. This can be written as (Bahadori and Haghighat, 1985):

$$Q_n = \Delta P / R_o \qquad \textbf{(3.4)}$$

Where Q_n is airflow rate through an opening n (m^3/s), ΔP is the pressure difference across that opening (Pa), and R_o is flow resistance at the opening ($Pa.m^{-3}.s$).

R_o can be estimated from the following equation:

$$R_o = \frac{\sqrt{0.5\rho\Delta P}}{A_n C_d} \qquad \textbf{(3.5)}$$

Where, C_d is the discharge coefficient of the opening, and A_n is opening area (m^2). Substituting equation 3.5 into equation 3.4 gives:

$$Q_n = A_{eff}\sqrt{(2\Delta p / \rho)} \qquad \textbf{(3.6)}$$

Where A_{eff} is the effective area of a window. This effective area depends on the opening type, and is equal to the free opening area multiplied by its discharge coefficient. Figure 3.5 illustrates the effective area measured for different window types.

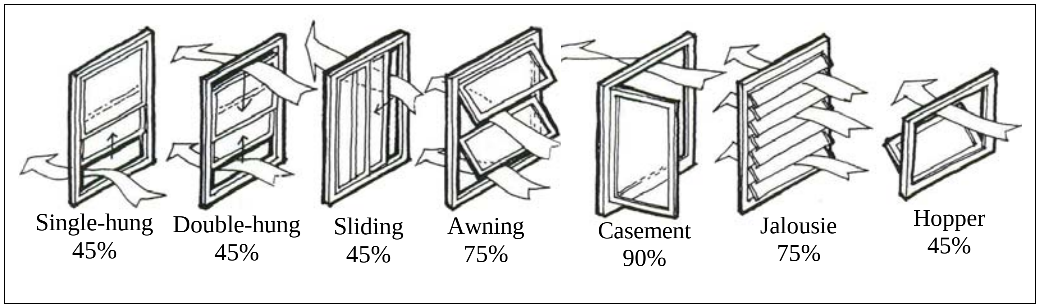

Figure 3.5: Effective area of some windows types

Source: (Moore, 1993)

Pressure difference across the opening, mentioned in the previous equation, can be estimated using the following common equation:

$$\Delta P = 0.5\ \rho V^2 \left|(C_{pn} - C_{pi})\right| \qquad \textbf{(3.7)}$$

Where, C_{pn} is pressure coefficient at opening n, and C_{pi} is pressure coefficient inside the space. This equation shows that pressure difference, and consequently ventilation rate, is highly sensitive to wind speed value. This means that any change in wind velocity will affect airflow rate more than pressure coefficient difference. If pressure difference is known, e.g. measured or modelled, then it is possible to solve equation 3.6 directly to obtain airflow rate through the opening, i.e. without using equation 3.7. Otherwise, it is essential to use equation 3.7 in order to calculate internal pressure coefficient C_{pi}, as explained below. Law of Mass Conservation states that the sum of airflow mass through N number of openings should be zero. This can be written as:

$$\sum_{N=1}^{n} Q_n = 0 \qquad \textbf{(3.8)}$$

Substituting equation 3.7 into equation 3.6 one gives:

$$Q_n = A_{eff} V \left(C_{pn} - C_{pi}\right)\left|\left(C_{pn} - C_{pi}\right)\right|^{-1/2} \qquad \textbf{(3.9)}$$

Where Q_n is positive when (C_{pn} - C_{pi}) is positive. Combining this equation with equations 3.8, results in:

$$\sum_{n=1}^{N} A_{eff} V \left(C_{pn} - C_{pi}\right) \left|\left(C_{pn} - C_{pi}\right)\right|^{-1/2} = 0 \qquad \textbf{(3.10)}$$

Therefore, it is possible to estimate internal pressure coefficient using equation 3.10 and then airflow rate using equation 3.9. However, external pressure coefficient for any opening can be obtained by many ways including wind tunnel tests. In fact, in the case of having many zones, calculation process using this model is a long process. In the case of parametric studies, any change in the design will result in repeating this process, with possibly new wind tunnel tests.

3.2.4 CFD model

Computational Fluid Dynamics (CFD) model is based on the concept of dividing the solution domain into sub-zones. Then, for each zone, the mass, momentum, and energy conservation equations are solved. This is done utilising the processing power of computers, which performs calculations more easily and, in comparison with the Network model, gives more detailed results. For example, it is possible through this method to estimate both airflow rate and heat transfer. CFD modelling was originally developed for industrial applications, but today it is used also for building applications, as shown in Figure 3.6 (Graça *et al.*, 2002). For example, CFD codes have been used to predict air jet diffusion, air velocity and temperature values, airflow patterns inside and around buildings, indoor air quality, and others more (Fluent Inc., 2004). Many softwares based on CFD codes have been developed like, Fluent, Flovent, Phoenics, and others. These softwares may have other supplementary tools for different applications, including solution mesh generation.

Nowadays, the use of (CFD) has become a standard tool in ventilation research. As described by CIBSE (1997, p.60), CFD is “a very powerful technique” in predicting air movement and characteristics. In the last two decades, extensive work has been done using CFD. Comparisons of CFD results with wind tunnel tests have been usually reported to show good agreement. However, it is recommended to validate the CFD modelling results presented in this study by another modelling or experimental method. This is recommended in order to ensure that the software, which is essential to be a sophisticated one with a variety of settings, has been implemented correctly (Oakley, 2002). In spite of being powerful in natural ventilation prediction, CFD model requires an experienced user and its relative cost still high.

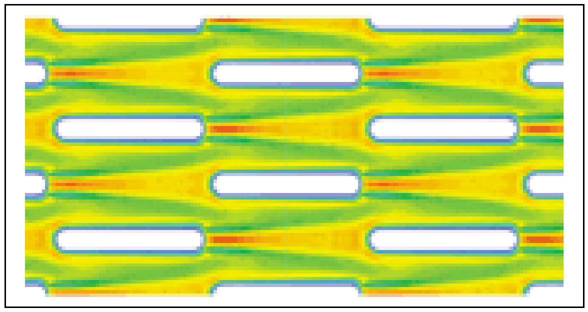

Figure 3.6: Using CFD to simulate airflow around buildings

Source: (Fluent Inc., 2004. Available online: http://www.fluent.com/solutions/hvac/index.htm)

3.3 Criteria of the adoption of airflow rate prediction model

As it is clear from the previous summarised explanation, natural ventilation prediction methods vary from simple and direct to complicated and iterative. Table 3.4 summarises the main advantages and disadvantages of these models. Choosing the appropriate model for any study depends on a balance between these advantages and disadvantages. This includes:

- Nature of the study programme.
- Nature of the required results.
- The available budget.

Table 3.4: Advantages and disadvantages of some commonly used models in natural ventilation prediction

Method	Advantages	Disadvantages
Empirical model	- Suitable for simple cases and design drafting stage. - Sets of equations, tables, and curves are ready for use.	- Assumptions they include affect their accuracy. - Limited applicability.
Wind tunnel	- Good for large-scale projects. - Gives data of pressure distribution around buildings.	- Limited outputs. - Costly and time consuming
CFD	- Powerful flow simulation tool, for both ventilation and heat transfer. - More practical for parametric studies.	- Relatively expensive tool - Requires good background to use the software correctly.
Network model	- More flexibility in system configuration than empirical models. - Calculations process is reasonable and less complicated than other models.	- Data of pressure coefficient is required prior to airflow rate calculations.

Concerning this architectural study, the use of CFD, as a main modelling tool, has been found to be more appropriate to serve its parametric methodology. It is also helpful, since this study has no access to laboratory or full-scale testing facilities. However, this requires a validation study of the implemented CFD code. Thus, the Network mathematical model will be used for this purpose. The CFD software that will be used is Fluent 5.5, which is powerful and commonly used in research. Section 3.4 provides more details about the implementation of this software for room air infiltration problems.

3.4 The use of Fluent 5.5 software for airflow modelling in buildings

CFD model has been introduced in Section 3.2.4. In this section, the implemented CFD software is explained in a detailed manner. This includes explanation of Fluent 5.5 software and its complementary software Gambit 1.3. Fluent 5.5 can be used to examine airflow characteristics in buildings. It is possible through this simulation tool to obtain many outputs of natural ventilation in buildings for any assumed reference wind velocity and direction. It is also possible to find out airflow rate through the building. Before explaining the use of this software, it is essential to introduce the Gambit 1.3 software, which is used to draw the building model and generate the calculation grid. However, more specific details related to the practical use of Fluent and Gambit programs are given in the validation study in Chapter 5.

3.4.1 Gambit software

Gambit is a pre-processor software, which facilitates the use of Fluent 5.5 software. Its CAD interface facilitates drawing two and three-dimensional building models, defining their boundary conditions, and generating the calculation mesh. This calculation mesh is exported to Fluent 5.5 software, which is mainly used as a calculation tool. These three stages are explained briefly in the following sections. Other details can be found by referring to Gambit 1.3 help menu (Fluent Inc., 1988).

A. Drawing of the building model

The Graphical User Interface (GUI) of this software is mainly a CAD interface with different commands. These commands have been set to draw the main components of the building, i.e vertices, edges, faces, and volumes. In the case of having a complicated case, it is possible to draw it in any CAD software and import it as a DXF file. It is possible to draw two-dimensional models using edges and faces, or to draw three-dimensional models using faces and volumes.

In fact, using two-dimensional modeling for room ventilation problems can give un-realistic outputs. The reason is that this method ignores some fundamental factors in determining airflow, such as airflow separation over the building sharp edges. However, this method significantly increases calculation mesh size and requires more computer memory. This stage is an important one, and requires high level of accuracy. For example, it is also important to draw the different zones of the problem in a way that facilitates the generation of the calculation mesh, as is explained in Section 5.2.2 of Chapter 5.

B. Definition of boundary and continuum conditions

This is a shared task between Fluent and Gambit programs. However, the initial definition should be done in Gambit. Considering three-dimensional modelling, the type of each entity at the external boundary of the domain should be defined. This can be pressure inlet, velocity inlet, wall, fans, voids, etc. In addition, every entity inside the domain should be defined as fluid, porous or solid. This is essential for a correct calculation process.

C. Generation of the mesh

After drawing the building model, the calculation grid is generated using the available options. The generated grid can be as fine and accurate as required, but this is limited by the factors of time and computer speed. By generating the grid, the domain representing the air is divided into small zones, faces or volumes. For these zones, calculation of the three basic conservation equations of mass, momentum and energy can be performed using Fluent 5.5 software.

Many options for mesh type are available, like regular hexahedral, tetrahedral, and hybrid. Mesh type does not affect calculation process, but it gives flexibility to find an appropriate mesh for different building forms. It is important to ensure that mesh quality is acceptable. Gambit provides many methods for mesh quality specifications. This includes: aspect ratio, diagonal ratio, and mesh skew. Once the mesh is ready, it can be exported to Fluent 5.5 program in order to perform the calculations, which may take several hours depending on the size and complexity of each individual case.

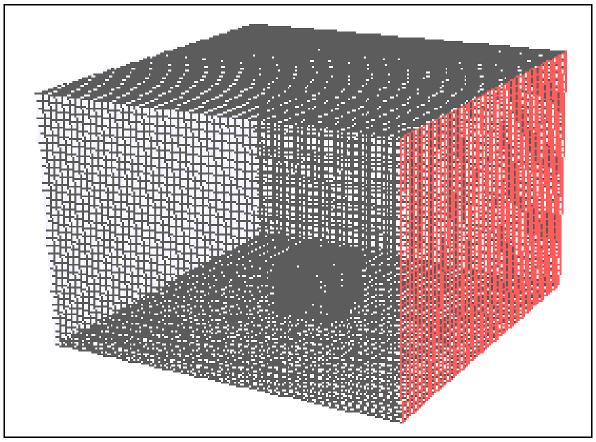

Figure 3.7: The use of quad-map mesh

3.4.2 Fluent 5.5 software

Fluent 5.5 is introduced here, with a focus on the settings that are relevant to this study. This is mainly obtained from Fluent 5.5 help menu (Fluent Inc., 1998). It is important to point out that further discussions on specific applications of this software will be raised wherever required during explanation of the empirical study. It is possible using Fluent 5.5 software to simulate airflow under the influence of various parameters, such as air velocity, location and size of openings, etc. However, it is crucial to define the program settings correctly, which requires a good background about the software. Some relevant software settings here are:

A. Turbulence model

Most airflow problems in buildings consider airflow to be turbulent. Thus, a correct definition of turbulent model is required to solve the transport equations. Awbi (2003) gave an overview of many turbulence models in use for CFD applications. He claimed that due to the complex nature of airflows in buildings, there is no single model that is ideal in all situations, except of the Direct Numerical Solution, which is out of reach of most users because of the high computer capacity it requires. However, the standard k-ε model is believed to be the most used and developed turbulence model. This model is most likely to predict reasonable results for airflow studies in buildings.

k-ε model is described as a semi-empirical model based on model transport equations for the turbulent kinetic energy (k), and its dissipation rate (ε). In the derivation of this model, the flow is assumed to be fully turbulent. In the transport equation of the turbulent kinetic energy, both mean velocity gradient and buoyancy effects are considered. The results of the two transport equations of this model are eventually combined to compute the turbulent viscosity. In the standard k-ε viscous model panel, illustrated in Figure 3.8, many constant parameters are used to control the solution. These constants have been determined experimentally for air and water and are most widely accepted.

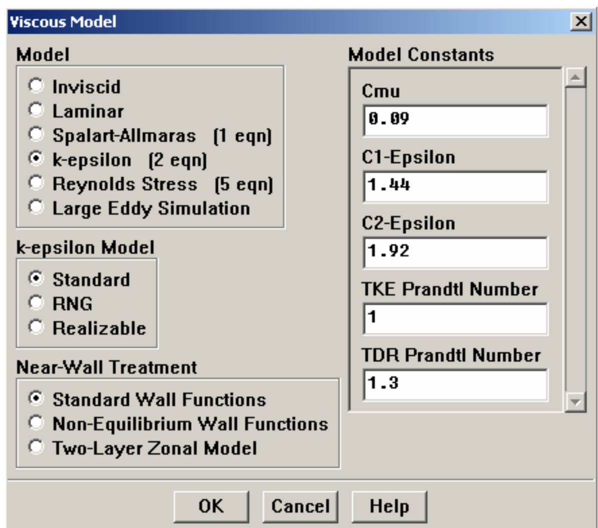

Figure 3.8: Viscous model panel in Fluent 5.5 software, showing the Standard k-ε model activated

B. Solver definition

Solver is defined using the Solver panel, shown below. This panel consists of many fields to specify three things: the solution method to be used in the calculation process, the dimensionality nature of the solution domain, and whether the flow is steady or unsteady. Segregated solver has been used in previous versions of Fluent and still widely used in CFD modelling. In this solver, the fundamental equations are solved sequentially or segregated from each other in the iteration loop. The solution reaches the end when the convergence criteria are met.

The Coupled solver enables a coupled solution algorithm. Time section has two options for the solution: steady and unsteady. Velocity Formulation section allows the user to specify whether the velocity is absolute, which is recommended for not-rotating fluids, or relative. In this study, all calculation will be done using the absolute velocity, and in the steady state.

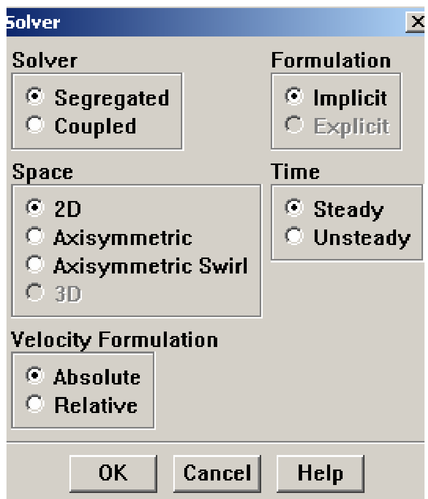

Figure 3.9: Solver panel in Fluent 5.5 software, showing Segregated solver activated

Source: (Fluent Inc., 1998)

C. Definition of boundary conditions

Boundary conditions specify different variables on the boundaries of a modelling case. In Fluent 5.5, boundary conditions should be initially defined in Gambit software, as explained in Section 3.4.1 (B). Then, the relevant settings in Fluent 5.5 software can be completed, so that the solution will be ready for processing. In the case shown below, air velocity is estimated in a room with an inlet and outlet. To do so, the inlet should be initially defined in Gambit as a velocity inlet, then the relevant settings can be completed in Fluent software as shown in Figure 3.10.

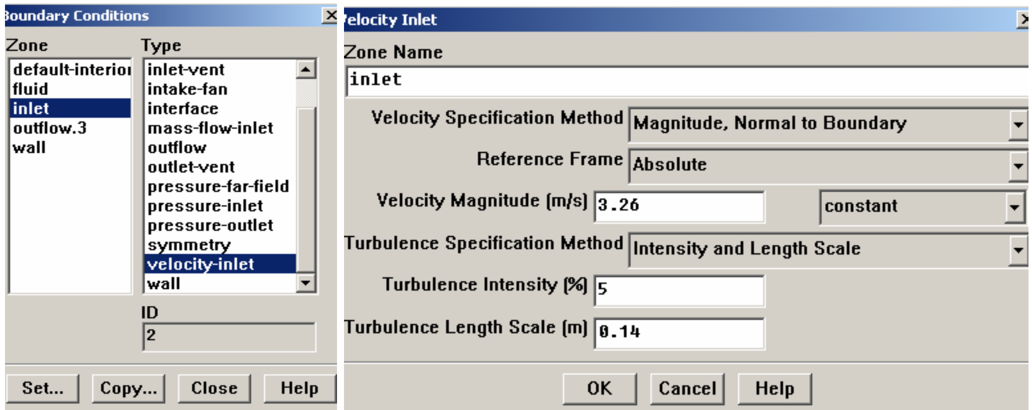

Figure 3.10: Boundary Conditions panel and Velocity Inlet Panel in Fluent 5.5 software

For the Segregated solver, the inputs for a velocity inlet boundary are: wind velocity magnitude and direction or velocity components, temperature (if energy model is enabled), and the turbulence parameters. If the Velocity Specification Method is set to be Normal to the Boundary, then it is only required to define the velocity magnitude. If it is set to the Magnitude and Direction option, then it is required to enter the magnitude of the velocity vector and the direction of the vector. Positive or negative sign for x, y, and z velocities indicate flow in the positive or negative x, y, and z directions. In three-dimensional modelling, it is possible to rotate the whole building inside the solution domain in order to simulate wind direction.

In room airflow problems, it is possible to use Intensity and Length Scale option to specify the turbulence parameters. Turbulence intensity is the ratio of the root-mean-square of the velocity fluctuations to the mean flow velocity. Its value varies depending on these two factors. Generally, turbulence intensity of 1% or less is considered low, while turbulence intensity greater than 10% is considered high. The turbulence length scale is related to the size of the inlet. This can be approximately estimated by multiplying the inlet height by a constant equals to 0.07.

D. Energy settings

Wind-induced ventilation is believed to be obviously more effective in hot climates, when compared with stack-induced one. This is because of the relatively lower temperature difference between indoor and outdoor temperatures, which is main factor affecting stack ventilation (Chow, 2004). Therefore, energy option is normally set off in wind-induced ventilation cases. If the energy option is enabled, more accurate results can be obtained. However, this will increase the time required for the solution to converge.

D. Residual monitors

By completing all the relevant settings, Fluent starts to perform the calculations in an iterative manner until a sufficient error tolerance, defined by the user, is achieved. This means that solution will converge after the achievement of that minimum error. Generally, calculation time will increase when a smaller error is defined.

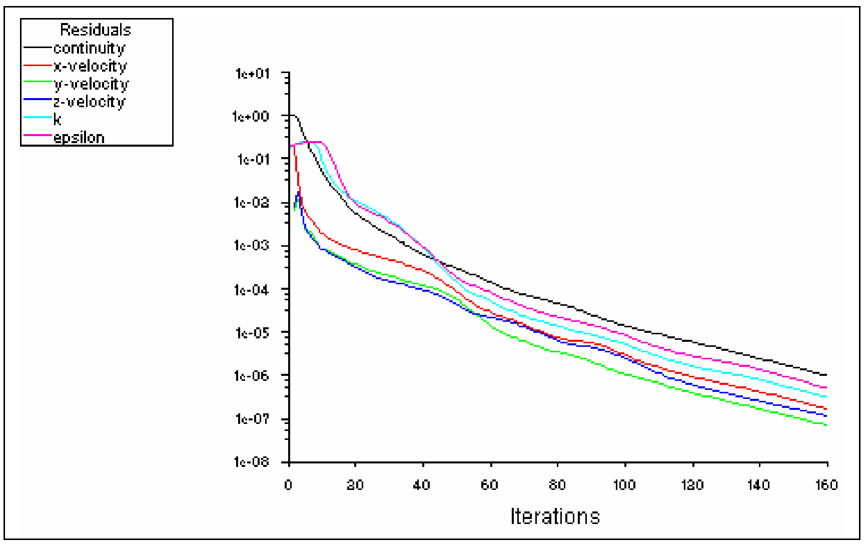

Figure 3.11: Example of residuals monitoring plot of a converged solution

G. Modelling outputs

Many outputs in different presentation methods can be obtained from Fluent 5.5 software. Various examples of these outputs can be found in the empirical study, namely Chapters 5 to 8. This includes:

- Contours of different parameters: like velocity, pressure, and turbulence. In case of three-dimensional models, the contours can be displayed on different sectional planes defined by the user.
- Velocity vectors: this show velocity direction in addition to its magnitude.
- Flux Report: this option helps the user compute the following parameters for a specified boundary zone: the mass flow rate, heat transfer rate, and radiation heat transfer rate.

- Animation: this option allows the user to specify key frames to define movement of an animated sequence. This option is useful in many cases like smoke spread modelling.

3.5 Conclusions

This chapter has presented some common methods that are used in natural ventilation prediction. This has been introduced by an explanation of wind pressure on buildings. It has been found that wind pressure, and accordingly air flow rate, is highly dependant on wind speed. This is because wind pressure is in proportion to the square of wind speed. Two more factors are considered in the pressure coefficient, which are wind direction, and building shape, materials, and surroundings. Therefore, these three parameters are important to be considered in the empirical study. Designers usually use official standards and buildings regulations for natural ventilation design, where simplified methods are usually applied. However, and for research purpose, the use of more detailed models is required.

Providing the advantages and disadvantages of some common models, CFD model has been chosen for this study. This is intended to facilitate the parametric study, and to cope with the available research facilities. Therefore, a further investigation of the CFD model has been carried out. It has been found that the studies CFD software, which is Fluent 5.5, has a wide variety of applications, including air infiltration. Therefore, a good background knowledge about the relevant software code is essential. In addition, this code should be validated prior to the modelling study. This is discussed in Chapter 5 of this study.

CHAPTER 4 : UTILISATION OF CURVED ROOFS AND TOWERS AS WIND-INDUCING ELEMENTS IN BUILDINGS

Introduction

The last two chapters have illustrated many concepts and applications related to natural ventilation in buildings. This is in addition to the prediction methods used to evaluate natural ventilation performance in buildings. This chapter serves as an essential architectural background to the empirical study. It aims to demonstrate the potential application of natural ventilation in buildings incorporating the targeted architectural elements in this study, i.e. domed and vaulted roofs, and towers. This is introduced by a brief illustration of the architectural relationship between these elements, and the need to re-introduce them.

To do so, the factors that affect the application of natural ventilation in buildings have been analysed, with reference to the case of curved roofs and towers. Firstly, the urban factors have been illustrated briefly. After that, the architectural factors related to the dome, vault and tower have been discussed. This includes a historical background, the operation mechanism of these elements for natural ventilation, in addition to some relevant background studies.

4.1 Dome, vault and tower in architecture

Domes and vaults are common roofing elements in the vernacular architecture of the Middle East. They have been used together in many types of buildings, and in different regions for many centuries. In many cases, tower is used with these curved roofs in a unique architectural scene. For example, Escring (1998) has highlighted the role of dome and tower in the architecture of the Mediterranean region. Escring mentioned that almost every city with a modern or ancient architecture is characterised by the use of this architectural couple. In addition to this, architects have commonly used vaulted roofs. This was a response to a functional need of roofing elements, and developed nowadays to have an additional dimension of symbolism. Nowadays, the architectural elements of dome, vault, and tower can be found in many types of buildings, like: residential, religious, and cultural buildings.

From an environmental point of view, the important role of these elements in formulating the architectural style of the place of their existence can also be utilised to serve the applications of sustainable architecture. This is expected to increase public awareness to the importance of such applications and encourage further use of them. On the other hand, this will directly contribute to the energy savings need, which increases their symbolic value.

Figure 4.1: Curved roofs and towers have been used together in the architecture of the Middle East

Source: a to d: (ArchNet, no date. Available online: http://archnet.org), f & g: (Steele, 1997)

In fact, the symbolic use of these elements in the contemporary architecture has raised an argument on their necessity. For example, and according to Holod and Khan (1997), dome and minaret (tower) in mosque architecture have been considered as optional design elements in the architectural school of modernism. The opposite opinion can be found in the vernacularism school. However, re-introducing these elements in a contemporary architectural frame is suggested in the post-modernism school.

This school aims to link the contemporary designs with the historical models in order to maintain a continuity in the architectural history. As shown in Figure 4.1, the contemporary use of curved roofs and towers features a variety of ideas, which combine between the use of traditional architectural elements and contemporary materials and construction methods. Whatever the case is, this argument will have an additional dimension when it is handled from an environmental point of view. For that reason, it is required that such architectural elements should be seen in a more modern perspective. This is necessary in order to give their existence in the contemporary context a real function, beside the role of inspiration and heritage linkage.

One of the common historical applications of curved roofs and towers in this regard is natural ventilation. Many studies have focused on the utilisation of these elements as wind-inducing devices, as will be discussed in Sections 4.3 and 4.4. However, the main aim of this study is to investigate the integration and combination of both curved roofs and towers in order to improve natural ventilation performance in buildings, and give more value to the architectural relationship between these two elements, as discussed above.

4.2 Factors affecting the use of curved roofs and towers for natural ventilation in buildings

One of the main tasks in any building design is to plan an effective natural ventilation system. This requires a series of investigations of the different interacting factors, and considers some helpful rules of thumb. As a result, it will be possible to establish a systematic approach in investigating the role of curved roofs and towers in natural ventilation. Figure 4.2 summarises this approach. Although it seems sometimes that some of the related factors are interacting, separating them serves the need for a systematic analysis. In fact, it is not an easy task to explain all of these factors in a detailed manner here. However, some of the relevant factors will be addressed in a summarised manner.

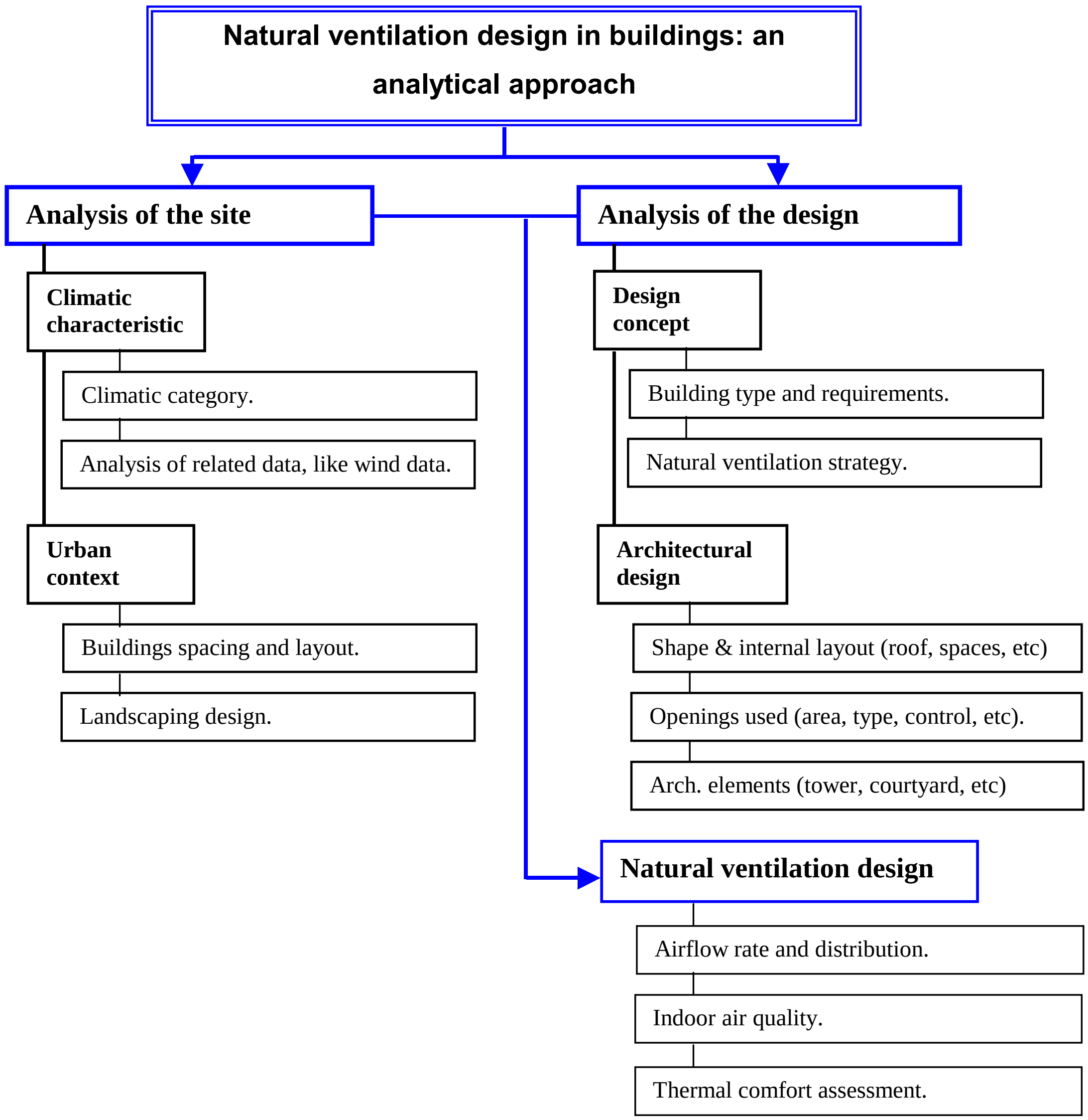

Figure 4.2: Factors affecting natural ventilation design in buildings

4.2.1 Analysis of building site

Two main issues can be addressed here:

A. Climatic characteristics

In order to plan an effective natural ventilation system, it is required to analyse the relevant climatic data, like wind speed and direction, and both indoor and outdoor air temperatures. Nature of data required depends mainly on the mathematical model used in the design. It also depends on the dominant driving force of natural ventilation. This driving force, as discussed in Section 2.5, can be either pressure or temperature difference, or a combination of both of them. Also, and in an advanced stage of the design, it depends on the thermal comfort model used.

There are many climatic zones in the world and different methods of classification. One of the most widely used climate classification systems is Koeppen System. In this system, each climatic zone is defined according to a combination of the annual and monthly average temperature and precipitation, and the distribution of natural vegetation within that zone. Two relevant climatic categories can be distinguished in the study zone, i.e. the Middle East. These categories are:

- *Hot-humid climate*

This zone is known for its high temperatures and large amount of rain all year round. It has an average temperature of 18 °C or higher (Wikipedia, 2006b). One of the main environmental design principles in this climatic zone is to maximise ventilation rates in order to increase the effectiveness of sweat evaporation, and therefore reduce internal temperature (Marsh, 1998b). This is why buildings located in this climatic zone are characterised by the use of large openings.

- *Hot-dry climate*

This zone is known for its little rain and low humidity levels. Also, it is known for its large daily temperature range between day and night (Marsh, 1998b). Therefore, direct natural ventilation is usually not enough. Air should be cooled down before admitted into the space in order to adapt the outdoor temperature swing. A common strategy here is the use of evaporative cooling. Another strategy is the use of building materials with high thermal capacity in order to benefit from night-time ventilation in cooling down the structure, as explained in Section 2.6.3. This cools down the air when becomes in contact with it at daytime.

B. Urban context

Urban planning has a direct effect on airflow behaviour around buildings. For example, wind speed, which is the main climatic parameter in the case of wind-induced ventilation, increases when building height increases. This consequently results in higher flow rates in the building. Also, wind speed is highly affected by the surrounding buildings or landscaping. In high urban densities, wind speed at street level is less than that of the free stream. This makes the use of roof-level openings, including domes, vaults, and wind catchers, more effective for natural ventilation. This issue has also been discussed numerically in Section 3.1.1.

4.2.2 Analysis of building design

Two main issues can be addressed here:

A. Design concept

To increase the efficiency of natural ventilation as a passive cooling technique, it is important to initially plan the design itself for that cause. This includes planning for an effective natural ventilation strategy. In the case of wind-induced natural ventilation, this should be intended to achieve sufficient air exchange between outdoor and indoor zones. This can be achieved by creating airflow paths to reduce internal air temperature and improve thermal comfort conditions. This also helps maintaining an acceptable indoor air quality.

However, provision of an appropriate airflow rate should be controlled to avoid any adverse effect like undesired draughts. For example, and according to ASHRAE standards, ventilation rate for domestic and office buildings should not exceed 0.75 to 1 air change per hour. Ventilation rate above this limit will cause discomfort (Goulding *et al.*, 1992).

B. Architectural design

After having sufficient data related to the site and the design requirements, the detailed design process starts. Many factors here can affect natural ventilation. This includes:

- Building layout: i.e. number of zones, height of the building, etc.
- Openings used: window type and area, control system, etc.
- Architectural elements used, and how they can be utilised for natural ventilation: for example: wind towers, courtyards, wall fins, etc.

The last point is much related to the modelling study. Thus, the following two sections give more details about the use of curved roofs and towers for natural ventilation in buildings. This includes a historical background about their architecture, the physical mechanism of their utilisation for natural ventilation, and the architectural factors that affect that use.

4.3 The use of curved roofs for natural ventilation

Curved roofs, namely domes and vaults, are widely used in many types of buildings. However, few studies of their use for natural ventilation could be found. The following review discusses this use through the following axes:

4.3.1 Historical background

Historically, dome and vaults are amongst the oldest roofing forms that have been used since the earliest times. Domed and vaulted roofs have been used in many civilizations including the Roman, Greece, Byzantine, in addition to the contemporary architecture (Gympel, 1996). They have been considered efficient shapes for covering large spans. In some areas, like Iran, this was possibly a result of the shortage of tember, which has been used in other areas to construct flat roofs (Bahadori and Haghighat, 1985).

According to Statham (1927, p.186 & 201), dome is “a built roof circular in plan and either semicircular or in some other arch shape in section”, and vault is “any solidly built arched roof over a building, with the exception of a dome, which is in fact a form of vault, but not generally called by that name”. In other words, if an arch is rotated in three dimensions about its centre, this will generate a dome. If this arch is arrayed along a straight axis, this will generate a vault.

Domes have been used in historical architecture in different styles. The simplest shape of the dome is the hemispherical one. The onion dome possesses a shape that has more than a half sphere. This may also be pointed at the top. Another form is the saucer dome, or a low dome, which possesses a shape that has less than a half sphere. A melon, or an umbrella dome, is a dome divided by radiating ribs into sections or gores. Unlike vaulted roofs, the resulting space bellow a domed roof does not possess straight sides, which obstructs dividing the space enclosed by the dome.

To overcome this problem, Byzantine architects used the curved triangle-shaped spherical segments, known as the pendentives. This has facilitated the transition from square to circular shape. Concerning dome size, it was related to the available building materials and construction methods. The earliest domes were smaller than the subsequent ones. The largest Roman dome is the Pantheon, which has a span of this dome is 43.4 m (Roth, 1998).

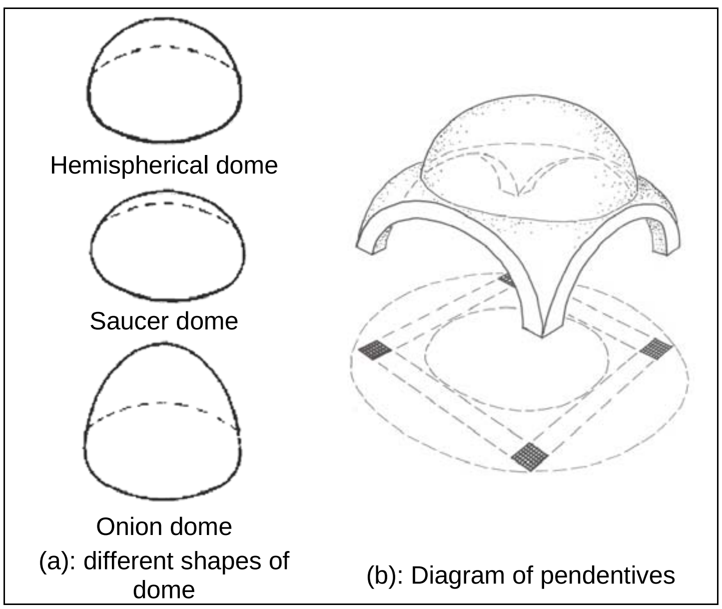

Figure 4.3: Different shapes of domes, and the use of pendentives

Source: a: (Elseragy, 2003), b: (Roth, 1998)

Vaults have been used in different shapes in historical architecture as well. According to Roth (1998), the simplest form of vaults is known as the barrel or tunnel vault. This is simply a half cylinder. When two tunnel vaults intersect in a right angle, the resulting vault is known as the groin vault. If the tunnel vault is curved into a circle, the resulting vault is known as the annular vault. Another form is the rib vault, which is a variation on the tunnel vault. The difference here is a structural one, where vault surface is divided into webs separated by arch ribs, which form the real construction. After that, the intervening spaces are filled in with lighter masonry supported by the ribs, which reduces the weight of the structure. Barrel vaults can have steeper or flatter profiles, which creates the segmental or catenary vaults, respectively (Elseragy, 2003).

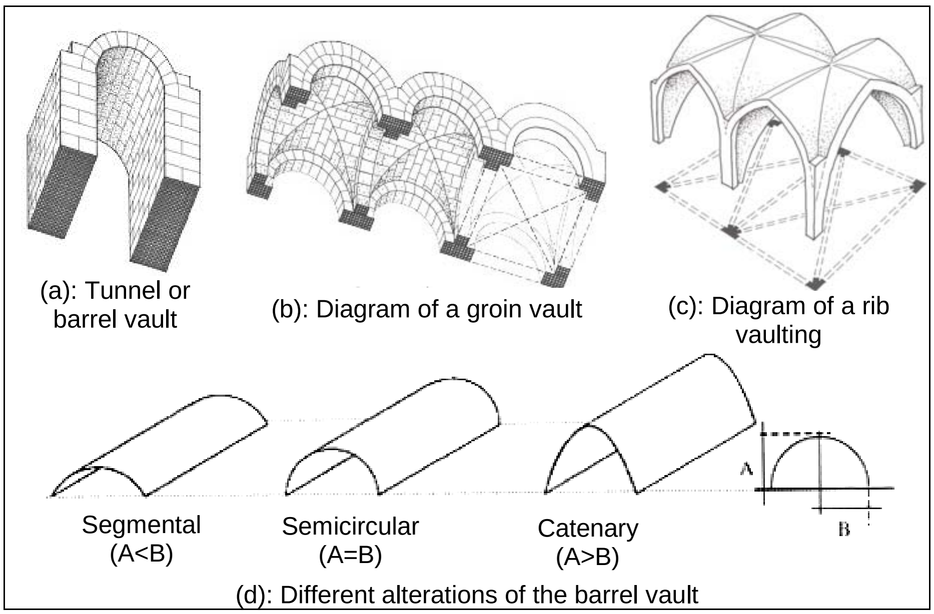

Figure 4.4: Different shapes of vaults

Source: a to c: (Roth, 1998), d: (Elseragy, 2003)

4.3.2 Operation concept

Before explaining the use of curved roofs for natural ventilation, it is useful to consider some of their environmental advantages. Curved roofs helps energy savings for cooling due to the fact that they have no corners, where heat is likely to be trapped. This encourages the natural circulation of internal air. Another benefit is saving in building materials. For example, dome has approximately one-third less surface area when compared to a box-style building (Fearnley, 2002). Elseragy (2003) compared solar behaviour of flat, vaulted, and domed roofs in different aspect ratios and orientations. Elseragy found that the use of hemispherical and pointed domes is helpful to reduce the received solar radiation in summer, compared to an equivalent flat roof, by about 70% and 50%, respectively. However, little effect has been recorded in the case of the saucer dome. This is also true in the case of semicircular, pointed, and segmental vaulted roofs in different orientations.

Concerning natural ventilation, Bahadori and Haghighat (1985) pointed out that domed roofs have been found to increase airflow rate due to wind effect, when compared with flat roofs. According to Bahadori (see: Bensalem, 1991), vaulted roofs have the same advantage. This is due to the similarity in natural ventilation operation concept, as explained below, especially when vaulted roofs are built with their long axis perpendicular to the prevailing wind. The use of curved roofs for natural ventilation is useful for both wind-induced and thermal-induced natural ventilation strategies. This is, on one hand, because curved roofs reformulate pressure zones around buildings, and encourages suction ventilation. On the other hand, their height allows the utilisation of stack effect to encourage vertical air movement.

As a general observation, roofs of buildings are the elements that are subjected to the highest suction (Sachs, 1978). This has attracted the interest of researchers in many studies. The main advantage of the use of curved roofs for natural ventilation is that air velocity increases as wind passes over the dome and around its base, and over the vault. This is true when air passes over a dome from any direction and, ideally, when wind direction is perpendicular to vault long axis. In the case of dome, this increase occurs at its apex and around its drum, or base. In the case of vault, this increase occurs along the top, or peak, of the vault. This increase in air velocity causes a reduction in its pressure. In other words, kinetic energy of the air will increase at the account of pressure energy. This increases the potential of the curved roofs for encouraging suction ventilation (Priolo, 1998).

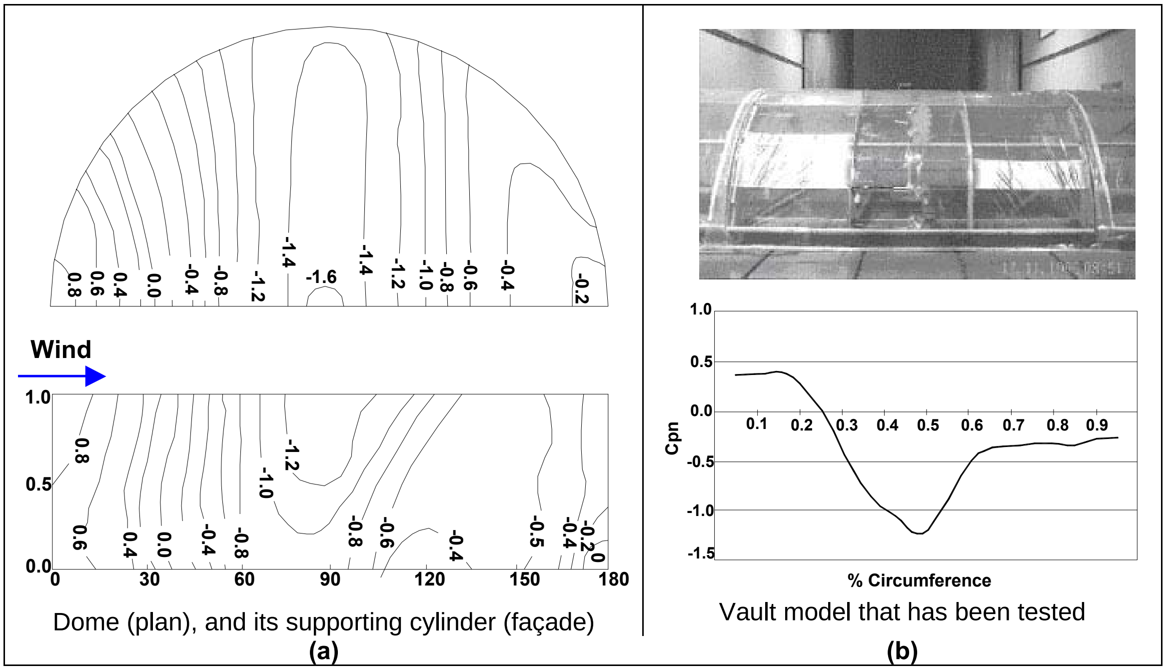

Dome (plan), and its supporting cylinder (façade)
(a)

Vault model that has been tested
(b)

Figure 4.5: Pressure distribution over domes and vaults

Source: a: (Scruton, 1981), b: (Robertson *et al.*, 2002).

Figure 4.5 illustrates pressure distribution for a hemispherical dome and its drum, and for a vaulted roof, subjected to a normal wind. In the case of the dome, it is clear that pressure coefficient value is negative at the top of the dome and its leeward. The maximum value is recorded in the apex (-1.6). In the dome base or drum, the maximum value is recorded in the middle (-1.2). In the case of the vaulted roof, pressure coefficient value is positive in the vault windward, then it converts to minus nearly at 25% of the vault circumference before it reaches its peak (about –1.2) at the top.

4.3.3 Architectural factors

It is common practice in research to investigate the effect of different architectural design parameters on building environmental performance. For example, Kindangen *et al.* (1997) performed a CFD analysis of ten roof shapes to study their impact on wind-induced natural ventilation. The methodology adopted in this study has the advantage of dealing with many interdependent parameters, like wind direction, roof shape, overhangs and building height.

To establish the comparison between different roof shapes, a basic model with fixed dimensions was assumed and modeled in Fluent 4 software. The interacting parameters were examined in turn, so that while examining a specific parameter, all other ones are assumed constants. Although wind and stack effect are acting together in the real cases, this study has focussed only on the wind-induced ventilation. Considering the case of curved roofs, many architectural parameters affect building natural ventilation performance as well. This includes:

A. Shape of the roof

The historical shapes of domes and vaults have been discussed in Section 4.3.1. Nowadays, domes and vaults can be integrated with different roof shapes, like flat and pitched roofs. It is possible also using the advanced construction methods to build them in larger spans and different designs and materials, including steel, concrete, and glass.

As mentioned by Yaghobi (1991), dome has a larger wind shadow area when compared with flat roofs. This is also true in the case of vaulted roofs. This limits heat transfer between hot outdoor air and building envelope, and reduce heat gains in hot climates. This is due to the curvature of the roof, so that wind passes over it with less resistance. Yaghobi carried out this investigation using simple models in a low speed wind tunnel. Several features of the airflow, such as flow separation, wind shadow area, turbulence, and flow circulation, were visualised by smoke flows.

In terms of the span and aspect ratio of the curved roofs, the author could not find any specific architectural guidelines, except of the applications of proportion and visual stability of the design. However, it is a common practice in research to carry out numerical analyses of buildings environmental performance in order to produce such guidelines. For example, the work of Elseragy (2003) is a good example in this regard, as has been explained in Section 4.3.2.

Another example is the work of Walker *et al.* (1993a). This work has reviewed natural ventilation in courtyards. Walker claimed that aerodynamics has a fundamental impact on the design of courtyards, and not only day lighting as mentioned in building regulations of the UK. For example, these regulations stipulate that the height of the wall above an opening in a closed courtyard shall be less than twice the distance to the facing wall. However, and using CFD modeling, the study concluded that a minimum courtyard area of 1 m^2 per 50 m^2 of the habitable building floor area should be maintained to ensure an effective natural ventilation in the courtyard.

B. Location of the openings

Roof-level openings at domed and vaulted roofs can have several configurations, as discussed below:

- *Domed roofs*

The historical review carried out for the traditional domed roofs showed that openings can be created at dome apex or drum, which is “the circular wall over which the dome is raised” (Statham, 1927, p.186). Bahadori and Haghighat (1985) openings at dome apex encourage suction forces acting over the dome. This in turn encourages airflow circulation inside the building, and increases airflow rate compared to flat roofs. The advantage of domed roofs here is that they are independent of wind direction. The Network mathematical model was adopted by Bahadori & Haghighat to estimate flow rates through the dome due to the wind, and employing domed roof. The Network model established was for a room with four openings in its wall and one opening in the apex of its domed roof. Pressure coefficients were obtained from a previous wind tunnel study.

Therefore, it was possible to carry out a comparison between domed and flat roofs in terms of airflow rate, considering different wind directions and speeds. The study considered two cases: when the building is wind-shaded and not wind-shaded. Also, it examined different windows arrangements. The main conclusion was that domed roofs, with opening in the dome apex, always increase airflow rate through buildings, especially when all openings are located in one wall.

Airflow rate estimation did not consider the stack effect, since it is limited in low-rise buildings and hot climates. In Herat, Afghanistan, another configuration is used, where a cap covers the apex opening. This cap is designed as a square scoop to catch the air, and admit it inside the dome. This is an interesting system, since it utilises the dome as air-catching device (Hallet, 1980).

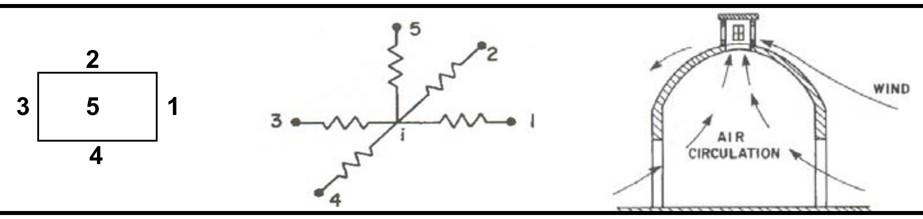

Opening distribution		Not wind-shaded			Wind-shaded		
Opening no.	Opening area	Flat roof	Domed roof	Increase in ventilation (%)	Flat roof	Domed roof	Increase in ventilation (%)
1	1	93	100	7.5	39.5	45	13.9
2	1						
3	1						
4	1						
1	2	82.75	139.5	69.6	37.7	52.8	39.9
2	0						
3	2						
4	0						
1	2	61.1	86.4	41.4	37	55	48.6
2	0						
3	0						
4	2						
1	4	0	44.9	∞	0	34.8	∞
2	0						
3	0						
4	0						

Flow rates are in m^3h^{-1}/m^2 of floor area. Opening area is presented as % of floor area

Figure 4.6: Average ventilation recorded in Bahadori & Haghighat's study with flat and domed roofs at a reference wind velocity of 5 m/s

Source: (Bahadori and Haghighat, 1985).

The other case is to place openings at dome nick, or drum, which is very common in the contemporary architecture due to the development of structural systems. Openings here are used also for day lighting for the central zone of the building. However, the author could not find any detailed study examining this configuration in terms of natural ventilation. The early findings of this study indicated that this kind of openings does not seem to work in cross ventilation mode as may be presumed. However, it works in the suction mode, depending on the same concept explained in the case of using dome apex. This is a subject of a further investigation in this study in order to interpret the different phenomena related to this airflow behaviour, as will be explained in Chapter 6.

- *Vaulted roofs*

The historical review carried out for the traditional vaulted roofs showed that openings are not created at the vault itself. Instead, they are usually created in the front wall built directly under the vault. This is because this wall, unlike the literal walls, has no structural role. This is true in the case of the barrel vault, see Figure 4.5. Sometimes, the entire face of the vault is utilised as an opening, but filled in using brick with large openings to secure both privacy and ventilation at the same time. In the case of the groin vault, where two or more vaults intersect at right angle, it is possible to utilise the front faces of the intersecting vaults as openings for the main intersected vault. If both vaults intersect in the same level, it is possible to integrate a dome in the middle, in which openings can be utilised.

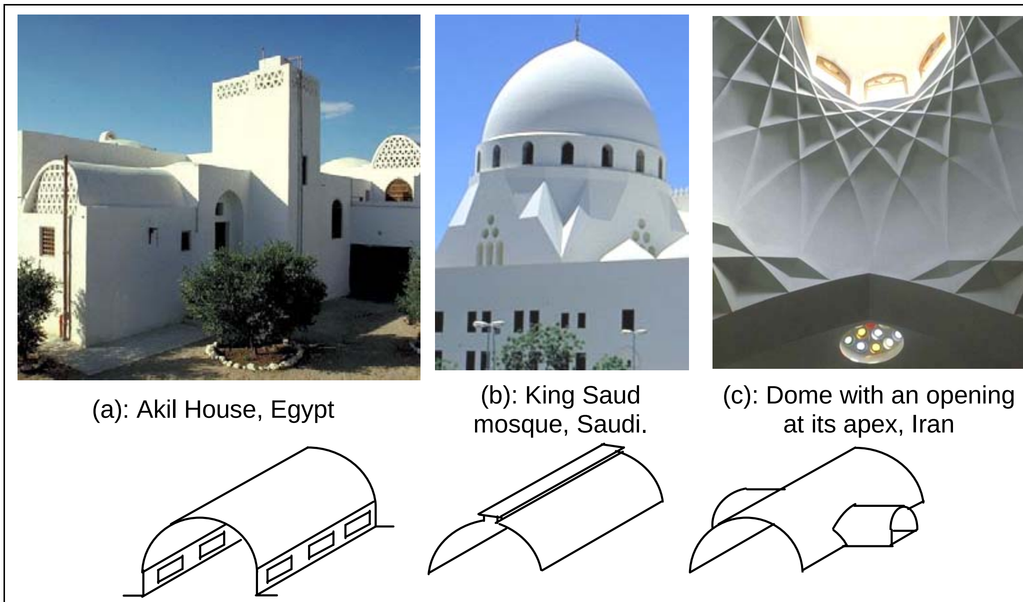

(a): Akil House, Egypt

(b): King Saud mosque, Saudi.

(c): Dome with an opening at its apex, Iran

(d): Different configurations to provide vaulted roofs with openings

Figure 4.7: Different configurations of openings are used at domed and vaulted roofs

Source: a to c: (ArchNet, no date. Available online: http://archnet.org)

The use of the rib vault facilitates creating openings at the vault body. This is because the structural part is the arch ribs, while the intervening spaces are only fillings supported by the ribs. Nevertheless, it is possible using the contemporary construction methods and materials to create openings at the top of the vault or at its literal walls in order to facilitate the suction ventilation as explained in Section 4.3.2.

4.4 The use of towers for natural ventilation

The use of the architectural element of tower as a wind tower or catcher is a common practice in architecture. A typical wind tower or catcher is mainly a chimney that is opened from its top to the outdoor air, and from the bottom to building interior (Bahadori, see: Bensalem, 1991). Towers can be built initially for natural ventilation, or reused for this purpose. For example, Bahadori (1994) recalled the attention to reuse the existing towers for passive cooling application. Wind towers and catchers are one of the unique architectural elements that have been used for natural ventilation in both vernacular and contemporary architecture. Thus, they have attracted the attention of many researches and architects for their performance analysis, improvement, and reuse. This is well reviewed in many studies. This includes the works of Al-Koheji (2003), Al-Qahtani (2000), Fariga (1997), Bahadori (1994 and 1985), and Yaghobi *et al.* (1991).

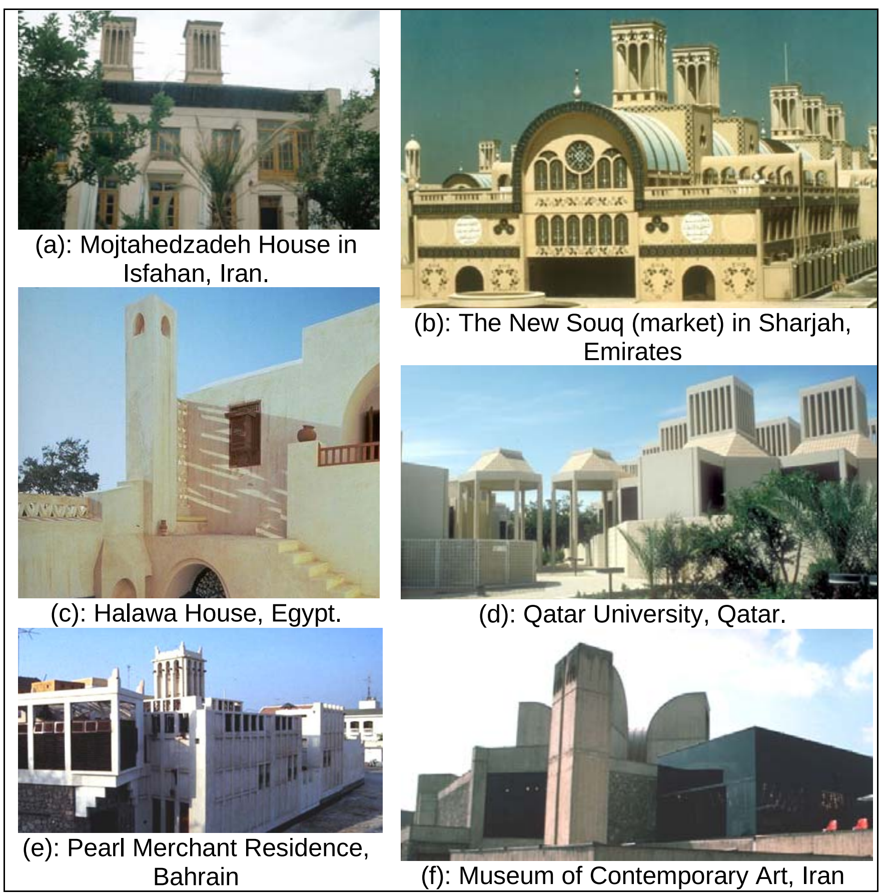

(a): Mojtahedzadeh House in Isfahan, Iran.
(b): The New Souq (market) in Sharjah, Emirates
(c): Halawa House, Egypt.
(d): Qatar University, Qatar.
(e): Pearl Merchant Residence, Bahrain
(f): Museum of Contemporary Art, Iran

Figure 4.8: The use of wind towers and catchers in different buildings types

Source: (ArchNet, no date. Available online: http://archnet.org)

4.4.1 Historical background

Wind towers and catchers have been used in the Middle East for many centuries for buildings passive cooling at both hot arid and humid climates. This is not limited to the residential buildings, but included some other building types. Some of the designs have utilised the new building materials and methods, while others have implemented the same traditional methods, like works of the Egyptian architect Hassan Fathy. In fact, reviewing the historical use of wind towers and catchers is important. This is because researchers in the field of sustainable design unanimously stated that vernacular architecture has shown a high sensitivity to human thermal comfort requirements (Farija, 1997).

Nowadays, development of structural systems and materials has given architects a wider margin to introduce an innovative ideas for tower design. Many contemporary designs over the world became landmarks of their place of existence. Tower can be utilized for natural ventilation, as a wind tower or catcher. Generally, the difference between them is that wind tower is multidirectional, while wind catcher is unidirectional. This means that the first one has many openings facing different wind directions, while the second one has only one opening. This will be discussed in Section 4.4.2. The following explanation summarises a historical background of the use of wind towers and catchers for natural ventilation.

A. Wind towers

Many examples of wind towers can be found in many countries in the Middle East. Some of them are:

- *Wind towers of Iran*

Wind towers are commonly used in Iran. For example, Yazd city in Iran is known as the city of wind catchers. Roaf (see: Al-Koheji, 2003) documented many wind tower forms used in this city, including square, rectangular, hexagonal, heptagonal, octagonal, and the rounded form. Figure 4.9 illustrates a cross section of a typical conventional Iranian wind tower, or Baud-Geer, as it is known in that area. Bahadori (1994) described this conventional design as a masonry-type square structure designed to catch and cool down the high-level ambient wind from any opening of the four openings provided at the top, depending on wind direction. Openings height starts from 2 m up to 20 m above the roof level. Airflow passage in the tower is divided into four parts.

As the difference in between day and night air temperature is considerable in the hot-arid climate of Iran, the use of night ventilation strategy has been found to be useful. However, Bahadori listed some disadvantages of this conventional design. This includes:

- Dust and insects can enter the building through the tower.
- Part of the admitted air, with a positive pressure coefficient, can leave the tower through other openings of the tower, which have less pressure coefficient.
- Thermal capacity of the tower is not enough to significantly reduce air temperature.

(a): A conventional wind tower in Iran

(b): A conventional wind tower in Bahrain.

Figure 4.9: Vernacular designs on wind towers

Source: a: (ArchNet, no date. Available online: http://archnet.org), b: (Al-Koheji, 2003)

- *Wind towers of the Arabian Gulf*

Al-Koheji (2003) mentioned that most of the historical wind towers in this region have been demolished. In Dubai, about forty wind towers still there in the Bastakia quarter, in which Iranian immigrants used to live. This is why wind towers in this area are similar to those used in Persia. The use of wall openings, which open to an attached courtyard, has facilitated the role of wind catcher here.

B. Wind catchers

Many examples of wind catchers could be found in many countries in the Middle East. Some of them are:

- Wind catchers in Egypt

Wind catchers in Egypt are named *al-Malqaf* and have been used since centuries. They are built facing the prevailing wind direction to catch the high-level air, which has a higher velocity and less temperature, and admit it to the summer living space of the building. In some cases, they might be integrated with some roof vents that cover the main living hall, *al-Qa'a*, in order to form a vertical cross ventilation system. This is discussed in Section 4.5. The roof of the catcher tilts forward in order to facilitate wind catching. This wind catcher might be connected to the space through a shaft or an opening in the roof (Fathy, 1986).

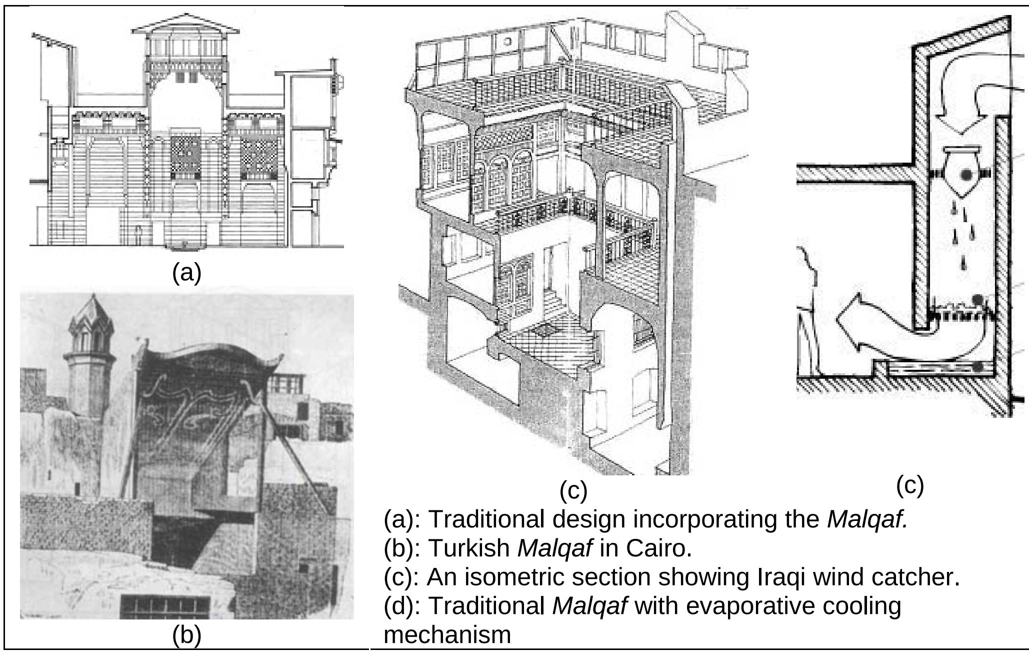

(a): Traditional design incorporating the *Malqaf.*
(b): Turkish *Malqaf* in Cairo.
(c): An isometric section showing Iraqi wind catcher.
(d): Traditional *Malqaf* with evaporative cooling mechanism

Figure 4.10: Vernacular designs on wind catchers

Source: a & b: (Fathy, 1986), c: (Al-Koheji, 2003)

- Wind catchers in Iraq

The roof of the tower is tilted at 45^{o} angle to facilitate air admission (Al-Koheji, 2003). The prevailing climate is hot and arid. Therefore, it is required to increase air humidity and reduce its temperature before admitting it into the living space. This requires the encouragement of two mechanisms:

- Convective heat transfer, due to the lower temperature of the earth and the thermal mass of the used building material. To improve the convective heat transfer between the air and the body of the catcher, catcher shaft is divided into several and small segments, ranging between 0.15 – 0.2 m in depth by 0.5, 0.6, 0.9-1.2 m in width. Another idea is to drive the air to a basement before passing it to the living space.
- Evaporative heat transfer, by implementing some traditional mechanisms of evaporative cooling. One idea is that wind towers and catchers are integrated with an evaporative cooling part, where water sprays are used to help cooling down the air before driving it to the internal space of the building. Another idea is to pass air over water containers or surfaces before admitting it into the space.

4.4.2 Operation concept

Wind towers and catchers operate in a simple mechanism. As pointed out in the previous section, the difference between a wind tower and catcher is that wind towers have many openings facing different wind directions, while wind catchers only face the prevailing wind direction. The main operation principle of both of them is to generate air movement within the building by utilising the movement of high-level air currents. However, the use of wind catcher is more effective wherever wind has a prevailing direction. This is assumed to be the case in this study. Thus, more details on operation mechanisms of wind catchers are given below.

- *During day-time*

a. The usual operation mechanism is dependant on wind effect due to the difference in air pressure. Wind catcher traps channels the air down at a higher velocity and less pressure, which is known as Venturi effect (Moore, 1993). This is more effective in the case of wind catchers, compared to wind towers, where the whole amount of air that entered the tower is driven to the building.
b. The other possibility is that there is no wind at daytime. In this case the hot ambient air enters the tower and is cooled down when it comes in contact with tower walls, which have been cooled down during the night or using

evaporative cooling. This creates air movement from the tower to the building, in an opposite manner of the stack effect.

- *During night-time*

a. When there is wind during night-time, then mechanism (a) mentioned above is applicable, but utilising the relatively lower outdoor air temperature. This is known as night-time ventilation, by which the building structure is cooled down by air movement, so that it can absorb heat gains at day time.

b. When there is no wind, the heat released by the tower body at the beginning of night-time heats up the air and encourages air movement from the building to the tower and then outside it, where air temperature is lower. This mechanism is dependant on stack effect due to the difference in air temperature and density. This is more effective in hot dry regions, where diurnal variation in ambient temperature is high.

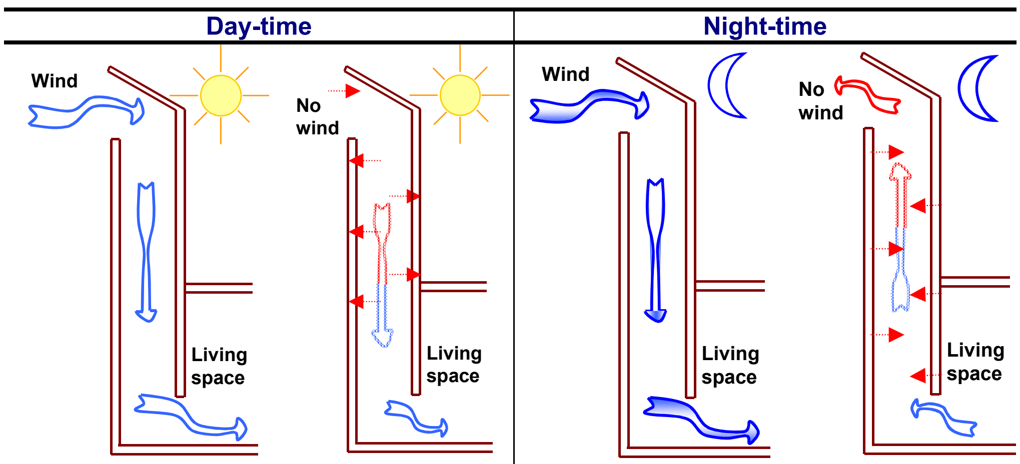

a: sufficent wind: wind effect. Air enters the building and may be cooled down.	b: no wind: downdraught. Opposite of what happens in the stack effect.	a: sufficent wind: wind effect. Cold air enters the building and cooles it down.	b: no wind: stack effect. Air leaves the building.

Figure 4.11: Different operation mechanisms of wind towers and catchers during day and night times

4.4.3 Architectural factors

Many factors affect the use of wind towers and catchers for wind-induced natural ventilation. Some of them are:

A. Dimensions of the tower

Fathy (1986) recommended the use of small sectional area of the tower when the external temperature is higher than the thermal comfort level, given that air should be cooled down before being admitted into the living space. The opposite case is true, i.e. the use of large sectional area of the tower when the external temperature is low. For example, in Iraq, where summer temperature reaches 45^{o}C, a small sectional area of wind catchers is used with shaft area ranging between 0.15 – 0.2 m in depth by 0.5, 0.6, 0.9-1.2 m in width (Al-Koheji, 2003). This is to help maximising airflow rates and cooling effect of the tower, since air passes over its internal walls and possibly the evaporative cooling part. However, this is a very general rule of thumb and Fathy did not mention any numerical indications in this regard.

To determine tower dimensions, and considering the case of wind-driven ventilation, it is a usual practice to analyse fluid flow through the tower in order to achieve the required pressure difference between tower inlet(s) and outlet(s). This is done considering the local climatic and urban conditions. Initially, it is required to know the relevant wind pressure coefficient values, which depends on the above-mentioned conditions. This can be obtained experimentally in wind tunnels. Then, and applying the Network model, as explained in Section 3.2.3, it is possible to determine air pressure drop along the tower and the resulting air velocity. If this velocity does not meet the required criteria to achieve thermal comfort, tower design, including its height, can be modified and, then, airflow rate can be recalculated.

Bahadori (1985) has implemented this approach systematically and for different sites and climatic conditions of hot arid areas. It was possible to determine dimensions of the tower, including its height, and to calculate air velocity at different points along the tower, including air velocity at the occupied level of the building in order to account for occupants thermal comfort. Badran (2002) has adopted this mathematical approach, considering the climatic conditions and building codes of Jordan. He found that the height of the tower could be less than 9 m. However, this mathematical approach requires a predetermined experimental data of pressure coefficients, which is time-consuming process. Alternatively, it is possible to use CFD codes to test different sizes of the tower.

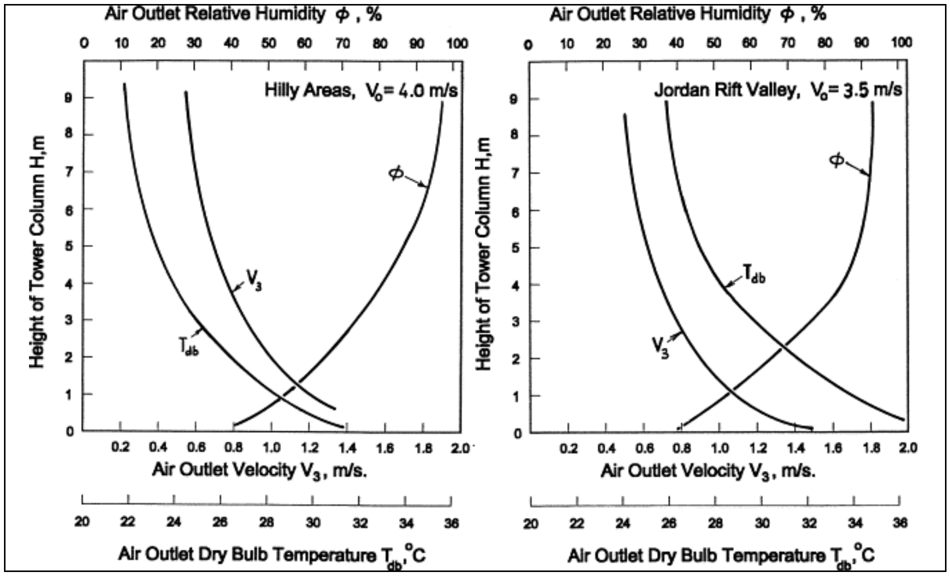

Figure 4.12: Effect of the height of tower evaporative column on velocity, humidity, and temperature airflow at tower outlet

Source: (Badran, 2002)

B. Orientation and location of the tower

Orientation of the tower is limited to the use of wind catchers, which are oriented with respect to the prevailing wind direction. The tower can work as a wind catcher when openings face the wind, or otherwise as a wind chimney when openings are located in the opposite direction. In the latter case, wind creates a negative pressure and suction forces similarly to what has been explained in Section 4.3.2. Regarding its location, many interesting ideas can be implemented.

For example, the tower can be attached to the main volume of the building at its windward or leeward face. In both cases, it can be utilised as a wind catcher or chimney. Another application is to separate the tower from the building as a response to the structural requirements and in order to facilitate the use of underground cooling. This can be achieved using an underground tunnel to convey airflow to the interior space of the building. The depth of this tunnel is another parameter, which may affect its cooling performance.

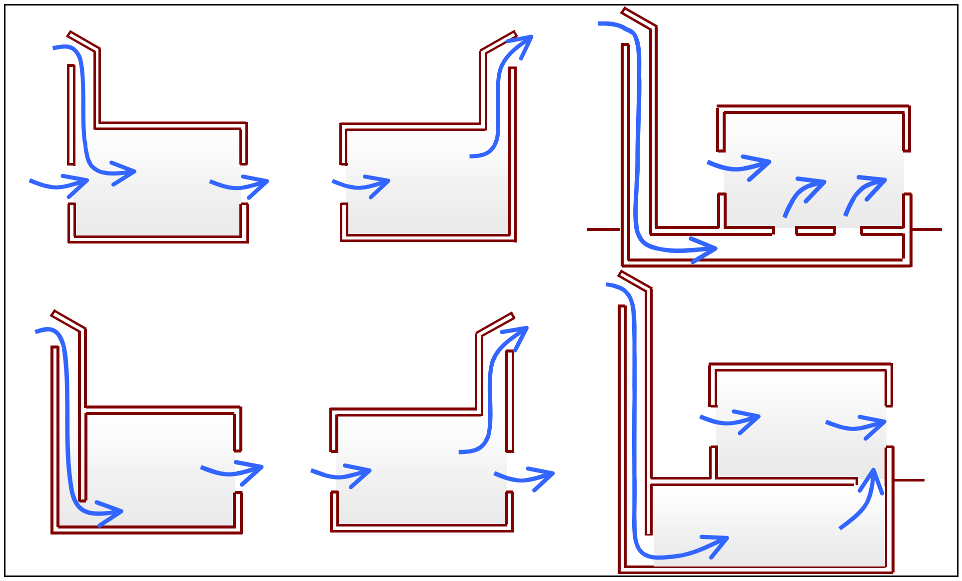

Figure 4.13: Different configurations of the orientation, location, and openings of wind catcher

Chand *et al.* (1990) has studied in wind tunnel many parameters related to wind catcher design. This catcher is installed on a room model, which has one window at the leeward wall. The parameters that have been evaluated are: façade area of the catcher, size and shape of catcher outlet, the use of overhang, and the replacement of the catcher by a window. The numerical output that has been used in the assessment is indoor wind velocity magnitude, as a percent of the reference wind velocity.

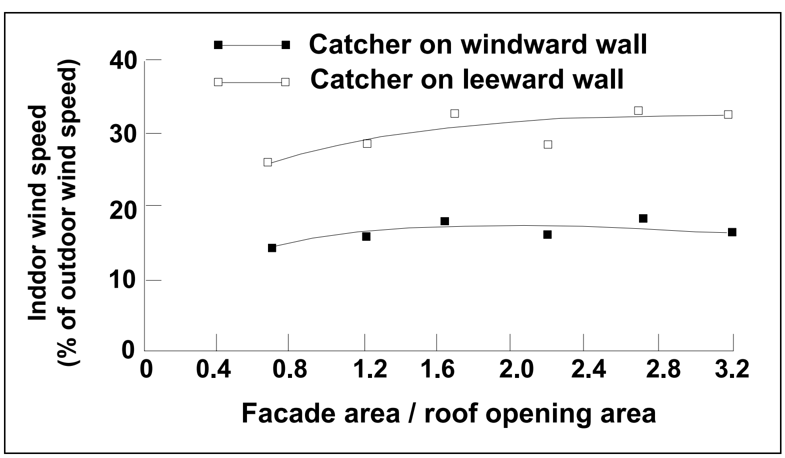

Figure 4.14: Effect of wind catcher façade area on the average indoor wind speed, considering two locations of the catcher

Source: Chand *et al.* (1990).

The study has considered two locations of the catcher: on the windward wall, and on the leeward one. Amongst many conclusions, the study concluded that locating the catcher on the leeward wall leads to a significant increase at air provision to the room. This is found to be true for the different tested façade areas of the catcher. The study has also concluded that a catcher outlet located at the bottom of the catcher shaft results in a higher indoor air speed, when compared to an outlet located at the literal wall of the shaft. This is because in the second configuration, air leaving the catcher loses more kinetic energy to overcome the abrupt changes in airflow path.

C. Design of the tower head

It is important to ensure that this part of the tower is designed in a way that optimises tower performance. Bahadori (1985) presents an analysis of the design of wind towers, where many factors should be taken into consideration. For example, the shape of the tower head has a crucial effect on pressure distribution around it. Also, increasing the pressure difference between the tower's inlet and outlet is desirable in natural ventilation design. This pressure difference is given in this equation:

$$\Delta P = (Cp_i - Cp_o)0.5\,\rho V^2 \qquad \textbf{(4.1)}$$

Where Cp_i and Cp_o are pressure coefficients at the tower head inlet and outlet; ρ is air density (kg/m^3); V is wind velocity (m/s).

An important factor is the shape of the tower head. For example, it is possible to increase pressure difference using an inclined roof, which increases the internal angle between the tower's roof and wall. Using a flat roof can cause a negative pressure field in this internal corner, which reduces the flow's kinetic energy.

Other factors are the properties of the building materials. For example the roughness of the materials used, presented by its friction factor, is considered in the pressure coefficient of equation 4.1 above. In general, reducing the roughness of the internal face of the airshaft is a desired condition. In addition, the thermal properties of these materials are important. When applying ventilation strategies such as night time ventilation, building materials with high thermal capacity become desirable.

Bahadori (1985) proposed an improved design of wind towers in hot arid climates. The main improvements were intended the disadvantages associated with the use of the traditional wind towers, as explained in Section 4.4.1(C). Thus, he suggested the following adjustments to the tower head:

- The use of gravity-shut dampers in order to catch wind from any direction and prevent air from leaving the tower through the opposite opening.
- Therefore, the curved part of the entrance in the traditional tower has been eliminated, which reduces the construction cost.
- The use of screens on the openings to prevent dust, insects, etc from entering the tower. These screens are of large openings to reduce pressure loses.

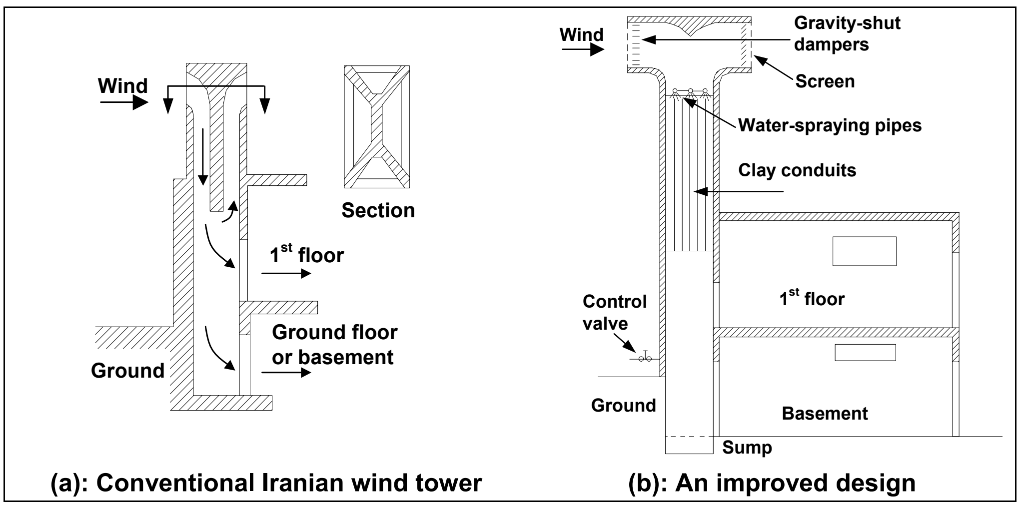

Figure 4.15: Bahadori's improved design of wind tower

Source: (Bahadori, 1985). Reproduced by the author.

Another study has been carried out by Al-Qahtani (2000), who had evaluated the performance of a wind tower building in Dammam, Saudi Arabia. The study involved full-scale measurements of airflow rate in an existing wind tower. After that, different parameters were varied in a wind tunnel study to find out their effect on the tower performance. Al-Qahtani recommended the use of the above-mentioned gravity-shut dampers. Furthermore, he recommended the use of automatic shutters, which allow the control of the incoming airflow rate. Another improvement at the tower head is the use of a pitched roof over it. This has increased suction forces acting over the tower. The outlet was located in a higher level than the inlet and was protected from the coming wind by a wing wall surrounding the tower head.

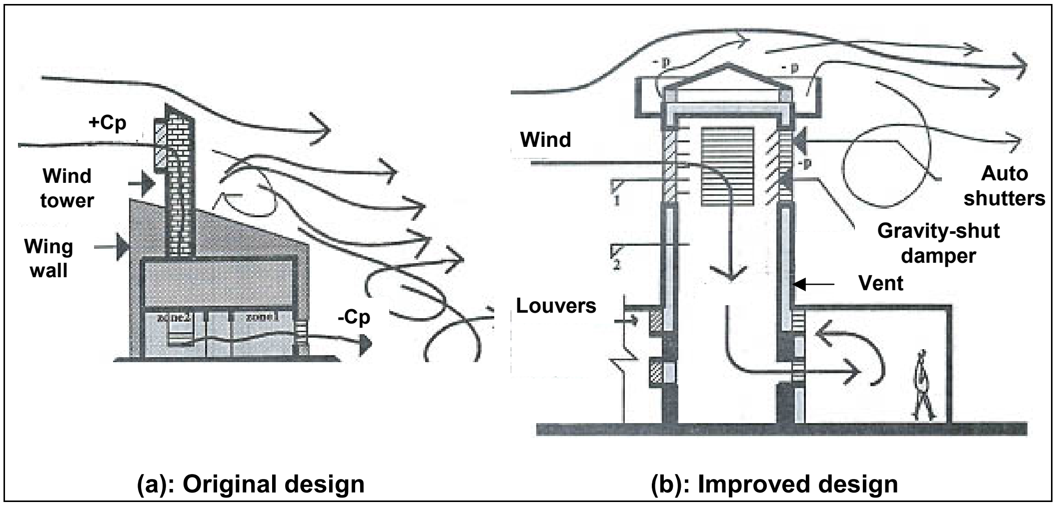

Figure 4.16: Al-Qahtani's improved designs of wind tower

Source: (Al-Qahtani, 2000).

In addition to the improvements implemented on the tower top part, two separate shafts for air entering and leaving the tower were constructed. The main shaft for coming air is in the tower centre, while the other shaft for leaving air is around the main shaft. The improved design then was constructed and mounted in the original one. Then, the full-scale measurements for both designs were compared. The following graph shows the dimensionless velocity ratio for both designs. Al-Qahtani claimed that the new design appears to provide an increase of 80% in the flow rate.

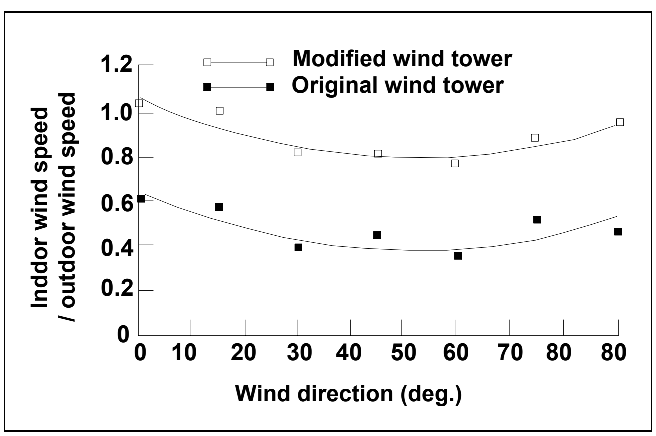

Figure 4.17: Comparison of ventilation provided by the original and improved wind tower designs in Al-Qahtani's study

Source: (Al-Qahtani, 2000).

The recent industrial development has facilitated the process of in-depth investigation of wind towers and catchers performance. This includes many interesting ideas, like:

- The provision of a fresh and a relatively non-contaminated air.
- The use of hybrid ventilation by integrating some mechanical devices like pumps.
- The incorporation of natural lighting devices. In this case, the term 'sun-catcher' is used sometimes.
- The utilisation of night-time cooling without compromising the security of the building. Some examples are shown in Figure 4.18.

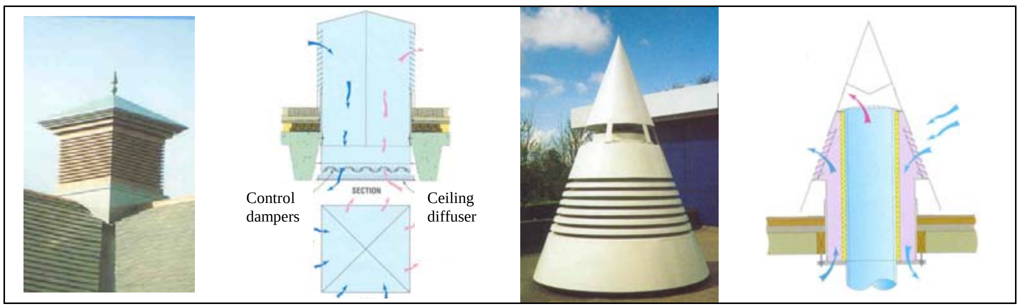

Figure 4.18: Examples on contemporary use of wind catchers

Source: (Monodraught, 2003)

4.5 Integration of curved roofs, towers, and the main building volume for natural ventilation

The previous sections have reviewed architectural and natural ventilation potential of curved roofs, namely domed and vaulted, and wind towers and catches. Priolo (1998) claimed that integrating dome with other natural ventilation devices like windows, wind towers, and wind catchers could increase the effectiveness of its suction ventilation. The same assumption can be applicable on the case of vaulted roofs. Many examples of this application could be found in the vernacular and contemporary architecture. However, the author could not find any detailed study of the potential of this integration for natural ventilation and thermal comfort improvement in the building. An early study on the combination between wind catcher and roof vents was carried out for the house of Othman Katkhuda in Cairo (Fathy, 1986). Figure 4.19 illustrates air velocity vectors, which shows velocity magnitudes and direction.

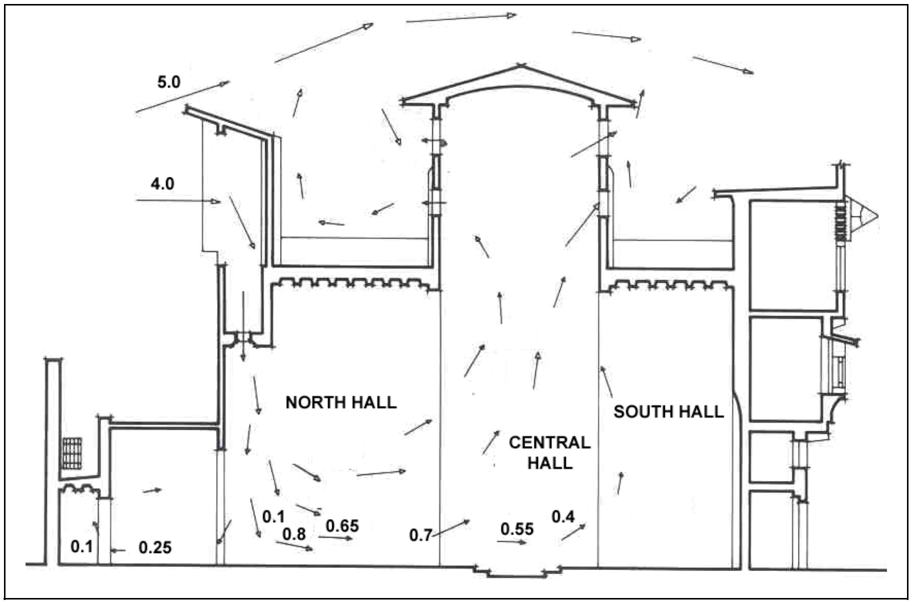

Figure 4.19: Section at Othman Katkhuda house in Cairo, showing airflow directions and velocity magnitudes in (m/s)

Source: (Fathy, 1986)

In this traditional house, a wind catcher has been built on the roof of a northern room, known in the traditional architecture as *Iwan.*. Air enters the wind catcher and accelerates towards building interior. Then, it passes though the northern *Iwan* slowly, before it accelerates towards the main and high living hall, known as *al-Qa'a.* The roof of *al-Qa'a* is covered by a pitched roof, which incorporates many roof vents installed at its base. According to Venturi effect, these vents are subjected to a negative pressure, which encourage ventilation by suction. Thus, air rises in the *Qa'a*, from the high-pressure zone to the lower-pressure zone, until it leaves through these roof vents.

It has been found in this study that when the upper openings in the central hall, known as wind escapes, are opened, airflow rate increases because of suction force acting on the roof. If airflow exceeds the desired rate, it is possible to open the wind escape opening provided in the catcher in order to reduce internal wind velocity. In addition to the effect of pressure difference, stack effect has an important role in encouraging this vertical air movement. This is more effective when the wooden *Qa'a* roof is heated up by solar radiation. This does not affect human thermal comfort negatively, due to the high level of this roof, compared to the adjacent living spaces. The use of this ventilation system justifies the fact theta this *Qa'a* space is designed to be in the middle of the building and surrounded by other spaces.

In spite of the interesting findings of this study, its numerical outputs are limited. Also, it is limited to the case that has been tested, and lacks the systematic approach from which variety of design guidelines can be concluded. This opens the door for a further investigation of the integration of the curved roofs and wind towers and catchers for natural ventilation in buildings.

4.6 Conclusions

This chapter has highlighted many aspects related to the targeted architectural elements in this study. These elements are curved roofs, namely domes and vaults, and wind towers and catchers. It has been concluded that there is a strong architectural relationship between these elements. This can be observed in many traditional and contemporary designs. Thus, re-introducing this relationship from an environmental point of view is expected to invest and give more value to the use of these elements in buildings. One possible application is the use of dome, vault and tower for natural ventilation, which is a common practice in the Middle East.

This has been reviewed in three main axes: a historical background, which showed the importance of studying vernacular architecture, the operation concept, and the architectural parameters that affect this use. It has been concluded that these elements have a high potential for natural ventilation in buildings. This could also be concluded from the related background studies that have been reviewed. However the integration of these architectural elements in one natural ventilation system is not investigated enough. Thus, this chapter has opened the door for the intended empirical study, which includes investigation of the potential of these three elements for wind-driven natural ventilation in buildings.

CHAPTER 5 : CFD CODE VALIDATION

Introduction

Computer modelling using CFD has been introduced in Section 3.2.4 of Chapter 3, where the code that is implemented in ventilation prediction has been explained in. The aim of this chapter is to describe the validation of this code, which was carried out in order to avoid any misleading results in the modelling study. This is crucial to ensure a correct implementation of the code, and this is why it is a common practice in CFD studies to compare both modelling and experimental results.

Due to time and budget constrains, this study is limited to the use of CFD modelling, and validation of the CFD code through a comparison between the CFD and mathematical models used to predict airflow rate. This means that the review presented in Sections 3.2.3 and 2.3.4 for the CFD and Network models is essential here. These two methods have been implemented on many building configurations and the results obtained have been compared and analysed. On the other hand, without this time and budget constrains, it would have been useful to undertake experimental studies and wind tunnel laboratory testing of the various configurations considered in this study.

5.1: Prediction of airflow rate using Network mathematical model, with normal wind direction

The Network mathematical model is used here to predict airflow rate driven by pressure difference across room large openings. It is possible to implement this model for any opening, knowing its area and wind static pressure coefficient. Prediction process here is divided into four stages: specification of the pressure coefficient data, specification of the study cases, calculations of internal pressure coefficient, and finally calculations of airflow rate.

5.1.1 Specification of pressure coefficient data

As discussed in Section 3.1.2, pressure coefficients are usually estimated in wind tunnels. As it was not possible in this study to carry out this experimental work, the author suggests using the wind pressure data presented by Liddament (1986), as tabulated below. These data are similar to those available in the British Standards (BSI, 1991), but they are more developed in terms of considering terrain type and more wind directions (Awbi, 2003).

Table 5.1: Surface averaged pressure coefficients for exposed low-rise buildings (up to 3 stories), with aspect ratios of 1:1 and 2:1

Source: (Liddament, 1986). Reproduced by the author

Surface

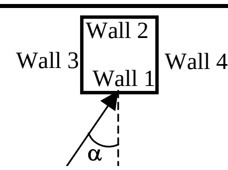

Wind pressure coefficient for wind angle α°

Building is not sheltered

	0°	45°	90°	135°	180°	225°	270°	315°
Wall 1	0.7	0.35	-0.5	-0.4	-0.2	-0.4	-0.5	0.35
Wall 2	-0.2	-0.4	-0. 5	0.35	0.7	0.35	-0. 5	-0.4
Wall 3	-0.5	0.35	0.7	0.35	-0.5	-0.4	-0.2	-0.4
Wall 4	-0.5	-0.4	-0.2	-0.4	-0. 5	0.35	0.7	0.35

Surface

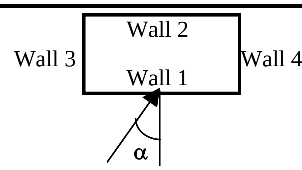

Wind pressure coefficient for wind angle α°

Building is not sheltered

	0°	45°	90°	135°	180°	225°	270°	315°
Wall 1	0.5	0.25	-0.5	-0.8	-0.7	-0.8	-0.5	0.25
Wall 2	-0.7	-0.8	-0. 5	0.25	0.5	0.25	-0. 5	-0.8
Wall 3	-0.9	0.2	0.6	0.2	-0.9	-0.6	-0.35	-0.6
Wall 4	-0.9	-0.6	-0.35	-0.6	-0.9	0.2	0.6	0.2

Liddament (1986) has presented pressure coefficients data for some common building configurations considering that building is exposed, sheltered, or semi-sheltered. This analysis assumes that buildings are exposed, i.e. located in the 'open country' terrain. This is because using second and third terrains requires details regarding the sheltering obstructions used in the wind tunnel tests that have been used to estimate wind pressure coefficients.

5.1.2 Specification of study cases

It is required here to propose building configurations that consider the different parameters affecting wind-induced natural ventilation. Namely, three parameters are varied here:

- Wind velocity magnitude: reference velocity magnitudes have been varied. A relatively low and high velocities have been used, namely 1 and 5 m/s.
- Wind direction: two wind angles are considered here: normal, and oblique (with an angle of 45^o). The first angle is examined in this section, while the other one is examined in the next section, as it requires different mesh type.
- Building geometry: different cases have been designed, so that they have nearly the same volume, but different aspect ratios. Aspect ratios of 1:1, 1:2 and 2:1 are considered here, as depicted in Table 5.2. This table illustrates the different three-dimensional cases used in the comparison process. It also shows values of the pressure coefficient, quoted from Table 5.1, with a reference number of the wall.

Table 5.2: **Illustration of the first six cases used in the Validation Study**

<table>
<tr><th>Cases</th><th>Illustration (showing C_{pn} values)</th></tr>
<tr><td rowspan="2">1 & 2</td><td>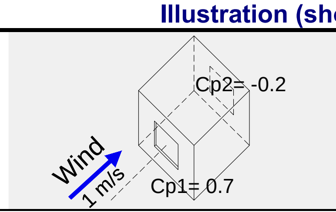

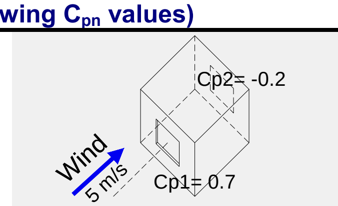
</td></tr>
<tr><td>Description: square, with 5 m length and 5 m height. (Room volume = 125 m^3).</td></tr>
<tr><td rowspan="2">3 & 4</td><td>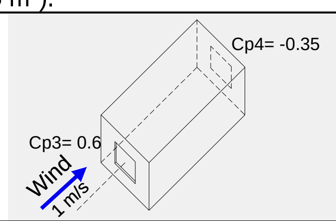

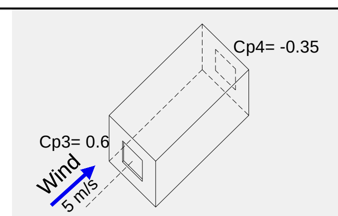
</td></tr>
<tr><td>Description: rectangular with 4 m length, 8 m width and 4 m height. (Room volume = 128 m^3).</td></tr>
<tr><td rowspan="2">5 & 6</td><td>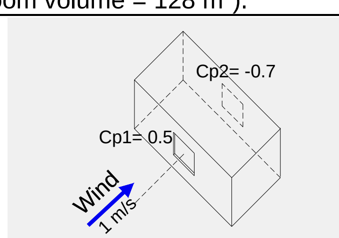

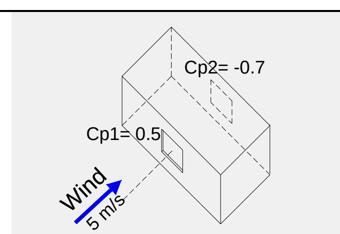
</td></tr>
<tr><td>Description: rectangular with 8 m length, 4 m width and 4 m height. (Room volume = 128 m^3).</td></tr>
<tr><td colspan="2">* In all cases, openings are assumed opposite openings located in the windward and leeward facades, with equal effective areas of 4 m^2.</td></tr>
</table>

5.1.3 Calculation of internal pressure coefficients

As explained in Section 3.2.3, internal pressure coefficient C_{pi} can be estimated using the following equation:

$$\sum_{n=1}^{N} A_{eff} V \left(C_{pn} - C_{pi}\right) \left|\left(C_{pn} - C_{pi}\right)\right|^{-1/2} = 0 \qquad \textbf{(5.1)}$$

Where, A_{eff} is opening effective area (m^2), C_{pn} is pressure coefficient at opening n, and C_{pi} is pressure coefficient inside the space.

In the case of using two windows, this equation may be written as:

$$A_{eff} V \left(C_{p1} - C_{pi}\right) \left|\left(C_{p1} - C_{pi}\right)\right|^{-1/2} + A_{eff} V \left(C_{p2} - C_{pi}\right) \left|\left(C_{p2} - C_{pi}\right)\right|^{-1/2} = 0$$

Given that reference wind velocity and the window effective area are the same for both windows; the equation may be simplified as follows:

$$\left(C_{p1} - C_{pi}\right) \left|\left(C_{p1} - C_{pi}\right)\right|^{-1/2} + \left(C_{p2} - C_{pi}\right) \left|\left(C_{p2} - C_{pi}\right)\right|^{-1/2} = 0,$$

$$\left|\left(C_{p1} - C_{pi}\right)\right|^{-1/2} + \left|\left(C_{p2} - C_{pi}\right)\right|^{-1/2} = 0,$$

And therefore:

$$\left|\left(C_{p1} - C_{pi}\right)\right|^{-1/2} = \left|\left(C_{pi} - C_{p2}\right)\right|^{-1/2} \qquad \textbf{(5.2)}$$

From the last simple equation, the internal pressure coefficient for cases 1 to 6 has been estimated, as shown below:

Table 5.3: Calculated internal pressure coefficients for the first six cases of the validation study

Case No.	Given external pressure coefficient values, C_{pn}	Calculated internal pressure coefficient values, C_{pi}
1 and 2	C_{p1} = 0.7, C_{p2} = -0.2	**0.25**
3 and 4	C_{p3} = 0.6, C_{p4} = -0.35	**0.125**
5 and 6	C_{p1} = 0.5, C_{p2} = -0.7	**-0.1**

5.1.4 Calculations of airflow rates

It is required to know air velocity at building height to implement the Network model for airflow rate estimation. This is possible using equation 3.3 and Table 3.1. This equation is given here again:

$$V = V_r * cH^a \qquad \textbf{(5.3)}$$

For cases 1 and 2, building height is 5 m. Knowing from Table 3.1 that c = 0.68 and a = 0.17, and given that reference wind velocity is 1 m/s, then V value can be estimated as follows:

$V = 1 * 0.68 * 5^{0.17} = 0.894$ m/s.

In the case of reference wind velocity of 5 m/s, V value is 4.47 m/s. For the other cases, building height is 4m. Thus V value is 0.861 m/s, for the lower reference wind velocity, and 4.31 m/s, for the higher reference wind velocity.

For any opening n, knowing its effective area, internal and external pressure coefficients, airflow rate Q_n through this opening can be estimated using the following equation:

$$Q_n = A_{eff} V (C_{pn} - C_{pi}) |(C_{pn} - C_{pi})|^{-1/2} \qquad \textbf{(5.4)}$$

This airflow rate is given in m^3/s. It is possible to convert it to mass flow rate, in kg/s, by multiplying it by air density. Value of air density should match the one under which pressure coefficient data were estimated. As there is no indication of this value in the related resource, this value will be assumed to be 1.225 kg/m^3, which is the default value used in Fluent 5.5 software and nearly the same as the standard air density value, i.e. 1.2 kg/m^3. Also it is possible to obtain airflow rate in ‘air change per hour’ by multiplying the output of this equation by 3600 then dividing it by the volume of the room. Table 5.4 shows the results of the airflow rate calculations.

Table 5.4: Calculated airflow rates for the first six cases of the validation study

Case number	Opening number	A_{eff} (m^2)	C_{pn}	C_{pi}	Q_n (m^3/s)	Q_n (kg/s)
1	1	4	0.7	0.25	2.40	**2.94**
	2	4	-0.2	0.25	-2.40	**-2.94**
2	1	4	0.7	0.25	11.99	**14.69**
	2	4	-0.2	0.25	-11.99	**-14.69**
3	3	4	0.6	0.125	2.37	**2.90**
	4	4	-0.35	0.125	-2.37	**-2.90**
4	3	4	0.6	0.125	11.85	**14.52**
	4	4	-0.35	0.125	-11.85	**-14.52**
5	1	4	0.5	-0.1	2.66	**3.26**
	2	4	-0.7	-0.1	-2.66	**-3.26**
6	1	4	0.5	-0.1	13.32	**16.32**
	2	4	-0.7	-0.1	-13.32	**-16.32**

5.2: Prediction of airflow rate using CFD modelling, in the case of normal wind direction

Using Fluent 5.5 software, it is possible to simulate airflow inside and around buildings, using three-dimensional modelling. It is also possible to estimate airflow rate across building openings. Modelling process includes the following four stages: drawing of the room model in Gambit software, generation of the calculation mesh, definition of the solution code in Fluent 5.5 software, and finally computing airflow rate.

5.2.1 Drawing of the room model

It is possible to draw the room model two or three-dimensionally. These two options were evaluated, and the author found that three-dimensional modelling is more accurate. It has been found to give more realistic airflow pattern and behaviour, which directly affects airflow rate. This explains the significant differences between results obtained using both methods in the early stage of this study.

Given that three-dimensional modelling is implemented, it is important to simulate the ambient air around the building. This is to consider wind deflection on its windward, which increases air pressure and causes airflow separation. Therefore, the modelled room will be placed inside a three-dimensional ‘box’, which is a common practice to simulate the ambient air in CFD studies.

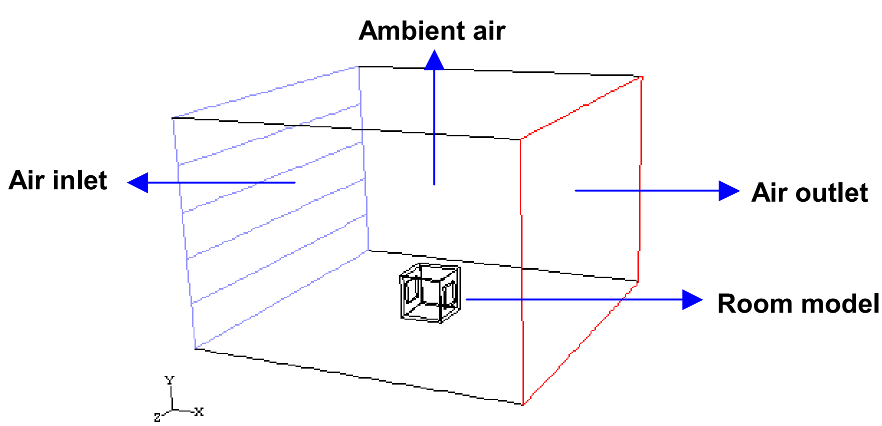

Figure 5.1: Simulation of the ambient air around buildings

After drawing the three-dimensional solution domain, the different boundary and continuum types of this domain should be defined in Gambit software. Because of the frictional effect of the ground over which wind blows, it is important to consider wind velocity variation with height in CFD modelling. It is possible to do so using equation 5.3, which is commonly used to express this relationship.

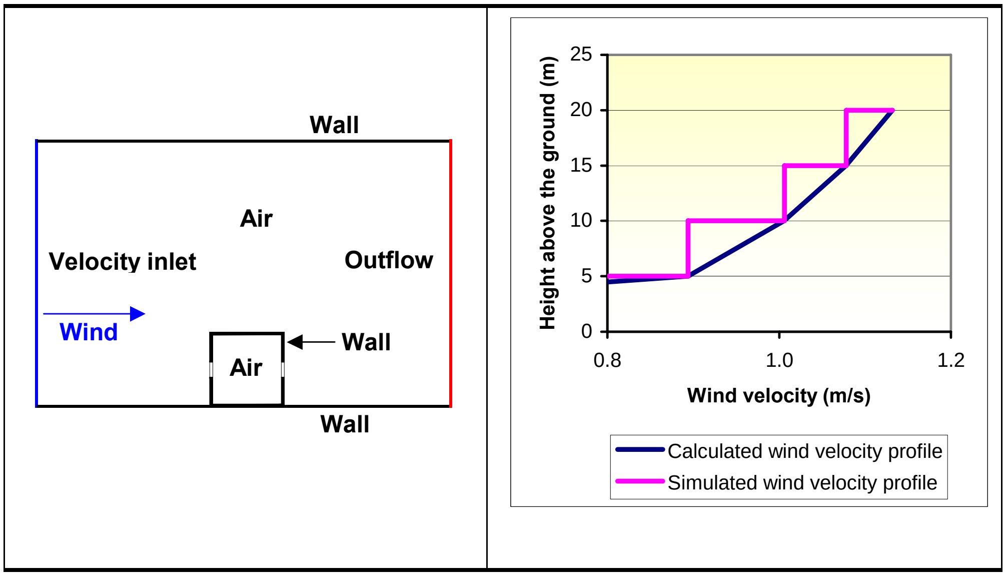

Figure 5.2: Boundary and continuum types used in the validation study, with illustration of the calculated and simulated wind velocity profile (for cases 1 & 2 and 1 m/s reference wind velocity, as an example)

Wind velocity profile can be defined along the velocity-inlet, as illustrated in Figure 5.2, using 'User Defined Function' option in Fluent software. However, application of this option in three-dimensional simulation requires some advanced C^{++} programming. It is possible, as an approximation method, to divide the large velocity inlet into many sub-inlets, so that each one has different air velocity magnitude depending on its height above the ground. These velocities are calculated using equation 5.3. This method has been found to be useful in terms of time saving, and good results have been obtained. Table 5.5 shows velocity values of each sub-inlet used in this method:

Table 5.5: Air velocities for the different heights used in the Validation Study

Cases 1 and 2 (Room height is 5m).				Cases 3 to 6 (Room height is 4m).			
Height above the ground (m)	Velocity sub-inlet number	Reference velocity magnitude, V_r		Height above the ground (m)	Velocity sub-inlet number	Reference velocity magnitude, V_r	
		1 m/s	5 m/s			1 m/s	5 m/s
5	1	0.894	4.47	4	1	0.861	4.305
10	2	1.006	5.03	8	2	0.968	4.84
15	3	1.078	5.39	12	3	1.037	5.185
20	4	1.132	5.66	16	4	1.089	5.447
-	-	-	-	20	5	1.132	5.658

5.2.2 Mesh generation and exportation

The use of three-dimensional simulation leads to think about the resulting files size and the required capacity of the processor. The use of a fine mesh has been found to be impractical for this study. For example, the use of 0.2 m mesh spacing in the meshing unit used was out of the available computer memory and speed. A common solution here is to create a hierarchy in mesh size, so that fine mesh is used inside the building and larger one is used around it. This required special treatment of the solution domain so that Gambit software connects the different sizes of the mesh.

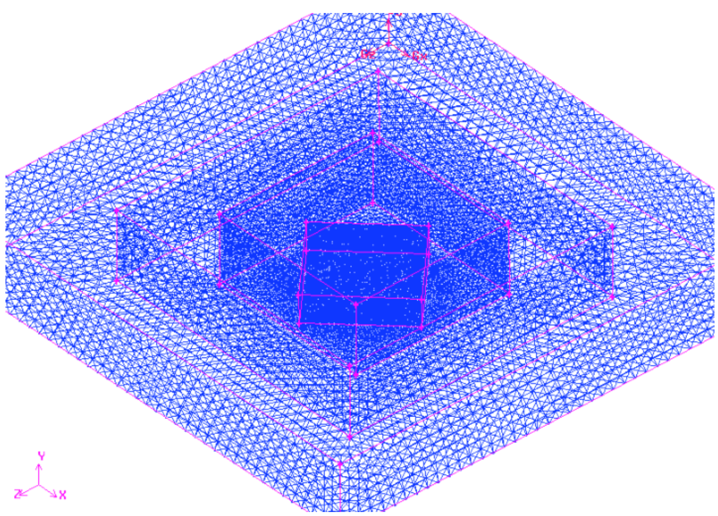

Figure 5.3: Example on creating hierarchy in mesh size in Gambit software

The use of this method, with relatively coarse mesh around the building, has been found to be acceptable. In any case, a trial-and-error process is recommended to find out the most appropriate mesh configuration. This is supported by Borth and Suter's study (see: Kindangen *et al.,* 1997), which found that rough mesh is suitable and sufficient in many CFD simulation cases. Generally, the following mesh configuration has been found to be acceptable:

- Meshing scheme: Hex-map or Hex-submap. Mesh elements here are hexahedral. This scheme is appropriate for the topological characteristics of the sharp-edged modelled cases. In case of oblique wind direction, Hex-map mesh has been used as well. However, the use of tetrahedral mesh has been found to give more accurate results, as will be discussed in section 5.5.
- Mesh node spacing: in the case of normal wind direction, hex-map and sub-map meshes were used with a unified size of 0.6 m. In the case of oblique wind direction, solution domain was divided into two zones: room interior, with 0.5 m hex-map mesh, and room exterior, with 1m tetrahedral mesh.

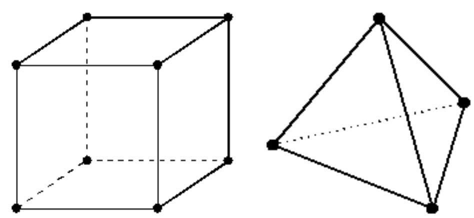

Figure 5.4: Hexahedron and tetrahedron mesh cells, showing their edge nodes.

In order to facilitate airflow rate estimation in Fluent software, solution domain should be divided into many zones. These zones are: room walls, which are defined as solid continuum and are not meshed, the ambient air, room interior, and the openings. The last three volumes are defined as fluid continuum.

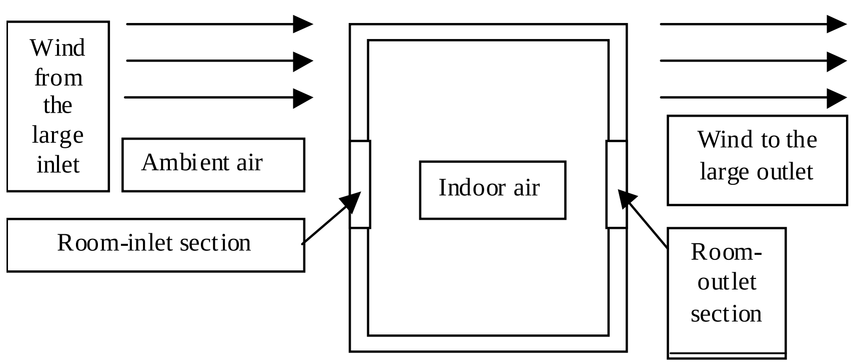

Figure 5.5: Mesh has been divided into many zones in order to estimate airflow rate

5.2.3 Definition of the solution code in Fluent 5.5 software

This stage has been explained in Section 3.4 of Chapter 3. In summary, the relevant settings are:

- Solver: Segregates.
- Viscous model: Standard *k-ε* model.
- Boundary conditions: velocity-inlet and outflow.
- Turbulence Intensity: 5%, depending on the domain size. Turbulence Height: 0.35m for cases 1 and 20, and 0.28m for other cases, depending on inlet height.
- Error tolerance in the velocity, continuity, and *k* parameter of the viscous model: e^{-6}.

5.2.4 Computing of airflow rate

After achieving solution convergence, it is possible to obtain the mass flow rate directly from the software, utilising the Surface Integrals option for the relevant inlet surface. Results obtained for the different cases are illustrated in the following table:

Table 5.6: Inflow rates for cases 1 to 6 in the validation study, as obtained from Fluent 5.5 software

Case	Inflow rate (kg/s)	Case	Inflow rate (kg/s)
1	3.19	**2**	15.89
3	2.98	**4**	14.87
5	3.30	**6**	16.46

Figure 5.6 illustrates the resulting airflow pattern for these cases, presented by contours of velocity magnitudes over a two-metre-height section. Generally, the observed airflow pattern has been found to be reasonable for such sharp-edge geometries. For example, when wind reaches the windward face, a high-pressure zone is formed there. This pressure pushes air inside, around, and over the building. Some standard features can also be observed. For example, airflow separation over building sharp edges. This phenomenon usually occurs when airflow layers hit building sharp edges, which reduces their momentum. After some distance, the separated airflow joins its original stream again in a point called the reattachment point. However, the separated airflow may randomly oscillate between reattaching and remain fully separated.

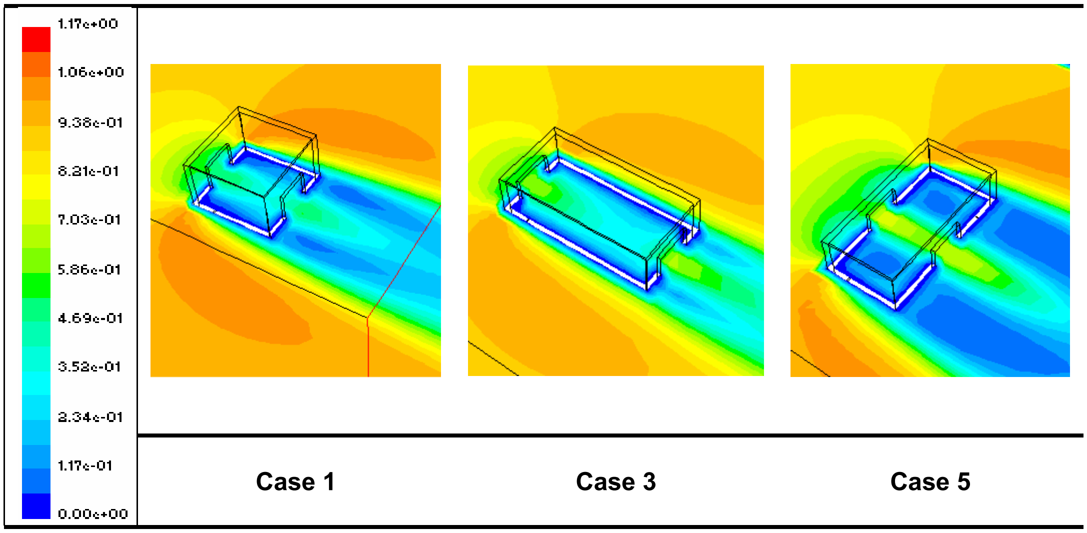

Figure 5.6: Airflow pattern, presented by contours of velocity magnitudes for cases 1, 3, and 5, in the case of normal wind incidence

5.3 Comparison between airflow rate prediction using Network and CFD models, in the case of normal wind direction

Table 5.7 shows a comparison between airflow rate predicted by Network and CFD models. The negative sign, if there is any, indicates that the modelled airflow rate is less than the calculated one.

Table 5.7: Discrepancy percentage between estimated and modelled airflow rate for cases 1 to 6 of the validation study

Case number	Opening number	Airflow rate Q_n (kg/s) (CFD)	Airflow rate Q_n (kg/s) (Network)	Discrepancy (%)
1	1	3.19	2.94	**7.8**
	2	-3.19	-2.94	
2	1	15.89	14.69	**7.6**
	2	-15.89	-14.69	
3	3	2.98	2.90	**2.7**
	4	-2.98	-2.90	
4	3	14.87	14.52	**2.4**
	4	-14.87	-14.52	
5	1	3.30	3.26	**1.2**
	2	-3.30	-3.26	
6	1	16.46	16.32	**0.9**
	2	-16.46	-16.32	

In general, this shows that a good agreement has been achieved. Discrepancy percentage observed is usually acceptable in airflow rate prediction, which is given as a snapshot and measured in kg/s. The differences observed can be justified by many reasons. One of them is the approximation method used in simulating air velocity profile, as explained in Section 5.2.1. This is because wind-induced airflow rate is dependant on pressure difference, which is dependent on wind velocity. As the square of air velocity is used in the estimation of this pressure difference, any error in air velocity results in a larger error in airflow rate value.

Another reason of the differences observed between both models is the approximation of the mathematical procedure used. This is, on one hand, because the used wind pressure coefficient values are approximate ones, as they have been averaged over the whole specified building face, and not a specified point on it. Liddament (1986, p. 3.10) highlighted this point and stated that: "accurate evaluation of this parameter (i.e. pressure coefficient) is one of the most difficult aspects of air infiltration modelling". On the other hand, air infiltration model used contains many assumptions to enable the estimation of airflow rate through a reasonable mathematical process. On the opposite, CFD considers the different values of air pressure on the opening, and calculate airflow rate as a summation their product.

One more possible reason is that pressure coefficient data used were generated in wind tunnel experiments, where air density, and therefore pressure, is affected by air temperature. CFD simulation carried out here is for wind-induced ventilation, which is solely dependant on pressure difference across an opening and used an assumed air density value. It has also been observed that discrepancy percentage is not sensitive to wind velocity magnitude, as the percentage is nearly the same in the case of same building geometry and different approaching wind speeds. This result supports what Liddement (1986) has mentioned that pressure coefficient is normally assumed to be independent of wind speed but not direction. Its value also is dependant on the position on the building surface and nature of the terrain. This reveals the need for a further investigation into airflow rate in the case of oblique wind direction.

5.4 Prediction of airflow rate using Network mathematical model, with oblique wind incident

The same procedures followed in Section 5.3.1 will be implemented here. Table 5.8 illustrates three more cases, which are used in the comparison between predicted and modelled airflow arte in the case of 45^{o} wind direction. It also shows values of pressure coefficient, quoted from pressure coefficient data presented in Section 5.3.2, with a reference number indicating the wall number. As error percentage has been found to be independent of wind velocity magnitude, the following investigation will be confined to a velocity magnitude of 1 m/s.

Table 5.8: **Illustration of cases 7 to 9 of the Validation Study**

Cases	Illustration (showing C_{pn} values)
7	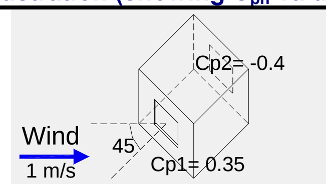
	Description: square, with 5 m length and 5 m height. (Room volume = 125 m^3).
8	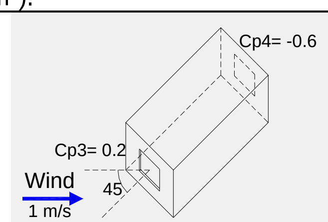
	Description: rectangular with 4 m length, 8 m width and 4 m height. (Room volume = 128 m^3).
9	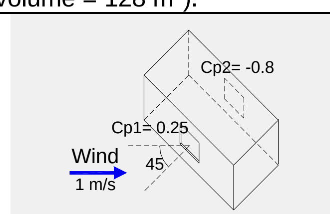
	Description: rectangular with 8 m length, 4 m width and 4 m height. (Room volume = 128 m^3).
* In all cases, openings are assumed opposite openings located in the windward and leeward facades, with equal areas of 4 m^2.	

Then, and using the same method explained in Section 5.3.1, internal pressure coefficients and airflow rate could be estimated. Table 5.9 shows the results of the calculation process. It is important to note that at oblique wind direction, effective area of a window is less. Knowing that wind angle is 45^{o}, window effective width can be simply calculated using Right Triangle Trigonometry. This width is 1.4 m. Thus, window effective area can be estimated by multiplying window width by its height, i.e. 1.4 * 2 = 2.8 m^2.

Table 5.9: Estimated internal pressure coefficients and airflow rates for cases 7 to 9 of the validation study

Case number	Opening number	A_{eff} (m^2)	C_{pn}	C_{pi}	Q_n (m^3/s)	Q_n (kg/s)
7	1	2.8	0.35	-0.025	1.53	**1.88**
	2	2.8	-0.4	-0.025	-1.53	**-1.88**
8	3	2.8	0.2	-0.2	1.52	**1.87**
	4	2.8	-0.6	-0.2	-1.52	**-1.87**
9	1	2.8	0.25	-0.275	1.75	**2.14**
	2	2.8	-0.8	-0.275	-1.75	**-2.14**

5.5 Prediction of airflow rate using CFD modelling, in the case of oblique wind direction

The same procedures followed in Section 5.3.2 will be implemented here. In Gambit software, rotating the room inside the ambient air in the required angle can be used to vary wind direction. This has been found to be useful solution, but requires a larger domain to ensure solution convergence. For example, the room in case 3 was placed in a box of square plan with length of 30 m and height of 20 m. This volume was enough for the solution to converge. If wind direction changed to 45°, extra sheer stresses, caused by the oblique building walls, cause reversed flows to occur. This leads the solution to diverge, and, therefore, made the use of a larger domain imperative. The domain was increased gradually until a size of 50 * 50 * 20 m was achieved.

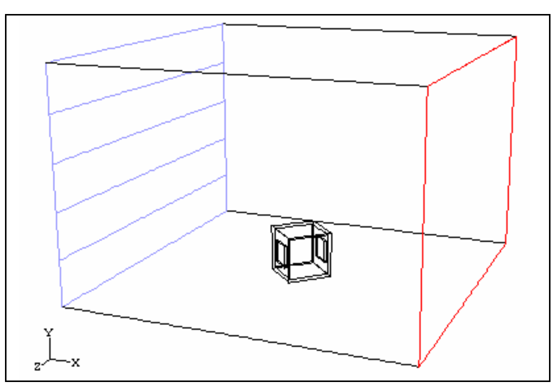

Figure 5.7: Solution domain for 45° wind direction

As has been discussed in Section 5.3.2, meshing such a large solution domain has been made considering time factor and the available computer speed. Mesh used here is a hex-map or sub-map mesh, with a node spacing of 0.6 m. The size of this mesh is 250,000 cells. Boundary conditions and case settings used are the same of the previous six cases, but with increasing turbulence intensity to be 10%, as a result of using a larger domain. Results obtained in the different cases are illustrated below.

Table 5.10: Inflow rates for cases 7 to 9 of the validation study, as obtained from Fluent 5.5 software

Case	Inflow rate (kg/s)
7	1.78
8	1.69
9	1.92

Figure 5.8 illustrates airflow pattern modelled for these three cases, represented by velocity magnitudes in 2-metre-height sections:

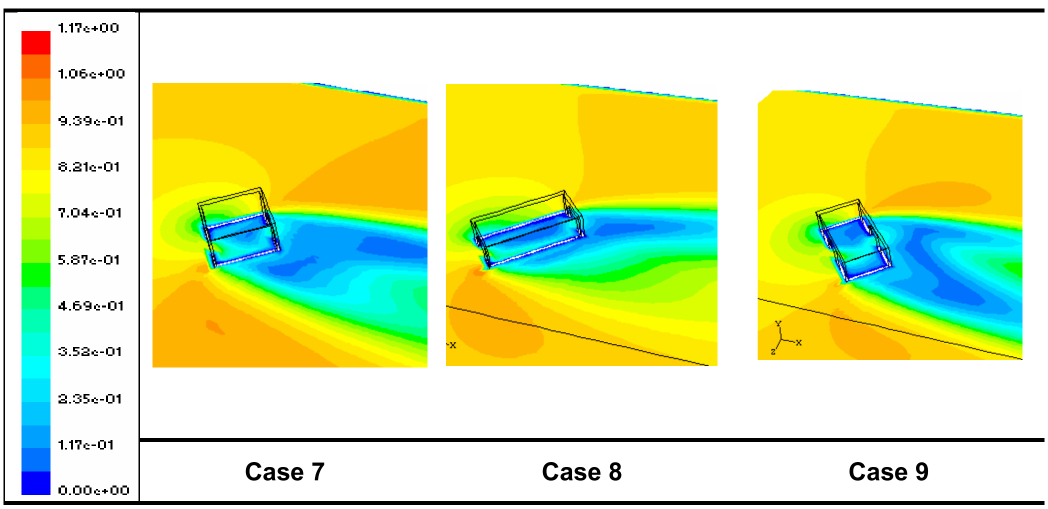

Figure 5.8: Airflow pattern, presented by contours of velocity magnitudes for cases 1, 3, and 5, with 45^o wind incident

5.6 Comparison between airflow rate prediction using Network and CFD models, in the case of oblique wind direction

Table 5.11 shows a comparison between results obtained from both mathematical model and CFD code for cases 7 to 9, using hex-map and sub-map meshes. Negative sign, if there is any, indicates that modelled value is less than predicted one. In general, this shows that a good agreement has been achieved.

However, discrepancy percentage in general is higher, compared to the case of normal wind direction, as illustrated in Table 5.7. CFD code used here is the same of that one used with the first six cases, in which less discrepancy has been observed. However, one difference here is the quality of the mesh used. The mesh used in cases 7 to 9 is a hex-map or sub-amp mesh. This mesh found to give convergence within an acceptable time and file size.

Table 5.11: Discrepancy percentage between estimated and modelled airflow rate for cases 7 to 9 of the validation study

Case number	Opening number	Airflow rate Q_n (kg/s) (CFD)	Airflow rate Q_n (kg/s) (Network)	Discrepancy (%)
7	1	1.78	1.88	**-5.6**
	2	-1.78	-1.88	
8	3	1.69	1.87	**-10.7**
	4	-1.69	-1.87	
9	1	1.92	2.14	**-11.5**
	2	-1.92	-2.14	

However, in the case of oblique wind direction, where buildings are rotated by 45^o inside the solution domain, tilted walls resulted in an obvious angular skew between edges in mesh cells. Skew between edges should not exceed the value of 0.75. However, lower values are recommended. For example, an excellent mesh has a skew less than 0.25 (Fluent Inc., 1988). Figure 5.9 illustrates that the skew observed in the current case is about 0.7.

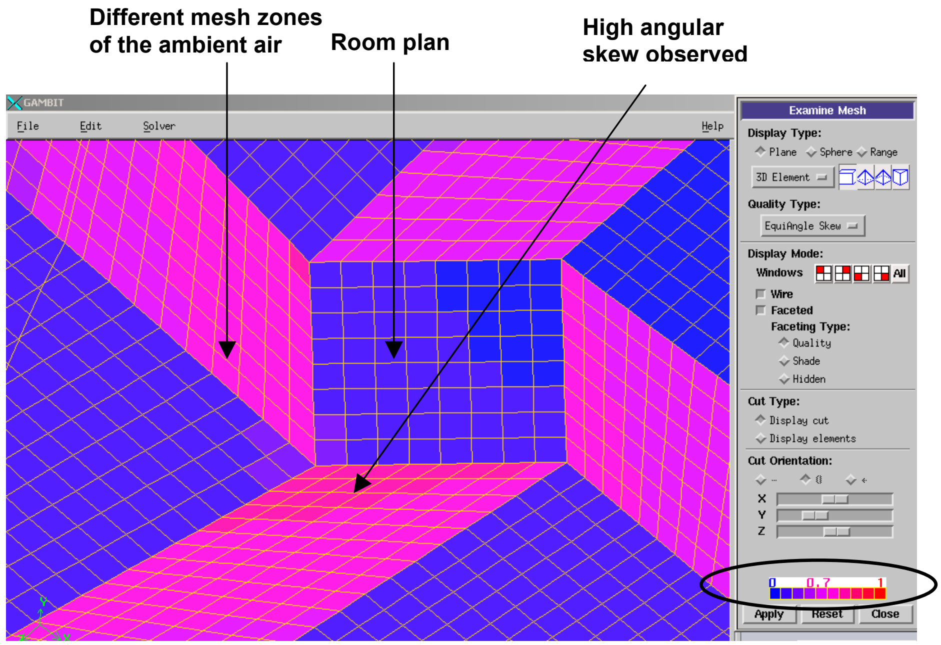

Figure 5.9: Skew observed in the hex-map and sub-map meshes used in the case of 45^o wind direction

Therefore, changing mesh type may improve the results obtained. Tetrahedral mesh has flexibility in meshing geometries having sharp edges, and therefore was chosen for meshing the ambient air zone, with a size of 1 m. However, hex-map mesh is still used for room interior, with a size of 0.5 m. As explained before, this size was used in order to cope with the available computing speed. The size of this mesh is 300,000 cells. Table 5.12 shows a recalculation of the comparison held between results obtained from both mathematical and CFD models in the case of oblique wind direction.

Table 5.12: **Discrepancy percentage between estimated and modelled airflow rate for cases 7 to 9 of the Validation Study, after changing mesh type**

Case number	Opening number	Airflow rate Q_n (modelled) (kg s-1)	Airflow rate Q_n (predicted) (kg s^{-1})	Discrepancy (%)
Case 7	1	1.84	1.88	**-2.2**
	2	-1.84	-1.88	
Case 8	3	1.83	1.87	**-2.2**
	4	-1.83	-1.87	
Case 9	1	2.26	2.14	**5.3**
	2	-2.26	-2.14	

Change of mesh type seems to have good effect, since discrepancy percentage has been significantly reduced in all the three cases. The remaining difference between the calculated and modelled airflow rates can be justified in the same way explained in Section 5.3. However, one more reason that may be added here is related to the pressure coefficient data used. These data were originally generated in wind tunnels for solid models.

According to Al-Qahtani (2000), air pressure distribution around a solid model changes if it is provided with openings. In the case of 45^o wind incidence, building model has two windward faces. In the case of a solid model, average pressure coefficient over these windward faces is the same for the square cases, and has a relatively small difference in the rectangular one, as illustrated in Table 5.1.

In the case of placing an opening at one of these two windward faces, it is expected that air pressure distribution will change, and there will be no more balance at its distribution on these two windward faces. This is because a solid windward face receives more wind deflection. On the opposite, a porous windward face receives less wind deflection, and therefore wind pressure will be less too.

To explain this, a look at pressure coefficient data related to square-plan buildings, illustrated at Table 5.1, shows that pressure coefficient values on the windward faces (faces 1 and 3) in case of 45^o wind direction are the same, i.e. +0.35. This is true for solid models. However, in the case of placing an opening in any of the building two windward faces, some change of surface pressure regime has been observed. Values of pressure coefficient for the two windward faces in Fluent have been found to be different, i.e. +0.28 for face 1, which has the window, and +0.32 for face 2, which is solid. This can be noted in Figure 5.10, which shows contours of static pressure magnitude.

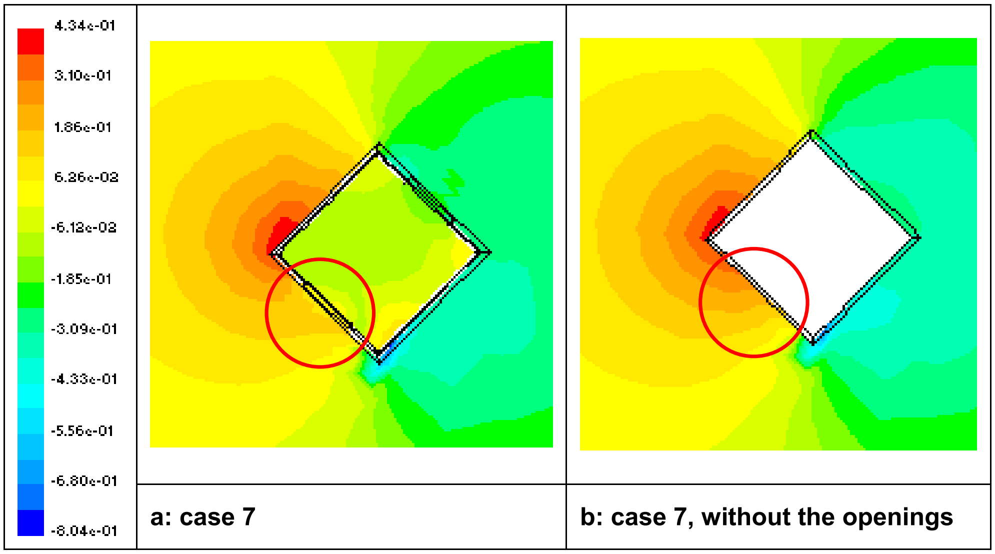

Figure 5.10: Contours of pressure magnitude, showing different pressure distributions in the modelled cases and the standard solid ones

5.7 Conclusions

In this chapter, validation of the CFD code that is used in the modelling study has been explained. This includes a comparison between the calculated airflow rate using the mathematical Network model and the modelled one using Fluent 5.5 software. Many cases with a variety in building geometry and wind velocity have been considered, which was a good opportunity to practice the use of the code prior to the modelling study.

This study has revealed that the choice of mesh type and size, in addition to the domain size is critical in three-dimensional CFD modelling. Results obtained support the use of the developed CFD code. The comparison between the mathematical and CFD models, in cases of normal and oblique wind directions, has shown a good agreement. This supports the reliability of the software and encourages further use of it in the investigation of wind-induced ventilation in buildings.

CHAPTER 6 : EFFECT OF DOME UTILISATION ON NATURAL VENTILATION PERFORMANCE

Introduction

This chapter aims to examine the potential of the dome, integrated with the main building volume, as a wind inducement device for natural ventilation. As introduced in Chapter 1, this will be demonstrated through a parametric approach and using CFD simulation. The literature review of this potential, introduced in Section 4.3, serves as an essential background of this chapter.

This chapter is divided into many sections. Firstly, the relevant climatic parameters, with a reference to the Middle East, are specified. Then, the geometrical parameters of the models tested are defined, and the parametric study programme is outlined. This programme compares building natural ventilation performance before and after dome utilisation for natural ventilation, considering different parameters, including: wind speed, wind direction, building form, and building plan area.

Results obtained from Fluent 5.5 software are then analysed in three main sections: airflow rate through the dome, airflow rate through wall openings, and airflow distribution in the occupied level of the building. This is expected to improve the understanding of natural ventilation performance in such building configurations, and to provide some design guidelines regarding the utilisation of domed roofs for natural ventilation in buildings.

6.1 Specification of the climatic parameters

For wind driven ventilation prediction, it is crucial to specify both wind speed and direction for the geographical site of interest. In environmental design research, two main approaches can be distinguished in this regard:

- Choice of a specific site as a reference of the study, and analysing the relevant climatic data of that site. This approach is very specific and its outputs are more accurate and practical. It is necessary to obtain data of the frequencies of occurrence of different wind speeds and directions. This is usually available from the local meteorological stations. This also helps establishing time-dependent results, which can be used to assess thermal comfort conditions.
- Choice of an entire climatic zone or a geographical region. Study results here are more general and usually based on some assumptions. They are also applicable wherever these climatic data occur.

The choice of the second approach is more appropriate for this study, which aims to deal with the research problem stated in Chapter 1 on a regional level. This is because the targeted architectural traditional elements are not only used in a specific city or country. Rather, they exist in many countries in the Middle East, and in a variety of local architectural styles. Nevertheless, the first approach mentioned above, still has its obvious importance and would be recommended for future studies for specific sites or cities.

6.1.1 Wind velocity

Depending on the previous argument, an appropriate climatic data can now be selected. To make this process logical, an overview on the study zone should be the first step. One suggested method is to use the average values of wind meteorological data in order to give some sense of the limits of that range. Wind atlases are usually used in this case. For example, the following map shows the global wind speed averages.

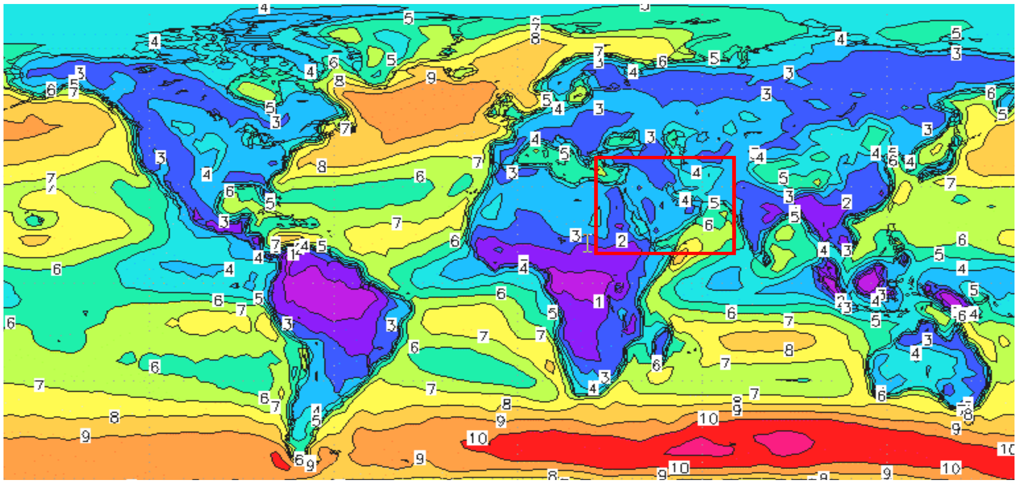

Figure 6.1: The mean wind speed in m/s measured at 10m above ground level for the period 1976-95, with Middle East region highlighted

Source: (Risø National Laboratory, 2006. Available online: http://www.windatlas.dk/World/Index.htm)

However, this method is inaccurate, because, on one hand, such maps give a broad outline of the global annual wind average speed. It is required to adapt these values, which are taken in the open country terrain, to consider the local terrain type. On the other hand, the use of these values is inappropriate in the case of passive cooling, which requires more specific data for summer months. Table 6.1 shows monthly average wind speed adapted to consider the city terrain for many cities in the study zone.

This table shows that wind speed data measured in the open country terrain vary in a wide range when compared with the similar data for the city terrain. In the latter case, wind speed varies between about 1.5 and 2.5 m/s. In summer period, it varies nearly within the same range, taking in account the majority of these values. However, these values cannot be used right now. As a common practice in building design, it is required to consider the worst cases, especially if they have a high frequency of occurrence. The worst cases can be those with very low wind speed value, which leads to overheat, or those with relatively high wind speed value, which leads to over draught. This requires details on the daily wind speeds.

Table 6.1: Average annual and monthly wind speed (m/s) for some capitals in the study zone for the Open Country and City terrains (at height of 10m)

Source: (Weatherbase, 2005. Available online: http://www.weatherbase.com). Adapted by the author

No	Country	City	Average wind speed (annual then monthly) for open terrains (m/s)												
			year	Jan	Feb	Mar	Apr	May	Jun	Jul	Aug	Sep	Oct	Nov	Dec
1	Bahrain	Manama	5.6	5.6	6.1	6.9	5.3	6.1	7.5	5.6	5.6	4.4	5.3	5.6	5.6
2	Egypt	Cairo	3.3	3.9	4.4	3.3	3.9	3.9	3.9	3.3	3.3	3.3	3.3	2.5	3.3
3	Iran	Tehran	5.3	5.3	5.3	5.6	6.9	6.1	5.6	4.7	3.3	4.7	5.6	5.6	5.6
4	Iraq	Baghdad	3.9	2.5	3.3	4.4	4.4	3.9	4.7	4.7	4.4	3.9	3.3	3.3	2.5
5	Jordan	Amman	4.4	4.7	5.3	4.7	4.7	4.7	4.4	4.4	3.9	3.9	3.3	4.4	4.7
6	Oman	Muscat	3.3	2.5	3.3	2.5	2.5	4.4	4.4	4.4	4.7	4.4	4.4	1.7	1.7
7	Saudi	Riyadh	3.9	3.3	3.9	3.9	4.4	4.4	5.3	4.7	4.7	4.4	2.5	2.5	3.3
8	Syria	Damascus	3.9	4.4	4.4	4.4	4.7	3.9	4.4	4.7	4.7	3.9	1.1	1.7	1.7
9	Turkey	Ankara	3.3	2.5	3.3	2.5	4.4	3.9	3.3	3.9	3.9	3.3	3.3	2.5	2.2
10	Yemen	Sanaa	4.7	3.9	5.3	5.3	4.4	4.4	4.7	4.7	5.3	4.7	4.4	3.9	3.9
No	Country	City	Average wind speed (annual then monthly) for city terrains (m/s)												
			year	Jan	Feb	Mar	Apr	May	Jun	Jul	Aug	Sep	Oct	Nov	Dec
1	Bahrain	Manama	2.5	2.5	2.7	3.1	2.4	2.7	3.4	2.5	2.5	2.0	2.4	2.5	2.5
2	Egypt	Cairo	1.5	1.7	2.0	1.5	1.7	1.7	1.7	1.5	1.5	1.5	1.5	1.1	1.5
3	Iran	Tehran	2.4	2.4	2.4	2.5	3.1	2.7	2.5	2.1	1.5	2.1	2.5	2.5	2.5
4	Iraq	Baghdad	1.8	1.1	1.5	2.0	2.0	1.7	2.1	2.1	2.0	1.7	1.5	1.5	1.1
5	Jordan	Amman	2.0	2.1	2.4	2.1	2.1	2.1	2.0	2.0	1.7	1.7	1.5	2.0	2.1
6	Oman	Muscat	1.5	1.1	1.5	1.1	1.1	2.0	2.0	2.0	2.1	2.0	2.0	0.7	0.7
7	Saudi	Riyadh	1.8	1.5	1.7	1.7	2.0	2.0	2.4	2.1	2.1	2.0	1.1	1.1	1.5
8	Syria	Damascus	1.7	2.0	2.0	2.0	2.1	1.7	2.0	2.1	2.1	1.7	0.5	0.7	0.7
9	Turkey	Ankara	1.5	1.1	1.5	1.1	2.0	1.8	1.5	1.8	1.8	1.5	1.5	1.1	1.0
10	Yemen	Sanaa	2.1	1.7	2.4	2.4	2.0	2.0	2.1	2.1	2.4	2.1	2.0	1.7	1.7

In fact, carrying out this work for such a wide geographical zone is an intensive statistical task, which is out of the scope of this study. Therefore, and as a common practice in ventilation studies, choosing a theoretical range with reasonable increment is an acceptable solution. Thus, the author suggests the use of two wind velocities that can represent climatic data analysed in Table 6.1. These two velocities are 1 and 3 m/s to represent respectively low and high wind speeds.

6.1.2 Wind direction

Usually, a theoretical range of wind directions with a reasonable increment is considered in natural ventilation research. This is to account for the different possible orientations of a building with respect to the prevailing wind direction, if there is any, or to deal with the different local wind directions. The author here suggests the use of three wind directions: 0^o, 45^o, and 90^o. In some cases, changing of wind direction from 0^o to 90^o is mainly intended for roof openings, and not for wall openings, which are symmetrical. Figure 6.2 shows the method of specifying wind directions with respect to building plan:

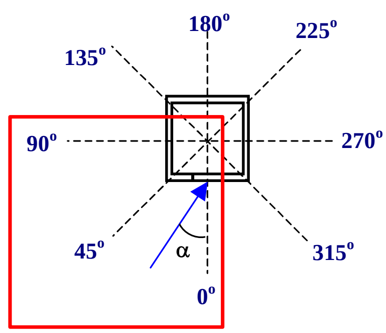

Figure 6.2: The three adopted wind directions of this study

6.2 Geometrical parameters

Concerning the main volume geometry, two common plan shapes are examined: square and rectangular forms. Generally, and assuming the case of single-cell building, cross ventilation is the most straightforward natural ventilation strategy (Smith, 2001). Thus, openings are provided in each of the four walls in order to examine the effect of the different possible wind directions. Implementation of cross ventilation strategy requires a shallow plan. A rule of thumb given by CIBSE (1997) states that cross ventilation is sufficient up to a building depth equals or less than five times its height. In fact, this rule of thumb cannot be taken as an absolute rule, since cross ventilation penetration into any space depends on wind speed and building shape as well. Therefore, modelled cases will include different depth values more and less than the CIBSE recommended value.

In the case of square-plan configurations, building relative length and width are equals. Their values are varied to be: 3H, 4H, and then 5H. This results in a plan area of 225, 400, and 625 m^2, respectively. In the case of rectangular-plan configurations, building relative length and width have been recalculated to give an equivalent area of the relevant square case, given that building aspect ratio is confined to 1:1.5. Recommended airflow rate is assumed to be 8 l/s per person. This value is recommended by CIBSE (1988, p. A1-9) for open-plan offices and other public building types, and will be assumed here as a rule of thumb. The floor plan area required for a person is assumed 1 m^2. Therefore, the required airflow rate can be presented for the floor plan area as 8 l/s per m^2.

The main volume height, H, it is usually specified according to the different architectural needs, like acoustics, lighting, and ventilation. As a general rule, buildings should have reasonable heights that are proportion to the plan area and number of occupants. In the design process for a specific case, it is possible to estimate the height according to the recommended volumetric ventilation rate in building codes. To explain that, and for an example, the minimum area required for a person in a rectangular hall is assumed 0.85 m^2, and the minimum ventilation rate 3 m^3/ hour/person. This means that hall minimum height is about 3 m^3 / 0.85 m^2 = 3.5 m. In this study, the height of the building will be assumed 5 m above the ground.

Porosity of the main volume is also assumed fixed. As a rule of thumb, recommended by Smith (2001), the minimum value required to implement cross ventilation is 5%. However, since the modelled building volume is higher than the normal one, due to its height and the additional volume of the dome, porosity will be assumed 10% of floor plan area.

The dome modelled here is a semi-spherical dome raised on a cylindrical base in which eight openings are placed to face the different possible wind directions. These openings are uniformly distributed with an increment of 45^o. Some previous studies, as mentioned in the up-to-date review in Chapter 5, investigated the potential of the dome with an opening at its apex. However, this study will examine the above-mentioned design, i.e. openings at dome nick instead of its apex, which is a common configuration in the contemporary architecture. Dome is centred on the flat roof of the main building volume. Relative dome diameter is calculated knowing the dome area, which is assumed 7.5% of the plan area. This gives an acceptable architectural proportion between the dome and the main volume. Thus, three diameters of the dome will be tested: 4.6, 6.2, and 7.8 m.

Porosity of the dome is assumed 13% of its plan area. This technically will allow eight openings at the dome base. Each opening is facing a different wind direction, with an increment of 45°. Figure 6.3 illustrates the resulting building configurations, in addition to the dome openings distribution. CAD illustrations with dimensions can be found in Section A.1 in Appendix A.

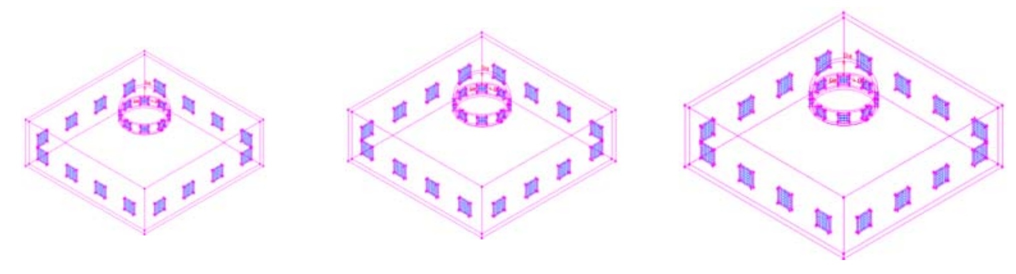

D1-s1	D2-s2	D3-s3
(Plan area = 225 m^2)	(Plan area = 400 m^2)	(Plan area = 625 m^2)

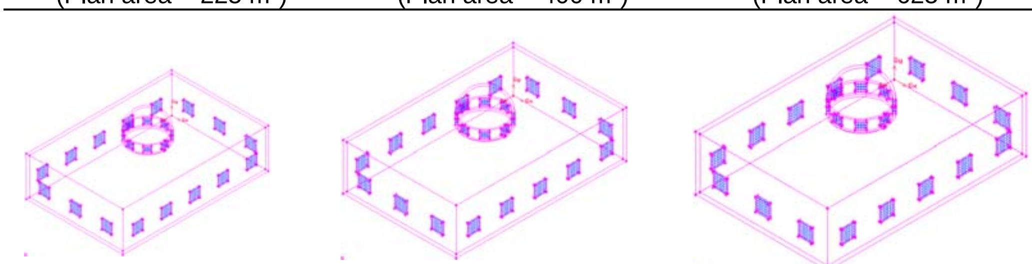

D1-r1	D2-r2	D3-r3
(Plan area = 225 m^2)	(Plan area = 400 m^2)	(Plan area = 625 m^2)

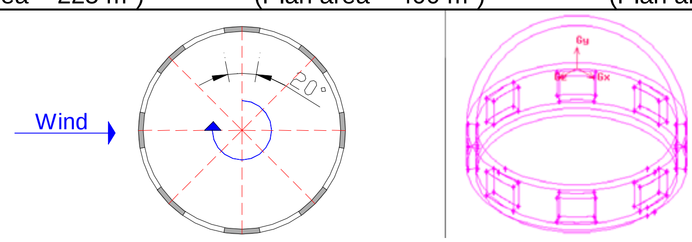

Figure 6.3: Different building configurations tested in the Dome Study, including illustration of the dome openings distributing

6.3 Dome modelling study: terminology and programme

The different cases are designated with a 'D' letter to refer to the dome study. This letter is associated with 'o' letter, to indicate that dome openings are opened, or 'c' letter, to indicate the opposite case. 'D' letter is followed by 's' or 'r' letters, in order to indicate, respectively, the square or rectangular form of the plan, which has also a serial number from 1 to 3 to indicate its area, i.e. 225, 400, or 625 m^2, respectively. Two more numbers follow this symbol: the first one indicates wind angle: 0, 45, or 90, and the second one indicates reference wind speed: 1 or 3. Figure 6.4 illustrates an example of this coding system.

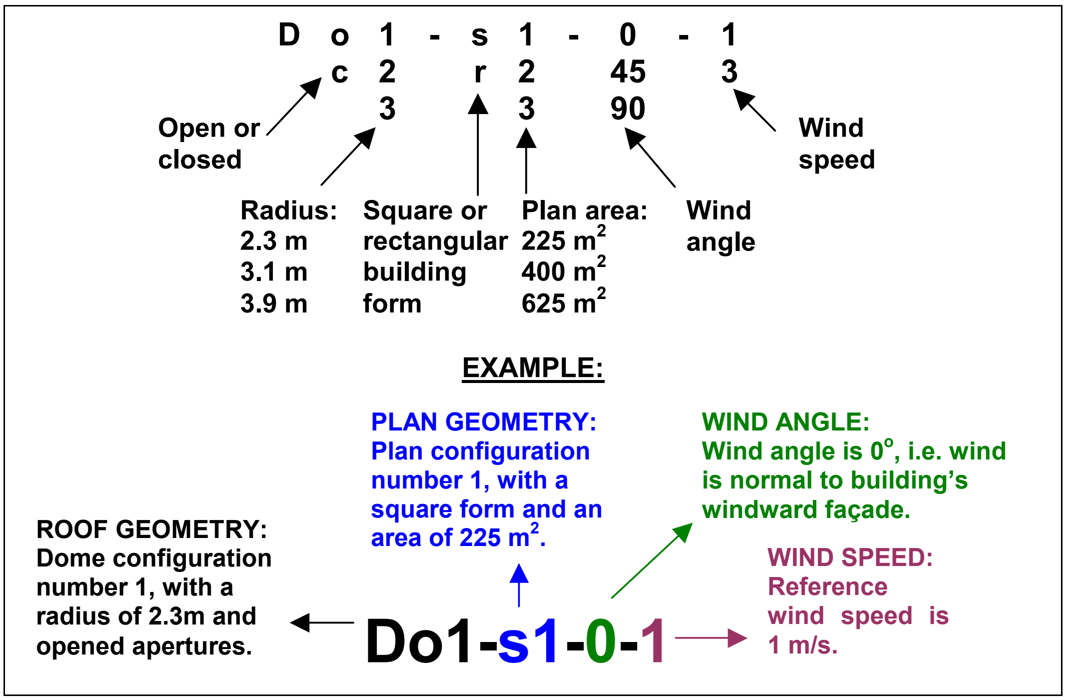

Figure 6.4: Coding method implemented in the Dome Study

Finally, it is important to note that the prototype considered here does not represent comprehensively all the possible design options. Nevertheless, it helps assessing many common design aspects, like: the use of wall openings for different building depths, the use of different building shapes, the use of dome openings for ventilation, and the effect of wind direction and speed. Table 6.2 lists the cases that are modelled in this study.

Table 6.2: Dome Study modelling programme

Config.	Description	Test no.	Test code	Wind angle	Wind speed (m/s)
D1-s1	**Form:** square. **Plan area:** 225m^2 **Wall opening area:** 22.5m^2 **Dome opening area:** 2.2m^2	1&2	Dc1-s1-0-1 & Do1-s1-0-1	0^o	1
		3&4	Dc1-s1-0-3 & Do1-s1-0-3	0^o	3
		5&6	Dc1-s1-45-1 & Do1-s1-45-1	45^o	1
		7&8	Dc1-s1-45-3 & Do1-s1-45-3	45^o	3
		9&10	Dc1-s1-90-1 & Do1-s1-90-1	90^o	1
		11&12	Dc1-s1-90-3 & Do1-s1-90-3	90^o	3
D2-s2	**Form:** square. **Plan area:** 400m^2 **Wall opening area:** 40m^2 **Dome opening area:** 3.9m^2	13&14	Dc2-s2-0-1 & Do2-s2-0-1	0^o	1
		15&16	Dc2-s2-0-3 & Do2-s2-0-3	0^o	3
		17&18	Dc2-s2-45-1 & Do2-s2-45-1	45^o	1
		19&20	Dc2-s2-45-3 & Do2-s2-45-3	45^o	3
		21&22	Dc2-s2-90-1 & Do2-s2-90-1	90^o	1
		23&24	Dc2-s2-90-3 & Do2-s2-90-3	90^o	3
D3-s3	**Form:** square. **Plan area:** 625m^2 **Wall opening area:** 62.5m^2 **Dome opening area:** 6.5m^2	25&26	Dc3-s3-0-1 & Do3-s3-0-1	0^o	1
		27&28	Dc3-s3-0-3 & Do3-s3-0-3	0^o	3
		29&30	Dc3-s3-45-1 & Do3-s3-45-1	45^o	1
		31&32	Dc3-s3-45-3 & Do3-s3-45-3	45^o	3
		33&34	Dc3-s3-90-1 & Do3-s3-90-1	90^o	1
		35&36	Dc3-s3-90-3 & Do3-s3-90-3	90^o	3
D1-r1	**Form:** rectangular. **Plan area:** 225m^2 **Wall opening area:** 22.5 m^2 **Dome opening area:** 2.2m^2	37&38	Dc1-r1-0-1 & Do1-r1-0-1	0^o	1
		39&40	Dc1-r1-0-3 & Do1-r1-0-3	0^o	3
		41&42	Dc1-r1-45-1 & Do1-r1-45-1	45^o	1
		43&44	Dc1-r1-45-3 & Do1-r1-45-3	45^o	3
		45&46	Dc1-r1-90-1 & Do1-r1-90-1	90^o	1
		47&48	Dc1-r1-90-3 & Do1-r1-90-3	90^o	3
D2-r2	**Form:** rectangular. **Plan area:** 400m^2 **Wall opening area:** 40m^2 **Dome opening area:** 3.9m^2	49&50	Dc2-r2-0-1 & Do2-r2-0-1	0^o	1
		51&52	Dc2-r2-0-3 & Do2-r2-0-3	0^o	3
		53&54	Dc2-r2-45-1 & Do2-r2-45-1	45^o	1
		55&56	Dc2-r2-45-3 & Do2-r2-45-3	45^o	3
		57&58	Dc2-r2-90-1 & Do2-r2-90-1	90^o	1
		59&60	Dc2-r2-90-3 & Do2-r2-90-3	90^o	3
D3-r3	**Form:** rectangular. **Plan area:** 625m^2 **Wall opening area:** 62.5m^2 **Dome opening area:** 6.5m^2	61&62	Dc3-r3-0-1 & Do3-r3-0-1	0^o	1
		63&64	Dc3-r3-0-3 & Do3-r3-0-3	0^o	3
		65&66	Dc3-r3-45-1 & Do3-r3-45-1	45^o	1
		67&68	Dc3-r3-45-3 & Do3-r3-45-3	45^o	3
		69&70	Dc3-r3-90-1 & Do3-r3-90-1	90^o	1
		71&72	Dc3-r3-90-3 & Do3-r3-90-3	90^o	3

6.4 Computer modelling considerations

The relevant modelling procedures using Fluent 5.5 software have been explained in Section 3.4 of Chapter 3 and validated in Chapter 5. Thus, this section only presents some special considerations that have been applied in the modelling study. One of the main challenges in this study is to simulate the ambient air around the building and to create an appropriate mesh in terms of quality and resolution. To overcome these challenges, an extensive work has been carried out prior to the modelling study to demonstrate the different available options. This has been done in terms of:

6.4.1 Size of the solution domain

It is important to find the minimum dimensions of this three-dimensional domain in order to account for mesh size. This has been found to be 3.75 times the length of the longest side of the building. This is in the case of 0^o wind incidence. In the case of oblique wind incidence, this value should be increased up to 6 times the length of the longest side of the building. The height of the ambient air box is 4 times the building height, i.e. 20 m in all cases. In the case of 0^o and 90^o wind incidence, the ambient air is divided into two zones: Ambient1, which is closer to the building, and Ambient2. In the case of 45^o wind incidence, it is divided into 3 zones, to allow for a further hierarchy in mesh size, as shown below.

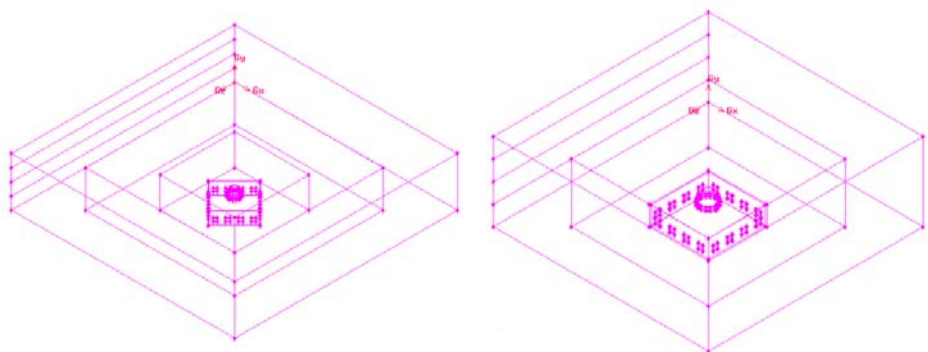

Figure 6.5: Method of dividing the ambient air in the case of normal and non-normal wind directions

6.4.2 Mesh size and resolution

Size and type of calculation mesh should be chosen to give an acceptable resolution within the available computer memory and speed. In this study, the maximum possible mesh size is about ½ million cells. Thus, all cases should be managed to fall within this range. As wall openings along building perimeter are not the same, symmetry boundary type cannot be a solution. Therefore, and as explained in Section 5.2.2, a hierarchy in mesh size has been created. Mesh type used is the tetrahedral one, which found to be appropriate for meshing the curved dome surface. However, this type gives a larger mesh size, nearly the double of the hex-map type, since its basic unit has less volume. This means that tetrahedral mesh with a size of 0.4 m is nearly equivalent in terms of resolution to a hex-map mesh with a size of 0.2 m.

Extra care has been given to the mesh of building openings, where airflow rate is recorded. Hex-map mesh has been used in these openings with a size of 0.2 m.

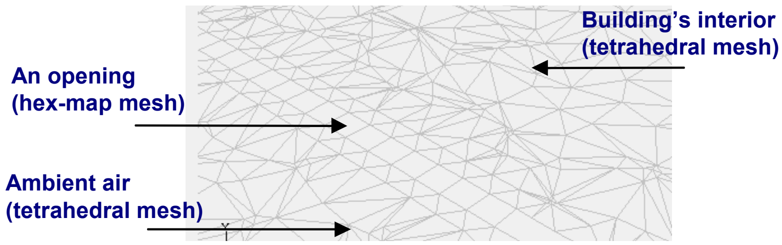

Figure: 6.6: Mesh size is finer within the building openings zone

It is worth mentioning here that files total size of cases involved in this modelling study, as listed in Table 6.2, is 6.4 GB. Table 6.3 list the different mesh sizes used for each case in this study:

Table 6.3: different mesh sizes used in the cases listed in Table 6.1

Wind direction	Building configuration	Mesh size in different building zones (m)					Approx. mesh volume (cell)
		Building openings	Building interior	Ambient air 1	Ambient air 2	Ambient air 3	
Normal wind incidence	D1-s1	0.2	0.6	1.2	1.8	-	300,000
	D2-s2	0.2	0.6	1.2	1.8	-	350,000
	D3-s3	0.2	0.6	1.2	1.8	-	480,000
	D1-r1	0.2	0.6	1.2	1.8	-	250,000
	D2-r2	0.2	0.6	1.2	1.8	-	425,000
	D3-r3	0.2	0.6	1.4	2.2	-	460,000
90° wind incidence	D1-s1	0.2	0.6	1.2	1.8	-	300,000
	D2-s2	0.2	0.6	1.2	1.8	-	350,000
	D3-s3	0.2	0.6	1.2	1.8	-	480,000
	D1-r1	0.2	0.6	1.2	1.8	-	250,000
	D2-r2	0.2	0.6	1.2	1.8	-	410,000
	D3-r3	0.2	0.6	1.4	2.2	-	470,000
45° wind incidence	D1-s1	0.2	0.6	1.2	1.2	1.8	400,000
	D2-s2	0.2	0.6	1.2	1.8	1.8	460,000
	D3-s3	0.2	0.8	1.6	2.4	3.2	300,000
	D1-r1	0.2	0.6	1.2	1.8	1.8	360,000
	D2-r2	0.2	0.8	1.6	1.6	2.4	480,000
	D3-r3	0.2	0.8	1.6	2.4	3.2	370,000

6.4.3 Air velocity variation with height

Wind velocity varies with the height above ground. Depending on the urban site roughness, wind velocity profile can be identified. This has been theoretically explained in Section 3.1.1. The adopted method for simulating this profile in Fluent software has been explained in Section 5.2.1. The profile that is used here is the

'City' profile, which assumes that the building is exposed to a wind speed that is modified by a city-like terrain. Table 6.4 shows velocity values for each sub-inlet used in this study.

Table: 6.4: Air velocities for different heights used in CFD modelling

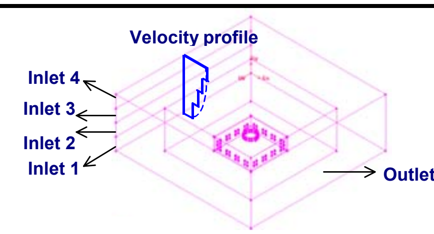

Height above the ground (m)	Velocity sub-inlet number	Reference velocity magnitude, V_r	
		1 m/s	3 m/s
5	1	0.894	2.682
10	2	1.006	3.018
15	3	1.078	3.234
20	4	1.132	3.396

6.4.4 Under-Relaxation Factors

Segregated Solver uses Under-Relaxation Factors to control the update of the computed variables iteratively. In few cases, and when the solution starts to progress very slowly towards the conversion, values of these factors have been adapted. It is recommended by Fluent Inc. (1998) to reduce values of these factors from their default values to values not less than 0.2, 0.5, 0.5, and 0.5 for pressure, momentum, k, and ε respectively. This speeds up the convergence and saves time.

6.4.5 Presentation of results

Two output types will be mainly used to analyse the modelling results in terms of airflow quantity and distribution: airflow rate and contours of velocity magnitudes. Airflow rate will be recorded for the four facades of the building. Inflow rate will be indicated by a positive sign and vice versa. This is also the case for the dome openings. Values obtained from Fluent are for mass flow rate in (kg/s). These values have been converted to volumetric flow rate in l/s to facilitate data processing, since mass flow rate usually possesses small values. Then, the resulting volumetric flow rate has been normalised for the floor unit area in order to establish the comparison between the different configurations tested in this study.

Thus, the average volumetric flow rate for the unit area of the building floor has been computed. This has also the advantage of relating the obtained results to the building capacity and natural ventilation standards, which specify the required airflow rate for the unit area as discussed in Section 6.2. It is important here to mention that this study is not a design project. This means that the main concern here is to observe the effect of specific parameters on building natural ventilation performance; regardless of the actual obtained values. In order to calculate airflow rate for every opening, these openings have been named, as presented Figure 6.7. Concerning contours of velocity magnitude, values have been recorded over two planes: Plane 1, which represents x-z plane at window-level (assumed 1.7m above the ground) and Plane 2, which represents y-x plane passing at the dome mid-axis, and following wind direction, as illustrates below.

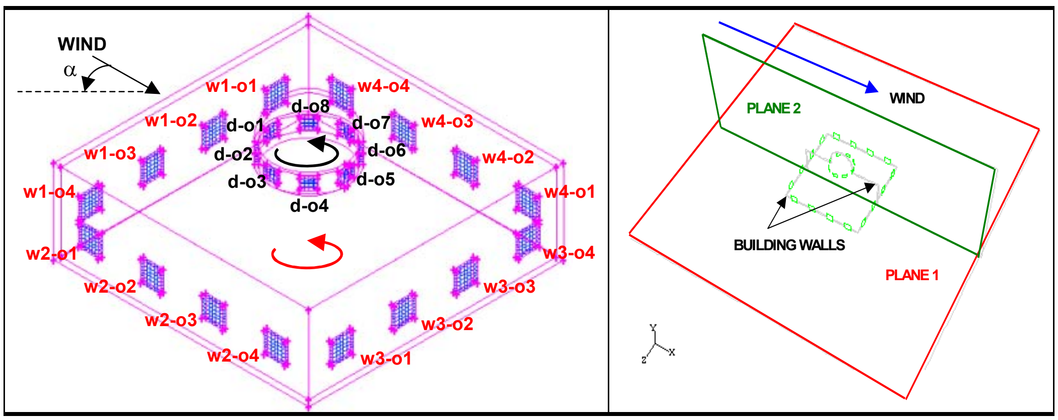

Figure 6.7: Method adopted to name different openings and planes in the modelling study

Table 6.5 summarises numerically airflow rates estimated, which shows the reliability of the results obtained according to the Law of Conservation of Mass. The following two sections discuss ventilation performance before and after the utilisation of the dome for natural ventilation in the different cases illustrated in Table 6.2. This compares:

- Square and rectangular-plan shapes.
- Normal and oblique wind directions.
- Relatively low and high wind speeds.
- Opened and closed dome openings.

Table 6.5: Summary of airflow rates recorded in the different cases modelled in the Dome Study, where dome openings are utilised for natural ventilation

	Wind angle 0^o Wind velocity 3 m/s					Wind angle 45^o Wind velocity 3 m/s					Wind angle 90^o Wind velocity 3 m/s				
Case Code	**Inflow (dome)**	**Inflow (walls)**	**Outflow (dome)**	**Outflow (walls)**	**Total**	**Inflow (dome)**	**Inflow (walls)**	**Outflow (dome)**	**Outflow (walls)**	**Total**	**Inflow (dome)**	**Inflow (walls)**	**Outflow (dome)**	**Outflow (walls)**	**Total**
Do1-s1	0.13	54.54	-10.66	-44.01	**0.00**	3.87	64.38	-13.84	-54.41	**0.00**	0.13	54.54	-10.66	-44.01	**0.00**
Do2-s2	0.49	54.15	-8.49	-46.16	**-0.01**	3.06	65.66	-11.23	-57.49	**0.00**	0.49	54.15	-8.49	-46.16	**-0.01**
Do3-s3	0.47	54.85	-7.10	-48.22	**0.00**	2.52	66.92	-9.36	-60.09	**-0.01**	0.47	54.85	-7.10	-48.22	**0.00**
Do1-r1	0.00	66.06	-14.23	-51.83	**0.00**	3.77	65.61	-13.51	-55.89	**-0.02**	1.34	39.31	-8.12	-32.55	**-0.02**
Do2-r2	0.00	66.40	-10.83	-55.56	**0.01**	3.08	66.42	-10.80	-58.70	**0.00**	0.71	40.03	-6.52	-34.22	**0.00**
Do3-r3	0.00	66.44	-9.23	-57.21	**0.00**	2.31	66.39	-8.60	-60.09	**0.01**	0.77	40.39	-5.75	-35.41	**0.00**

* All values are in $(l/s)/m^2$.

6.5 Airflow rate through dome openings

It has been found that ventilation performance varies for different building geometries and different wind speeds. However, the effect of these parameters was not as dramatic as the effect of wind angle. Therefore, the following analysis will be presented according to the different considered wind directions. It has been observed that all the dome openings, except of the one that is normal to the wind, function in the suction mode. Data presented below show outflow rate as a total of these openings. Thus, the main focus in the following analysis will be the role of the dome in inducing airflow from buildings. Some numerical examples are given. However, all other values can be found by referring to appendices A.2 and A.3.

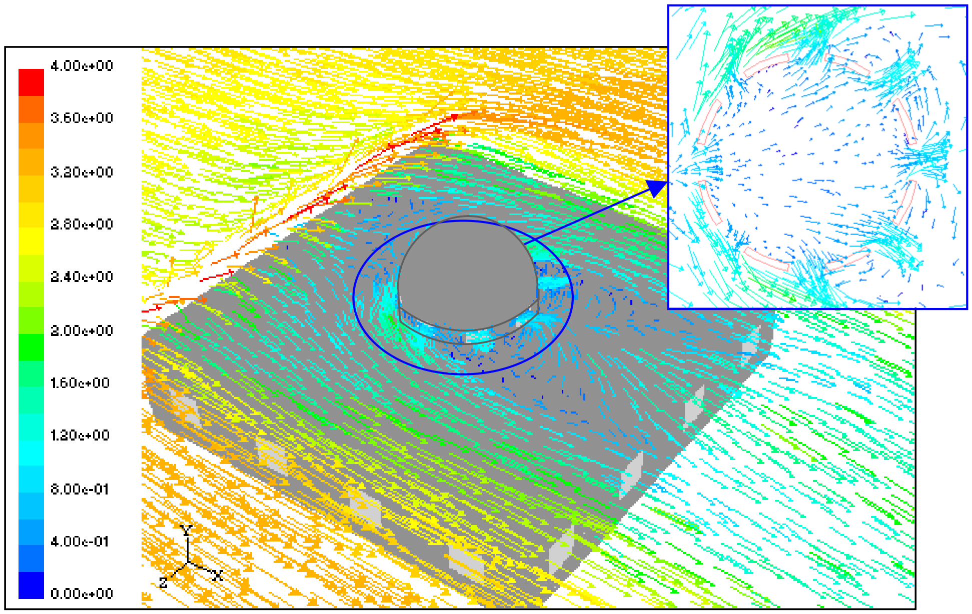

Figure 6.8: Airflow pattern over building roof, as illustrated by air velocity vectors (m/s), showing that dome openings function mainly in suction

6.5.1 In the case of 0° wind incidence

Figure 6.9 summarises airflow rates recorded for the different configurations tested, and for both 1 and 3 m/s air velocities.

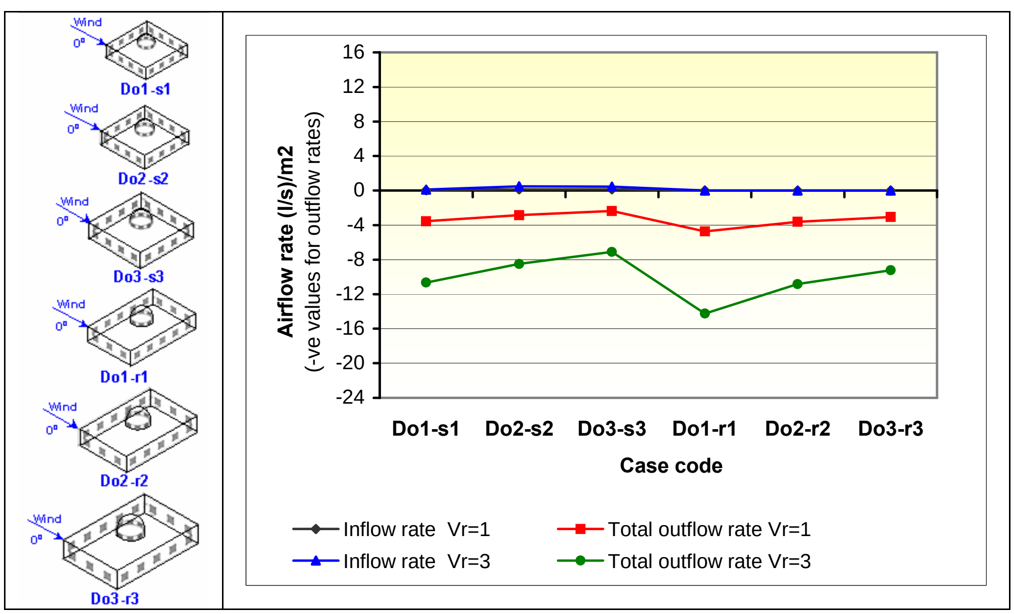

Figure 6.9: Volumetric airflow rates through dome openings presented for building unit area for 0° wind angle and 1 and 3 m/s reference wind velocities

Figure 6.9 shows that all configurations recorded, generally, the same outflow rate behaviour at both reference wind speeds. Outflow rate through the dome decreases as building area, or depth, increases. This behaviour is more pronounced in the case of high wind speed. For example, in the case of square configurations and 3m/s wind speed, outflow rate drops from –10.66 to –7.1 (l/s)/m^2, with a difference of about 33%. The reason is that any increase in the plan area means that the distance between the dome body and the roof windward sharp edge will increase. Accordingly, this reduces the intensity of the negative pressure field surrounding the dome, which reduces its potential for suction. This is illustrated in Figure 6.10.

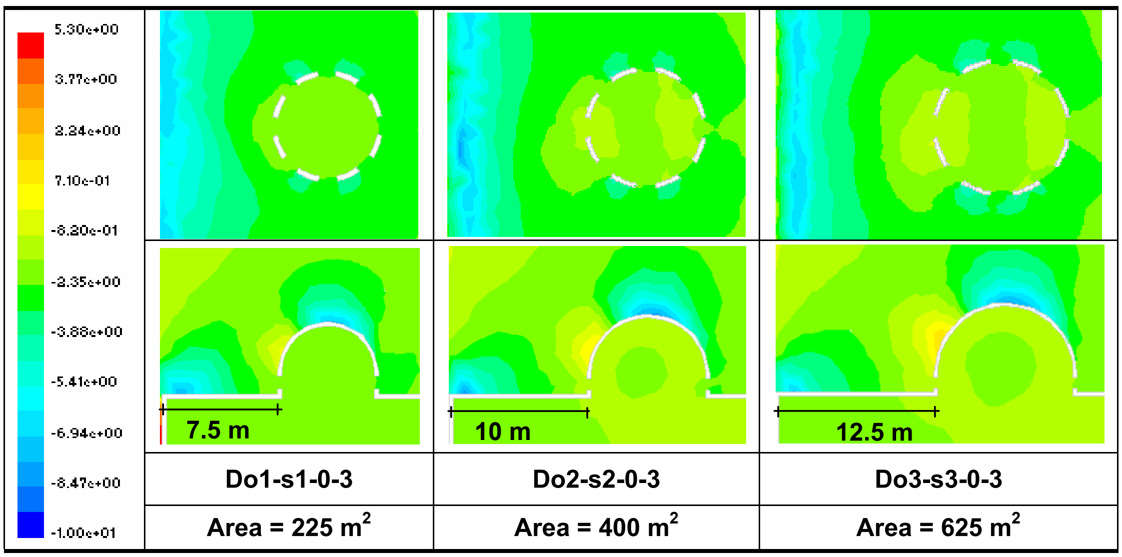

Figure 6.10: Contours of static pressure magnitude (Pa) in roof level of the indicated cases, showing that pressure magnitude inside and around the dome increases as building area increases

This is also true for the rectangular cases. For example, in the case of 3m/s wind speed, the dome has an average outflow rate range from –14.23 to -9.23 (l/s)/m^2, with a difference of about 35%. However, outflow rate recorded higher values in these cases. This is because the effect of airflow separation at the roof sharp edge is stronger here. This may be due to two reasons:

- The distance between the dome centre and the windward edge is shorter (compared to the square cases, as illustrated in Figure 6.10). This equals 6.1, 8.15, 10.2 m for cases Do1-r1, Do2-r2, and Do3-r3, respectively.
- Rectangular cases generally are characterised as elongated geometries. This means that airflow prefers to blow above the building instead of around it, following the fewer resistance. This increases the intensity of airflow separation

and, therefore, the local suction forces around the dome.

Concerning inflow rate, Figure 6.9 shows that inflow rate through the dome inlet has recorded a low value in the square configurations at both reference wind velocities. This can be explained by the existence of a trapped air vortex in the corner between the flat roof and the dome cylindrical base, in which dome openings are located. Air vortex may be defined as "a rotating mass of air, which eventually dissipates its energy by friction in turbulence" (Bain *et al.,* 1971, p.15). It is possible to observe air vortices in many places, including building roof, corners, and wake region. Also, it is usually associated with airflow separation, which is the case here. However, in the case of shorter distance between the dome inlet and the building windward edge, like rectangular cases, this vortex has more kinetic energy, which reduces the potential of air to penetrate the dome inlet. In general, this vortex can be considered as an advantage because it increases the potential of the dome for air suction.

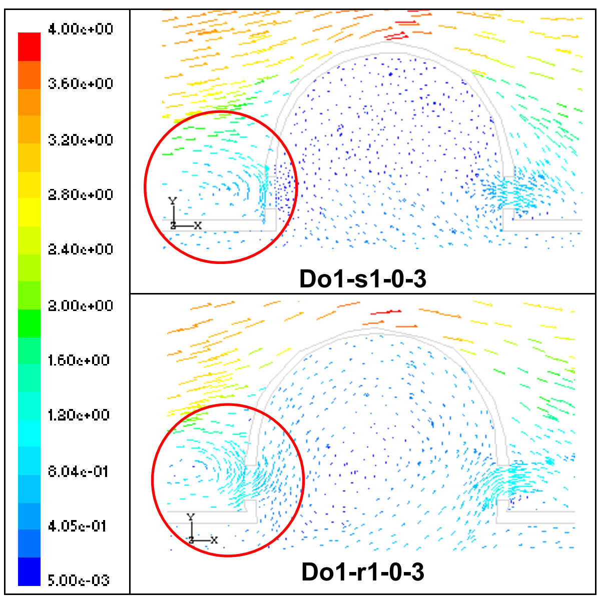

Figure 6.11: Velocity vectors for the indicated cases at 0° wind angle, showing a stronger air vortex before the dome inlet in cases that have smaller area

In order to explore airflow rate behaviour under different reference velocities, cases Do2-s2-0 and Do2-r2-0 have been modelled again, with a reference wind velocity of 5 m/s. Figure 6.12 shows that the relationship between outflow rates recorded at the dome outlets, and the different reference wind velocities of 1, 3, and 5 m/s, is a linear relationship, which has been found to be consistent with the other results obtained through out this study. This, for example, can be noticed in Section A.3 of Appendix A. However, increasing wind velocity has more effect on the rectangular-plan case, since dome is more affected by suction forces resulting from airflow separation over the windward sharp edge of the building, as has been explained in this section.

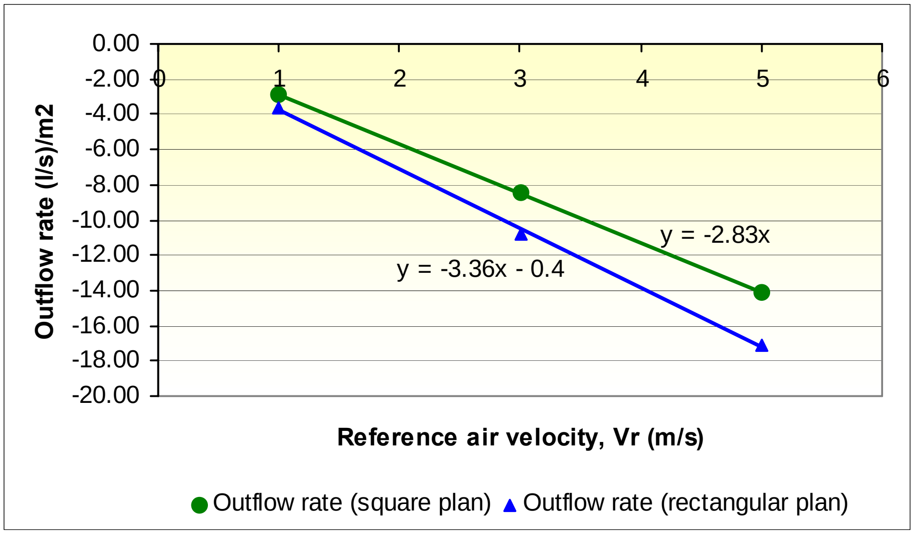

Figure 6.12: Relationship between average airflow rates through dome openings and reference wind velocity, at 0^{o} wind angle, and for the indicated cases

6.5.2 In the case of 45^{o} wind incidence

Figure 6.13 summarises airflow rates recorded for the different configurations tested, and for both 1 and 3 m/s air velocities. Outflow rate values present the same behaviour observed in the case of 0^{o} wind direction, i.e. it is inversely proportional to the area of the building. This can be interpreted in the same way explained in the previous wind direction. It has been explained in Section 6.5.1 that the high value of outflow rate through dome opening in the case of 0^{o} wind direction is caused by airflow separation over the windward sharp edge of building main volume. This is also true in the case of 45^{o} wind incidence, but with some differences. Airflow here is generally attached on the two upstream building faces and then separates at the outer corners. According to Merony (1982) this forms a wide re-circulating wake region, associated with strong and persistent air vortices along the windward roof edges. This encourages air local suction through dome openings and increases outflow rates through the dome.

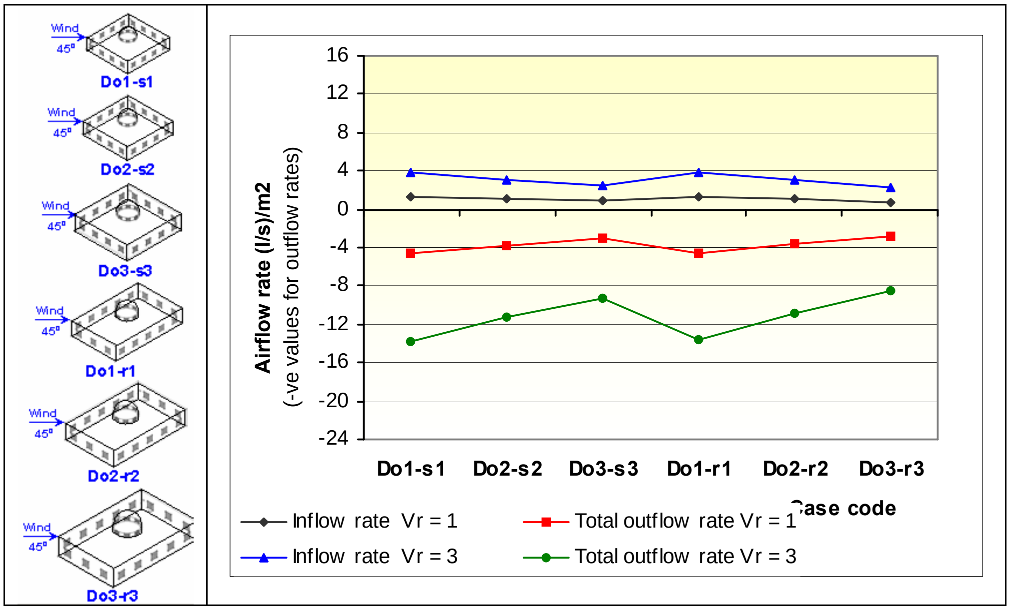

Figure: 6.13: Volumetric airflow rates through dome openings presented for building unit area for 45^{o} wind angle and 1 and 3 m/s reference wind velocities

This airflow separation seems to have the same effect of the one observed in the normal wind direction in the case of rectangular building form, since outflow rate values are nearly the same at both cases for both wind velocities tested. However, outflow rate here has increased by about 30% in the square cases, which indicates more effect of airflow separation in this wind direction. Considering the net outflow rate, dome potential for suction at both square and rectangular cases has been negatively affected by the observed higher inflow rate, compared to the case of 0^{o} wind direction. This is because it has been observed that airflow that enters through the dome inlet leaves through its outlets, which reduces the potential of the dome for air suction. This higher inflow rate is because no frontal air vortices have been observed, which is not the case in the normal wind direction. Therefore, airflow move freely to penetrate the dome inlet, as illustrated in Figure 6.14.

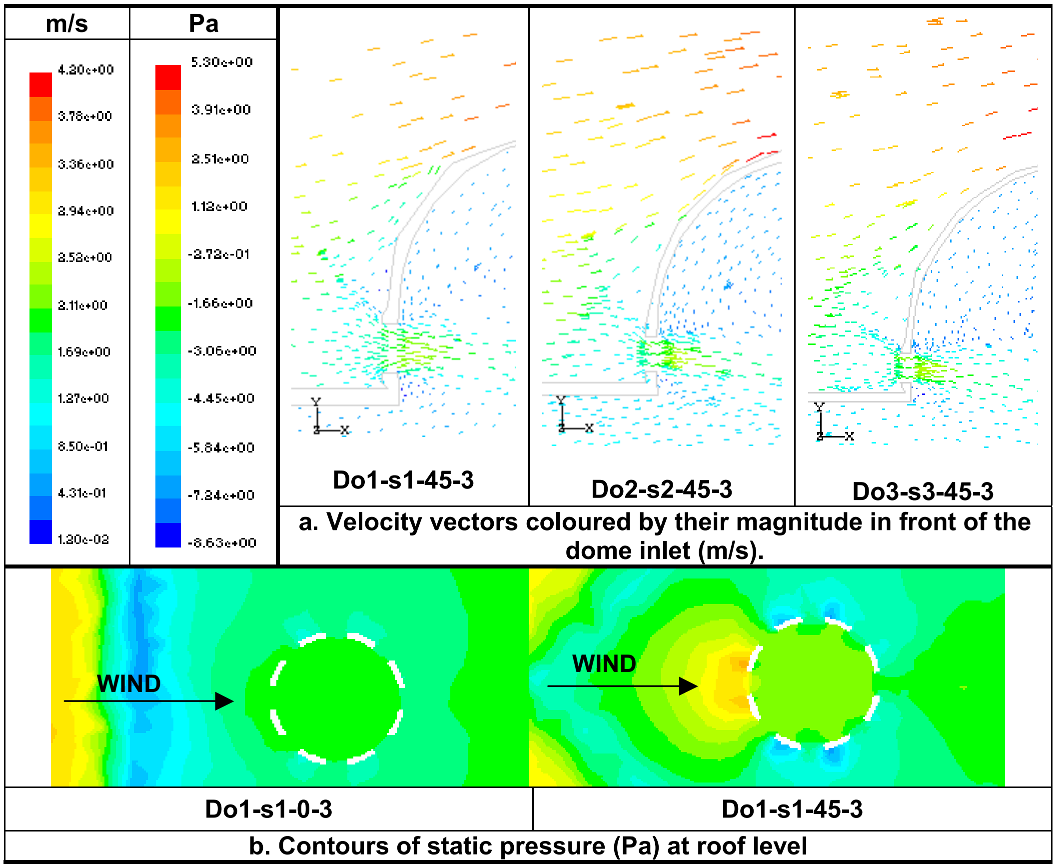

a. Velocity vectors coloured by their magnitude in front of the dome inlet (m/s).

b. Contours of static pressure (Pa) at roof level

Figure 6.14: No air vortex has been observed before the dome inlet in the case of 45° wind direction, which results in a higher air pressure acting on this inlet

This means that closing the dome opening that faces the wind is expected to increase the net outflow rate. This has been done for cases Do2-s2-45-3 and Do2-r2-45-3. Results observed showed that the net outflow rate through the dome has increased by about 25% at both square and rectangular cases. Net outflow rate has increased from 8.2 to 10.6 (l/s)/m^2 in the square case, and from 7.7 to 10.2 (l/s)/m^2 in the rectangular case. This has positively affected airflow rates through wall openings, as discussed in Section 6.6.2. Generally, inflow and outflow rates have presented a regular behaviour, compared to the 0° wind direction. Inflow rate value decreases when the plan area increases. This indicates that the suction force acting on the dome outlets openings induces inflow rate through the dome inlet. This behaviour occurs in a higher rate in the case of a higher wind velocity.

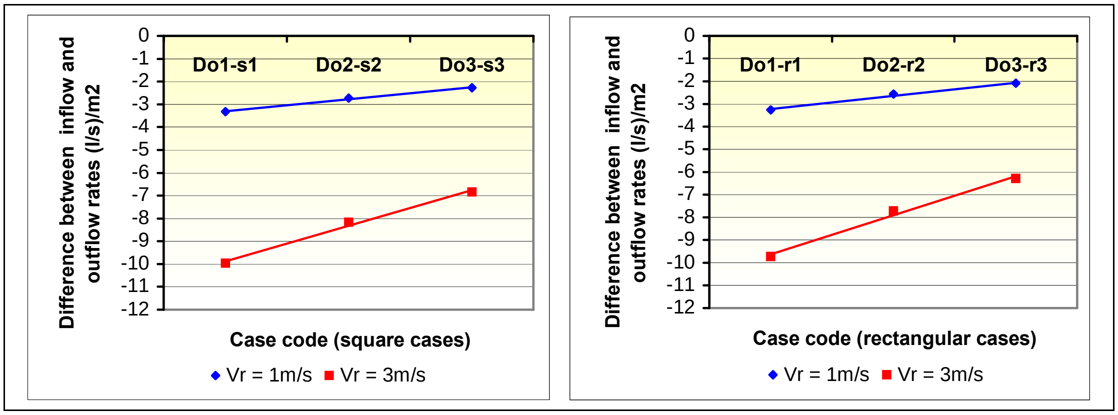

Figure 6.15: A uniform relationship has been observed between volumetric inflow and outflow rates in the case of 45° wind direction

6.5.3 In the case of 90° wind incidence

Figure 6.16 summarises airflow rates recorded for the different configurations tested, and for 1 and 3 m/s air velocities.

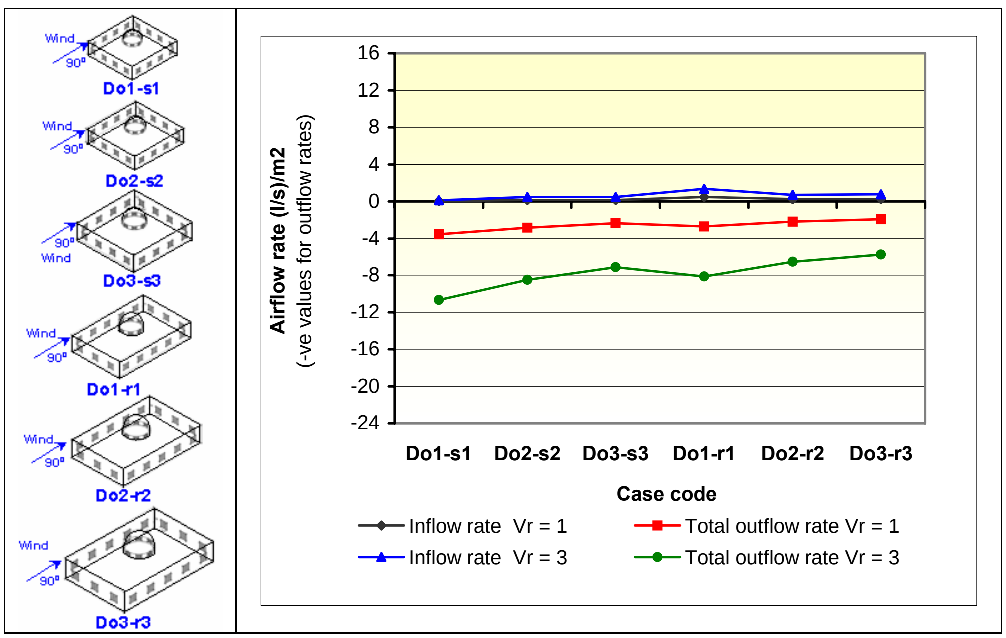

Figure: 6.16: Volumetric airflow rates through dome openings presented for building unit area for 90° wind angle and 1 and 3 m/s reference wind velocities

Outflow and inflow rate values in the square cases show the same behaviour presented and discussed in the case of normal wind direction. This is because square cases are symmetrical around both their axes. Unlike the case of 0° wind direction, net outflow rate in the rectangular cases, compared to the square ones, presented fewer values (less by 30%), due to the significant increase in plan depth in this orientation. This causes airflow to lose more kinetic energy before it reaches the dome. This long distance results also in a positive inflow rate due to the absence of the air vortex that has been observed in the case of normal wind direction.

6.6 Effect of dome utilisation on airflow rate through wall openings and internal airflow distribution

Mass flow rate through every opening of the 16 wall openings in every case has been computed by Fluent software. It has been then converted to volumetric flow rate and averaged for the unit area, as discussed in Section 6.5. All of these airflow rate values can be comprehensively found in Appendix A.2. Figures 6.17 and 6.18 compare this average airflow rate in the case of closed and opened dome windows. Thus, this will help demonstrating the effect of the utilisation of dome openings on airflow rates through wall openings, which are located around the occupied level of the building. This leads to assess airflow distribution in that level. To assess airflow distribution at building interior, contours of air velocity magnitudes have been used, since air velocity is a main factor that affects thermal comfort. This technique in Fluent software presents air velocity distribution on a defined plane and according to a defined velocity scale. The default range of this scale has been used, which consists of 20 air velocities. The minimum is always 0 and the maximum has been unified for all cases possessing the same reference velocity.

To give this analysis ‘more value’, a numerical criterion has been adopted in order to calculate the plan-area that have the same air velocity. Knowing the total plan area, area of every internal velocity zone has been estimated as a percentage of the total plan area. This has been done using AutoCAD software, where any air velocity zone can be traced following Fluent contour lines in order to calculate its area. To carry out this task, internal air velocities recorded on the horizontal, Plane 1, has been divided into four zones, which has been found to be reasonable and practical, as illustrated in Figure 6.20, and for both reference air velocities tested in this study. As both low and high reference air velocities have resulted in the same airflow rate and distribution behaviours, numerical examples given in the following discussion are limited to the high air velocity, where differences between different values observed are easier to be distinguished.

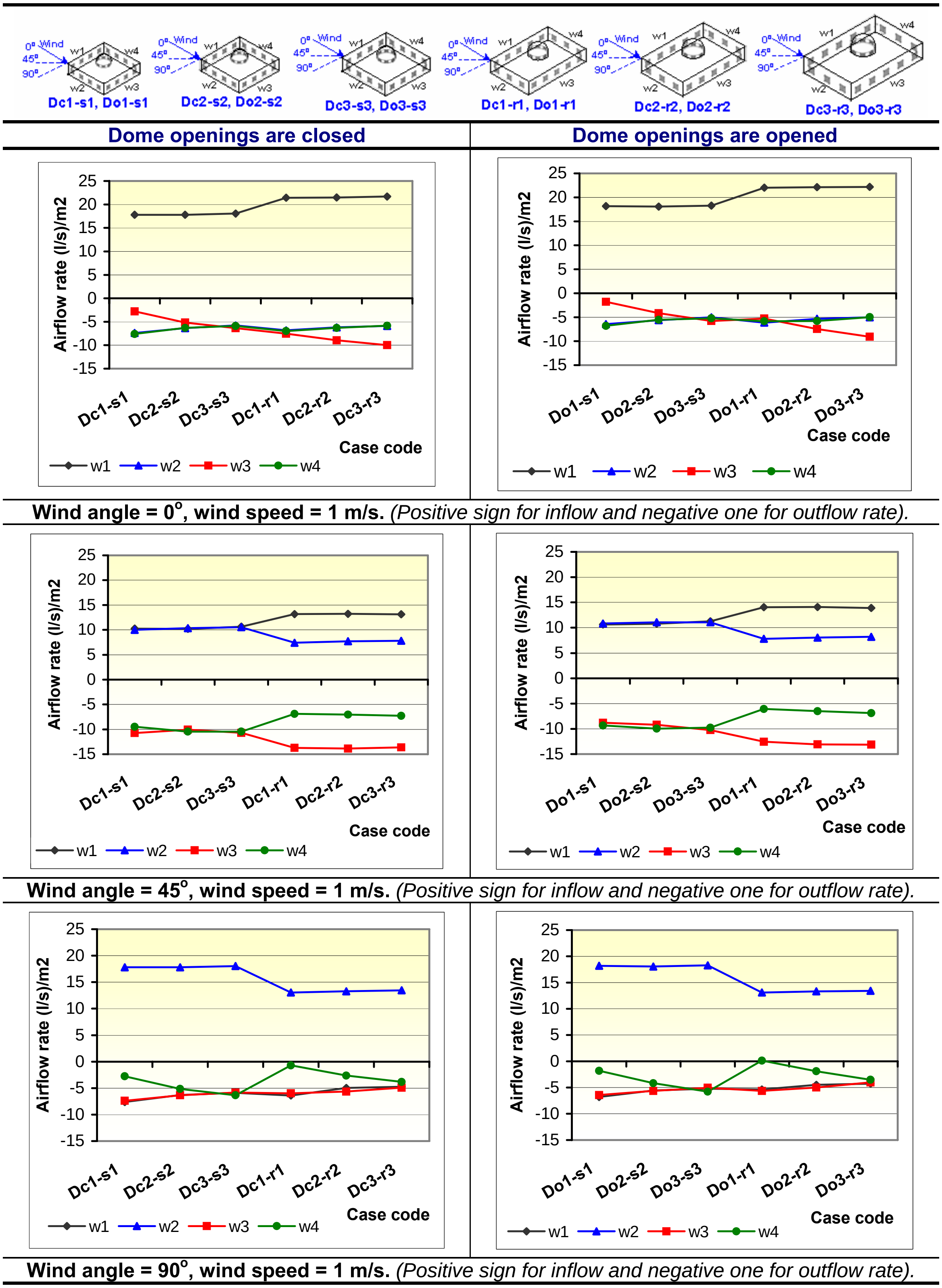

Figure 6.17: Average volumetric airflow rate (for building unit area) through wall openings recorded in the Dome Study at a reference wind speed of 1 m/s

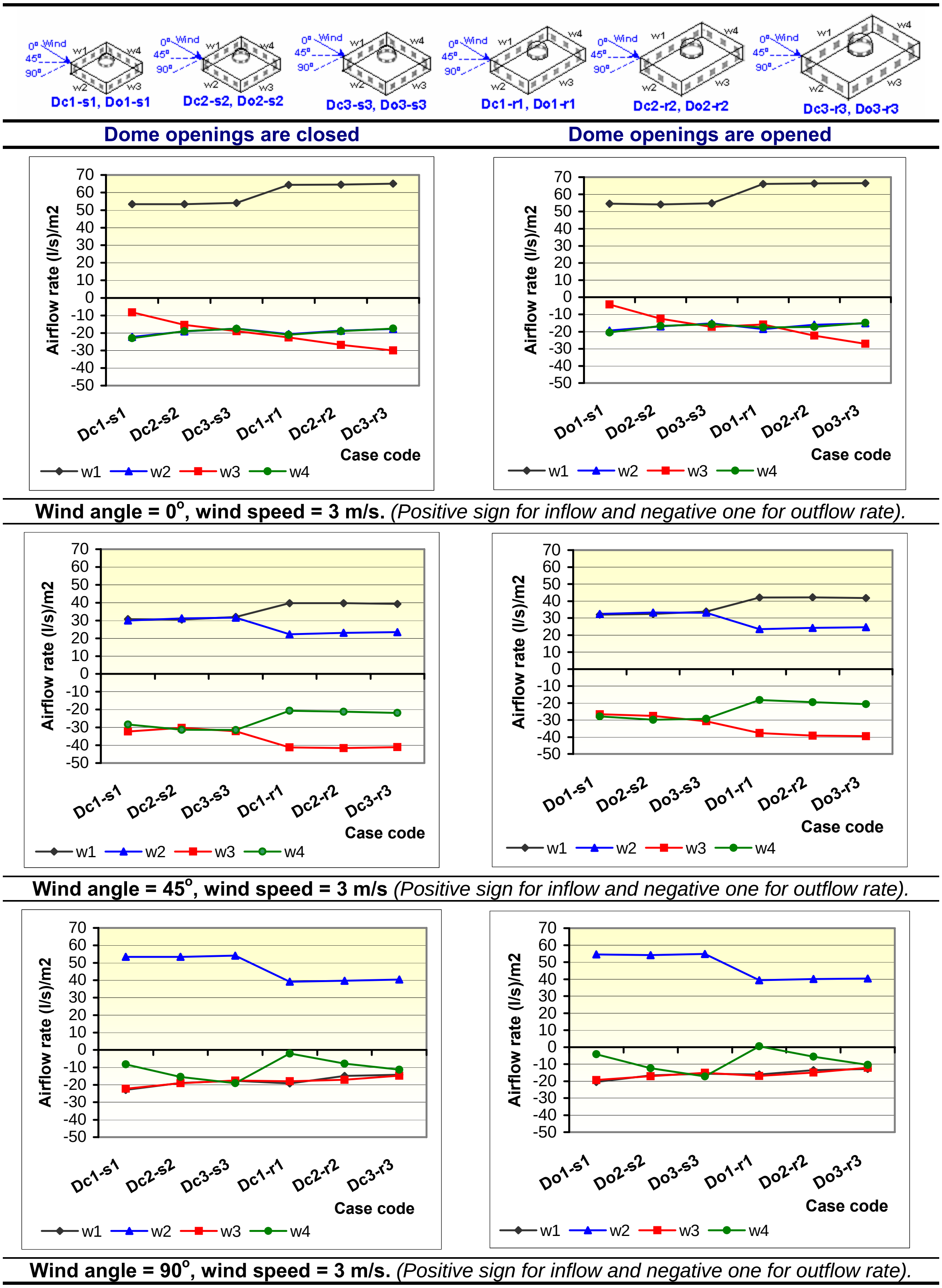

Figure 6.18: Average volumetric airflow rate (for building unit area) through wall openings recorded in the Dome Study at a reference wind speed of 3 m/s

6.6.1 In the case of 0^o wind incidence

Table 6.6 illustrates inflow and outflow rates recorded in this wind direction. Figures 6.20 and 6.21 are used to assess this internal flow distribution using contours of air velocity magnitude, as discussed at the beginning of Section 6.6. It has been found that both reference air velocities used in the study have resulted in the same internal air distribution, but with different velocity values. This is supported by that although air pressure is proportional to the square of the wind speed, its distribution does not change with speed for most sharp-edged buildings (Dalgliesh and Schriever, 1965). Thus, images depicted in Figures 6.20 and 6.21 have been found true for both wind velocities, considering the different velocity scales attached to them.

Table 6.6: The effect of dome openings operation on inflow and outflow rates through wall openings in the case of 0^o wind direction and 3m/s wind speed

Case	Inflow rate		Diff. (%)	Outflow rate		Diff. (%)
	Closed dome	Opened dome		Closed dome	Opened dome	
D1-s1	53.39	54.54	**+2.2**	-53.39	-44.01	**-17.6**
D2-s2	53.42	54.15	**+1.4**	-53.42	-46.16	**-13.6**
D3-s3	54.14	54.85	**+1.3**	-54.14	-48.22	**-10.9**
D1-r1	64.31	66.06	**+2.7**	-64.31	-51.83	**-19.4**
D2-r2	64.50	66.40	**+3.0**	-64.50	-55.56	**-13.9**
D3-r3	65.12	66.44	**+2.0**	-65.12	-57.21	**-12.2**

* All airflow rate values are in (l/s)/m^2.

Inflow rates increase was observed as a result of dome utilisation for natural ventilation. This is due to the suction force acting on the dome. This is supported by the findings of Bahadori and Haghighat (1985), as discussed in Section 4.3.2, that the utilisation of dome for natural ventilation always increases inflow rates in buildings. Dome also attracts some of the air that enters the building to leave through it instead of walls outlets, which are located in the literal building faces, w2 and w4, in addition to the leeward building face, w3, as can be noticed in Figures 6.17 and 6.18. This resulted in a reduction in outflow rate, which is in proportion to the suction forces acting on the dome. This suction is higher when building area is less, as discussed in Section 6.5.1. This redistribution of air results in a more active air movement in the central zone of the building.

One phenomenon that affects internal airflow distribution in this wind direction is that, and in some cases, airflow penetrates the space diagonally. This results in an active airflow movement in the higher level of the space. It seems that there is a conflict between two forces in this regard:

- Suction forces acting on walls openings, which cause airflow to penetrate the space horizontally.
- Dragging forces acting on the roof due to airflow separation on the windward roof edge. This causes airflow to penetrate the space diagonally in the high level of the space and towards the opposite outlets. This results in a weak air movement in the downstream zone of the occupied level. Suction forces acting over the dome, in addition to the low height of the building, increase this effect.

In the case of building with smaller depth, for example case Dc1-r1, air penetrates the space horizontally because the effect of suction forces acting on the leeward wall openings is more dominant than the dragging effect on the windward wall openings. This has resulted in a good internal airflow distribution, which is characterised by a small still-air zone (only 13%). Utilising dome openings has caused air movement to become diagonal, which increased area of the still-air zone, as in case Do1-r1, by about 100%. In the other two cases, i.e. Dc2-r2 and Dc3-r3, building depth is higher. Thus airflow penetrates the space diagonally, which reduced the quality of internal airflow distribution, compared to case Dc1-r1. Utilising the dome for natural ventilation has enhanced this diagonal air movement. The only difference is that airflow leaves through dome openings instead of wall openings. This is why internal air distribution has, positively or negatively, recorded slight changes.

In the square cases, the higher building depth has resulted in a diagonal air movement in all cases. Thus, a larger area of the still-air zone, about 30%, has been observed in the downstream zone, when dome openings are closed. When dome openings are opened, air penetrates the space more deeply, and is attracted towards the central zone of the building. This reduces the still-air zone by about 5% in the first two cases. Consequently, air velocity increases in zone B, i.e. 0.07m/s and 0.2m/s respectively for the low and high wind velocities. However, a large area of the still-air zone is still observed, especially in the third case, which has the largest depth.

In fact, this diagonal air movement can be considered as an advantage that supports the interest in creating a vertical air movement within the space. Although this phenomenon has initially reduced the overall internal airflow quality, since it has been found to occur even in the case of using flat roofs, i.e. without the dome, in such deep buildings, it has improved the internal airflow distribution in the upstream zone of the building. One possible solution here is to propose air provision system to the downstream zone of the building, as will be discussed in Chapter 8 of this study.

Another phenomenon that affects internal airflow distribution in this wind direction is the existence of the literal wall openings, especially in the square cases. Contours of velocity magnitude over plane 1 in Figure 6.19 show that large amount of airflow leaves the building directly through the literal openings, where suction force is higher than the one acting on the leeward wall openings. This is assumed to reduce the quality of internal airflow distribution.

To demonstrate this phenomenon, case D2-s2-0-3 has been modelled again but with closed literal wall openings. Results showed an improved internal airflow distribution. This is supported by a rule of thumb mentioned by Smith (2001) that outlets on opposite walls are more effective for cross ventilation than the adjacent wall. Also, reducing the number of outlets located at building walls has increased the importance of dome openings in suction. This is why outflow rate through the dome has increased from 8.0 to 15.0 (l/s)/m^2, i.e. by about 85%. However, these literal openings will be kept in the rest of cases tested in this parametric study in order to consider their benefit in the oblique wind direction, since both windward faces of the building work in opposite cross ventilation mode with the other opposite two faces. On the other hand, using these openings is important for other environmental systems in such deep buildings, like day lighting.

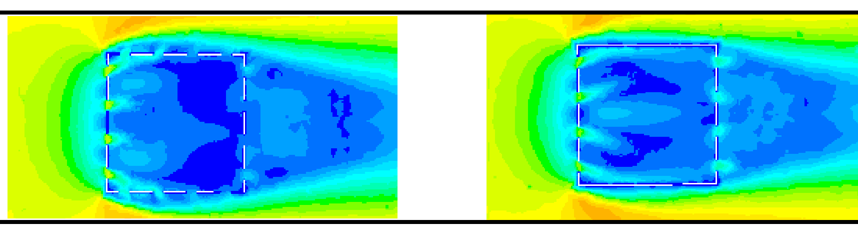

Figure 6.19: Internal airflow distribution for case Do2-s2-0 in the case of using openings at all building walls, and openings at only opposite walls

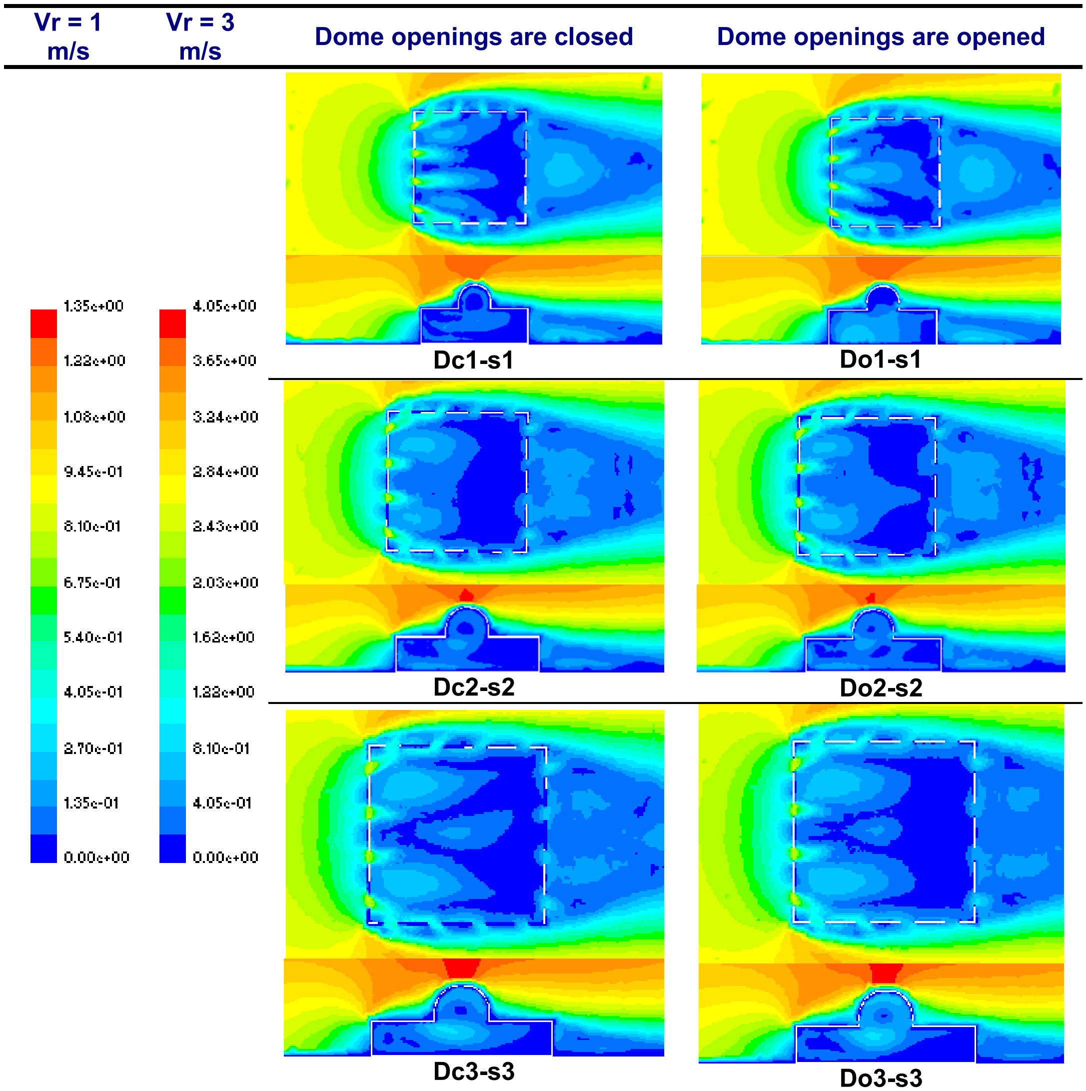

* Contours of velocity magnitude shown above are presented in Plane1 and 2 (Scale 1:1000), with normal wind direction, and both 1 and 3 m/s reference wind velocities.

Air velocity contour	Vi (Vr=1m/s)	Vi (Vr=3m/s)	% of total plan area (square cases)					
			Dc1-s1	Do1-s1	Dc2-s2	Do2-s2	Dc3-s3	Do3-s3
A	0.0	0.0	30.9	26.4	37.0	31.2	33.1	34.7
B	0.07	0.2	30.3	38.1	28.8	37.8	28.5	26.3
C	0.14	0.4	15.3	15.5	15.9	14.1	17.5	16.7
D *& above*	$0.14<Vi<Vi_{max}$	$0.4<Vi<Vi_{max}$	23.5	20.0	18.3	16.9	20.9	22.3

Figure 6.20: Comparison of internal airflow distribution presented by internal air velocity Vi distribution before and after utilising the dome openings in the square building form at 0° wind direction

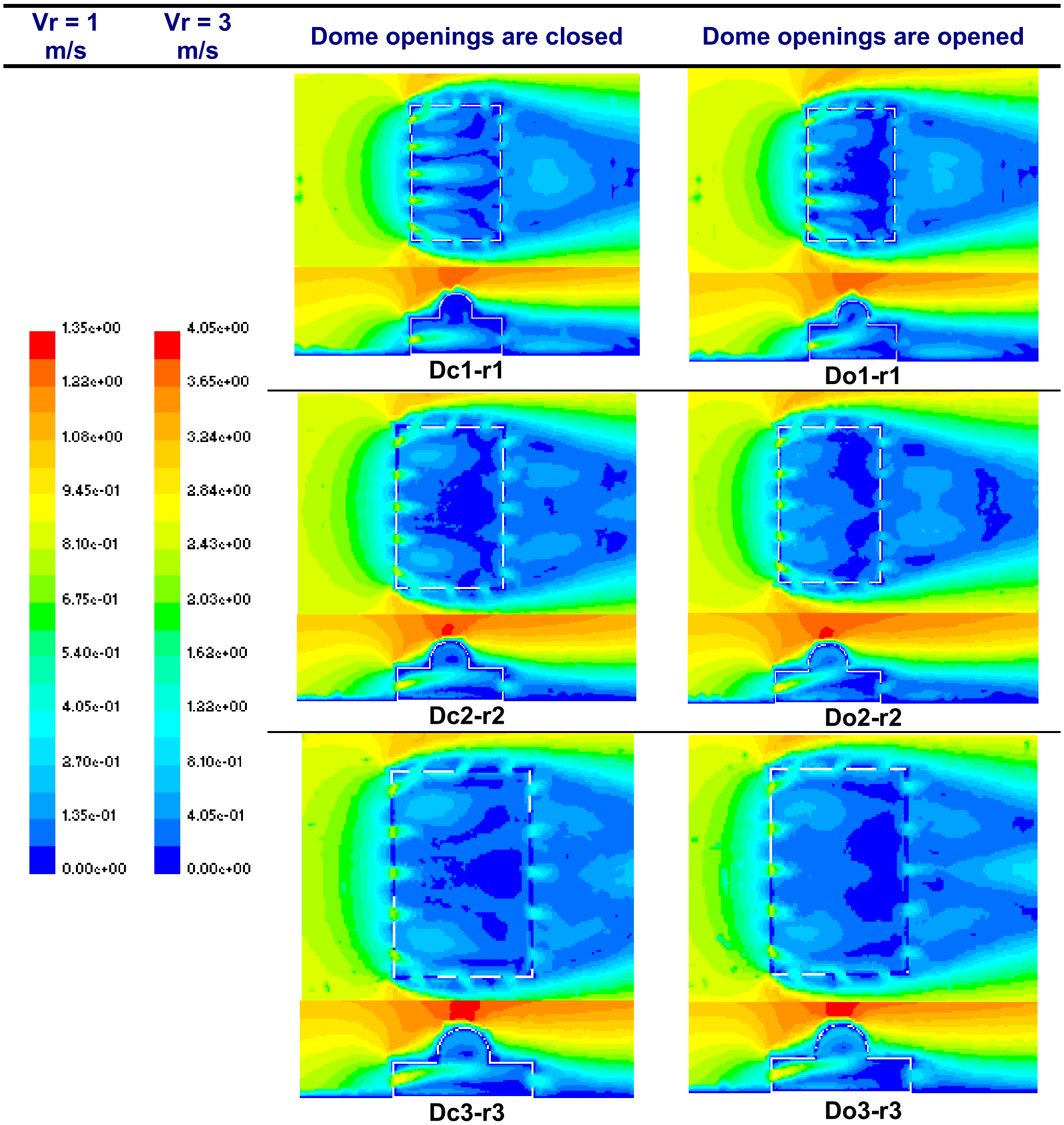

* Contours of velocity magnitude shown above are presented in Plane1 and 2 (Scale 1:1000), with normal wind direction, and both 1 and 3 m/s reference wind velocities.

Air velocity contour	Vi (Vr=1m/s)	Vi (Vr=3m/s)	% of total plan area (rectangular cases)					
			Dc1-r1	Do1-r1	Dc2-r2	Do2-r2	Dc3-r3	Do3-r3
A	0.0	0.0	13.0	27.8	27.8	21.7	19.0	20.7
B	0.07	0.2	42.9	33.8	36.8	40.5	45.3	42.4
C	0.14	0.4	17.2	15.4	16.4	21	17.6	22.9
D *& above*	$0.14<Vi<Vi_{max}$	$0.4<Vi<Vi_{max}$	26.9	23.0	19.0	16.8	18.1	13.4

Figure 6.21: Comparison of internal airflow distribution presented by internal air velocity Vi distribution before and after utilising the dome openings in the rectangular building form at 0^o wind direction

6.6.2 In the case of 45^o wind incidence

Table 6.7 presents inflow and outflow rates recorded in this wind direction. Figures 6.22 and 6.23 present internal airflow distribution using contours of air velocity magnitude for both square and rectangular building cases.

Table 6.7: The effect of dome openings operation on inflow and outflow rates through wall openings in the case of 45^o wind direction and 3m/s wind speed

Case	Inflow rate		Diff. (%)	Outflow rate		Diff. (%)
	Closed dome	Opened dome		Closed dome	Opened dome	
D1-s1	60.69	64.38	**+6.1**	-60.69	-54.41	**-10.4**
D2-s2	61.67	65.66	**+6.5**	-61.67	-57.49	**-6.8**
D3-s3	63.54	66.92	**+5.3**	-63.54	-60.09	**-5.4**
D1-r1	61.84	65.61	**+6.1**	-61.84	-55.89	**-9.6**
D2-r2	62.81	66.42	**+5.8**	-62.81	-58.70	**-6.6**
D3-r3	62.86	66.39	**+5.6**	-62.86	-60.09	**-4.4**

* All airflow rate values are in (l/s)/m^2.

In this wind direction, natural ventilation system works in the cross-ventilation mode, where airflow entering and leaving the building from opposite openings. This means that the effect of the literal openings, as has been observed in the case of 0^o wind direction, is no more valid here. The fact that two facades here are facing the wind did not result, however, in the gross inflow rate through these two facades to be the double of the one observed in the case of normal wind incident. This is because the effective area of any opening oriented obliquely with respect to the wind is less. For example, the gross effective area of the four inlets is 10.24 m^2 in case Do1-s1-0-3. In the case Do1-s1-45-3, this gross area is 7.25 m^2.

Inflow rate through wall openings has significantly increased when dome openings are opened. As explained in the case of 0^o wind direction, this is because suction forces acting over the dome are inducing more air to enter the building. The higher gross area of inlets, as explained above, increases the potential of the dome for inducing inflow through these inlets. Suction forces acting over and around the dome also attract some of the air to leave through the dome instead of wall openings. This reduces outflow rates through wall openings, as can be observed in Table 6.7. However, reduction in outflow rate here is less than in the case of 0^o wind direction. This is due to the smaller area of outlets, which reduces the potential of the dome for attracting some of the outflow that leave through these outlets.

In the case of closing the dome inlet, as explained in Section 6.5.2, the role of the dome in suction has significantly increased. Results observed showed that the net outflow rate through the dome has increased by about 25% in the tested square and rectangular building cases. This, on one hand, has caused an additional increase in inflow rate by about 1.7% in the square case Do2-s2, and by about 1.2% in the rectangular case Do2-r2. On the other hand, it has caused an additional reduction in outflow rate by about 2.4% in the square case, and by about 3% in the rectangular-plan case.

The above-mentioned opposite cross ventilation system has resulted in an improved internal airflow distribution, compared to the normal wind direction. This is characterised by a less area of the still-air zone, and higher air velocities in the other zones. In the square cases, dome utilisation in the first two cases has caused some increase in the area of the high velocity zone (zone D).

In the third square case, which possesses the largest depth, the still-air zone area has increased in the downstream zone of the building. This is because part of airflow leaving through dome openings instead of wall outlets. This is also true for the rectangular configurations, especially for the last case that has the largest depth. However, the resulting airflow distribution is unsymmetrical, since the still-air zone occurs in the downstream internal corner. This is because pressure difference across the lower corner is higher due to wind deflection on buildings windward facades.

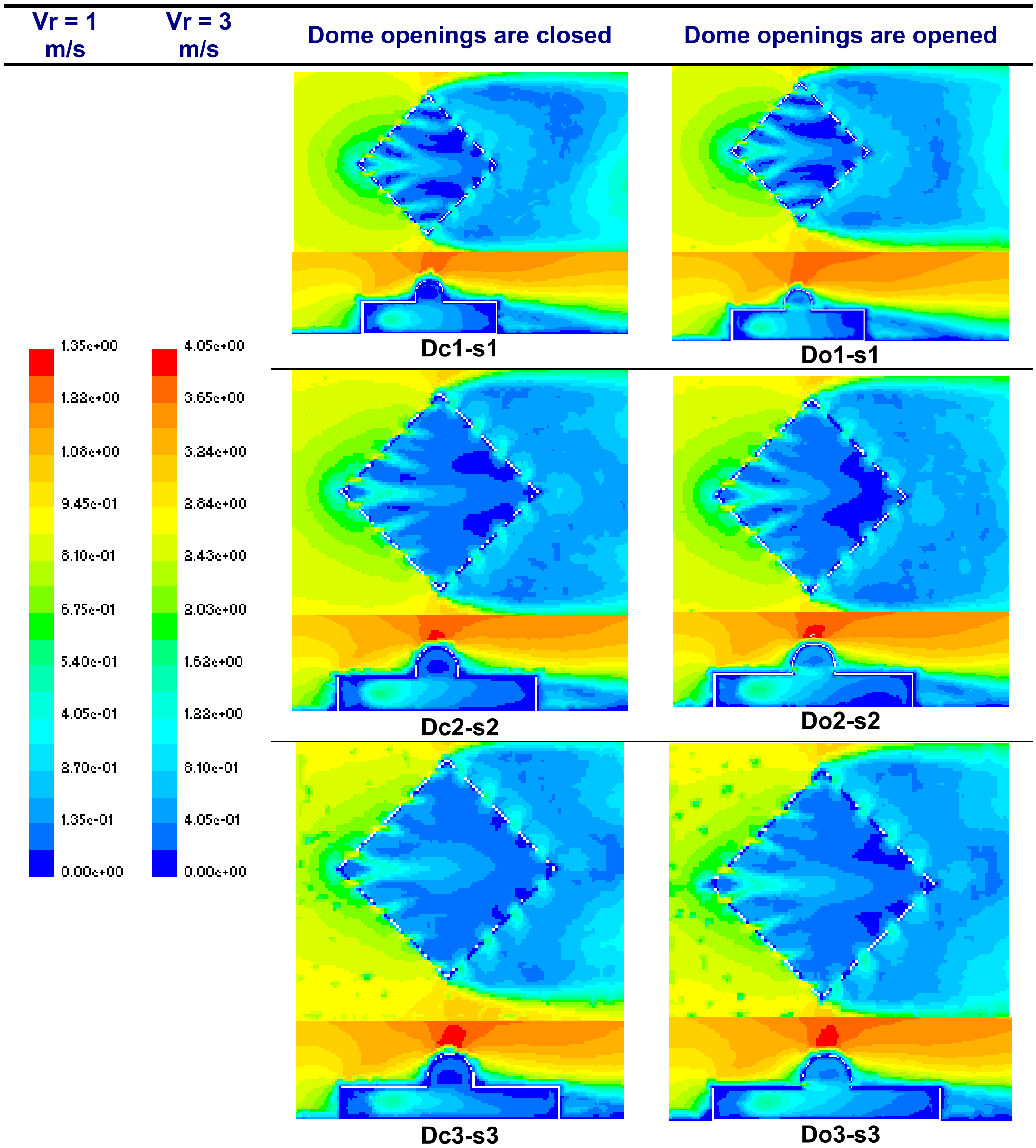

* Contours of velocity magnitude shown above are presented in Plane1 and 2 (Scale 1:1000), with 45° wind direction, and both 1 and 3 m/s reference wind velocities.

Air velocity contour	Vi (Vr=1m/s)	Vi (Vr=3m/s)	% of total plan area (square cases)					
			Dc1-s1	Do1-s1	Dc2-s2	Do2-s2	Dc3-s3	Do3-s3
A	0.0	0.0	17.5	18.7	11.2	13.3	2.8	7.4
B	0.07	0.2	34.5	30.8	52.9	45.5	49.9	44.8
C	0.14	0.4	16.6	16.9	18.7	16.8	26.7	27.8
D *& above*	$0.14<Vi<Vi_{max}$	$0.4<Vi<Vi_{max}$	31.4	33.6	17.2	24.4	20.6	20.0

Figure 6.22: Comparison of internal airflow distribution presented by internal air velocity Vi distribution before and after utilising the dome openings in the square building form at 45° wind direction

Vr = 1 m/s	Vr = 3 m/s	Dome openings are closed	Dome openings are opened

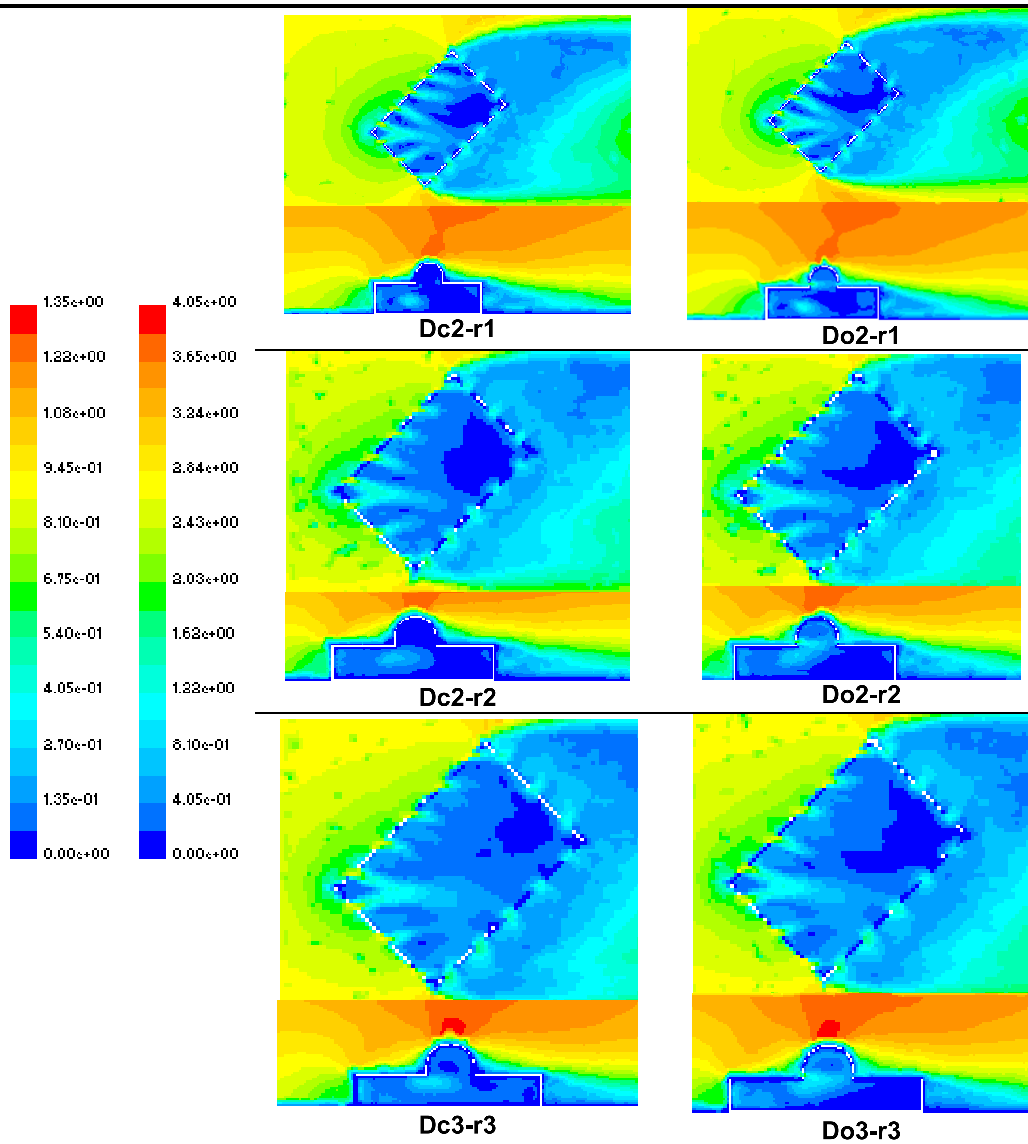

* Contours of velocity magnitude shown above are presented in Plane1 and 2 (Scale 1:1000), with 45° wind direction, and both 1 and 3 m/s reference wind velocities.

Air velocity contour	Vi (Vr=1m/s)	Vi (Vr=3m/s)	% of total plan area (rectangular cases)					
			Dc1-r1	Do1-r1	Dc2-r2	Do2-r2	Dc3-r3	Do3-r3
A	0.0	0.0	15.3	13.4	17.8	15.7	8.3	17.3
B	0.07	0.2	33.9	39.7	43.8	44.1	44.0	35.9
C	0.14	0.4	19.0	17.3	16.2	18.5	26.5	24.3
D *& above*	$0.14<Vi<Vi_{max}$	$0.4<Vi<Vi_{max}$	31.8	29.6	22.2	21.7	21.2	22.5

Figure 6.23: Comparison of internal airflow distribution presented by internal air velocity Vi distribution before and after utilising the dome openings in the rectangular building form at 45° wind direction

6.6.3 In the case of 90^o wind incidence

Table 6.8 presents inflow and outflow rates recorded in this wind direction. Figure 6.24 presents the observed internal airflow distribution using contours of air velocity magnitude.

Table: 6.8: The effect of dome openings operation on inflow and outflow rates through wall openings in the case of 90^o wind direction and 3m/s wind speed

Case	Inflow rate		Diff. (%)	Outflow rate		Diff. (%)
	Closed dome	Opened dome		Closed dome	Opened dome	
D1-s1	53.39	54.54	**+2.2**	-53.39	-44.01	**-17.6**
D2-s2	53.42	54.15	**+1.4**	-53.42	-46.16	**-13.6**
D3-s3	54.14	54.85	**+1.3**	-54.14	-48.22	**-10.9**
D1-r1	39.17	39.31	**+0.4**	-39.17	-32.55	**-16.9**
D2-r2	39.76	40.03	**+0.7**	-39.76	-34.22	**-13.9**
D3-r3	40.36	40.39	**+0.1**	-40.36	-35.41	**-12.3**

* All airflow rate values are in (l/s)/m^2.

Airflow rates and distribution in the square cases behave in the same way explained in the case of 0^o wind direction, due to building symmetry. Regarding the rectangular cases, the reduction in outflow rates is generally higher. This is because some openings in the leeward wall, especially the middle ones, act as inlets. This is because suction forces acting on the long literal faces of the building drag airflow in the wake zone. The utilisation of the dome supports this dragging effect and cause the air to be reversed inside the building again. For example, average airflow rate through the leeward wall (w4) is positive in case Do1-r1.

Concerning airflow distribution in the rectangular cases, area of the still-air zone in the downstream wing is significantly high due to the relatively large building depth. When dome openings are opened, slight improvement has been observed. Area of the still-air zone has been reduced by about 5%, with a corresponding increase in other wind velocity zones. However, area of the still-air zone in the leeward wing still large (about 30% of the total area).

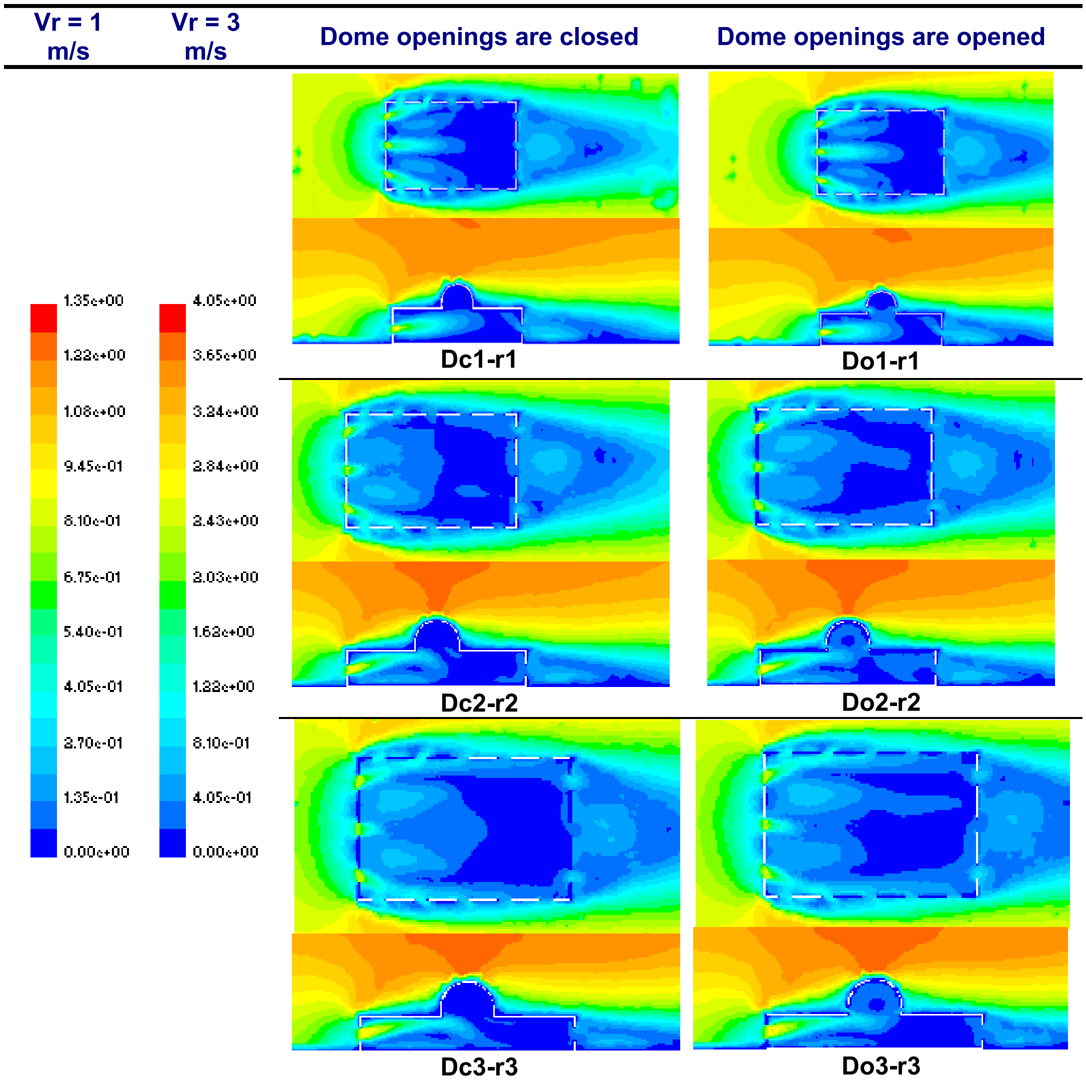

* Contours of velocity magnitude shown above are presented in Plane1 and 2 (Scale 1:1000), with 90^o wind direction, and both 1 and 3 m/s reference wind velocities.

Air velocity contour	Vi (Vr=1m/s)	Vi (Vr=3m/s)	% of total plan area (rectangular cases)					
			Dc1-r1	Do1-r1	Dc2-r2	Do2-r2	Dc3-r3	Do3-r3
A	0.0	0.0	45.0	41.0	36.2	30.6	33.7	28.7
B	0.07	0.2	24.7	25.4	32.5	36.2	28.2	30.5
C	0.14	0.4	10.9	12.8	17.5	19.3	18.1	21.7
D *& above*	0.14<Vi<Vi_{max}	0.4<Vi<Vi_{max}	19.4	20.8	13.8	13.9	20.0	19.1

Figure 6.24: Comparison of internal airflow distribution presented by internal air velocity Vi distribution before and after utilising the dome openings in the rectangular building form at 90^o wind direction

6.7 Conclusions

This chapter aimed to investigate the effect of dome employment for natural ventilation on the performance of wind-induced ventilation in the modelled building prototypes. This has been presented in terms of airflow rate and internal airflow distribution. A general look at some climatic data related to the Middle East has led to specify the data that will be implemented in this study. Two wind velocities have been considered: 1 m/s, as a low wind velocity, and 3 m/s, as a high one. Three wind directions have been examined: 0^o, 45^o, and 90^o. Then, the geometrical parameters have been specified. This has considered: square and rectangular building forms, wall openings at building four faces, three different areas of building plan, and a centralised hemispherical dome with openings at its base.

More than 70 cases have been modelled using Fluent 5.5 software. The main findings related to dome performance in natural ventilation are:

- Dome with openings at its base works mainly in suction, where at least 87.5% of its opening area serves as air outlets.
- This suction increases as the distance between dome and roof windward sharp edge(s) decreases, i.e. when building area is smaller.
- In the case of 0^o and 90^o wind directions, inflow rate through the dome is low due to the generated air vortex before it. This has been found to be useful for increasing dome potential for suction.
- In the case of 45^o wind direction, inflow rate is higher due to the absence of this air vortex. Thus, closing dome inlet has been found to cause a significant improvement in its performance (about 25% in the configuration tested).

The main findings related to airflow rate through walls openings, and internal airflow distribution, are:

- Dome openings always induce more inflow rate through building windward face, especially in the case of oblique wind direction (about 6%). This is in inverse proportion to the building area.
- Dome utilisation always reduces outflow rate through walls openings, since it attracts some air to leave through it, especially in the case of 0^o and 90^o wind

directions (about -14%). This is also in inverse proportion to the building area.

- The above-mentioned two observations has generally improved internal airflow distribution in the upstream and central zone of the building, but has not guaranteed this in the downstream one.

Thus, dome can be integrated with an air supply system in order to encourage air movement in the building, especially in its downstream wing. As discussed in Chapter 4, the architectural relationship between domes and towers can be utilised to serve the above-mentioned need. This will be the research problem of Chapter 8 of this study.

CHAPTER 7 : EFFECT OF VAULT UTILISATION ON NATURAL VENTILATION PERFORMANCE

Introduction

This chapter focuses on the potential of the vault for improving wind-induced natural ventilation in buildings. Vault is a common configuration of the curved roofs that has been used in buildings for centuries. This potential has been discussed in Section 4.3 of the literature review. It has been concluded that there is a similarity between both domed and vaulted roofs in increasing airflow rates due to suction forces acting upon and around them. Thus, this chapter aims to examine and quantify the effect of the vault, integrated with the main building volume, on wind-induced natural ventilation performance. This will be demonstrated through a parametric approach using CFD simulation, implementing the same methodology used in Chapter 6. Conclusions revealed from Chapter 6 helps reducing the range of parameters tested here.

This chapter starts by illustrating the geometrical parameters that will be examined in the CFD modelling. Results obtained are discussed in many sections, including airflow rate and distribution in the building before and after the utilisation of different configurations of vaults and different climatic parameters. Many parameters have been varied, like: building form, vault plan area, wind direction, and wind speed. After that, many observations have been concluded, which are believed to improve designers' understanding of the utilisation of vaulted roofs for natural ventilation.

7.1 Geometrical parameters

In this study, geometry of the two main elements of the main building volume and the vault is varied. It has been indicated in Chapter 6 that the use of square configurations in some cases has resulted in a better natural ventilation performance, compared to the rectangular ones, and vice versa. However, in some cases and due to different considerations, including site planning, the use of the less appropriate form may be mandatory. Therefore, this study will be carried out for both square and rectangular forms. These are namely configurations D2-s2 and D2-r2 presented in Section 6.2 in Chapter 6, but with a vault instead of the dome. This means that the main volume area will be confined to 400 m^2, which is the middle area tested in the Dome Study. This is because the three different areas tested in Chapter 6 have resulted generally in the same natural ventilation behaviour. Main volume height is 5 m, and its porosity is 10%, which produces 16 uniformly distributed wall openings.

However, the plan area of the vault will be varied here. Thus, three configurations are examined:

- Configuration 1: a square-plan vault, with a length equal to the corresponding dome diameter, i.e. 6.2 m. This vault possesses the same opening area of the dome, i.e. 3.85 m^2. As has been practiced in Chapter 6, openings will be located in the base of the curved roof instead of its top. Thus, two opposite large openings are used in the base of the vault, with dimensions of 0.6 * 3.2 m.
- Configuration 2: the square-plan vault has been stretched to a length equals the double of its original length, keeping the width fixed. This resulted in the second vault geometry, with plan dimensions of 6.2 * 12.4 m. Thus, four openings of the same size mentioned above are used.
- Configuration 3: the third geometry represents a relatively long vault that has the same width, but a length that equals 18.6 m, i.e. three times of the dome diameter. Thus, six openings of the same size mentioned above are provided here.

The vault shape used here is semi-circular raised on a cubical base, in which the openings are placed. These openings are located in the windward and leeward faces of the base, considering the case of normal wind direction. Figure 7.1 shows illustrations of the cases of this modelling study. CAD illustrations with dimensions can be found in Appendix B.1.

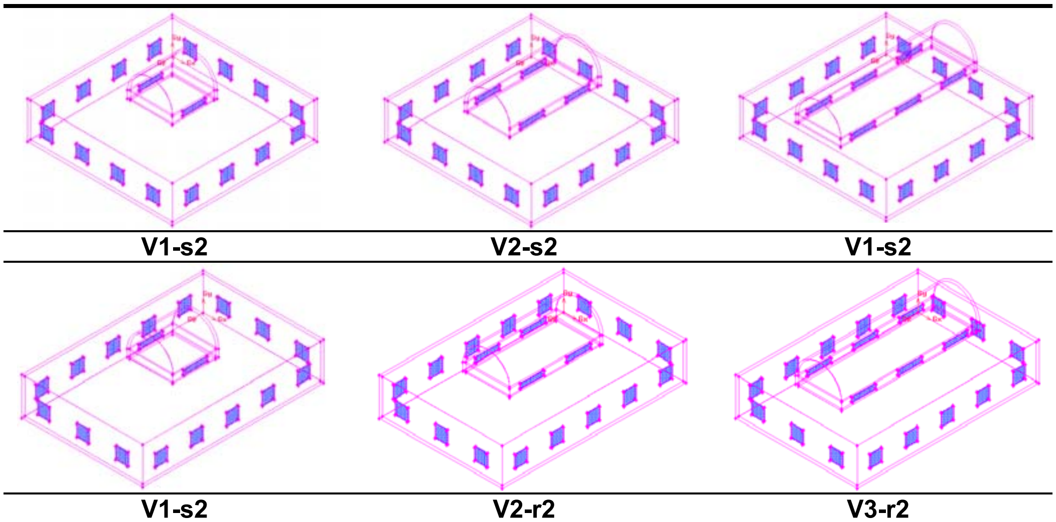

Figure 7.1: Different building configurations tested in the Vault Study

7.2 Vault modelling study: terminology and programme

The same method explained in Section 6.3 has also been used here. The different cases tested are designated with a ‘V’ letter to refer to the Vault Study. This letter is associated with either ‘o’ letter, to indicate that vault openings are opened, or ‘c’ letter, to indicate the opposite. ‘V’ letter is also associated with a serial number, from 1 to 3, to refer to the vault configuration tested, as explained in Section 7.1. One of two letters then follows the resulting symbol, ‘s’ letter to represent a square plan of the main building volume or ‘r’ letter to represent a rectangular one.

Building area, confined to 400 m^2, has been referred to in Chapter 6 by two symbols: ‘s2’ for the square-plan case, and ‘r2’ for the rectangular-plan one. Thus, these two symbols are used here as well. Two more numbers follow the resulting symbol: the first one indicates wind angle: 0, 45, or 90, and the second one indicates reference wind speed: 1 or 3. For example Vo1-s2-0-3 indicates that the test is targeting the vault configuration number 1, which has an opened windows and is placed on a square roof. Wind direction is 0^o and reference wind speed is 3 m/s. Table 7.1 summarises the cases that will be modelled in this study.

Table 7.1: Vault Study modelling programme

Config.	Description	Test no.	Test code	Wind angle	Wind speed (m/s)
V1-s2	**Form:** square. **Plan area:** 400m^2 **Wall opening area:** 40 m^2 **Vault opening area:** 3.85m^2	1 & 2	Vc1-s2-0-3 & Vo1-s2-0-3	0^o	3
		3 & 4	Vc1-s2-45-3 & Vo1-s2-45-3	45^o	3
		5 & 6	Vc1-s2-90-3 & Vo1-s2-90-3	90^o	3
V2-s2	**Form:** square. **Plan area:** 400m^2 **Wall opening area:** 40m^2 **Vault opening area:** 9.7m^2	7 & 8	Vc2-s2-0-1 & Vo2-s2-0-1	0^o	1
		9 & 10	Vc2-s2-45-1 & Vo2-s2-45-1	45^o	1
		11 & 12	Vc2-s2-90-1 & Vo2-s2-90-1	90^o	1
		13 & 14	Vc2-s2-0-3 & Vo2-s2-0-3	0^o	3
		15 & 16	Vc2-s2-45-3 & Vo2-s2-45-3	45^o	3
		17 & 18	Vc2-s2-90-3 & Vo2-s2-90-3	90^o	3
V3-s2	**Form:** square. **Plan area:** 400m^2 **Wall opening area:** 40m^2 **Vault opening area:** 14.55m^2	19 & 20	Vc3-s2-0-3 & Vo3-s2-0-3	0^o	3
		21 & 22	Vc3-s2-45-3 & Vo3-s2-45-3	45^o	3
		23 & 24	Vc3-s2-90-3 & Vo3-s2-90-3	90^o	3
V1-r2	**Form:** rectangular (1:1.5). **Plan area:** 400m^2 **Wall opening area:** 40m^2 **Vault opening area:** 3.85m^2	25 & 26	Vc1-r2-0-3 & Vo1-r2-0-3	0^o	3
		27 & 28	Vc1-r2-45-3 & Vo1-r2-45-3	45^o	3
		29 & 30	Vc1-r2-90-3 & Vo1-r2-90-3	90^o	3
V2-r2	**Form:** rectangular (1:1.5). **Plan area:** 400m^2 **Wall opening area:** 40m^2 **Vault opening area:** 9.7m^2	31 & 32	Vc2-r2-0-1 & Vo2-r2-0-1	0^o	1
		33 & 34	Vc2-r2-45-1 & Vo2-r2-45-1	45^o	1
		35 & 36	Vc2-r2-90-1 & Vo2-r2-90-1	90^o	1
		37 & 38	Vc2-r2-0-3 & Vo2-r2-0-3	0^o	3
		39 & 40	Vc2-r2-45-3 & Vo2-r2-45-3	45^o	3
		41 & 42	Vc21-r2-90-3 & Vo2-r2-90-3	90^o	3
V3-r2	**Form:** rectangular (1:1.5). **Plan area:** 400m^2 **Wall opening area:** 40m^2 **Vault opening area:** 14.55m^2	43 & 44	Vc2-r2-0-3 & Vo2-r2-0-3	0^o	3
		45 & 46	Vc2-r2-45-3 & Vo2-r2-45-3	45^o	3
		47 & 48	Vc2-r2-90-3 & Vo2-r2-90-3	90^o	3

It has been found, similarly to Chapter 6, that wind direction has the most dramatic effect on the observed ventilation performance. Therefore, results here are presented according to the different wind directions. Regarding reference wind speed, it has been concluded that both low and high wind velocities, 1 and 3 m/s respectively, have resulted generally in the same behaviour of airflow rate and internal airflow distribution. Therefore, the higher wind velocity is examined here. However, the lower wind velocity is only examined in the second and fifth geometries. This is, on one hand, to examine whether that the observed similarity of the resulting airflow behaviour between both reference wind velocities is applicable in the vault case or not. On the other hand, these cases will be used in Chapter 8, where the role of wind catcher will be tested.

It is worth mentioning here that files total size of this modelling study is 5.9 GB. The same computer modelling considerations explained in Section 6.4 of the Chapter 6 are applicable here. Specifically:

- Division of solution domain at both normal and oblique wind directions.
- Air velocity variation with height.
- Creation of mesh size hierarchy in order to reduces total mesh size.

Table 7.2 summarises numerically airflow rates estimated, and shows the reliability of the results obtained according to the Law of Conservation of Mass.

Table 7.2: Summary of airflow rates recorded in the different cases modelled in the Vault Study, where vault openings are utilised for natural ventilation

	Wind angle 0° Wind velocity 3 m/s					Wind angle 45° Wind velocity 3 m/s					Wind angle 90° Wind velocity 3 m/s				
Case Code	**Inflow (vault)**	**Inflow (walls)**	**Outflow (vault)**	**Outflow (walls)**	**Total**	**Inflow (vault)**	**Inflow (walls)**	**Outflow (vault)**	**Outflow (walls)**	**Total**	**Inflow (vault)**	**Inflow (walls)**	**Outflow (vault)**	**Outflow (walls)**	**Total**
Vo1-s2	1.89	53.94	-3.48	-52.35	**0.0**	4.00	63.92	-8.07	-59.83	**0.02**	0.00	54.78	-11.30	-43.48	**0.0**
Vo2-s2	2.80	54.82	-8.38	-49.25	**-0.01**	8.01	65.49	-13.25	-60.25	**0.0**	0.00	56.97	-20.43	-36.54	**0.0**
Vo3-s2	8.72	55.51	-12.53	-51.70	**0.0**	13.10	67.33	-19.03	-61.39	**0.01**	0.00	60.13	-22.07	-38.06	**0.0**
Vo1-r2	0.00	65.70	-5.40	-60.30	**0.0**	3.18	63.86	-8.02	-59.02	**0.0**	0.00	41.12	-10.09	-31.04	**-0.01**
Vo2-r2	2.42	66.23	-9.15	-59.50	**0.0**	6.24	65.18	-13.22	-58.20	**0.0**	0.00	43.19	-16.19	-27.00	**0.0**
Vo3-r2	6.40	67.74	-13.81	-60.34	**-0.01**	11.37	67.10	-18.94	-59.53	**0.0**	0.00	45.69	-19.38	-26.31	**0.0**

* All values are in (l/s)/m^2.

7.3 Airflow rate through vault openings

This section discusses ventilation performance of the tested vaulted roofs, as presented by airflow rate through their apertures. The resulting airflow rates and internal airflow distribution in the main volume of the building are discussed in Section 7.4. It is intended here to examine the performance of vaulted roofs with openings at vault base. Considering the study programme presented in Table 7.1, it is possible here to compare the effect of different porosities of the vault, square and rectangular forms, in addition to the different tested wind directions and velocities.

As wind direction seems to have the most dramatic effect on the results obtained, the following analysis is divided according to the three considered wind directions, which are: wind is normal to the vault, wind is inclined at an angle of 45^{o} with respect to the vault axis, and wind is parallel to the vault. It has been observed that vault openings located at its base function mainly in suction. This is because outflow rate is always higher than inflow rate, as will be presented over the following three sections. In the following analysis, some numerical examples will be given. However, all other values can be found in Appendix B.

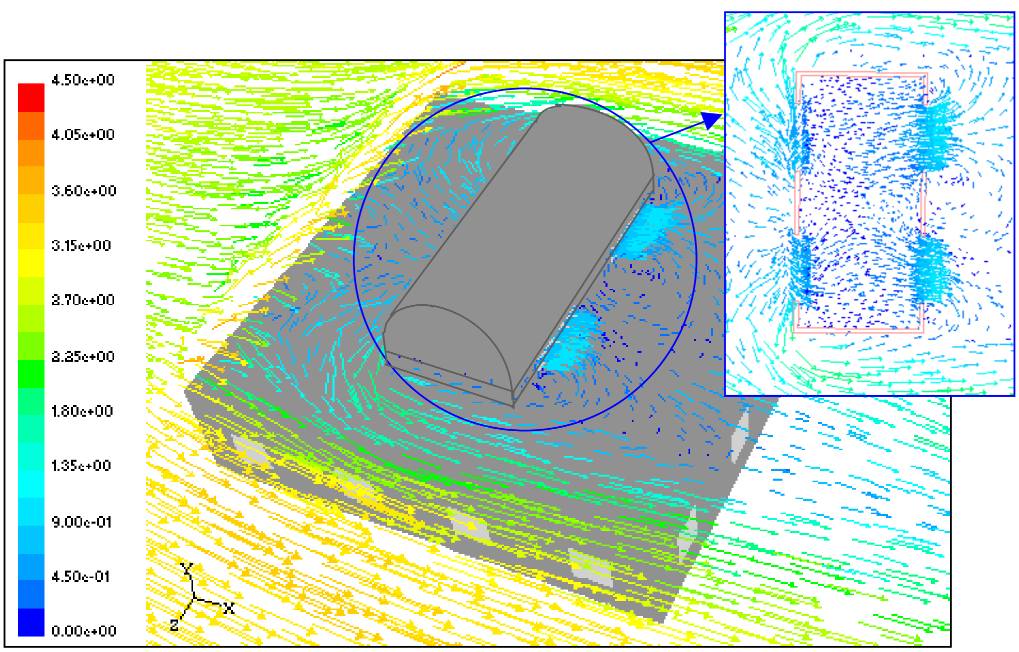

Figure 7.2: Airflow pattern over building roof, as illustrated by air velocity vectors (m/s), showing that vault openings function mainly in suction

7.3.1 In the case of 0° wind incidence

Figure 7.3 summarises airflow rates recorded for cases Vo1-s2 to Vo3-r2 at reference wind velocity of 3 m/s and 0° wind direction.

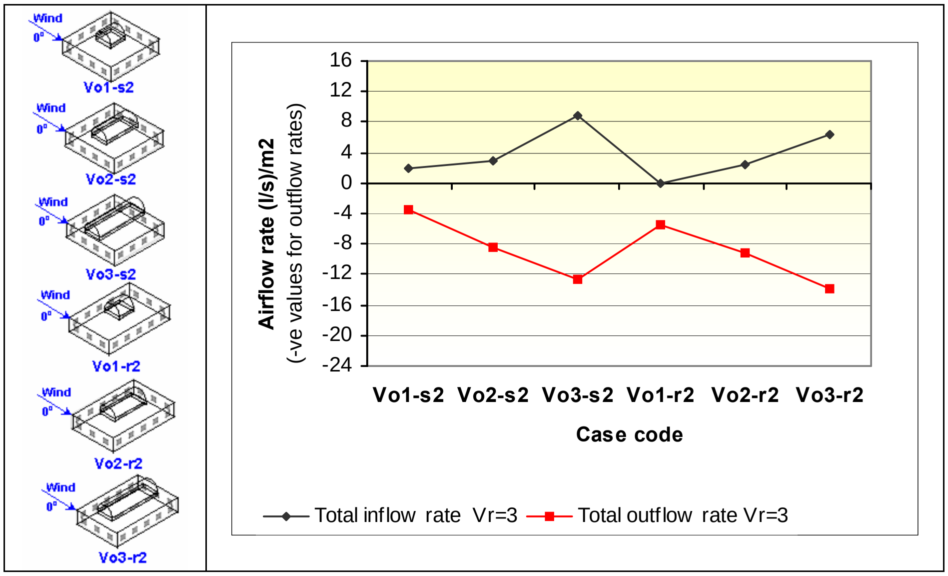

Figure 7.3: Volumetric inflow and outflow rates through vault openings presented for plan-unit area of the indicated cases and for 3m/s reference wind velocity and 0° wind angle

It can be noticed in Figure 7.3 that outflow rate is always higher than inflow rate, when wind is normal to the vault. This seems to be an interesting finding, since it might be presumed that the equal opening areas located at the windward and leeward vault faces will allow equal amount of air to penetrate vault openings at these two faces. However, this is not the case. For example, inflow rate in the case Vo1-r2 is zero. This is due to the nature of airflow pattern around the vault, which is quite turbulent. This is characterised by air vortices before the vault inlet(s) as a result of airflow separation over the windward sharp edge of the flat roof and the sharp edges of the vault itself. As explained in Section 6.5.1 of the Chapter 6, this is more pronounced in the rectangular building form. This is because the distance between the inlets and the roof windward edge is shorter.

Generally, inflow and outflow rates through vault openings increase as the plan area of the vault increases. This is logical, since openings area increase when the vault plan area increases. However, it generally seems that the intensity of suction force is not affected by increasing the vault plan area. Changing the form of the building from square to rectangular seems to have more effect on the observed outflow rate, compared to the case of the dome.

For example, net outflow rate in the Dome Study for case Do2-r2 is higher by 35% than case Do2-s2. In the Vault Study, this increase is more than 200% by comparing case Vo1-r2 to Vo1-s2. It has been found that in the Dome Study that when the distance between the dome inlet and the windward sharp edge of the roof decreases, inflow rate decreases and, consequently, outflow rate increases. This behaviour should be more pronounced in the case of using the vault, because its inlet area is significantly larger (50% of the total roof opening area, compared to 12.5% in the case of the dome). This means that the vault configuration tested is more sensitive to changing building plan depth in the normal wind direction.

7.3.2 In the case of 45^o wind incidence

Figure 7.4 summarises airflow rates recorded for cases Vo1-s2 to Vo3-r2 at reference wind velocity of 3 m/s and 45^o wind direction.

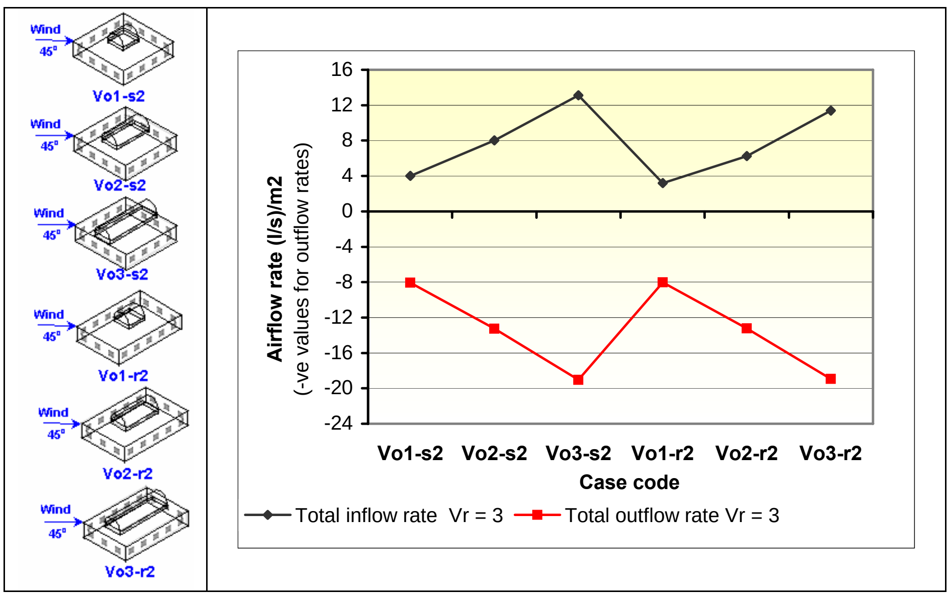

Figure 7.4: Volumetric inflow and outflow rates through vault openings presented for plan-unit area of the indicated cases and for 3m/s reference wind velocity and 45^o wind angle

Generally, airflow rates observed here present the same behaviour observed in the previous wind direction. Inflow and outflow rates are proportional to the opening area of the vault, as explained in Section 7.3.1, but in higher values. Concerning inflow rate, this is due to the absence of air vortex in front of the vault inlet. This is true for both square and rectangular building forms, as could be observed using the tool of velocity vectors in Fluent 5.5 software. Thus, inflow rates for both square and rectangular forms are nearly the same. Concerning outflow rate, the higher value observed is because building roof in the case of oblique wind direction is subjected to a higher suction forces, as explained in Section 6.5.2 in Chapter 6. Additionally, this is due to airflow separation over the vault corners. This can be noticed in Figure 7.5, which shows that the vault outlet in the oblique wind direction is subjected to a higher negative pressure caused by the above-mentioned airflow separation.

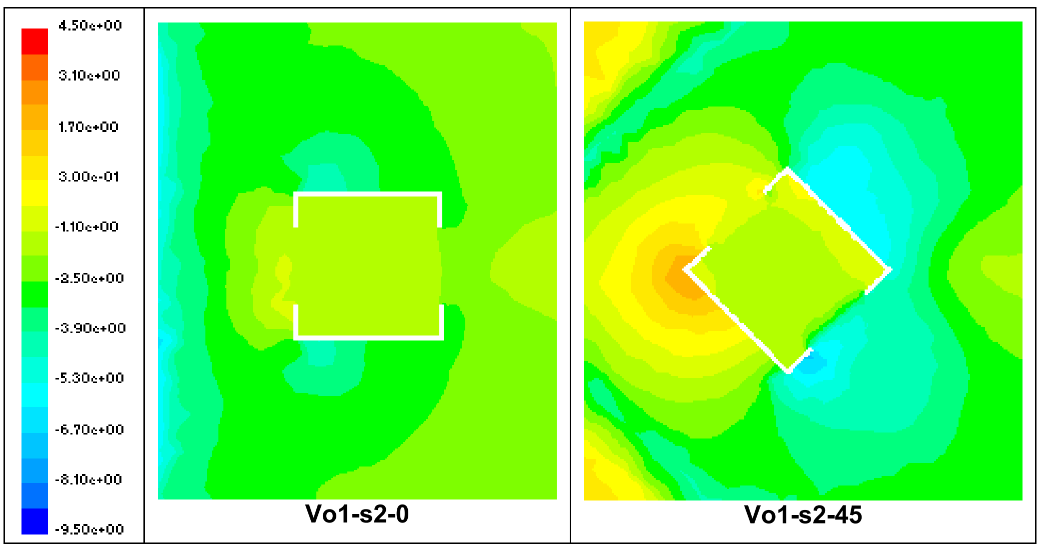

Figure 7.5: Contours of static pressure (Pa) in a horizontal plane passing through vault openings, showing that the vault outlet in the oblique wind direction is subjected to a higher negative pressure

7.3.3 In the case of 90^o wind incidence

Figure 7.6 summarises airflow rates recorded for cases Vo1-s2 to Vo3-r2 at reference wind velocity of 3 m/s and 90^o wind direction.

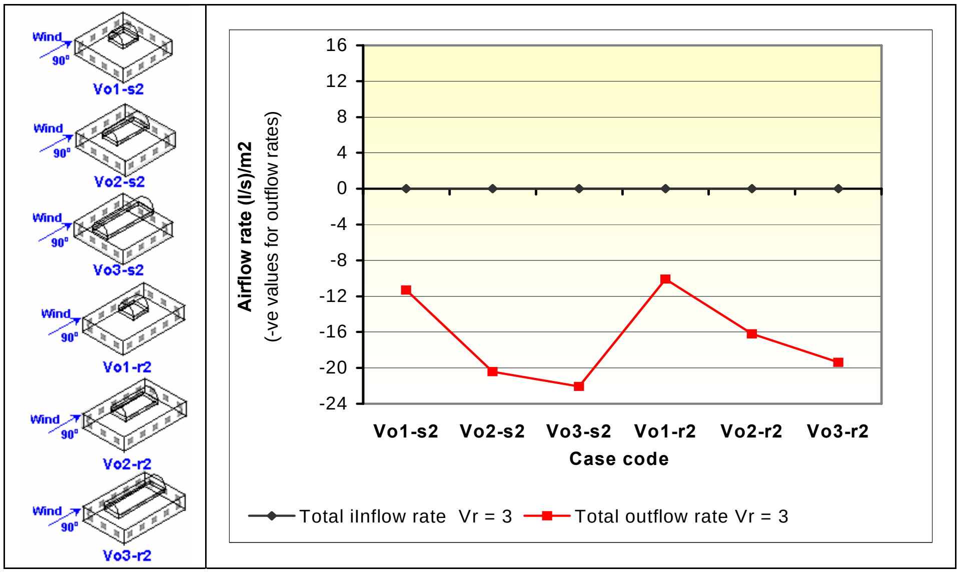

Figure 7.6: Volumetric inflow and outflow rates through vault openings presented for plan-unit area of the indicated cases and for 3m/s reference wind velocity and 90° wind angle

It is clear in Figure 7.6 that all vault openings function in suction, since inflow rate is zero in all cases. This has led to a significant increase in outflow rates compared to the previous two wind directions. Wind here is parallel to the vault. This means that airflow separation occurs over the sharp edges of the vault base and the curved edges of the vault itself. This results in large negative pressure fields surrounding the literal facades of the vault, in which vault openings are located.

Another observation is that outflow rate through vault openings in the case of square cases is higher, when compared to the rectangular ones in this wind direction. Figure 7.7 shows that the square roof is subjected to a higher negative pressure, compared to the rectangular one. This can be explained by that when airflow separates over the building windward sharp edge, larger amount of the air, compared to the rectangular roof, prefers to pass over the building instead of around it following the shorter distance. This results in a more active air motion over the roof and, thus, a higher difference in pressure around the vault apertures.

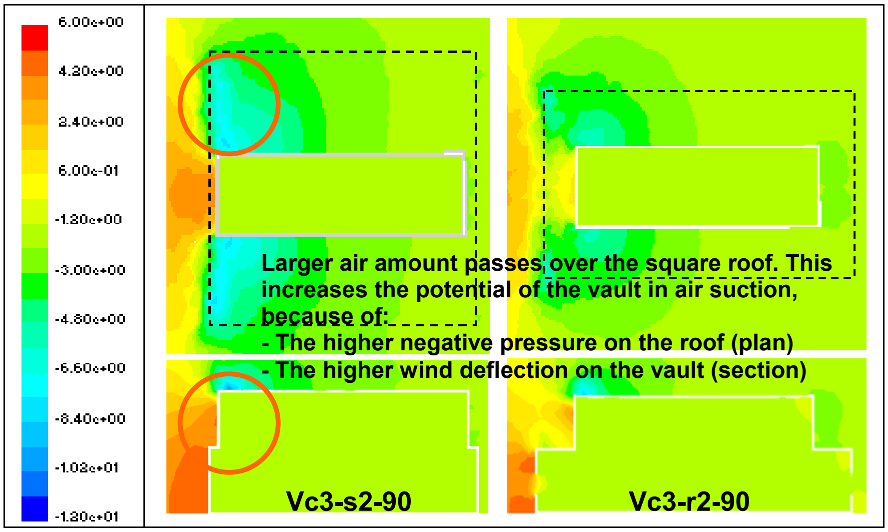

Figure 7.7: Contours of static pressure (Pa) at roof' level of the indicated cases, showing that square roof is subjected to a higher negative pressure

7.4 A comparison between the potential of domed and vaulted roofs for inducing ventilation by suction

This section compares in a summarised manner net outflow rates recorded at the tested domed and vaulted roof configurations. Two equivalent domed and vaulted roofs, in terms of the plan area of the roof and the main volume, have been chosen. These configurations are Do2 and Vo1, for both square and rectangular building forms. So, four cases in total will be compared, as illustrated at the top of Figure 7.8.

This comparison is also intended to show the effect of closing roof inlet on increasing net outflow rate through the curved roof. It is important to mention that the configurations tested here have different opening areas, as illustrated in Table 7.3. Thus, these different areas have been normalised by dividing the recorded net outflow rate by outlet opening area, instead of dividing it by the main volume area. Thus, it will be possible to compare natural ventilation performance of both configurations under the same conditions.

Table 7.3: Outlet opening area of the compared dome and vault cases

Roof configuration	Outlet opening area (m2)		
	0^o	45^o	90^o
Do2	3.41	3.41	3.41
Vo1	1.93	1.93	3.85

By comparing the vault configuration Vo1 to the dome configuration Do2, it is possible to notice that the difference between domed and vaulted roofs performance is highly dependant on wind angle. It is also clear that closing roof inlet always increases outflow rate through its outlet openings. This is in exception of Vo1 in the case of 90^{o} wind direction, where all vault openings work as outlets

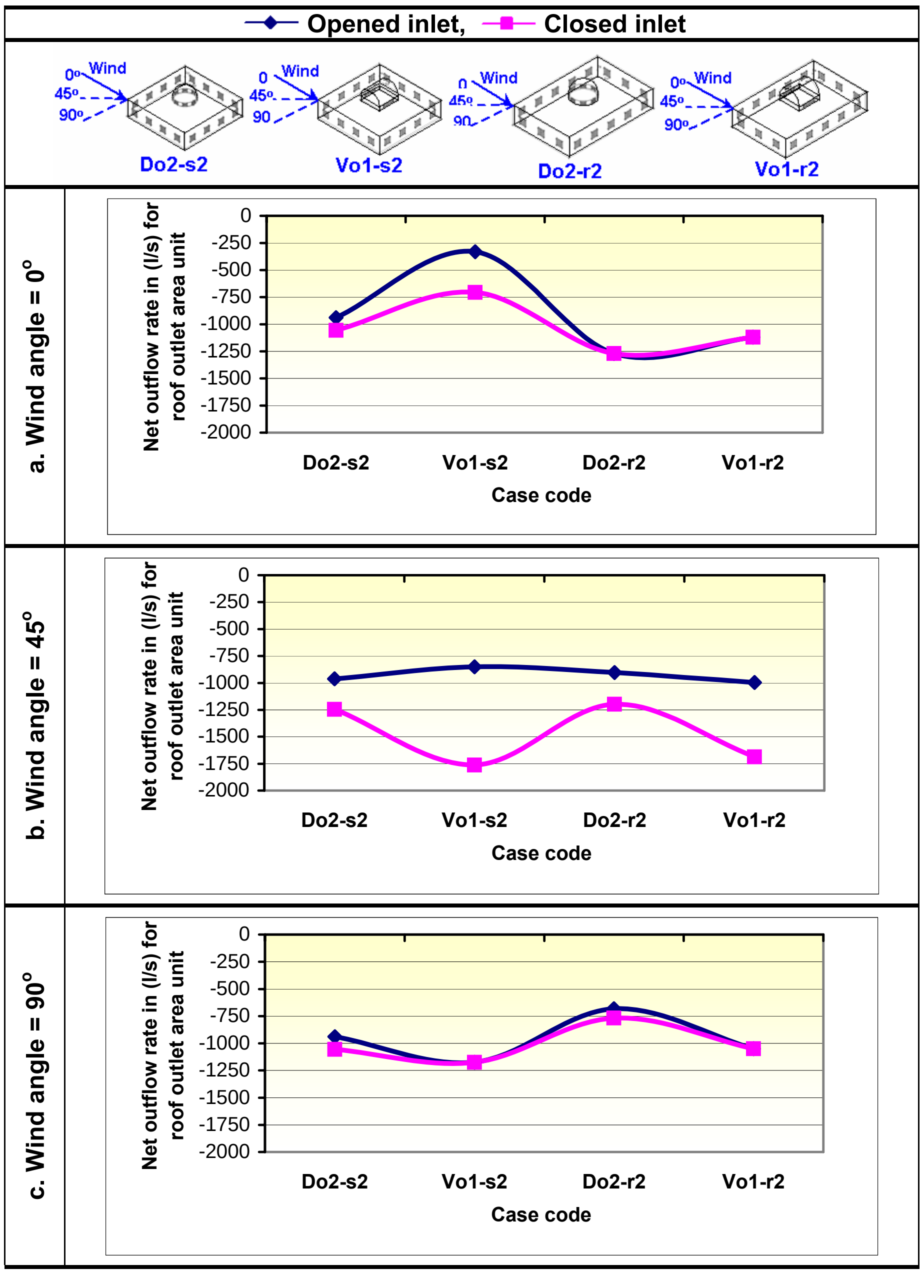

Figure 7.8: A comparison between the potential of domed and vaulted roofs for air suction, considering square and rectangular building forms, and 3 m/s reference wind velocity

In the case of 0^o wind incidence, net outflow rate is generally higher in the case of using the dome. This is only significantly higher in the square building form, where the difference is 65%, while it is only 12% in the rectangular building form. The significant difference in the square cases is due to the higher value of inflow rate through vault openings, which limits its rule in air suction, as explained in Section 7.3.1. On the opposite, inflow rate for both rectangular cases is zero. However, the difference observed between these cases shows that dome geometry is more efficient in air suction. Closing roof inlet has no effect in the case of rectangular cases due to the originally zero inflow rate. In the square case, suction potential has been mainly improved in the vault by about 100%. This has reduced the difference in net outflow rate between the dome and the vault in the square cases to 33%, compared to 65% before closing the inlet. Practically, this difference is about 150 (l/s)/m^2 of outlets unit area, which is equivalent to the ventilation need of 25 persons, as explained in Section 6.2.

In the case of 45^o wind direction, the use of either roof shape has nearly the same advantage. Net outflow rate recorded through the dome is higher than the one recorded through the vault by 12% in the square cases, while it is less by 10% in the rectangular case. Closing roof inlet has more effect in improving the potential of the roof for air suction, compared to previous wind direction. In the square building form, this improvement is 30% and 100% respectively for the dome and the vault. In the rectangular building form, this improvement is 30% and 70% respectively for the dome and the vault. The significant improvement observed is due to the observed high inflow rate through the roof in this wind direction, as has been discussed in Section 7.4.2. Thus, the use of the vault here is more effective after closing roof inlet, which has increased its net outflow rate to be higher that the dome by 40% for both square and rectangular cases. This is expected to positively affect airflow rates through wall openings, and, accordingly, airflow distribution.

In the case of 90^o wind direction, net outflow rate is higher in the case of using the vault. This is because the parallel orientation of the vault with respect to the wind increases its potential for air suction, as discussed in Section 7.4.3, where more surface area of the vault is subjected to negative pressure. Net outflow rate recorded through the vault is higher by 25% and 55% than the one recorded through the dome for square and rectangular cases, respectively. Closing roof inlet, namely for the dome, has improved its potential for air suction by 12%. This has reduced the difference in net outflow rate. Net outflow rate recorded through the vault is now higher by 10% and 35% than the one recorded through the dome for square and rectangular cases, respectively.

7.5 The effect of vault utilisation on airflow rate through wall openings and internal airflow distribution

This section discusses mass flow rated through the 16 openings located in the walls of the main building volumes illustrated in Figure 7.1. The discussion considers the effect of vault utilisation for natural ventilation on airflow rates and distribution in the building. Mass flow rates have been computed by Fluent software, and then converted to volumetric flow rates for the floor unit area of the main volume. Figure 7.9 presents these flow rates. However, this can be found numerically for every opening in Appendix B. As both low and high air velocities resulted in nearly the same airflow behaviour, this discussion is limited to the high air velocity, where differences between different values are larger and easier to be handled.

The same method used in the Chapter 6 for internal airflow distribution assessment has been used here, as explained in details at the beginning of Section 6.6. It has been found that changing wind direction has the most dramatic effect here. Therefore, this section is divided according to the three different wind directions tested. It has also been found that both air velocities used in the modelled cases presented in Table 7.1 have resulted in the same internal air distribution, but with different velocity scales. Thus, the following airflow distribution results will be assumed applicable for both reference wind velocities in all cases tested here.

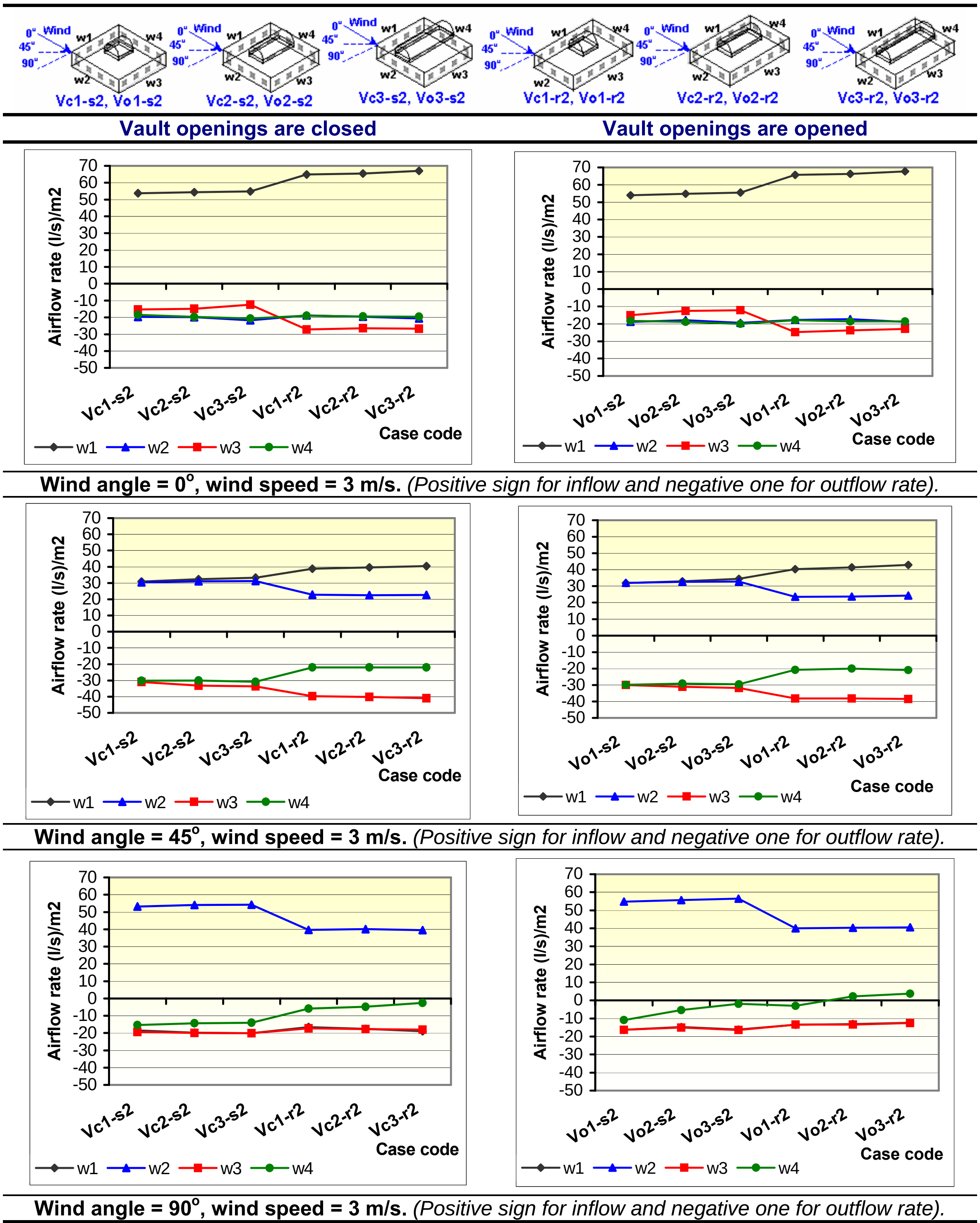

Figure 7.9: Average volumetric airflow rate (for building unit area) through wall openings recorded in the Vault Study at a reference wind speed of 3 m/s

7.5.1 In the case of 0^o wind incidence

Figure 7.9 shows the general behaviour of airflow through wall openings in the different building walls, where no dramatic change has been recorded after the utilisation of the vault for natural ventilation. These graphs show airflow rate for the floor unit area, where a slight change is important. Therefore, and to make more accurate assessment, numerical comparisons are held between airflow rates before and after the utilisation of the vault in the different wind directions. Table 7.4 presents inflow and outflow rates recorded in this wind direction. Figures 7.10 and 7.11 present internal airflow distribution using contours of air velocity magnitude for both square and rectangular cases.

Table 7.4: The effect of vault openings operation on inflow and outflow rates through wall openings in the case of 0^o wind direction and 3m/s wind speed

Case	Inflow rate		Diff. (%)	Outflow rate		Diff. (%)
	Closed vault	Opened vault		Closed vault	Opened vault	
V1-s2	53.65	53.94	**+0.54**	-53.65	-52.35	**-2.42**
V2-s2	54.41	54.82	**+0.75**	-54.41	-49.25	**-9.48**
V3-s2	54.84	55.51	**+1.22**	-54.84	-51.70	**-5.73**
V1-r2	64.86	65.70	**+1.30**	-64.86	-60.30	**-7.03**
V2-r2	65.43	66.23	**+1.22**	-65.43	-59.50	**-9.06**
V3-r2	66.98	67.74	**+1.13**	-66.98	-60.34	**-9.91**

* All airflow rate values are in (l/s)/m^2.

In the case of normal wind incidence, slight effect of the vault has been observed in increasing inflow rate through the building windward. The effect of the vault in attracting some of the air to leave through it instead of building literal and leeward faces is more significant. This can be noticed in Figure 7.9. This is because the percentage of reduction in outflow rate is always higher than the percentage of increase in inflow rate. Generally, vault effect is more significant when it is integrated with the rectangular building form. As has been discussed in Section 7.3.1, this is because the short distance between the vault inlet(s) in the rectangular case reduces inflow rate through the vault, and increases its potential for air suction.

However, the behaviour of outflow rates in each building form seems to be inconsistent. Roof configuration Vo3 seems to be less efficient, compared to Vo2 and Vo3. This is true at both square and rectangular forms. This is because as the vault area increases from Vo2 to Vo3, inflow rate has increased more rapidly, as illustrated in Figure 7.3. This is because roof configuration Vo3 has three inlets, compared to two in configuration Vo2 and one in configuration Vo1. This means that the middle inlet is less affected by airflow separation occurred over the vault literal sharp edges. This increases inflow rate through the vault in this wind direction, and reduces its advantage in attracting some of the air to leave through it instead of the wall openings.

Figures 7.10 and 7.11 illustrate contours of air velocity magnitude, integrated with a numerical assessment of internal airflow distribution in the occupied level of the building. A large area of the still-air zone has been observed. This is about 40% in the square configurations, and about 30% in the rectangular ones. This is because airflow penetrates the space diagonally, as discussed in Section 6.6.1. This increases still-air zone in the downstream part of the space. Utilising the vault has benefited from this airflow pattern, and has resulted generally in a more active air motion in the upstream and central zones of the building.

In the square cases, utilisation of the first vault configuration has nearly no effect, due to the small suction acting over it, and the large depth of the plan. In the other two cases, vault utilisation has slightly reduced the area of this still-air zone. This has increased the area of other zones that possess higher air velocity, like zone B in the second square case and zone D in the third square case. In the rectangular cases, area of the still-air zone is generally less, due to the smaller building depth. Utilisation of the vault in the first and second cases has improved airflow distribution. In the third case, vault utilisation has a reverse effect. This is because the suction acting on the vault has improved ventilation in the centre of the building on the account of its corners.

Vr = 1 (m/s)	Vr = 3 (m/s)	Vault openings are closed	Vault openings are opened
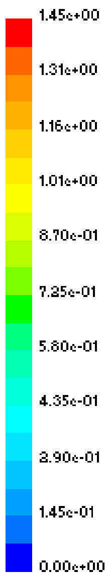	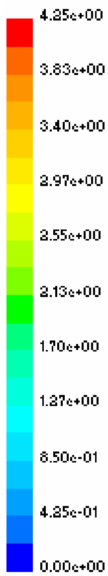	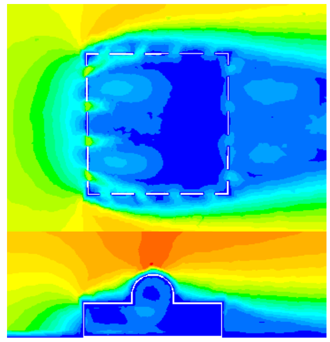 Vc1-s2	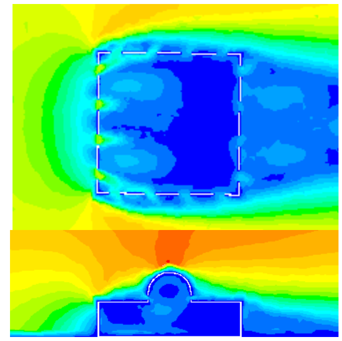 Vo1-s2
		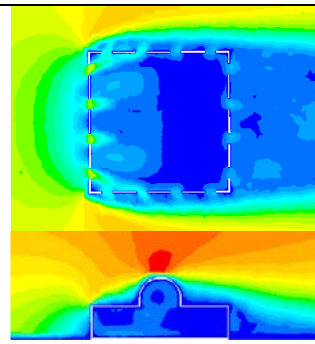 Vc2-s2	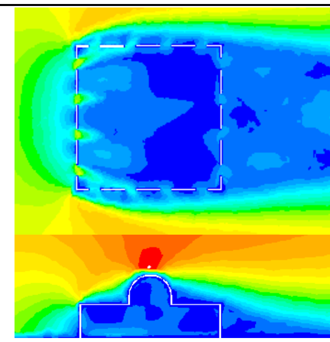 Vo2-s2
		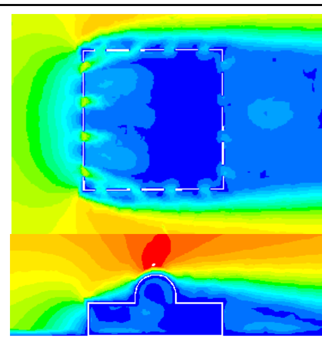 Vc3-s2	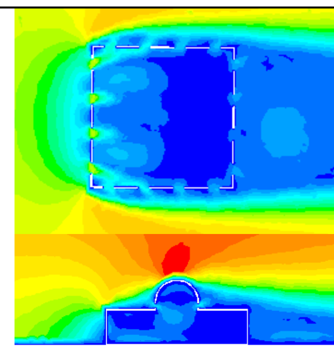 Vo3-s2

* Contours of velocity magnitude shown above are presented in Plane1 and 2 (Scale 1:1000), with normal wind direction, and both 1 and 3 m/s reference wind velocities.

Air velocity contour	Vi (Vr=1m/s)	Vi (Vr=3m/s)	% of total plan area (square cases)					
			Vc1-s2	Vo1-s2	Vc2-s2	Vo2-s2	Vc3-s2	Vo3-s2
A	0.0	0.0	42.0	41.8	44.6	39.8	46.5	44.6
B	0.07	0.2	27.6	27.1	26.2	33.3	23.0	24.3
C	0.14	0.4	15.6	15.4	15.2	15.5	17.1	14.1
D *& above*	$0.14<Vi<Vi_{max}$	$0.4<Vi<Vi_{max}$	14.8	15.7	14.0	11.4	13.0	17.0

Figure 7.10: Comparison of internal airflow distribution presented by internal air velocity Vi distribution before and after utilising the vault openings in the square building form at 0° wind direction.

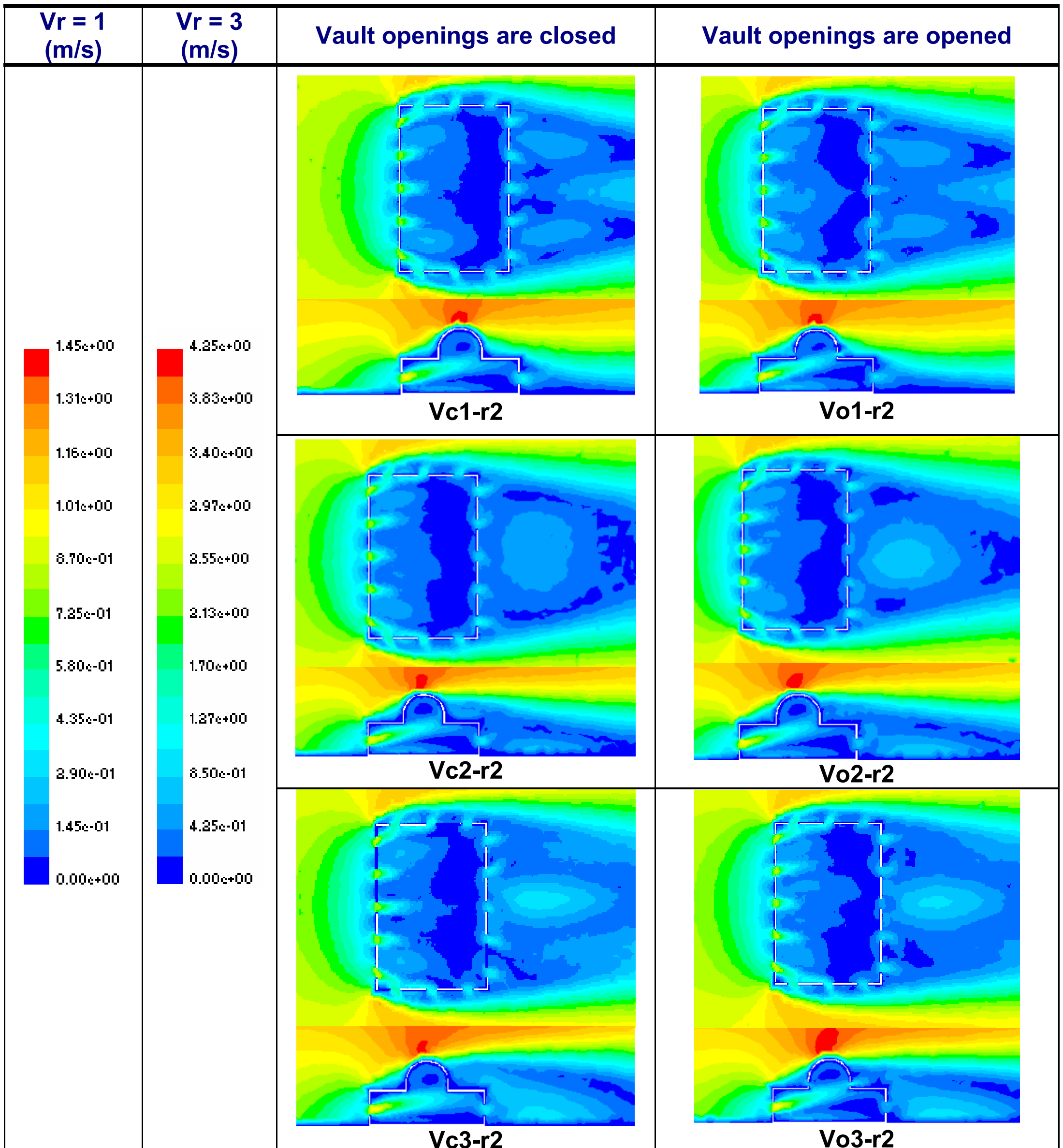

* Contours of velocity magnitude shown above are presented in Plane1 and 2 (Scale 1:1000), with normal wind direction, and both 1 and 3 m/s reference wind velocities.

Air velocity contour	Vi (Vr=1m/s)	Vi (Vr=3m/s)	% of total plan area (rectangular cases)					
			Vc1-r2	Vo1-r2	Vc2-r2	Vo2-r2	Vc3-r2	Vo3-r2
A	0.0	0.0	33.5	28.0	34.3	31.4	30.9	33.8
B	0.07	0.2	37.8	34.6	33.1	38.8	34.4	33.3
C	0.14	0.4	15.6	19.0	15.2	16.2	17.6	15.8
D *& above*	$0.14<Vi<Vi_{max}$	$0.4<Vi<Vi_{max}$	13.1	18.4	17.4	13.6	17.1	17.1

Figure 7.11: Comparison of internal airflow distribution presented by internal air velocity Vi distribution before and after utilising the vault openings in the rectangular building form at 0^{o} wind direction.

7.5.2 In the case of 45^o wind incidence

Table 7.5 presents inflow and outflow rates recorded in this wind direction. Figures 7.12 and 7.13 present internal airflow distribution using contours of air velocity magnitude for both square and rectangular cases.

Table 7.5: The effect of vault openings operation on inflow and outflow rates through wall openings in the case of 0^o wind direction and 3m/s wind speed

Case	Inflow rate		Diff. (%)	Outflow rate		Diff. (%)
	Closed vault	Opened vault		Closed vault	Opened vault	
V1-s2	61.24	63.92	**+4.38**	-61.24	-59.83	**-2.30**
V2-s2	63.37	65.49	**+3.35**	-63.37	-60.25	**-4.92**
V3-s2	64.49	67.33	**+4.40**	-64.49	-61.39	**-4.81**
V1-r2	61.65	63.86	**+3.58**	-61.65	-59.02	**-4.27**
V2-r2	62.08	65.18	**+4.99**	-62.08	-58.20	**-6.25**
V3-r2	63.04	67.10	**+6.44**	-63.04	-59.53	**-5.57**

* All airflow rate values are in (l/s)/m^2.

In the case of oblique wind direction, the observed increase in inflow rate for both square and rectangular cases is significantly higher than the case of normal wind direction. This occurred through the building windward facades due to the higher suction acting over the vault, as has been discussed in Section 7.3.2. This is expected to be even higher in the case of closing the vault inlet(s), as discussed in Section 7.4. In addition, inflow rate is higher because building in this orientation has more inlet area. On the opposite, the recorded reduction in outflow rates is less here because building has less outlet area.

Both square and rectangular cases have good internal air distribution, since the still-air zone area is less than 15% in the square cases and 25% in the rectangular ones. This is because building orientation here has facilitated the opposite cross ventilation, as has been discussed in Section 6.6.2. Utilisation of the vault generally has insignificant effect in the square cases and the first rectangular case. This indicates that the horizontal air movement at the building windward wing, which has been facilitated by the opposite cross ventilation, still stronger than the vertical one. In the last two rectangular cases, an adverse, but insignificant, effect of the vault utilisation has been observed. This is because airflow in such deep buildings, and under the increasing suction force, prefers to leave through vault openings instead of wall outlets, following the less resistance.

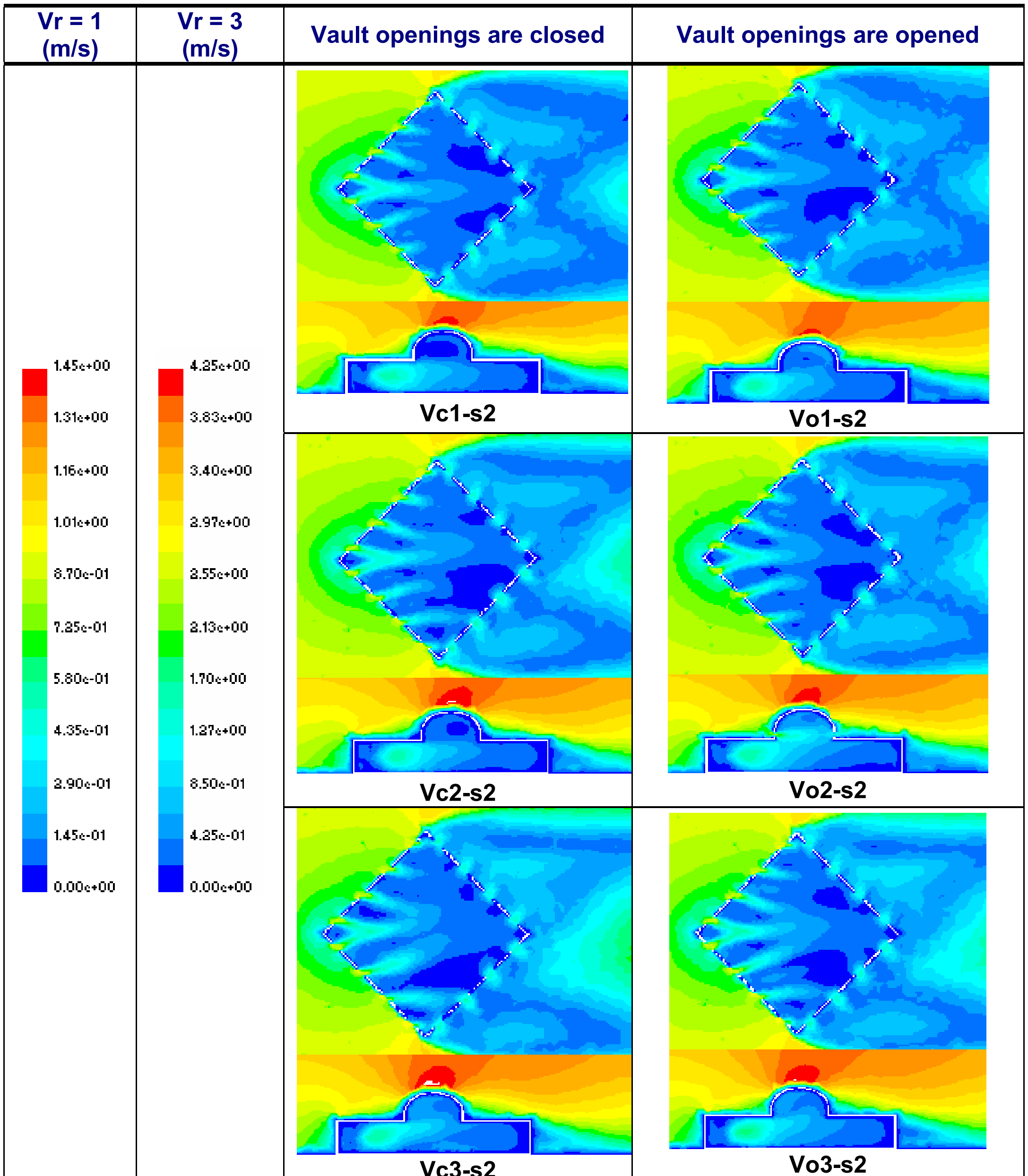

* Contours of velocity magnitude shown above are presented in Plane1 and 2 (Scale 1:1000), with 45° wind direction, and both 1 and 3 m/s reference wind velocities.

Air velocity contour	Vi (Vr=1m/s)	Vi (Vr=3m/s)	% of total plan area (square cases)					
			Vc1-s2	Vo1-s2	Vc2-s2	Vo2-s2	Vc3-s2	Vo3-s2
A	0.0	0.0	9.3	11.5	13.5	14.1	13.5	11.8
B	0.07	0.2	54.6	48.5	43.5	48.1	39.7	41.7
C	0.14	0.4	16.6	16.2	18.7	16.8	18.8	19.8
D *& above*	$0.14<Vi<Vi_{max}$	$0.4<Vi<Vi_{max}$	19.5	23.8	24.3	21.0	28.0	26.7

Figure 7.12: Comparison of internal airflow distribution presented by internal air velocity Vi distribution before and after utilising the vault openings in the square building form at 45° wind direction.

Vr = 1 (m/s)	Vr = 3 (m/s)	Vault openings are closed	Vault openings are opened
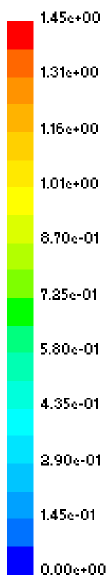	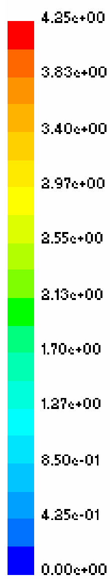	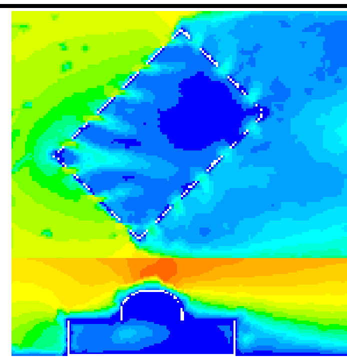 Vc1-r2	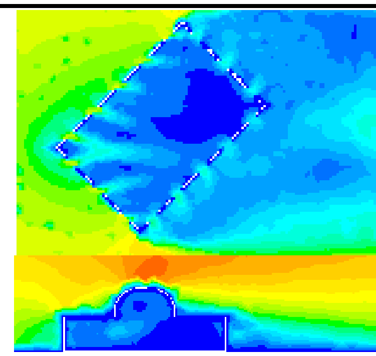 Vo1-r2
		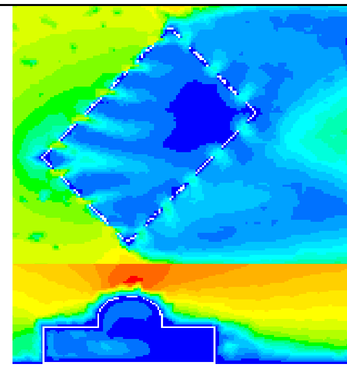 Vc2-r2	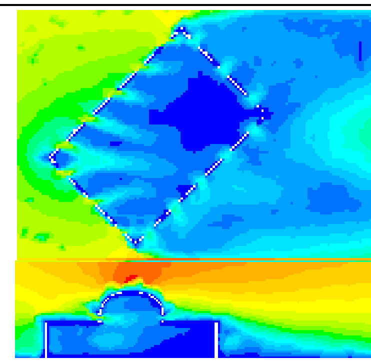 Vo2-r2
		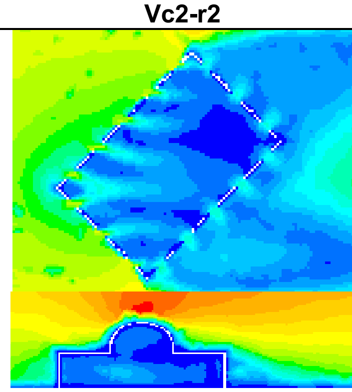 Vc3-r2	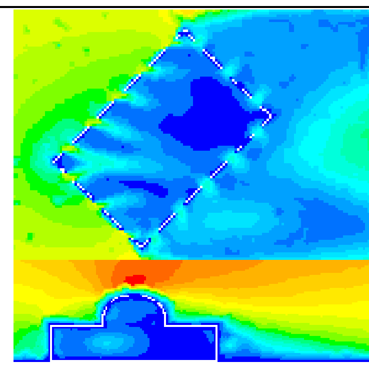 Vo3-r2

* Contours of velocity magnitude shown above are presented in Plane1 and 2 (Scale 1:1000), with 45^{o} wind direction, and both 1 and 3 m/s reference wind velocities.

Air velocity contour	Vi (Vr=1m/s)	Vi (Vr=3m/s)	% of total plan area (rectangular cases)					
			Vc1-r2	Vo1-r2	Vc2-r2	Vo2-r2	Vc3-r2	Vo3-r2
A	0.0	0.0	22.5	21.1	17.4	22.3	15.3	20.0
B	0.07	0.2	38.7	40.3	38.0	39.6	36.7	36.1
C	0.14	0.4	16.0	17.2	22.4	18.6	23.0	18.5
D *& above*	$0.14<Vi<Vi_{max}$	$0.4<Vi<Vi_{max}$	22.8	21.4	22.2	19.5	25.0	25.4

Figure 7.13: Comparison of internal airflow distribution presented by internal air velocity Vi distribution before and after utilising the vault openings in the rectangular building form at 45^{o} wind direction.

7.5.3 In the case of 90° wind incidence

Table 7.6 presents inflow and outflow rates recorded in this wind direction. Figures 7.14 and 7.15 present internal airflow distribution for both square and rectangular cases, using contours of air velocity magnitude.

Table 7.6: The effect of vault openings operation on inflow and outflow rates through wall openings in the case of 0° wind direction and 3m/s wind speed

Case	Inflow rate		Diff. (%)	Outflow rate		Diff. (%)
	Closed vault	Opened vault		Closed vault	Opened vault	
V1-s2	53.27	54.78	**+2.83**	-53.27	-43.48	**-18.38**
V2-s2	54.04	56.97	**+5.42**	-54.04	-36.54	**-32.38**
V3-s2	54.20	60.13	**+10.94**	-54.24	-38.06	**-29.83**
V1-r2	39.67	41.12	**+3.66**	-39.67	-31.04	**-21.75**
V2-r2	40.08	43.19	**+7.76**	-40.08	-27.00	**-32.63**
V3-r2	40.61	45.69	**+12.51**	-40.61	-26.31	**-35.21**
* All airflow rate values are in (l/s)/m^2.						

In this wind direction, a higher increase in inflow rate has been observed. This is associated with a significant reduction in outflow rates, due to the suction forces acting on the vault. Relationship between the increase in inflow rate and decrease in outflow rate is consistent, since it is in proportion to the opening area of the vault. This was not the case when wind was normal to the vault, as has been discussed in Section 7.5.1. The maximum increase in inflow rate reaches a value of about 11% in the case of square form and 12.5% in the case of rectangular form. It is clear that this increase is slightly higher in the case of rectangular configurations. This seems to be in disagreement with the findings of Section 7.3.3 that in this wind direction outflow rate through vault openings is higher in the case of square configurations.

However, the observed increase in inflow rate in the case of rectangular configurations has occurred due to the reversed airflow acting on the leeward façade, wall 4. This can be noticed by comparing airflow rates through wall 4, as depicted in Figure 7.9. Openings located in this façade are supposed to function as outlets. In the square cases, air passing over the roof has more kinetic energy, compared to the rectangular cases, especially when vault openings are closed. This increases its potential, after it reattaches in the wake zone, to resist the strong rotating air vortex that formulates at that zone due to airflow reattachment. On contrary, air passing over the rectangular roof has originally less kinetic energy. It also loses more kinetic energy during its journey along the roof, especially when vault openings are utilised. This is due to the generated vortices on the literal vault faces, as illustrated in Figure 7.14. Thus, it has less potential to resist the reversed airflow in the wake zone. This allows some air to enter the building again through wall 4.

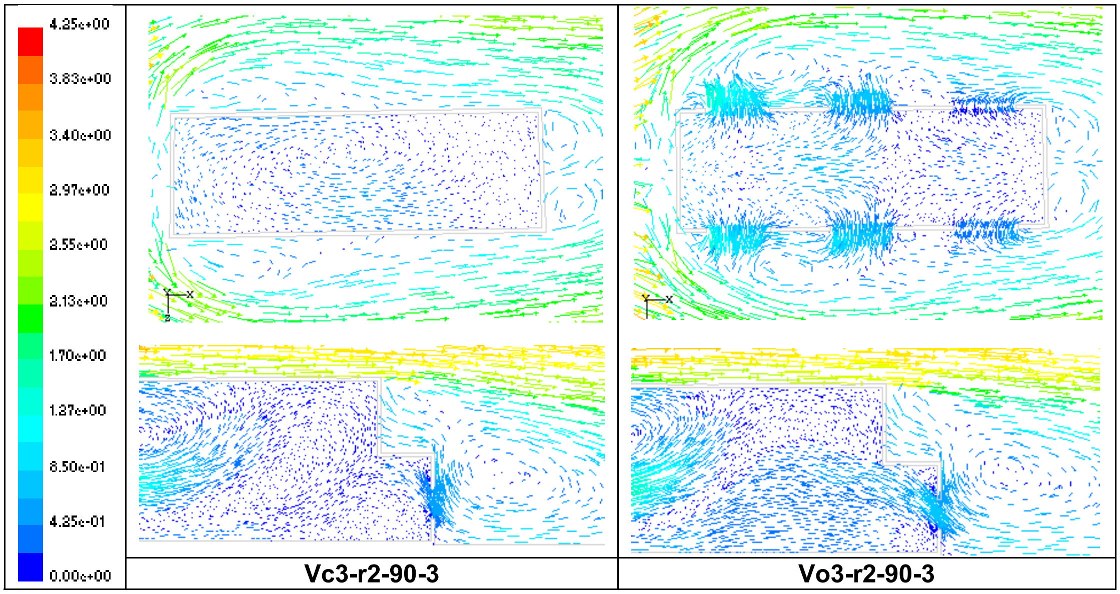

Figure 7.14: Velocity vectors for the indicated rectangular cases at roof level (above), which shows air vortices generated around the vault when its apertures are opened, and across plane 2 (below), which shows the reversed flow

In the first square configuration, a significant improvement in internal airflow distribution has been observed. This is due to the significant suction force acting on the vault, which drag airflow to the centre and towards the leeward wing of the building. When this suction increases in the other two square cases, it improves airflow distribution in the building centre on the account of its downstream corners. Rectangular cases have presented a more consistent behaviour, where the situation has been improved at all of the three cases. For example, area of the still air zone has been reduced by about 15%, compared to about 5% in the dome study. This is due to the extreme suction acting over the vault. This did not cause any adverse effect due to the less width of the building. The other reason is the occurrence of the reversed flow in the leeward façade, as explained above.

Vr = 1 (m/s)	Vr = 3 (m/s)	Vault openings are closed	Vault openings are opened

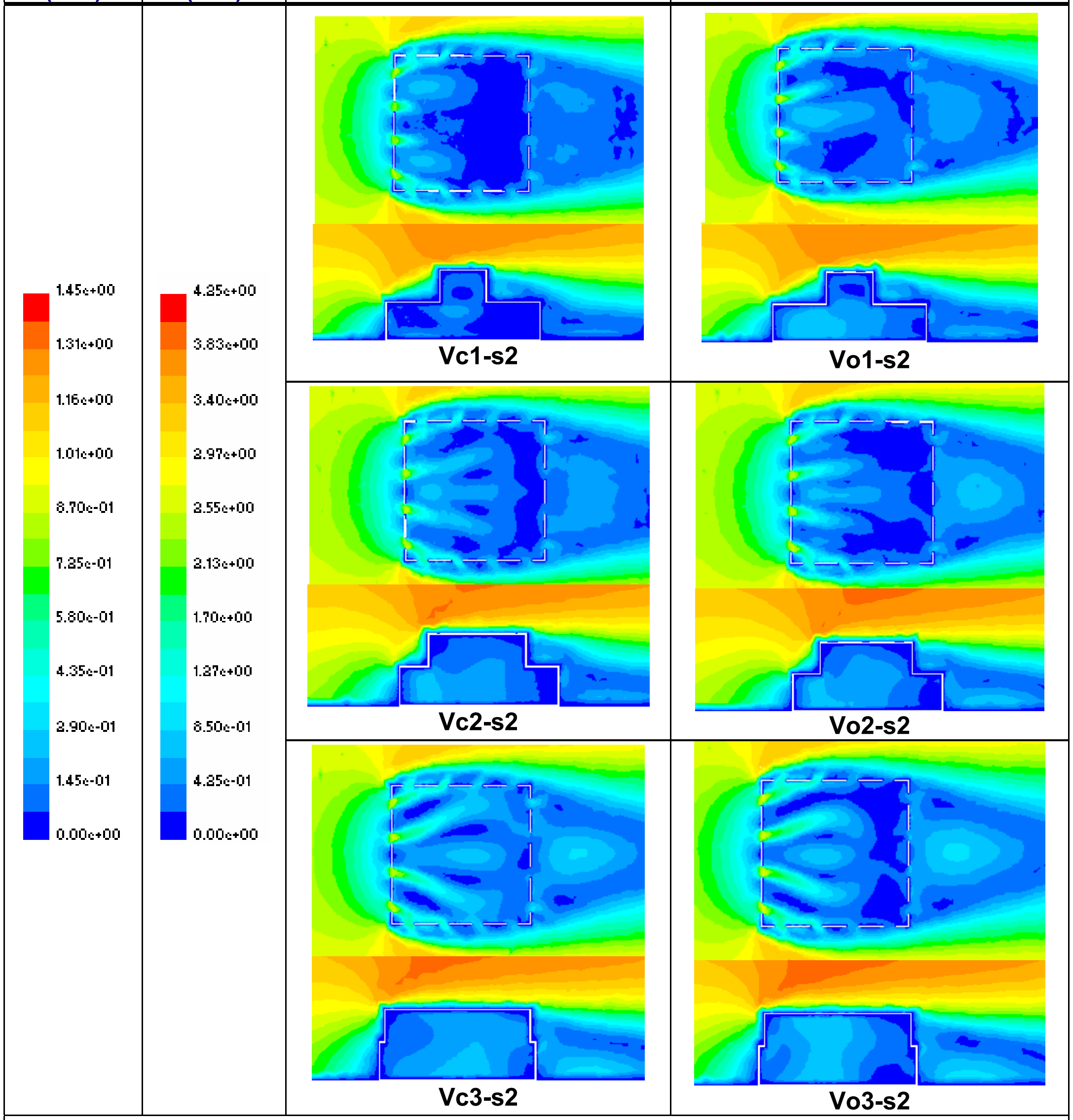

* Contours of velocity magnitude shown above are presented in Plane1 and 2 (Scale 1:1000), with 90° wind direction, and both 1 and 3 m/s reference wind velocities.

Air velocity contour	Vi (Vr=1m/s)	Vi (Vr=3m/s)	% of total plan area (square cases)					
			Vc1-s2	Vo1-s2	Vc2-s2	Vo2-s2	Vc3-s2	Vo3-s2
A	0.0	0.0	44.1	17.9	22.1	29.3	7.0	22.8
B	0.07	0.2	26.4	43.9	36.1	35.1	32.6	35.1
C	0.14	0.4	15.2	18.4	20.8	15.2	27.8	16.3
D *& above*	$0.14<Vi<Vi_{max}$	$0.4<Vi<Vi_{max}$	14.3	19.8	21.0	20.4	32.6	25.8

Figure 7.15: Comparison of internal airflow distribution presented by internal air velocity Vi distribution before and after utilising the vault openings in the square building form at 90° wind direction.

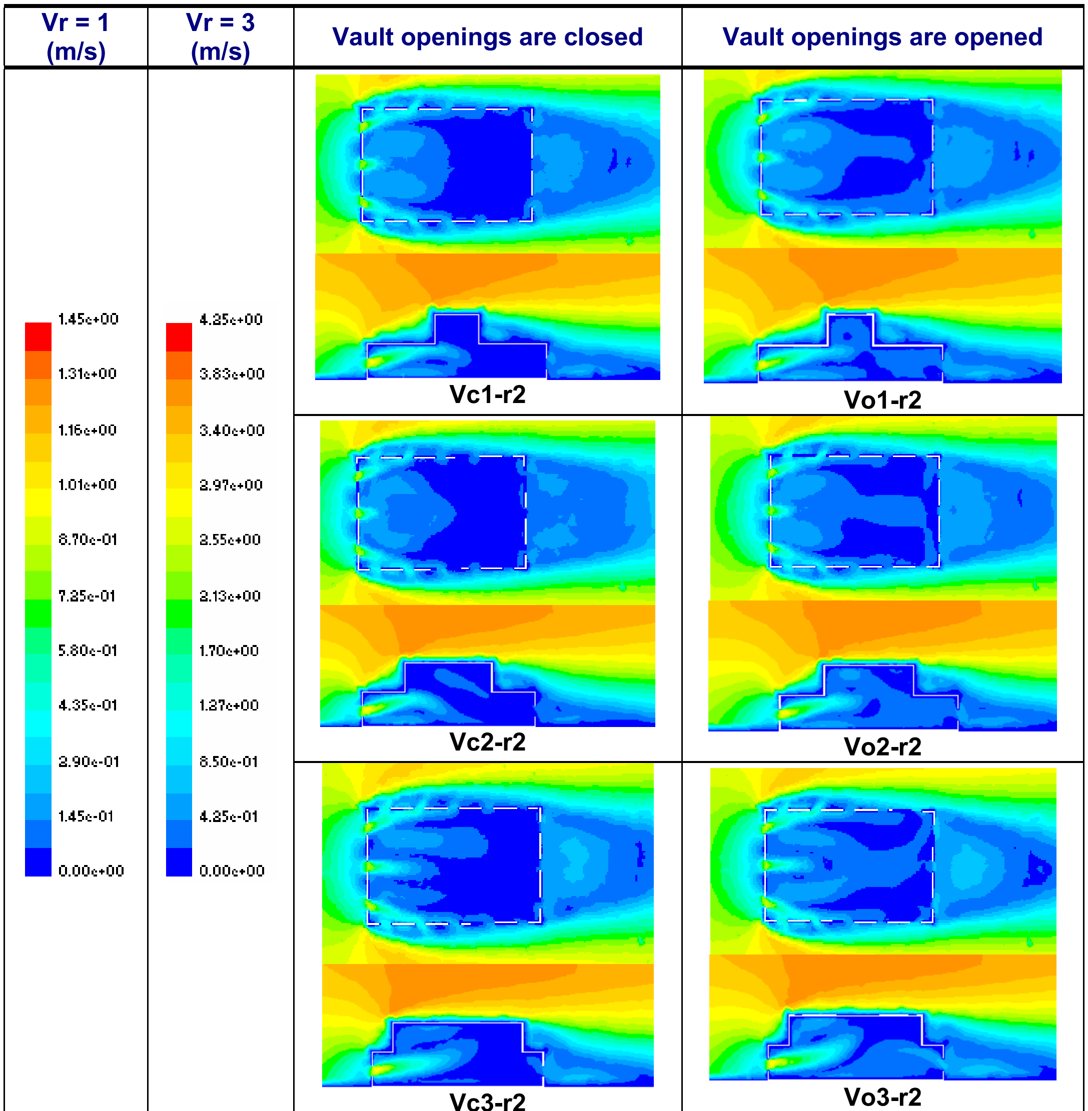

* Contours of velocity magnitude shown above are presented in Plane1 and 2 (Scale 1:1000), with 90° wind direction, and both 1 and 3 m/s reference wind velocities.

Air velocity contour	Vi (Vr=1m/s)	Vi (Vr=3m/s)	% of total plan area (rectangular cases)					
			Vc1-r2	Vo1-r2	Vc2-r2	Vo2-r2	Vc3-r2	Vo3-r2
A	0.0	0.0	49.6	31.7	50.4	36.0	50.0	27.5
B	0.07	0.2	21.3	35.5	23.5	39.2	24.6	44.9
C	0.14	0.4	14.3	19.8	14.3	15.0	11.0	14.3
D *& above*	$0.14<Vi<Vi_{max}$	$0.4<Vi<Vi_{max}$	14.8	13.0	11.8	9.8	14.4	13.3

Figure 7.16: Comparison of internal airflow distribution presented by internal air velocity Vi distribution before and after utilising the vault openings in the rectangular building form at 90° wind direction.

7.6 Conclusions

This study aimed to investigate the effect of vaulted roofs on wind-induced natural ventilation performance, presented by airflow rate and distribution at building interior. More than 50 cases have been modelled using Fluent 5.5 software. This has been done considering a variety of parameters, including form of the building, length and opening area of the vault, and wind direction. As practised in the dome study, openings have been located at vault base.

It has been concluded that there are many similarities between vaulted and domed roofs in terms of their natural ventilation performance. This includes:

- Vaulted roofs work mainly in suction, even with the half of its opening area being located at building windward façade. Inflow rate is restricted by the air vortex and negative pressure caused by airflow separation occurring over the windward sharp edges of the building and the vault.
- However, in the case of 90^o wind direction, no inflow rate has been observed, and outflow rate is significantly higher.
- Outflow rate through the vault increases as the distance between the vault and the roof windward sharp edge(s) decreases, i.e. when building form is square or rectangular. It also increases as the length and outlet area of the vault increases.
- Vault always induce more inflow rate through building windward face, and reduces outflow rate through walls openings. This is most effective in the case of 90^o wind directions, where inflow increase reaches 12%, and outflow reduction reaches 35%.
- The above-mentioned behaviour has generally improved internal airflow distribution in the upstream and central zones of the building, but has not guaranteed this in the downstream one.

This study has also compared natural ventilation performance of two equivalent cases of domed and vaulted roofs. Net outflow rate has been estimated and normalised for the unit area of the roof outlets at both cases. Results revealed that:

- The advantage of any roof shape in air suction is highly dependant on wind direction.

- In general, dome is more effective in inducing air outside the building in the case of 0^o wind direction, and square building form. In the case of rectangular building form, both roof configurations have the same advantage. This latter observation is true in the case of 45^o wind direction. However, vault has been found to be more effective in the case of 90^o wind direction.
- Closing roof inlet increases dome and vault outflow rate in the same significance. This is most significant at 45^o wind incidence, especially in the vault, due to the high inflow rate observed through the roof in this wind direction.

By comparing results concluded in the dome study to the ones concluded here, it seems that vault utilisation, similarly to the dome and especially when it is relatively long, has positively contributed to the observed increase of airflow rates. However, internal airflow distribution, especially in the downstream zone of the building still requires more improvement. As has been concluded in Chapter 6, one possible solution is to use an air supply system in that zone, which will be investigated in the Chapter 8 for both domed and vaulted roofs.

CHAPTER 8 : EFFECT OF INTEGRATING WIND CATCHERS WITH CURVED ROOFS ON NATURAL VENTILATION PERFORMANCE

Introduction

Chapters 6 and 7 have investigated the potential of different configurations of curved roofs, namely hemispherical domes and semicircular vaults, as wind-inducing devices in buildings. This has been carried out through parametric studies including different buildings forms, floor areas, wind directions, and wind speeds. It has been concluded that curved roofs utilisation improves airflow rate and internal airflow distribution in many cases. This is due to the fact that these roofs mainly operate in air suction, which induces more ventilation to the windward and central zones of the building. However, it has been observed that internal airflow distribution requires more improvement in the downstream wing of the deep-plan configurations.

Thus, this chapter aims to investigate the effect of integrating wind catcher, which has been used for centuries in building natural ventilation in the Middle East, with the previously investigated curved roofs. Similarly to Chapters 6 and 7, this study is intended to be a parametric one using CFD simulation. However, findings of these two chapters are used to reduce the variety of parameters in order to cope with the study limitations. Results obtained are quantitatively and qualitatively compared to the ones obtained in Chapters 6 and 7in terms of airflow rate and distribution.

8.1 Geometrical parameters

In this section, geometrical characteristics of the studied wind catcher are specified. The potential of wind catchers for natural ventilation has been reviewed in Section 4.4.3. It has been concluded that this role is affected by many geometrical parameters including: catcher height, form, and position. However, and as has been implemented in Chapters 6 and 7, the intention here is not to assess the detailed design of wind catchers, but the effect of integrating them with the curved roofs. Thus, three operation modes or systems of the catcher have been suggested here. These systems are illustrated in Table 8.1.

Table 8.1: The three wind-catcher systems considered in Chapter 8

No.	Illustration	Description
1	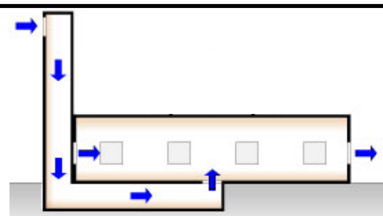	The higher aperture faces the prevailing wind. Catcher is connected to the centre of the plan by an underground tunnel. Depth of this tunnel affects its underground cooling effect. As this is not considered here, the tunnel is assumed just under building floor. Catcher provides air to the centre of the plan.
2	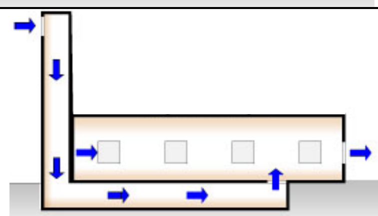	The higher aperture of the catcher faces the prevailing wind. Catcher is connected to the downstream wing of the building by an underground tunnel. Catcher internal aperture provides air to the space at a depth equals to ¾ of the total depth.
3		Catcher works as a wind chimney. The higher aperture is located in the back of the catcher. Catcher internal aperture opens to the space at the middle of the leeward face.

It is important to note that in each system, roof openings, being in a dome or a vault, and wall openings are still utilised for natural ventilation. Catcher form is assumed square, which is commonly used in both vernacular and temporary architecture. Cross sectional area is assumed 4.8 m^2, which is small compared to building plan area (400 m^2 in this study). Thus, catcher plan area is 1.2% of the total plan area, with a length of 2.2 m. Although this area represents an acceptable architectural proportion between different elements in the prototype tested, it has the advantage of reducing the construction cost as well. Catcher relative height is assumed 2.5 H, where H is the height of the main building volume, which is 5 m. Porosity is assumed 0.5% of the plan area. In the case of 0^o and 90^o wind directions, this is equivalent to two square opening (inlet and outlet), having a length of 1.4 m and area of about 2 m^2. In the case of 45^o, the top opening is equally divided into two openings located at both windward faces of the catcher.

8.2 Integration of domed roofs and wind catchers

This study, which is referred to as the 'Tower and Dome' study, aims to investigate the effect of integrating the domed roofs, tested in Chapter 6, with the different studied wind-catcher systems, illustrated in Table 8.1, on natural ventilation performance.

8.2.1 Tower and Dome study: terminology and programme

To facilitate the comparison between ventilation performance before and after integrating the catcher, modelling conditions implemented in Chapters 6 and 7 are also used here, with the same limitations, as explained in Section 7.2. Both low and high wind velocities are considered here. Figure 8.1 shows illustrations of the different cases of this modelling study. CAD illustrations with dimensions can be found in Section C.1 in Appendix C.

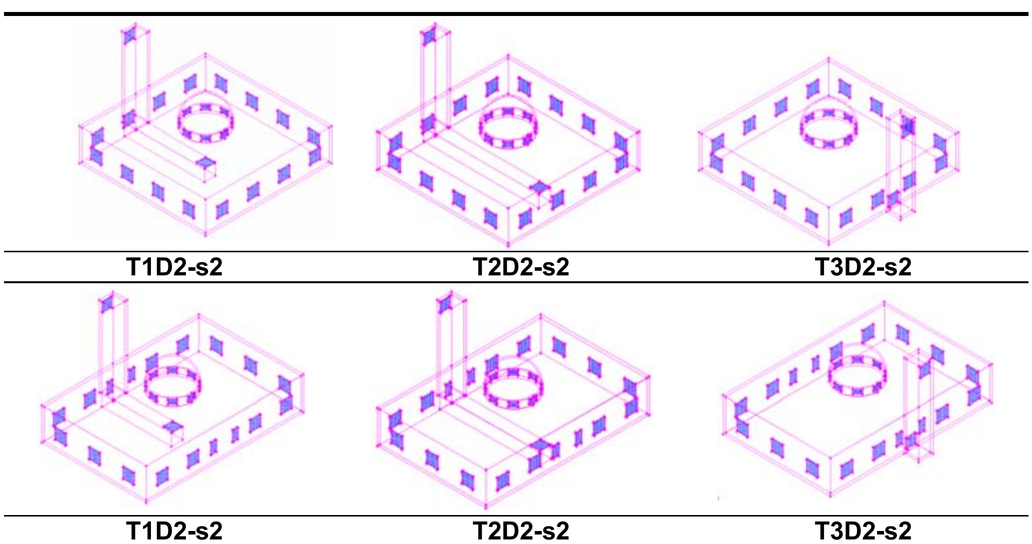

Figure 8.1: Different building configurations tested in the Tower and Dome study, illustrated in 0^o wind direction.

The different cases modelled in this study are designated with a ‘T’ and ‘D’ letters to refer to the ‘Tower and Dome’ study. ‘T’ letter is followed a serial number, from 1 to 3, to indicate the ventilation operation system of the catcher, as explained in Table 8.1. Using the same method implemented in Chapters 6 and 7, and explained in Section 6.3, ‘T’ and ‘D’ letters are followed by ‘s2’ or ‘r2’ symbols. These symbols indicate the square or rectangular form of the plan, respectively, with an area of 400 m^2. This presents the middle value of the three areas tested in Chapter 6. Two more numbers follow the resulting symbol: the first one indicates wind angle, 0^o, 45^o, or 90^o, and the second one indicates reference wind speed, 1 or 2 m/s. Figure 8.2 illustrates this coding method. Table 8.2 lists the different cases modelled in this study.

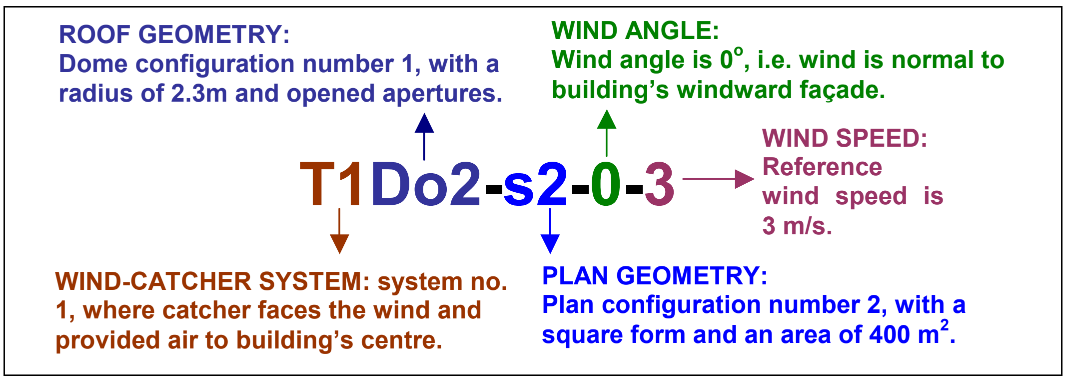

Figure 8.2: Coding method implemented in the Tower and Dome study

Table 8.2: CFD cases modelled in the Tower and Dome study

Config.	Description	Test no.	Test code	Wind angle	Wind speed (m/s)
T1Do2-s2	**Form:** square. **Plan area:** 400m^2 **Catcher operation:** wind catcher connected to the central zone of the plan.	1	T1Do2-s2-0-1	0^o	1
		2	T1Do2-s2-0-3	0^o	3
		3	T1Do2-s2-45-1	45^o	1
		4	T1Do2-s2-45-3	45^o	3
		5	T1Do2-s2-90-1	90^o	1
		6	T1Do2-s2-90-3	90^o	3
T1Do2-r2	**Form:** square. **Plan area:** 400m^2 **Catcher operation:** wind catcher connected to the central zone of the plan.	7	T1Do2-r2-0-1	0^o	1
		8	T1Do2-r2-0-3	0^o	3
		9	T1Do2-r2-45-1	45^o	1
		10	T1Do2-r2-45-3	45^o	3
		11	T1Do2-r2-90-1	90^o	1
		12	T1Do2-r2-90-3	90^o	3
T2Do2-s2	**Form:** square. **Plan area:** 400m^2 **Catcher operation:** wind catcher connected to the downstream zone of the plan.	13	T2Do2-s2-0-1	0^o	1
		14	T2Do2-s2-0-3	0^o	3
		15	T2Do2-s2-45-1	45^o	1
		16	T2Do2-s2-45-3	45^o	3
		17	T2Do2-s2-90-1	90^o	1
		18	T2Do2-s2-90-3	90^o	3
T2Do2-r2	**Form:** square. **Plan area:** 400m^2 **Catcher operation:** wind catcher connected to the downstream zone of the plan.	19	T2Do2-r2-0-1	0^o	1
		20	T2Do2-r2-0-3	0^o	3
		21	T2Do2-r2-45-1	45^o	1
		22	T2Do2-r2-45-3	45^o	3
		23	T2Do2-r2-90-1	90^o	1
		24	T2Do2-r2-90-3	90^o	3
T3Do2-s2	**Form:** square. **Plan area:** 400m^2 **Catcher operation:** wind chimney connected to the leeward wall of the building.	25	T3Do2-s2-0-1	0^o	1
		26	T3Do2-s2-0-3	0^o	3
		27	T3Do2-s2-45-1	45^o	1
		28	T3Do2-s2-45-3	45^o	3
		29	T3Do2-s2-90-1	90^o	1
		30	T3Do2-s2-90-3	90^o	3
T3Do2-r2	**Form:** square. **Plan area:** 400m^2 **Catcher operation:** wind chimney connected to the leeward wall of the building.	31	T3Do2-s2-0-1	0^o	1
		32	T3Do2-s2-0-3	0^o	3
		33	T3Do2-s2-45-1	45^o	1
		34	T3Do2-s2-45-3	45^o	3
		35	T3Do2-s2-90-1	90^o	1
		36	T3Do2-s2-90-3	90^o	3

It is worth mentioning here that files total size of the modelled cases of 'Dome and Tower' study is 3.20 GB. In the following sections, natural ventilation performance of the studied system will be discussed. Table 8.3 summarises numerically airflow rates estimated, and shows the reliability of the results obtained according to the Law of Conservation of Mass.

Table 8.3: Summary of airflow rates recorded in the different cases modelled in the Tower and Dome Study

	Wind angle 0° Wind velocity 3 m/s							Wind angle 45° Wind velocity 3 m/s							Wind angle 90° Wind velocity 3 m/s						
	Inflow rate			Outflow rate				Inflow rate			Outflow rate				Inflow rate			Outflow rate			
Case Code	Tower	Dome	Walls	Tower	Dome	Walls	Total	Tower	Dome	Walls	Tower	Dome	Walls	Total	Tower	Dome	Walls	Tower	Dome	Walls	Total
T1Do2-s2	8.32	0.00	55.18	---	-10.26	-53.24	**0.00**	5.06	3.29	63.71	---	-10.92	-61.12	**0.02**	8.32	0.00	55.18	---	-10.26	-53.24	**0.00**
T2Do2-s2	8.29	0.00	54.29	---	-9.69	-52.89	**0.00**	4.89	2.98	63.24	---	-11.06	-60.06	**-0.01**	8.29	0.00	54.29	---	-9.69	-52.89	**0.00**
T3Do2-s2	---	0.08	54.83	-3.63	-6.08	-45.19	**0.01**	---	3.06	69.01	-4.23	-7.94	-59.92	**-0.02**	---	0.08	54.83	-3.63	-6.08	-45.19	**0.01**
T1Do2-r2	8.19	0.00	66.02	---	-13.36	-60.85	**0.00**	4.93	2.35	67.65	---	-11.61	-63.32	**0.00**	8.11	0.00	40.71	---	-8.12	-40.69	**0.01**
T2Do2-r2	8.14	0.00	66.33	---	-13.21	-61.26	**0.00**	5.04	2.33	67.53	---	-11.43	-63.48	**-0.01**	7.98	0.00	39.10	---	-7.55	-39.55	**-0.02**
T3Do2-r2	---	0.22	67.44	-3.88	-8.35	-55.44	**-0.01**	---	3.47	69.15	-5.20	-7.51	-59.92	**-0.01**	---	1.04	40.84	-3.38	-3.63	-34.86	**0.01**

* All values are in (l/s)/m^2.

8.2.2 Effect of utilising wind catcher on airflow rate through dome openings

The same method used in Chapters 6 and 7 to compare natural ventilation performance is used here as well. Cases are compared before and after the integration of the different studied wind-catcher systems. For example, case Do2-s2 in the Dome Study will be compared to cases T1Do2-s2, T2Do2-s2, and T3Do2-s2. In the following analysis, some numerical values presented in the relevant graphs are given. However, all other values can be comprehensively found in Appendix C.2.

A. In the case of 0° wind incidence

Figure 8.3 summarises airflow rates through the dome at 0° wind direction. These airflow rates are recorded before utilising the catcher (the first case) and after that (the rest of the cases), and for both square and rectangular cases. It is clear that both velocities have presented the same behaviour. This is also true for the other wind directions tested. Therefore, numerical examples given here are limited to the 3 m/s wind velocity. It is also clear that the rectangular cases recorded higher outflow rates. This is because airflow separation at the windward sharp edge of the roof is stronger here due to the elongated nature of their geometry. Thus, larger amount of airflow blows above the building instead of around it, following the less resistance. This leads to higher suction forces acting on the dome.

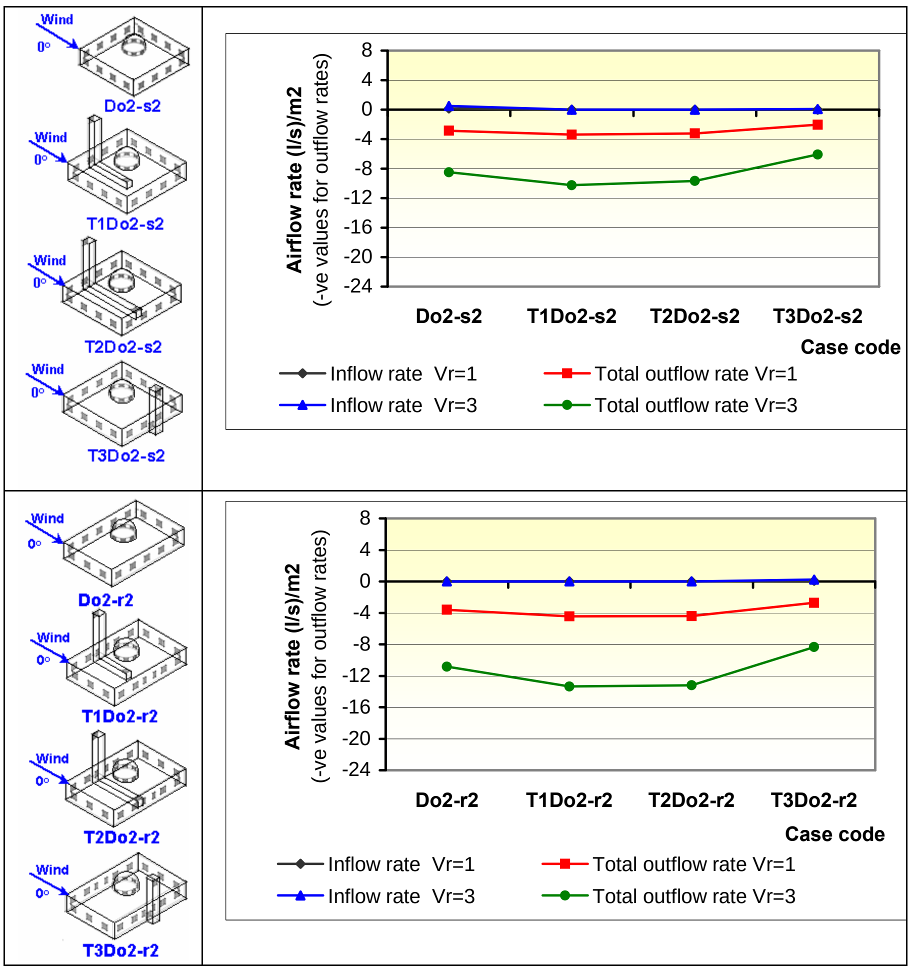

Figure 8.3: Airflow rate through the dome after utilising the different studied wind-catcher systems, where wind angle is 0^{o} and reference wind speed is 1 and 3 m/s

After utilising the first two wind-catcher systems, outflow rate through the dome has increased. This increase is slightly higher in the first system, where wind catcher supplies air to the centre of the space, i.e. directly under the dome. Numerically, this increase is about 20% in square cases and 23% in rectangular ones. In the case of utilising wind catcher as a wind chimney, significant reduction in the dome outflow rate has been recorded. This reduction is about 28% in square cases and 23% in rectangular ones. This is because wind catcher here attracts some of the air to leave through it instead of the dome. Observed internal airflow paths in the three studied wind-catcher systems are illustrated in Figure 8.4.

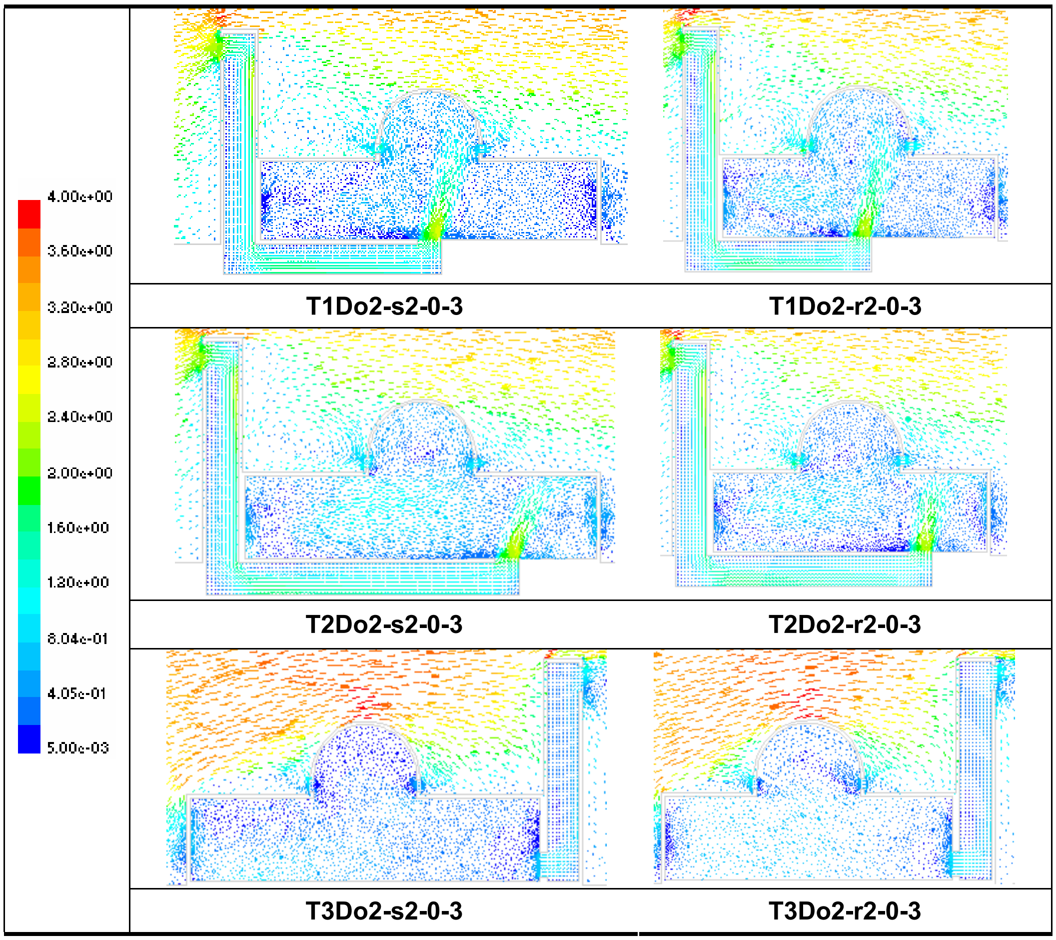

Figure 8.4: Internal airflow patterns in the three wind-catcher systems used, as illustrated by velocity vectors over a central vertical section

As explained in Chapters 6, inflow rate through the dome in this wind direction has recorded a relatively low value due to the generation of air vortex before the dome inlet. In the case of utilising wind catcher with the design, this value has been reduced even more to be zero, namely in the first two wind-catcher systems. This is due to the sheltering effect of wind catcher body, which is located in front of the dome inlet.

B. In the case of 45^o wind incidence

Figure 8.5 summarises airflow rates through the dome at 45^o wind direction. These airflow rates are recorded before utilising the catcher (the first case) and after that (the rest of the cases), and for both square and rectangular cases.

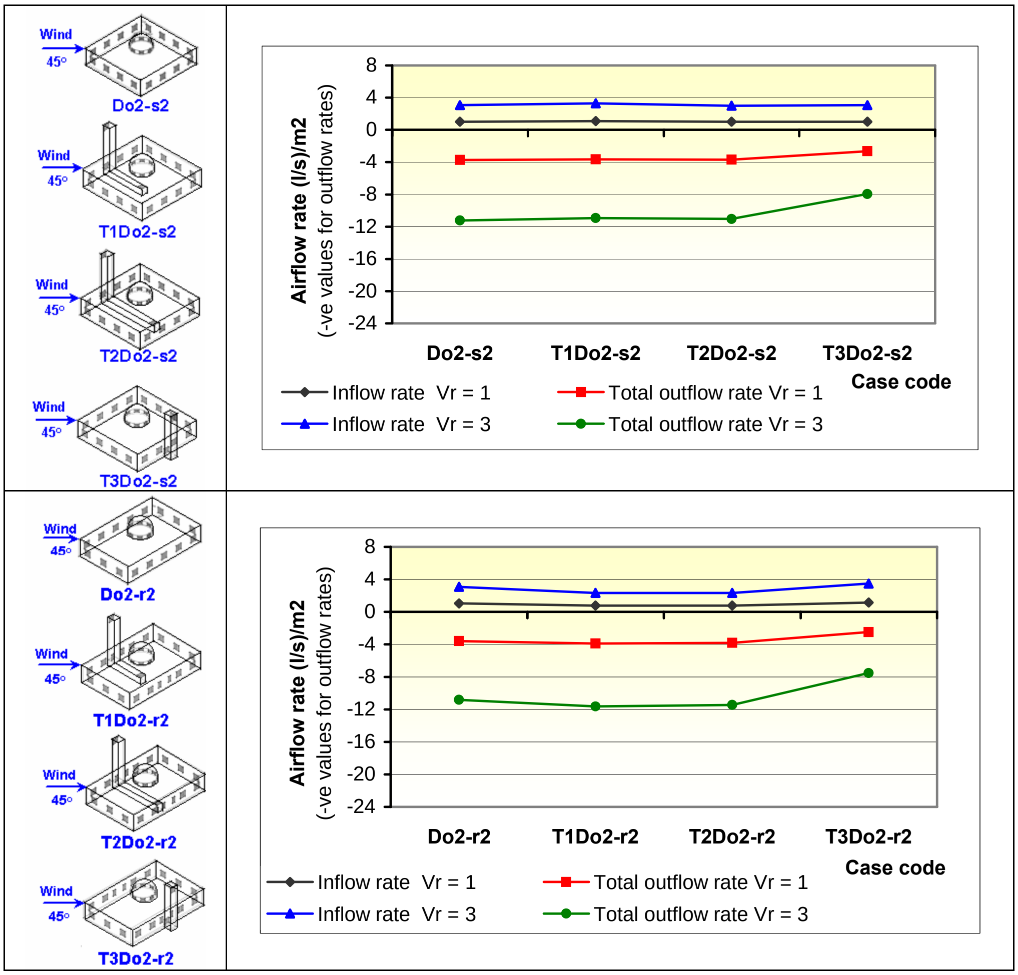

Figure: 8.5: Airflow rate through the dome after utilising the different studied wind-catcher systems, where wind angle is 45^o and reference wind speed is 1 and 3 m/s

The recorded inflow and outflow rates here present different behaviour, compared to the one observed in the previous wind direction. Airflow behaviour in 45^o wind direction has been explained in details in Section 6.5.2. In summary, inflow rate through the dome increases due to the absence of air vortex in front of its inlet. Outflow rate significantly increases in the square cases (about 30%) due to the generated air vortices at the windward sharp edges of the roof, which increases local suction around the dome. This is also true for the rectangular cases. After utilising the first two wind-catcher systems, slight change has been observed in inflow and net outflow rates through the dome. This is true for both square and rectangular configurations.

This indicates that suction forces acting over the dome do not have a significant effect on the catcher. Instead, catcher is more affected by suction forces acting on building walls. This will be illustrated in Section 8.2.3 (B). For example, the vertical section of case T1Do2-s2-0-3 shows a strong vertical air motion between the catcher outlet and the dome. This is not the case in T1Do2-s2-45-3, where the horizontal plan shows internal rotating air motion in the central zone of the plan. This means that suction forces acting on building leeward facades have more effect than the suction forces acting on the dome. The same observation is true in the case of rectangular building form, as could be concluded from the analysis of velocity vectors. This is also supported by the fact that outflow rate through wall openings in the case of oblique wind direction is always higher after the utilisation of wind catcher.

This is true for the first two wind-catcher systems. In the case of utilising the catcher as a wind chimney, significant reduction in outflow rate through the dome has been recorded. Numerically, this reduction is about 30% in both square and rectangular cases. This is because catcher inlet is subjected here to a negative air pressure. This has more effecting attracting air entering the building to leave through the catcher instead of the dome.

C. In the case of 90^{o} wind incidence

Figure 8.6 summarises airflow rates through the dome at 90^{o} wind direction. These airflow rates are recorded before utilising the catcher (the first case) and after that (the rest of the cases), and for both square and rectangular cases. Both inflow and outflow rates for the square configurations show the same tendency observed in the case of 0^{o} wind direction, due to building symmetry.

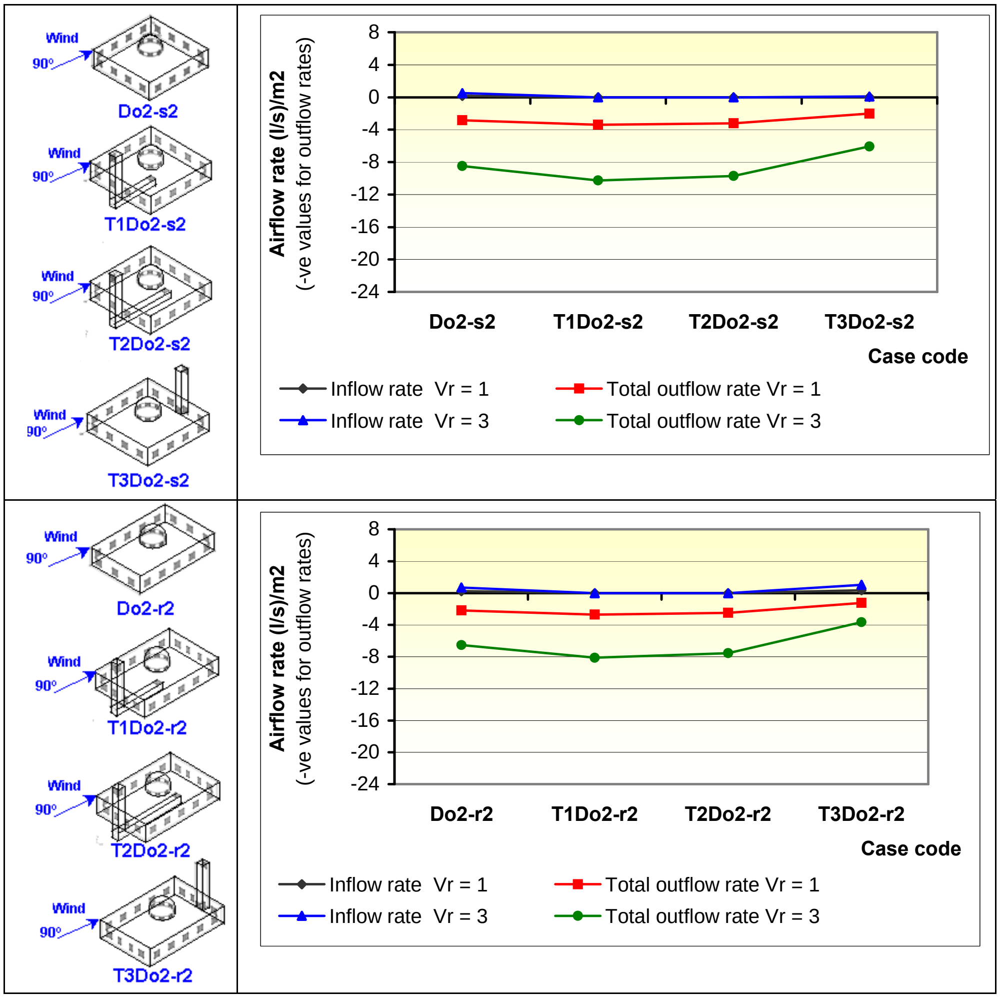

Figure: 8.6: Airflow rate through the dome after utilising the different studied wind-catcher systems, where wind angle is 90° and reference wind speed is 1 and 3 m/s

However, and as discussed in Sections 6.5.3 and 7.3.3 in Chapters 6 and 7, outflow rates through the dome in this wind direction are less when building form is rectangular. This is because building higher depth reduces suction forces acting on the roof. This is also true after utilising the catcher, especially in the third system, where the reduction reaches about 30%. This is due to the nature of rectangular geometries in this orientation, which possesses a deep plan. This reduces kinetic energy of airflow travelling over the building. This also reduces the effect of airflow separation over the roof windward sharp edge in generating suction forces around the dome, which is relatively away from this edge.

8.2.3 Effect of both wind catcher and dome on airflow rate through wall openings and internal airflow distribution

Mass flow rate through every opening of the 16 wall openings in every case has been computed using Fluent 5.5 software. It has been then converted to volumetric flow rate for the floor unit area. Figure 8.7 compares the general behaviour of airflow rates recorded through wall openings before and after utilising the catcher with the dome, for both square and rectangular cases. Additional tables are used during the discussion to facilitate a numerical comparison. These graphs also compare the three tested wind-catcher systems. As both reference wind velocities used here has resulted in the same airflow behaviour, numerical examples given in the discussion are limited for the higher wind velocity, 3 m/s. All other values, in addition to the graphs related to the low reference air velocity, can comprehensively be found in appendices C.2 and C.3.

The adopted method in assessing internal airflow distribution has been explained in Section 6.7 of Chapter 6. The same method is implemented here using the velocity contours tool in Fluent 5.5 software. Figure 8.7 shows these contours for both reference air velocities tested here. Results obtained are used to compare internal airflow distribution between the following cases:

- Configurations with cross ventilation through walls openings only, i.e. dome and catcher are not utilised.
- Configurations with cross ventilation through both walls and dome openings, i.e. catcher is not utilised.
- Configurations with cross ventilation through walls, dome, and catcher openings. These cases include the three wind-catcher systems tested here, as illustrated in Table 8.1. This also allows the comparison between these three wind-catcher systems.

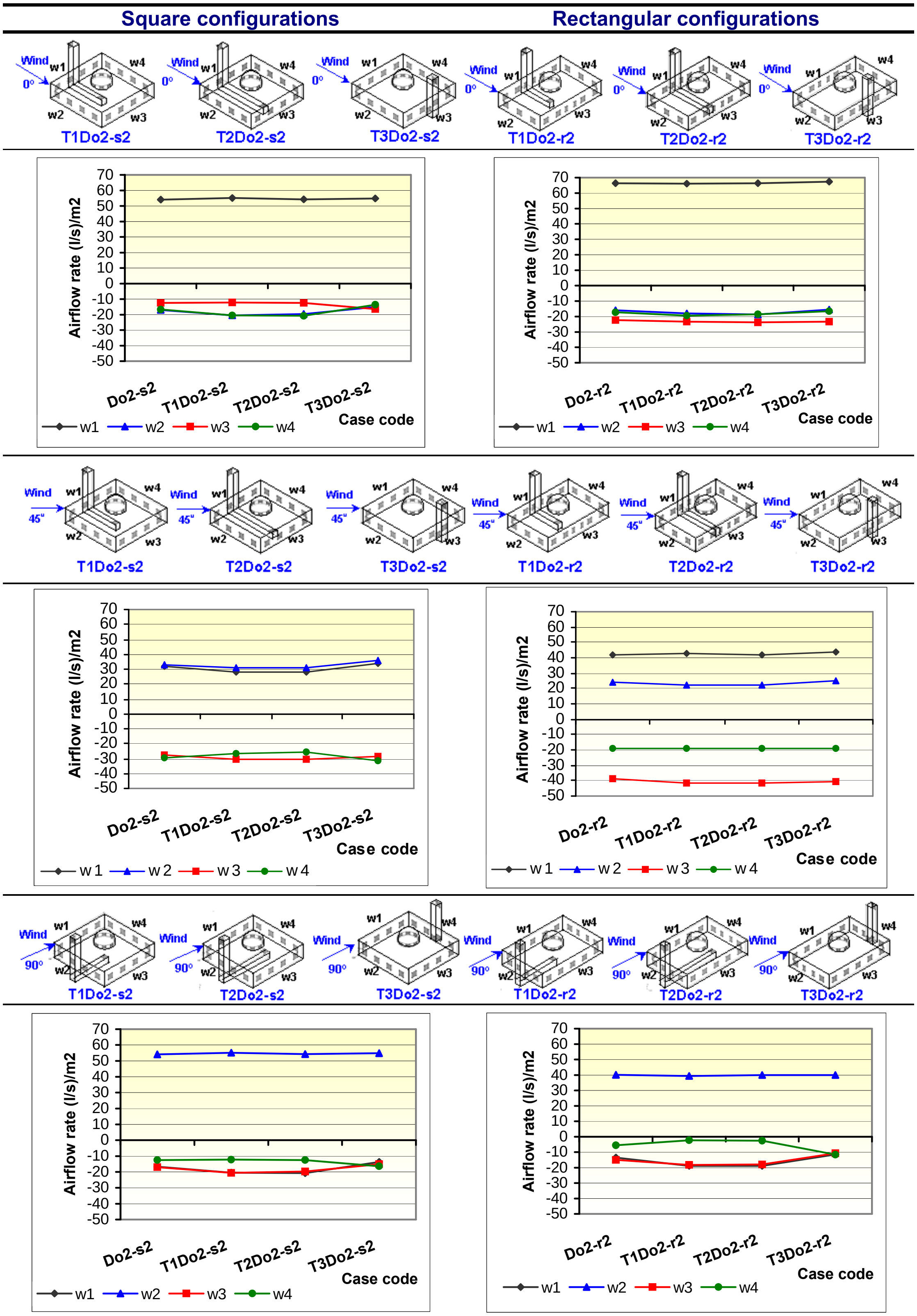

* Positive sign for inflow and negative one for outflow rate.

Figure 8.7: Average volumetric airflow rate through wall openings recorded in the Tower and Dome study at reference wind speed of 3 m/s

A. In the case of 0^o wind incidence

Table 8.4 presents inflow and outflow rates discussed here.

Table 8.4: The effect of wind catcher integration with the dome on inflow and outflow rates through wall openings in the case of 0^o wind direction and 3m/s reference wind speed

Inflow rate					Outflow rate				
Dome only		Dome & tower		Diff. (%)	Dome only		Dome & tower		Diff. (%)
Do2-s2	54.15	**T1Do2-s2**	55.18	**+1.9**	**Do2-s2**	-46.16	**T1Do2-s2**	-53.24	**+15.3**
		T2Do2-s2	54.29	**+0.3**			**T2Do2-s2**	-52.89	**+14.6**
		T3Do2-s2	54.83	**+1.3**			**T3Do2-s2**	-45.19	**- 2.1**
Do2-r2	66.40	**T1Do2-r2**	66.02	**- 0.6**	**Do2-r2**	-55.56	**T1Do2-r2**	-60.85	**+9.5**
		T2Do2-r2	66.33	**- 0.1**			**T2Do2-r2**	-61.26	**+10.3**
		T3Do2-r2	67.44	**+1.6**			**T3Do2-r2**	-55.44	**- 0.2**

* All airflow rate values are in (l/s)/m^2.

Utilising the catcher has caused a slight change in inflow rate through windward wall openings. However, significant increase in outflow rate in the first two wind-catcher systems has been recorded. This increase is about 15% in the square cases and about 10% in the rectangular ones. This increase has mainly occurred due to the air provided by the catcher. Part of this air leaves the building through the dome, and the rest leaves through the walls opening. In the square cases, the amount that leaves through the dome is less than the rectangular cases, due to the less suction that acts on the dome. This has been explained in Section 8.2.2 (A). Thus, the amount that leaves through the walls is higher.

However, it is important to note that square and rectangular cases presented different behaviours here, as can be noticed in Figure 8.7. In the square configurations, the increase at outflow rates in the first two wind-catcher systems has mainly occurred in the literal wall openings (w2 & w4). This is because of the higher suction forces acting over these faces. Utilising the catcher as a wind chimney increases suction forces acting over the leeward building face (w3). Thus, a significant increase in outflow rate through leeward wall openings has been observed. This is substituted by an equivalent decrease in outflow rate through literal walls openings. This is why there is no significant change in the total outflow rate after utilising the catcher. This means that utilising the catcher helps redistributing the internal airflow in different patterns. It also attracts more airflow to the still-air zone in building downstream wing. In the rectangular configurations, and for the first two systems, the situation is similar to what has been observed in the square cases. However, some additional increase at outflow rate through the leeward face (w3) has been observed. This is because building depth is smaller. In the third wind-catcher system, outflow rate through the literal wall openings ceases, but does not increase in the leeward wall openings. This is because suction forces acting over the dome are high here, compared to the square case, and have more effect than the suction caused by the catcher.

Figures 8.8 and 8.9 are used to assess internal airflow distribution. Generally, internal airflow distribution has been significantly improved after the utilisation of the catcher in both square and rectangular configurations, given that it is originally better in the rectangular ones due to the small depth of the building. Reduction in the still-air zone and increase in the higher-velocity zones have been observed. In the square configurations, the still-air zone is significantly less, when comparing Do2-s2 to T1Do2-s2, T2Do2-s2, and T3Do2-s2. The drop percentages are 12%, 21.4%, and 8% respectively. This resulted in an increase in air velocity zone C for the three cases, and in zone D for the first two ones. The improvement is more significant in the first two wind-catcher systems. Airflow entering the catcher is restricted by its walls, which increases airflow velocity. This can be noticed in the vertical sections of the buildings depicted in Figures 8.8 and 8.9. Thus, air pressure is reduced to compensate the observed increasein its kinetic energy (Moore, 1993). On the opposite, when airflow leaves the catcher, its velocity slows down and its pressure increases. This increases the potential of this air to be driven toward the dome or the adjacent wall openings, depending on the intensity of the surrounding suction forces. The second system is even more effective because catcher outlet is located more deeply in the building, which reduces the still-air zone. However, airflow distribution at the corners can also be improved using air distribution system.

In the rectangular configurations, two differences can be distinguished:

- The improvement observed in the first wind-catcher system is less, compared to the square building form. This is because the increased inflow rate provides more air to the centre of the plan, which is directly attracted by the suction acting on the dome.

- The improvement observed in the third wind-catcher system is the most significant. This is because the role of the dome has been limited here, as discussed in Section 8.2.2 (A). This allows more air to penetrate the space, which has smaller depth, so that it leaves through the tower instead of the dome. Thus, the still-air zone has nearly disappeared (only 4%), and the higher velocity zone has increased by about 13%.

Vr = 1 m/s	Vr = 3 m/s	Before utilising the catcher	After utilising the catcher

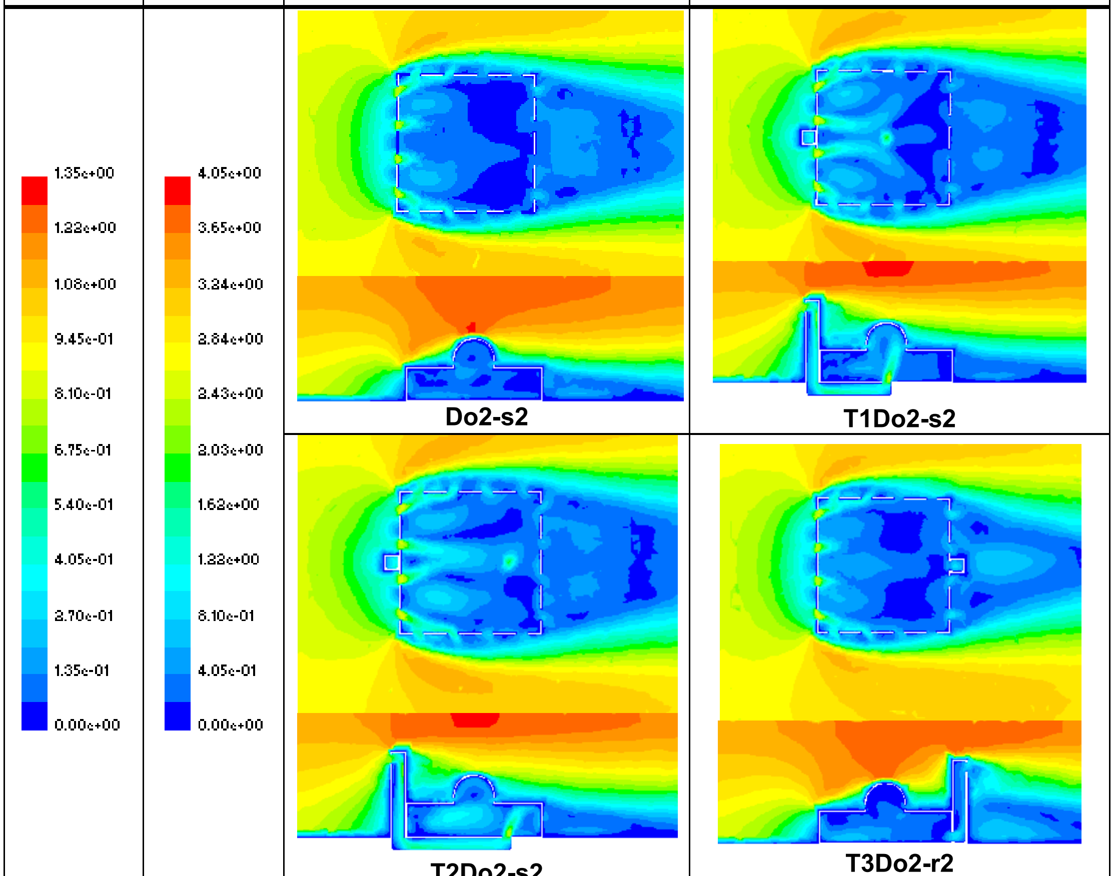

* Contours of velocity magnitude shown above are presented in Plane1 and 2 (Scale 1:1000), with normal wind direction, and both 1 and 3 m/s reference wind velocities.

Air velocity contour	Vi (Vr=1m/s)	Vi (Vr=3m/s)	% of total plan area (square cases)				
			Dc2-s2	Do2-s2	T1Do2-s2	T2Do2-s2	T3Do2-s2
A	0.0	0.0	37.0	31.2	18.6	9.4	22.6
B	0.07	0.2	28.8	37.8	32.9	35.1	37.0
C	0.14	0.4	15.9	14.1	19.9	22.3	24.5
D *& above*	$0.14<Vi<Vi_{max}$	$0.4<Vi<Vi_{max}$	18.3	16.9	28.6	33.2	15.9

Figure 8.8: Comparison of internal airflow distribution presented by internal air velocity Vi distribution before and after utilising the different wind-catcher systems with the dome in the square building form at 0^{o} wind direction.

Vr = 1 m/s	Vr = 3 m/s	Before utilising the catcher	After utilising the catcher
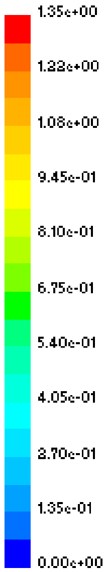	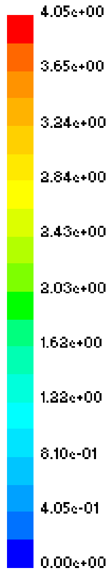	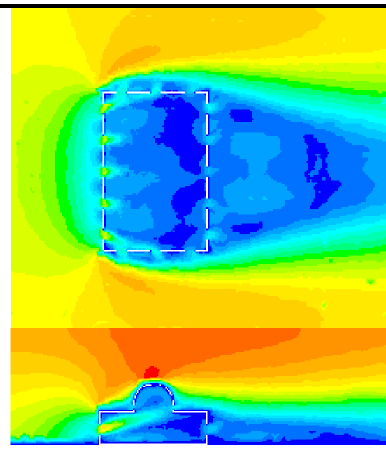 Do2-r2	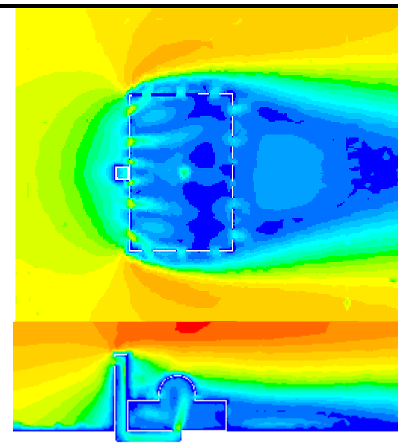 T1Do2-r2
		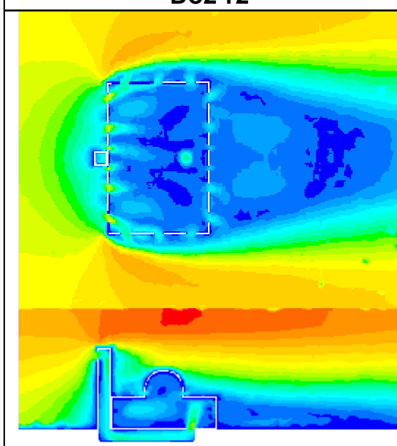 T2Do2-r2	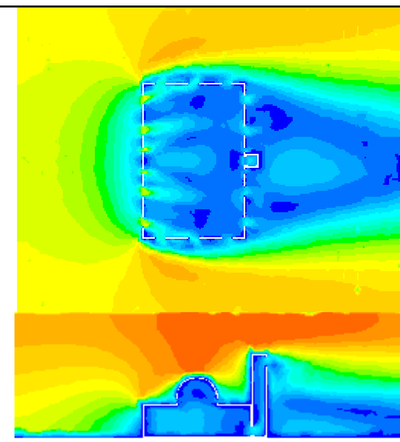 T3Do2-r2
* Contours of velocity magnitude shown above are presented in Plane1 and 2 (Scale 1:1000), with normal wind direction, and both 1 and 3 m/s reference wind velocities.			

Air velocity contour	Vi (Vr=1m/s)	Vi (Vr=3m/s)	% of total plan area (rectangular cases)				
			Dc2-r2	Do2-r2	T1Do2-r2	T2Do2-r2	T3Do2-r2
A	0.0	0.0	27.8	21.7	19.1	13.0	3.90
B	0.07	0.2	36.8	40.5	42.5	44.3	43.7
C	0.14	0.4	16.4	21	19.8	19.0	22.1
D *& above*	$0.14<Vi<Vi_{max}$	$0.4<Vi<Vi_{max}$	19.0	16.8	18.6	23.7	30.3

Figure 8.9: Comparison of internal airflow distribution presented by internal air velocity Vi distribution before and after utilising the different wind-catcher systems with the dome in the rectangular building form at 0^{o} wind direction.

B. In the case of 45^o wind incidence

Table 8.5 presents inflow and outflow rates discussed here.

Table 8.5: The effect of wind catcher integration with the dome on inflow and outflow rates through wall openings in the case of 45^o wind direction and 3m/s reference wind speed

Inflow rate					Outflow rate				
Dome only		Dome & tower		Diff. (%)	Dome only		Dome & tower		Diff. (%)
Do2-s2	65.66	**T1Do2-s2**	63.71	**- 3.0**	**Do2-s2**	-57.49	**T1Do2-s2**	-61.12	**+6.3**
		T2Do2-s2	63.24	**-3.7**			**T2Do2-s2**	-60.06	**+4.5**
		T3Do2-s2	69.01	**+5.1**			**T3Do2-s2**	-59.92	**+4.2**
Do2-r2	66.42	**T1Do2-r2**	67.65	**+1.8**	**Do2-r2**	-58.70	**T1Do2-r2**	-63.32	**+7.9**
		T2Do2-r2	67.53	**+1.7**			**T2Do2-r2**	-63.48	**+8.1**
		T3Do2-r2	69.15	**+3.9**			**T3Do2-r2**	-59.92	**+2.1**

* All airflow rate values are in (l/s)/m^2.

As discussed in Section 6.6.2, cross ventilation here is implemented between opposite walls only, which results in a more effective cross ventilation. However, the balance observed in ventilation between both building windward faces is no more valid after the utilisation of the first two systems of the catcher. This is due to the existence of catcher body on wall (w1), which weaken the role of the inlets located in this wall. This makes some of the air entering the building through wall (w2) to be attached to the leeward wall (w4), which causes an internal curved air motion. This can be observed in velocity contours, presented in Figure 8.10, and airflow rates recorded for the individual openings, as listed in Appendix C.2. In the rectangular configurations, a curved air movement has also been observed, but without air being reversed towards the windward façade (w1).

In the square configurations, inflow rate in cases T1Do2-s2 and T2Do2-s2 has been reduced, compared to case Do2-s2. This is because one opening at wall (w1) works as an outlet due to the sheltering effect of the wind catcher body, which is attached to this wall. Regarding outflow rate, the central rotating air movement has resulted in:

- Reducing outflow rate at wall (w4), due to the conflict between the curved air motion and the suction force act on this wall.
- Increasing outflow rate through the openings of (w3), which are at the wake of the curved air motion.

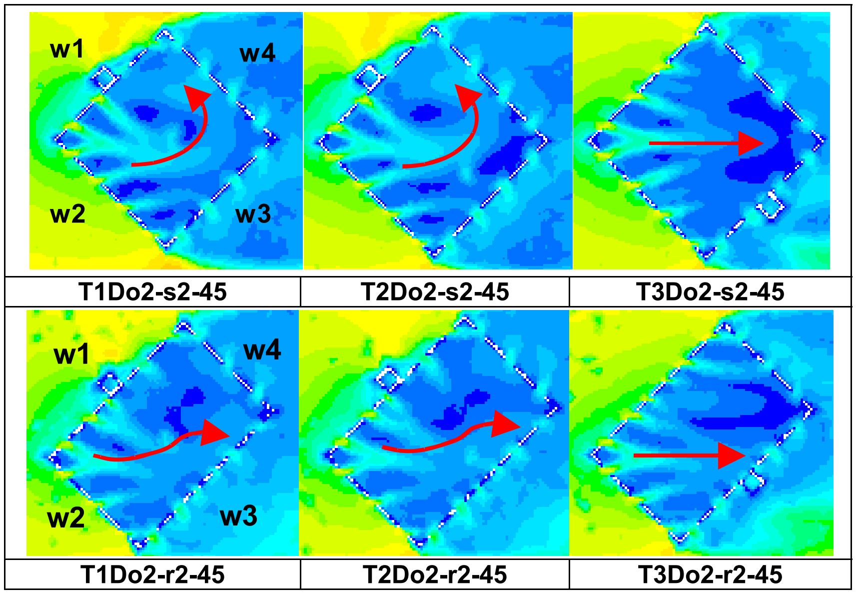

Figure 8.10: Contours of velocity magnitude showing different patterns of the internal air motion for the indicated cases, in the case of 45^{o} wind direction

In the rectangular configurations, inflow rate in cases T1Do2-r2 and T2Do2-r2 has slightly increased, compared to case Do2-r2. This is in spite of the fact that an opening at w1 works as an outlet, as discussed above. This is because internal suction forces generated by the wind catcher are strong enough to increase the total inflow rate, due to the smaller depth of the building. Regarding outflow rate, the central rotating air movement has resulted in:

- Insignificant change in inflow rate, because air is not reversed as observed in the square configurations.
- Increasing outflow rate through the openings of wall 3, due to the curved air deflection on that wall, and due to air provision by the catcher.

In the third wind-catcher system, where the catcher is employed as a wind chimney, both square and rectangular cases have presented a balanced and straight internal air movement, as could be noticed in Figure 8.10. As a result of the suction force caused by the catcher, both inflow and outflow rates have slightly increased at square and rectangular cases compared to the values recorded before employing the catcher.

Figures 8.11 and 8.12 are used to assess internal airflow distribution. In the square cases, the integration of the catcher with the dome in the first two wind-catcher systems has significantly improved the internal airflow distribution, after being slightly of poorer quality when the dome was solely employed. This indicates that the observed internal curved air motion has facilitated this improvement. The drop percentages in the area of the still-air zone are 8.7%, and 6% respectively. This resulted also in a reduction in air velocity zone B and increase in zone C. A significant increase has been observed also in the high-velocity zone, i.e. zone D, by 15.7% for the first wind catcher system, and 13% for the second one.

The resulting curved internal air movement has also improved internal airflow distribution the first two wind catcher systems in the case of rectangular building form. Area of the still-air zone has been reduced and limited at the central zone, instead of the downstream corner, as has been observed in the case of 0^o wind direction. The observed reduction is about 12%. This resulted also in a reduction in zone B and an increase in zone C. A significant increase has been observed also in the high-velocity zone, zone D, by about 10% for both cases.

This is not the case in the third wind-catcher system in the square cases, Do2T3-s2, where wind catcher works in suction, since insignificant improvement has been observed. This is because suction force generated by the catcher is not enough to cause significant improvement in internal airflow distribution. This is in spite of the fact that this suction has reduced outflow rate through the dome, as explained in Section 8.2.2 (B). However, and as has been explained in the normal wind direction, utilising the catcher as a wind chimney seems to be more efficient in the case of rectangular building form.

<table>
<tr><th>Vr = 1 m/s</th><th>Vr = 3 m/s</th><th>Before utilising the catcher</th><th>After utilising the catcher</th></tr>
<tr>
<td rowspan="2">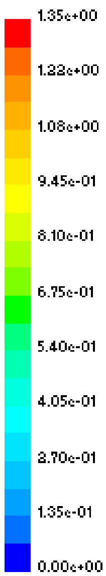
</td>
<td rowspan="2">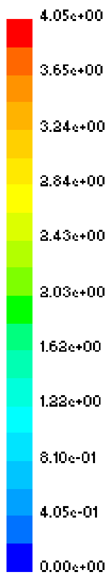
</td>
<td>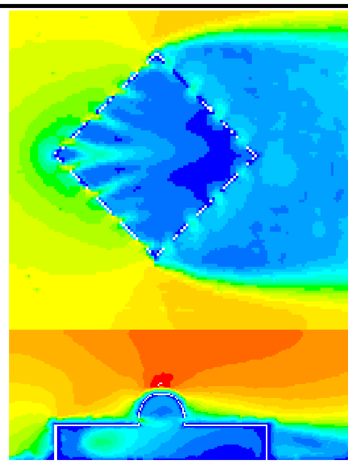
Do2-s2</td>
<td>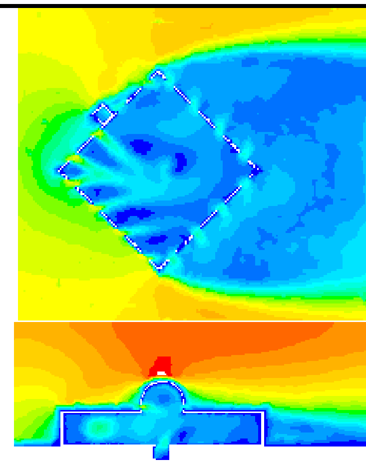
T1Do2-s2</td>
</tr>
<tr>
<td>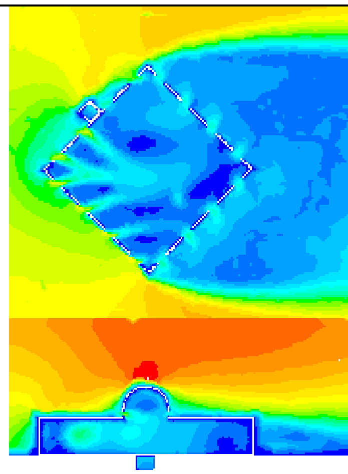
T2Do2-s2</td>
<td>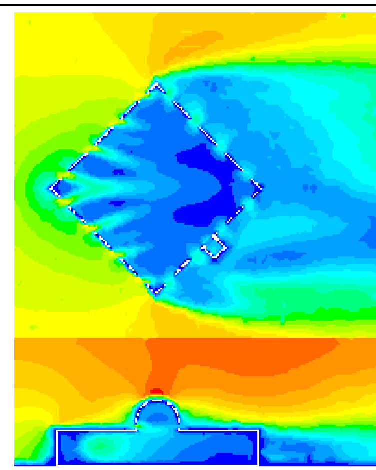
T3Do2-s2</td>
</tr>
<tr><td colspan="4">* Contours of velocity magnitude shown above are presented in Plane1 and 2 (Scale 1:1000), with 45° wind direction, and both 1 and 3 m/s reference wind velocities.</td></tr>
</table>

Air velocity contour	Vi (Vr=1m/s)	Vi (Vr=3m/s)	% of total plan area (square cases)				
			Dc2-s2	Do2-s2	T1Do2-s2	T2Do2-s2	T3Do2-s2
A	0.0	0.0	11.2	13.3	4.6	7.3	12.9
B	0.07	0.2	52.9	45.5	25.4	26.1	44.7
C	0.14	0.4	18.7	16.8	29.9	29.2	19.9
D *& above*	$0.14<Vi<Vi_{max}$	$0.4<Vi<Vi_{max}$	17.2	24.4	40.1	37.4	22.5

Figure 8.11: Comparison of internal airflow distribution presented by internal air velocity Vi distribution before and after utilising the different wind-catcher systems with the dome in the square building form at 45° wind direction.

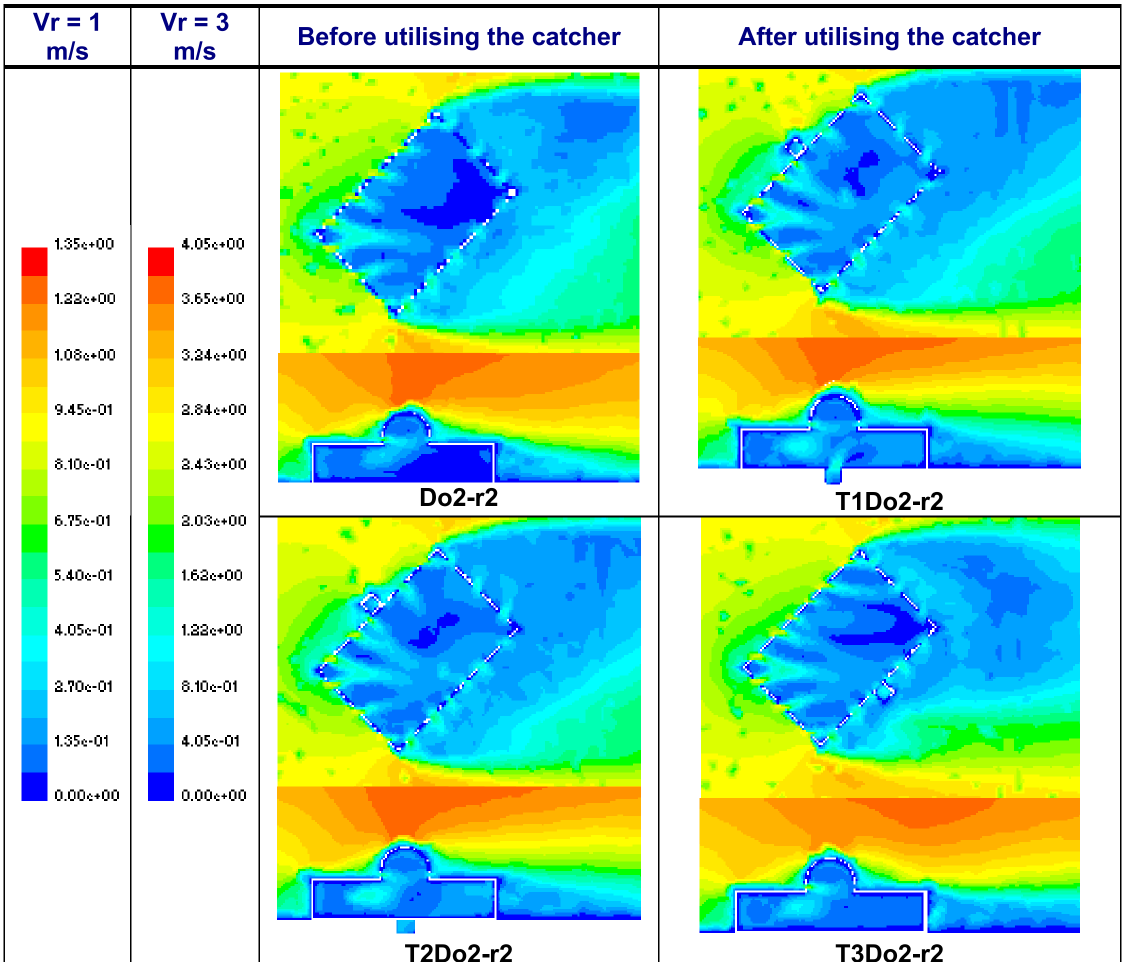

* Contours of velocity magnitude shown above are presented in Plane1 and 2 (Scale 1:1000), with 45° wind direction, and both 1 and 3 m/s reference wind velocities.

Air velocity contour	Vi (Vr=1m/s)	Vi (Vr=3m/s)	% of total plan area (rectangular cases)				
			Dc2-r2	Do2-r2	T1Do2-r2	T2Do2-r2	T3Do2-r2
A	0.0	0.0	17.8	15.7	3.7	3.6	9.4
B	0.07	0.2	43.8	44.1	32.1	34.8	30.7
C	0.14	0.4	16.2	18.5	32.5	29.6	35.4
D *& above*	$0.14<Vi<Vi_{max}$	$0.4<Vi<Vi_{max}$	22.2	21.7	31.7	32.0	24.5

Figure 8.12: Comparison of internal airflow distribution presented by internal air velocity Vi distribution before and after utilising the different wind-catcher systems with the dome in the rectangular building form at 45° wind direction.

C. In the case of 90^o wind incidence

Table 8.6 presents inflow and outflow rates discussed here.

Table 8.6: The effect of wind catcher integration with the dome on inflow and outflow rates through wall openings in the case of 90^o wind direction and 3m/s reference wind speed

Inflow rate					Outflow rate				
Dome only		Dome & tower		Diff. (%)	Dome only		Dome & tower		Diff. (%)
Do2-s2	54.15	**T1Do2-s2**	55.18	**+1.9**	**Do2-s2**	-46.16	**T1Do2-s2**	-53.24	**+15.3**
		T2Do2-s2	54.29	**+0.3**			**T2Do2-s2**	-52.89	**+14.6**
		T3Do2-s2	54.83	**+1.3**			**T3Do2-s2**	-45.19	**- 2.1**
Do2-r2	40.03	**T1Do2-r2**	40.71	**+1.7**	**Do2-r2**	-34.22	**T1Do2-r2**	-40.69	**+18.9**
		T2Do2-r2	39.92	**- 0.3**			**T2Do2-r2**	-39.53	**+15.5**
		T3Do2-r2	40.84	**+2.0**			**T3Do2-r2**	-34.86	**+1.9**
* All airflow rate values are in (l/s)/m^2.									

In the square cases, airflow rate and distribution behave in the same way explained in the case of 0^o wind direction, considering the change of walls naming after building has been rotated by 90^o. This is due to building symmetry. In the rectangular cases, some differences could be observed. In the first two wind-catcher systems, outflow rate has significantly ceased in the leeward openings for the benefit of the literal openings. This can be noticed in Figure 8.7. The resulting total increase in outflow rate is larger, compared to the case of normal wind direction. This is because large part of the air, provided by the catcher, chose to leave the building through these literal openings, which accommodate more outlets, due to the shorter distance. This is in addition to the effect of the reversed flow at building wake, as has been explained in Section 6.5.3. This is why the total outflow rate for these two cases is significantly higher for the first two wind-catcher systems by 19% and 16%, respectively, compared to about 10% in the normal wind direction.

In the case of the third system, where the catcher acts as a wind chimney, the opposite behaviour has been observed. Outflow rate through the leeward face has increased on the account of the literal openings and the dome. This is because the effect of the catcher here in suction is more dominant in attracting air to penetrate the building. This has also limited the role of the dome, since outflow rate through it has been reduced, as explained in Section 8.2.2 (C). This has caused a slight increase in outflow rate by 2%, compared to the normal wind direction.

Concerning internal airflow distribution in the rectangular cases, it has been discussed in Chapter 6 that utilising the dome alone has insignificant effect. This is because only the central zone of the building benefits from that utilisation, leaving the deep downstream wing of the building still. Utilising the first wind-catcher system has resulted in the same behaviour. This is why area of the still air zone has increased, even when is compared to Dc2-r2. However the still-air zone has been significantly reduced in the second wind catcher system by 14%. This resulted in a significant increase in zone B as well. This is because catcher provides air directly to the downstream zone, instead of the central zone.

In the third wind-catcher systems, the still-air zone has been significantly reduced by 18.5%. This also resulted in a significant increase in zones C and D. This seems to be an interesting result because the large building depth is expected to prevent air from penetrating the space. However, as explained above, the less suction acting on the dome, in addition to the observed reversed airflow, has allowed this improvement to occur.

Vr = 1 m/s	Vr = 3 m/s	Before utilising the catcher	After utilising the catcher
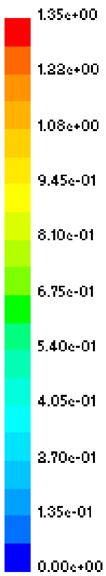	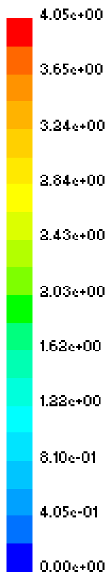	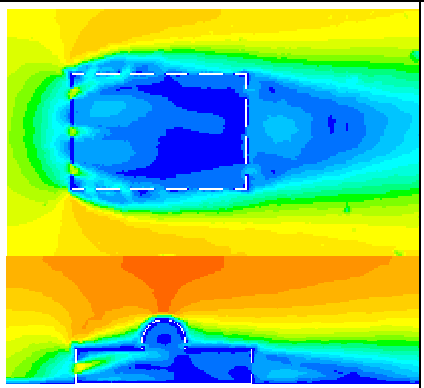 Do2-r2	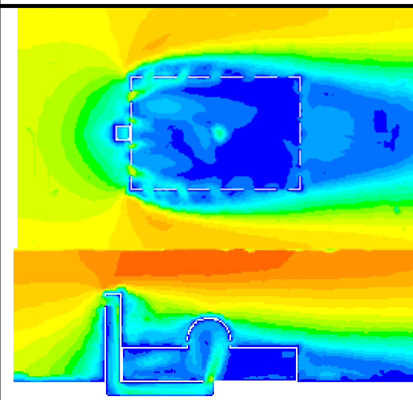 T1Do2-r2
		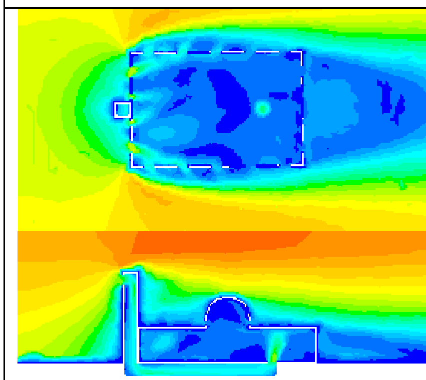 T2Do2-r2	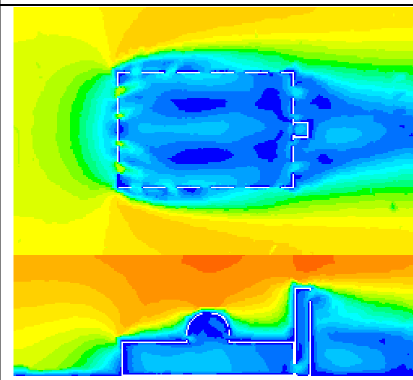 T3Do2-r2

* Contours of velocity magnitude shown above are presented in Plane1 and 2 (Scale 1:1000), with 90° wind direction, and both 1 and 3 m/s reference wind velocities.

Air velocity contour	Vi (Vr=1m/s)	Vi (Vr=3m/s)	% of total plan area (rectangular cases)				
			Dc2-r2	Do2-r2	T1Do2-r2	T2Do2-r2	T3Do2-r2
A	0.0	0.0	36.2	30.6	43.9	16.6	11.7
B	0.07	0.2	32.5	36.2	26.3	50.6	30.8
C	0.14	0.4	17.5	19.3	14.0	13.2	29.6
D *& above*	$0.14<Vi<Vi_{max}$	$0.4<Vi<Vi_{max}$	13.8	13.9	15.8	19.6	27.9

Figure 8.13: Comparison of internal airflow distribution presented by internal air velocity Vi distribution before and after utilising the different wind-catcher systems with the dome in the rectangular building form at 90° wind direction

8.3 Integration of vaulted roofs and wind catchers

This study, which is referred to as 'Tower and Vault' study, aims to investigate the effect of integrating wind catchers and vaulted roofs on natural ventilation performance at buildings. The following sections discuss the different related sides in this regard.

8.3.1 Tower and Vault study: terminology and programme

The same method implemented in the previous study in setting up the modelling programme is implemented here as well. Many similarities have been observed in the behaviour of domed and vaulted roofs tested. Thus, further reduction in the study parameters is considered here in order to cope with the study limitation. The following configurations will be considered in order to examine the effect of integrating wind catcher with vaulted roofs in general. This includes the second wind-catcher system, T2, and the second vault geometry, V2. Figure 8.14 shows illustrations of the different modelling cases. CAD illustrations with dimensions can be found in Appendix C.1.

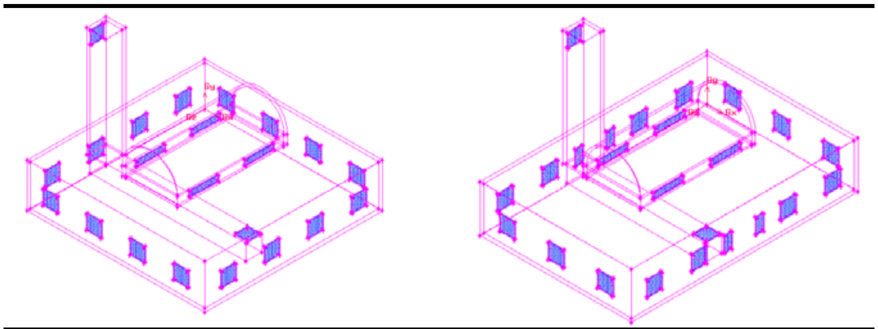

T2V2-s2 | T2V2-r2

Figure 8.14: Different building configurations tested in the Tower and Vault study, illustrated in 0^{o} wind direction

The different cases modelled in this study are designated with a 'T' and 'V' letters to refer to the 'Tower and Vault' study. The same method explained in Section 8.2.1 is implemented here. For example: T2Vo2-r2-45-3 indicates the second wind-catcher system integrated with the second vault configuration, with a rectangular main building volume that has an area of $400m^2$. The building is exposed to a 45^{o} wind incident with a reference speed of 3 m/s. Table 8.7 lists the different cases modelled in this study.

Table 8.7: CFD cases modelled in the Tower and Vault study

Config.	Description	Test no.	Test code	Wind angle	Wind speed (m/s)
T2Vo2-s2	**Form:** square. **Plan area:** 400m^2 **Catcher operation:** wind catcher connected to the central zone of the plan.	1	T2Vo2-s2-0-1	0^o	1
		2	T2Vo2-s2-0-3	0^o	3
		3	T2Vo2-s2-45-1	45^o	1
		4	T2Vo2-s2-45-3	45^o	3
		5	T2Vo2-s2-90-1	90^o	1
		6	T2Vo2-s2-90-3	90^o	3
T2Vo2-r2	**Form:** rectangle. **Plan area:** 400m^2 **Catcher operation:** wind catcher connected to the central zone of the plan.	7	T2Vo2-r2-0-1	0^o	1
		8	T2Vo2-r2-0-3	0^o	3
		9	T2Vo2-r2-45-1	45^o	1
		10	T2Vo2-r2-45-3	45^o	3
		11	T2Vo2-r2-90-1	90^o	1
		12	T2Vo2-r2-90-3	90^o	3

It is worth mentioning here that files total size of the modelled cases of 'Vault and Tower' study is 1.3 GB. In the following sections, natural ventilation performance of the studied system will be discussed. Table 8.8 summarises numerically airflow rates estimated, and shows the reliability of the results obtained according to the Law of Conservation of Mass.

Table 8.8: Summary of airflow rates recorded in the different cases modelled in the Tower and Vault Study

	Wind angle 0^o Wind velocity 3 m/s							Wind angle 45^o Wind velocity 3 m/s							Wind angle 90^o Wind velocity 3 m/s						
	Inflow rate			Outflow rate			Total	Inflow rate			Outflow rate			Total	Inflow rate			Outflow rate			Total
Case Code	Tower	Vault	Walls	Tower	Vault	Walls		Tower	Vault	Walls	Tower	Vault	Walls		Tower	Vault	Walls	Tower	Vault	Walls	
T2Vo2-s2	8.24	0.33	55.29	0.00	-10.76	-53.12	**-0.02**	4.96	6.24	65.45	0.00	-11.78	-61.24	**0.00**	8.39	0.00	55.27	0.00	-17.63	-46.02	**0.01**
T2Vo2-r2	8.20	0.00	67.04	0.00	-14.71	-60.51	**0.02**	4.98	4.12	69.88	0.00	-17.84	-61.14	**0.00**	8.10	0.00	41.49	0.00	-15.22	-34.37	**0.00**

* All values are in (l/s)/m^2.

8.3.2 Effect of utilising wind catcher on airflow rate through vault openings

Airflow rate through vault openings has been compared before and after the utilisation of wind catcher. This has been done for both square and rectangular cases, and for both low and high reference wind velocities. As has been observed in the previous comparisons, both velocities have presented the same behaviour at all wind directions tested. Therefore, numerical examples given here are limited to the 3 m/s wind velocity. All other values can be found by referring to Appendix C.2.

A. In the case of 0^{o} wind incidence

Figure 8.15 summarises airflow rates through the vault before and after utilising the catcher for both square and rectangular building forms.

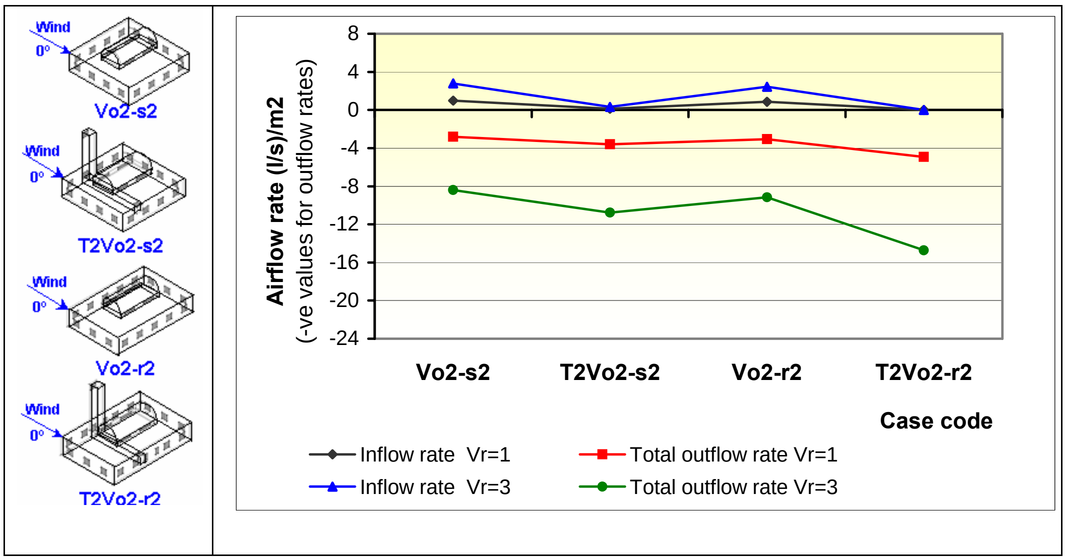

Figure 8.15: Airflow rate through the vault after utilising the studied wind-catcher system, where wind angle is 0^{o} and reference wind speed is 1 and 3 m/s

Catcher integration has been found to cause a significant improvement in terms of airflow rate through the vault. Location of the wind catcher at the middle of the windward façade of the building has caused a wind-shadow area between the catcher and the vault, as illustrated below. Thus, inflow rate through vault openings, which are located at the wake of the catcher, has been reduced. Both sheltering effect of the catcher and the air vortex observed before the inlets has reduced inflow rate value to a very low value at square cases and to zero in the rectangular ones. This significant decrease in inflow rate has increased the potential of the vault outlets for air suction from the building.

Thus, significant increase in outflow rate has been recorded (28% in the square cases and 60% in the rectangular cases). This, in fact, shows the advantage of closing the vault inlets in this wind direction in order to maximise outflow rate through the vault, as has been analysed in Section 7.4 of Chapter 7. The significant higher increase in outflow rate in the rectangular cases is due to the smaller depth of the building, which allows more amount of air provided by the catcher to leave the building through the vault.

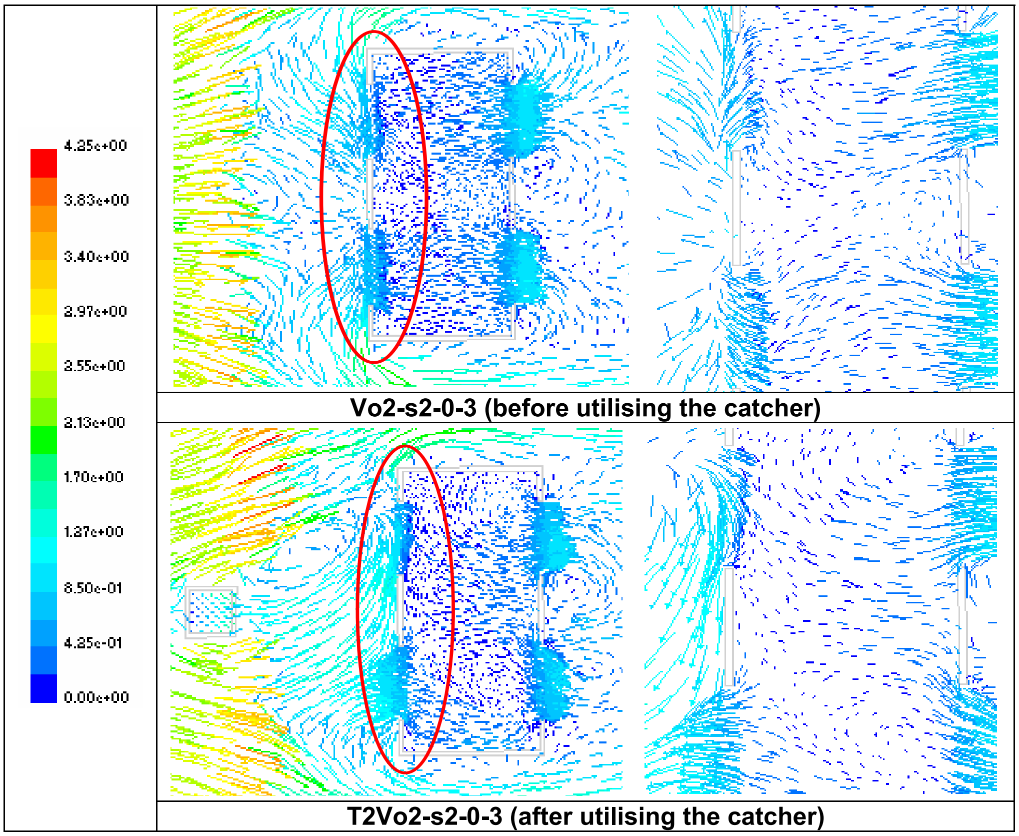

Figure 8.16: Velocity vectors showing the effect of wind catcher in reducing inflow rate through vault windward openings at 0^o wind direction

B. In the case of 45^o wind incidence

Figure 8.17 summarises airflow rates through the vault before and after utilising the catcher for both square and rectangular building forms at 45^o wind direction.

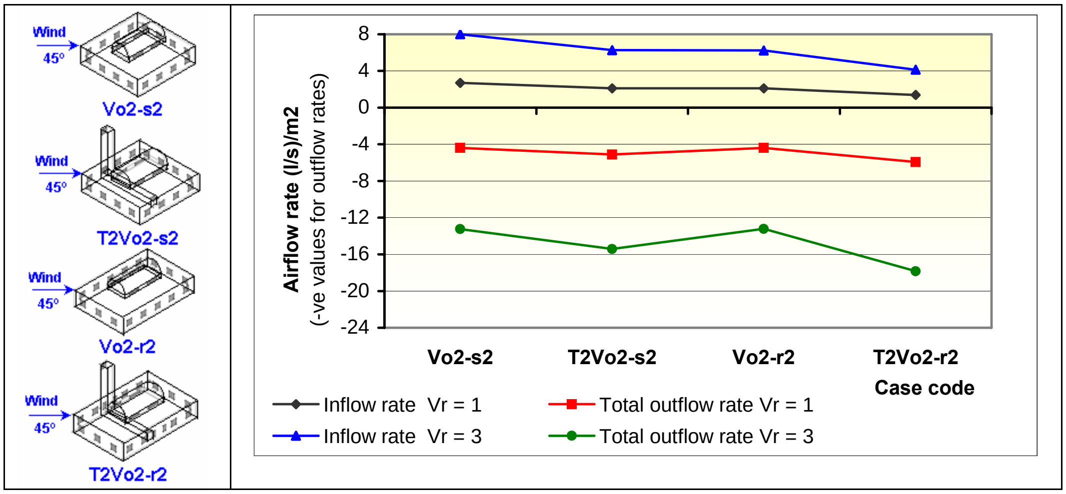

Figure: 8.17: Airflow rate through the vault after utilising the studied wind-catcher system, where wind angle is 45^o and reference wind speed is 1 and 3 m/s

The same observation explained in the previous section regarding the reduction in inflow rate is true here, with nearly the same percentage of reduction. However, inflow rate was originally high, due to the absence of the air vortex occurring before the vault inlets. This vortex has been always observed as a result of airflow separation over the roof windward sharp edge in the case of 0^o and 90^o wind directions. Therefore, inflow rate value does not approach zero here.

Using velocity vectors tool, and considering building plan, the observed reduction in inflow rate has only occurred at the top windward inlet of the vault, which is sheltered by the catcher. The other inlet is subjected to a positive pressure and provides larger amount of air to the closer vault outlet. Thus, outflow rate has mainly increased at the lower leeward outlet of the vault. The observed increase in outflow rate here is significant, but less than the one observed in the normal wind direction (16%, compared to 28% in the square cases, and 35%, compared to 60% in the rectangular cases).

C. In the case of 90^o wind incidence

Figure 8.18 summarises airflow rates through the vault before and after utilising the catcher for both square and rectangular building forms at 90^o wind direction.

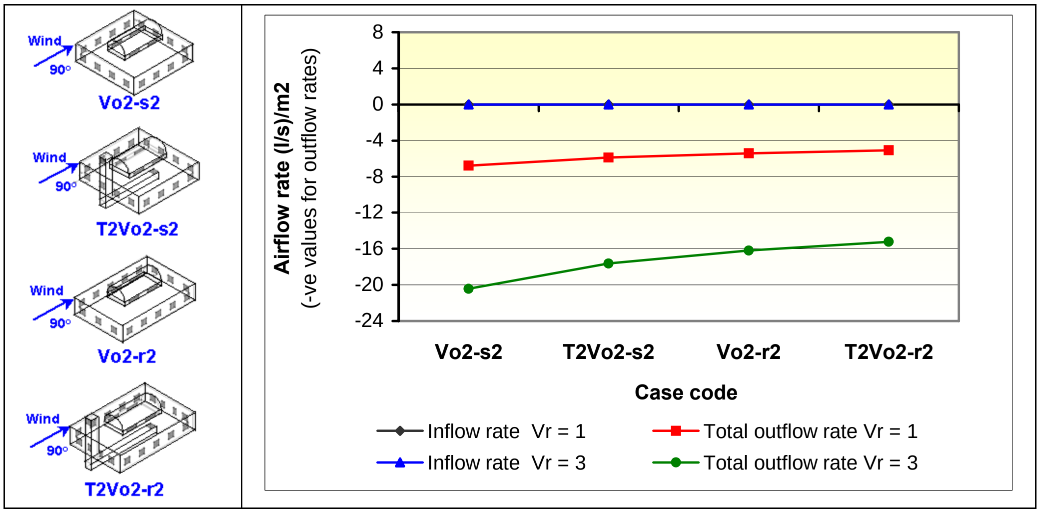

Figure: 8.18: Airflow rate through the vault after utilising the studied wind-catcher system, where wind angle is 90^o and reference wind speed is 1 and 3 m/s

Inflow rate recorded through the tested vault geometry is always zero in this wind direction, and the vault mainly works in suction. However, utilising the catcher has reduced outflow rate through the vault by 13% for the square case and 6% for the rectangular one. This means that airflow provided by the catcher has supported the role of walls openings in suction on the account of vault openings, as can be noticed in Figure 8.18. This means that providing air to the internal space by the catcher has improved the internal airflow distribution, as will be discussed in the following section.

8.3.3 Effect of both wind catcher and vault on airflow rate through wall openings and internal airflow distribution

Figure 8.19 compares airflow rate and distribution before utilising the catcher with the vault and after that for both square and rectangular cases. Additional tables are used in the discussion to facilitate a more accurate comparison. As both reference wind velocities used here has resulted in the same airflow behaviour, numerical examples given in the discussion are limited to the higher wind velocity, 3 m/s. All airflow values discussed here can be comprehensively and numerically found in Appendices C.2 and C.3.

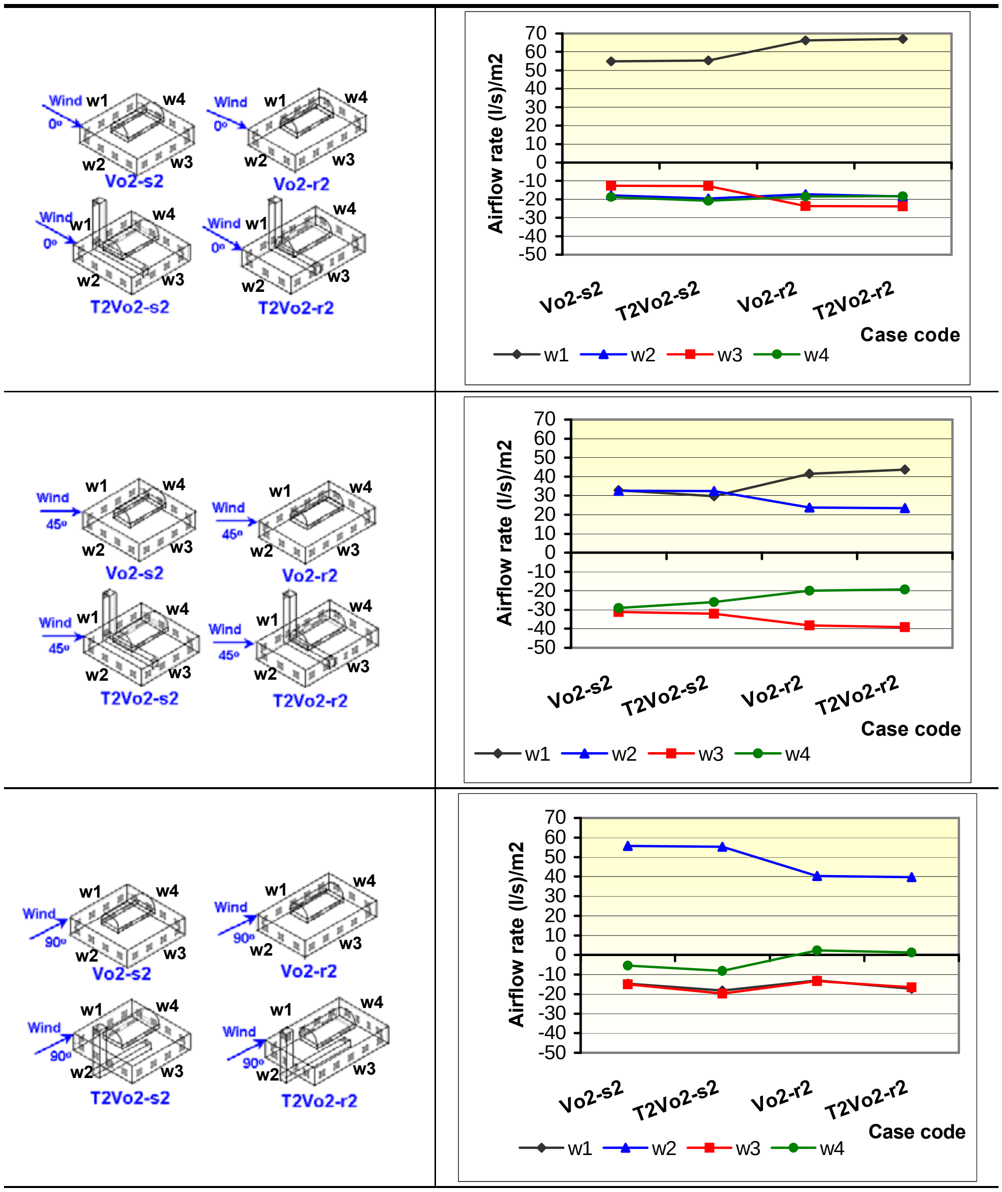

* Positive sign for inflow and negative one for outflow rate.

Figure 8.19: Average volumetric airflow rate through wall openings recorded in the Tower and Vault Study at reference wind speed of 3 m/s

A. In the case of 0° wind direction

Table 8.9 presents inflow and outflow rates discussed here.

Table 8.9: The effect of wind catcher integration with the vault on inflow and outflow rates through wall openings in the case of 0° wind direction and 3m/s reference wind speed

Inflow rate					Outflow rate				
Vault only		Vault & tower		Diff. (%)	Vault only		Vault & tower		Diff. (%)
Vo2-s2	54.82	**T2Vo2-s2**	55.29	**+0.9**	**Vo2-s2**	-49.25	**T2Vo2-s2**	-53.12	**+7.9**
Vo2-r2	66.23	**T2Vo2-r2**	67.04	**+1.2**	**Vo2-r2**	-59.50	**T2Vo2-r2**	-60.51	**+1.7**
* All airflow rate values are in (l/s)/m^2.									

It is clear that utilisation of wind catcher in both square and rectangular cases has slightly increased inflow rate. This is balanced by an increase in outflow rate, which is higher because the catcher provides some air to the space. However, the observed increase is only significant in the square case. This is because air provided by the catcher in the rectangular case mainly leaves the space through the vault and not the walls openings, as discussed in Section 8.3.2 (A).

Thus, outflow rate through vault openings is significantly higher for the rectangular case, while outflow rate through walls openings is significantly higher for the square case. This is why internal airflow distribution has been improved more significantly in the square case, after the utilisation of the catcher. This is presented in the Figure 8.20, which has been used to assess internal airflow distribution in this wind direction. Area of the still-air zone has been reduced in the square case by about 25%, with an equivalent increase velocity zone D. However, area of the still-air zone in the rectangular case has been reduced by about 5%, and increased by about 7% at air velocity zone D.

<table>
<tr><th>Vr = 1 m/s</th><th>Vr = 3 m/s</th><th>Before utilising the catcher</th><th>After utilising the catcher</th></tr>
<tr><td rowspan="2">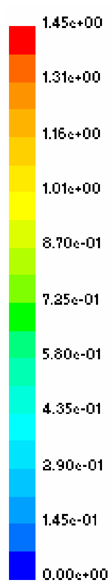
</td><td rowspan="2">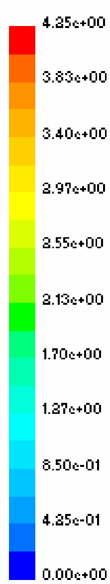
</td><td>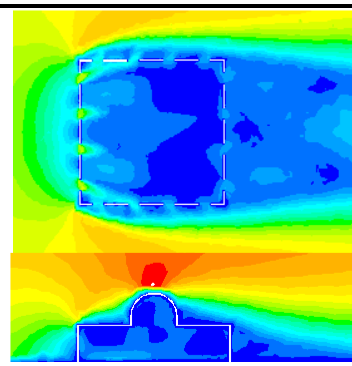
Vo2-s2</td><td>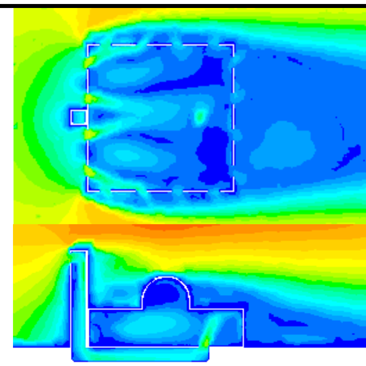
T2Vo2-s2</td></tr>
<tr><td>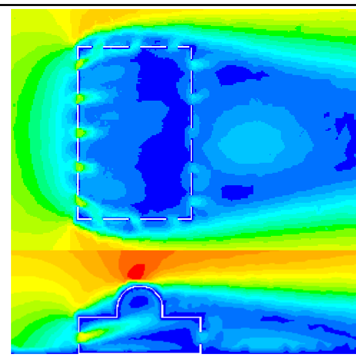
Vo2-r2</td><td>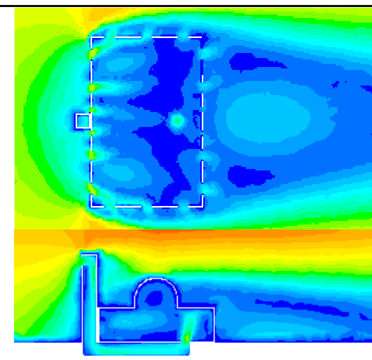
T2Vo2-r2</td></tr>
<tr><td colspan="4">* Contours of velocity magnitude shown above are presented in Plane1 and 2 (Scale 1:1000), with normal wind direction, and both 1 and 3 m/s reference wind velocities.</td></tr>
</table>

Air velocity contour	Vi (Vr=1m/s)	Vi (Vr=3m/s)	% of total plan area (square cases)		
			Vc2-s2	Vo2-s2	T2Vo2-s2
A	0.0	0.0	44.6	39.8	13.2
B	0.07	0.2	26.2	33.3	33.4
C	0.14	0.4	15.2	15.5	18.9
D *& above*	$0.14<Vi<Vi_{max}$	$0.4<Vi<Vi_{max}$	14.0	11.4	34.5

Air velocity contour	Vi (Vr=1m/s)	Vi (Vr=3m/s)	% of total plan area (rectangular cases)		
			Vc2-r2	Vo2-r2	T2Vo2-r2
A	0.0	0.0	34.3	31.4	26.1
B	0.07	0.2	33.1	38.8	35.2
C	0.14	0.4	15.2	16.2	18.2
D *& above*	$0.14<Vi<Vi_{max}$	$0.4<Vi<Vi_{max}$	17.4	13.6	20.5

Figure 8.20: Comparison of internal airflow distribution presented by internal air velocity Vi distribution before and after utilising the wind catcher with the vault at 0^o wind direction.

B. In the case of 45^o wind direction

Table 8.10 presents inflow and outflow rates discussed here.

Table 8.10: The effect of wind catcher integration with the vault on inflow and outflow rates through wall openings in the case of 45^o wind direction and 3m/s reference wind speed

Inflow rate					Outflow rate				
Vault only		Vault & tower		Diff. (%)	Vault only		Vault & tower		Diff. (%)
Vo2-s2	65.49	**T2Vo2-s2**	65.45	**-0.1**	**Vo2-s2**	-60.25	**T2Vo2-s2**	-61.24	**+1.6**
Vo2-r2	65.18	**T2Vo2-r2**	69.88	**+7.2**	**Vo2-r2**	-58.20	**T2Vo2-r2**	-61.14	**+5.1**
* All airflow rate values are in (l/s)/m^2.									

In the case of 45^o wind direction, the observed behaviour of airflow rates in the square case is similar to the one observed in the case of utilising the catcher with the dome, as explained in Section 8.2.3 (B). However, differences in airflow rates are less here. Airflow pattern, illustrated in Figure 8.21, shows that there is no curved air motion in the rectangular case after integrating then catcher. This is because the effect of the vault is more dominant than the potential of the curved air movement for reforming the internal airflow pattern.

Numerically, net outflow rate through the vault is higher than the one recorded through the dome by about 13% in the square form, and 50% in the rectangular form. This increases the potential of the vault for air suction on the account of the leeward walls, and thus weakens the internal curved air motion. In the rectangular case, this has significantly increased inflow rate. Thus, internal airflow distribution has been improved. In the square cases, area of the still-air zone has been reduced in the square case by about 6%, with an increase in velocity zone C by 15%. This is more significant in the rectangular cases. Area of the still-air zone has been reduced by 18%, with an increase by 7% in velocity zones B and C.

<table>
<tr><th>Vr = 1 m/s</th><th>Vr = 3 m/s</th><th>Before utilising the catcher</th><th>After utilising the catcher</th></tr>
<tr><td rowspan="2">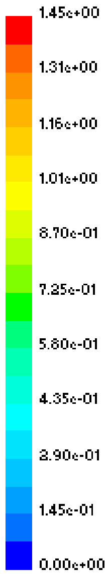
</td><td rowspan="2">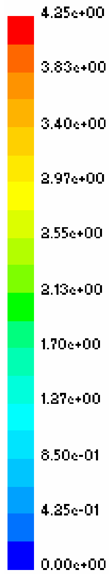
</td><td>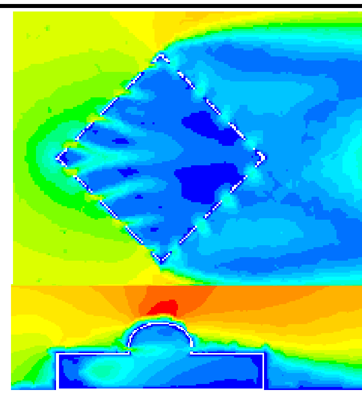
Vo2-s2</td><td>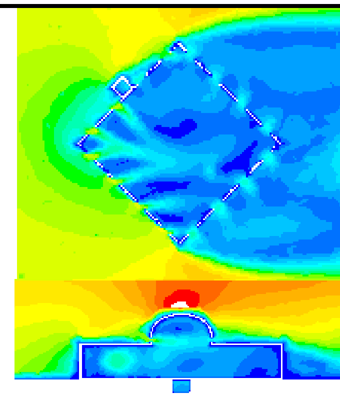
T2Vo2-s2</td></tr>
<tr><td>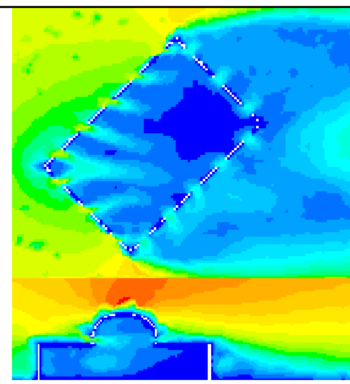
Vo2-r2</td><td>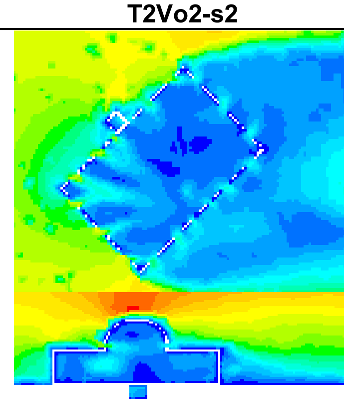
T2Vo2-r2</td></tr>
<tr><td colspan="4">* Contours of velocity magnitude shown above are presented in Plane1 and 2 (Scale 1:1000), with 45° wind direction, and both 1 and 3 m/s reference wind velocities.</td></tr>
</table>

Air velocity contour	Vi (Vr=1m/s)	Vi (Vr=3m/s)	% of total plan area (square cases)		
			Vc2-s2	Vo2-s2	T2Vo2-s2
A	0.0	0.0	13.5	14.1	7.8
B	0.07	0.2	43.5	48.1	34.3
C	0.14	0.4	18.7	16.8	32.0
D *& above*	$0.14<Vi<Vi_{max}$	$0.4<Vi<Vi_{max}$	24.3	21.0	25.9

Air velocity contour	Vi (Vr=1m/s)	Vi (Vr=3m/s)	% of total plan area (rectangular cases)		
			Vc2-r2	Vo2-r2	T2Vo2-r2
A	0.0	0.0	17.4	22.3	4.0
B	0.07	0.2	38.0	39.6	46.8
C	0.14	0.4	22.4	18.6	25.5
D *& above*	$0.14<Vi<Vi_{max}$	$0.4<Vi<Vi_{max}$	22.2	19.5	23.7

Figure 8.21: Comparison of internal airflow distribution presented by internal air velocity Vi distribution before and after utilising the wind catcher with the vault at 45° wind direction.

C. In the case of 90° wind direction

Table 8.11 presents inflow and outflow rates discussed here.

Table 8.11: The effect of wind catcher integration with the vault on inflow and outflow rates through wall openings in the case of 90° wind direction and 3m/s reference wind speed

Inflow rate					Outflow rate				
Vault only		Vault & tower		Diff. (%)	Vault only		Vault & tower		Diff. (%)
Vo2-s2	54.29	**T2Vo2-s2**	55.27	**+1.8**	**Vo2-s2**	-36.54	**T2Vo2-s2**	-46.02	**+25.9**
Vo2-r2	39.1	**T2Vo2-r2**	41.49	**+6.1**	**Vo2-r2**	-27.00	**T2Vo2-r2**	-34.37	**+27.3**
* All airflow rate values are in (l/s)/m^2.									

Inflow rate for both rectangular and square configurations has increased as a response to the integration of the catcher, as has been explained in the previous two wind directions. However, this increase is higher in the rectangular cases due to the observed reversed airflow through wall w4, as has been explained in Section 7.4. Although this reversed airflow is still observed here, the use of the catcher has limited its effect. Thus, the observed increase in inflow rate is less than it was before utilising the catcher (6%, when the vault is solely used, compared to 7.7%, when both the vault and the catcher are used).

Significant increase in outflow rate has been observed at both square and rectangular cases. This increase is about 25%, compared to a reduction in outflow rate by about 30% before utilising the catcher. This is because outflow rate through the vault has been significantly reduced after the utilisation of the wind catcher, as explained in Section 8.3.2 (C). The significant reduction at the vault outflow rate in addition to the air provided by the catcher increases the role of wall openings in sucking the air outside the building and thus, improves the internal airflow distribution. Figure 8.22 has been used to assess internal airflow distribution in this wind direction. Area of the still-air zone has been reduced in the square case by about 19%, with an increase in velocity zone D by 10%. In the rectangular case, area of the still-air zone has been reduced by about 13%, with an increase in velocity zone B by 10%.

<table>
<tr><th>Vr =
1 m/s</th><th>Vr =
3 m/s</th><th>Before utilising the catcher</th><th>After utilising the catcher</th></tr>
<tr><td rowspan="2">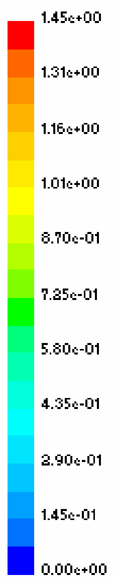
</td><td rowspan="2">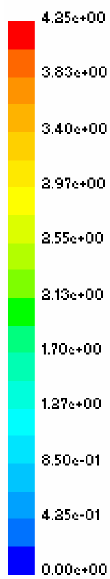
</td><td>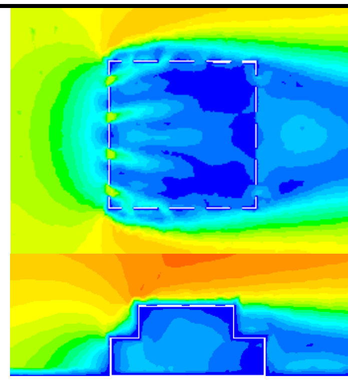
Vo2-s2</td><td>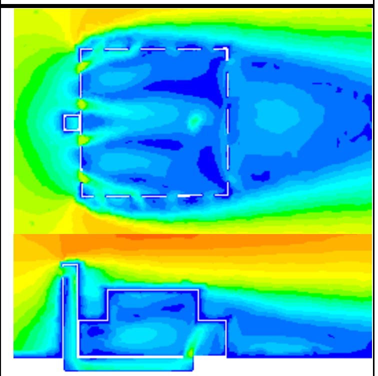
T2Vo2-s2</td></tr>
<tr><td>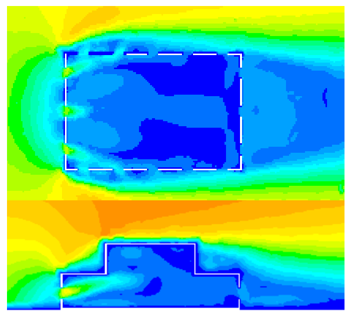
Vo2-r2</td><td>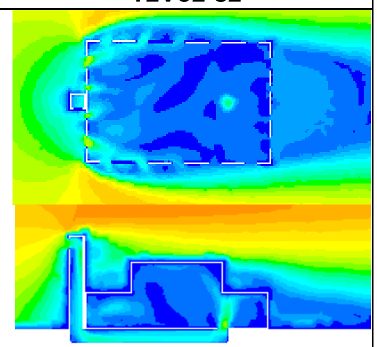
T2Vo2-r2</td></tr>
<tr><td colspan="4">* Contours of velocity magnitude shown above are presented in Plane1 and 2 (Scale 1:1000), with 90° wind direction, and both 1 and 3 m/s reference wind velocities.</td></tr>
</table>

Air velocity contour	Vi (Vr=1m/s)	Vi (Vr=3m/s)	% of total plan area (square cases)		
			Vc2-s2	Vo2-s2	T2Vo2-s2
A	0.0	0.0	22.1	29.3	10.6
B	0.07	0.2	36.1	35.1	36.2
C	0.14	0.4	20.8	15.2	21.7
D *& above*	$0.14<Vi<Vi_{max}$	$0.4<Vi<Vi_{max}$	21.0	20.4	31.5

Air velocity contour	Vi (Vr=1m/s)	Vi (Vr=3m/s)	% of total plan area (rectangular cases)		
			Vc2-r2	Vo2-r2	T2Vo2-r2
A	0.0	0.0	50.4	36.0	23.5
B	0.07	0.2	23.5	39.2	51.3
C	0.14	0.4	14.3	15.0	12.6
D *& above*	$0.14<Vi<Vi_{max}$	$0.4<Vi<Vi_{max}$	11.8	9.8	12.6

Figure 8.22: Comparison of internal airflow distribution presented by internal air velocity Vi distribution before and after utilising the wind catcher with the vault at 90° wind direction

8.4 Conclusions

This chapter has investigated the potential of wind catcher integration for improving natural ventilation in buildings. Wind catcher has been integrated with some configurations of the previously investigated curved roofs. More than 50 cases have been modelled in this investigation, considering different climatic and geometrical parameters. The intention in this study was to assess the studied ventilation strategy in general, and not the detailed design of the catcher. Thus, three wind-catcher systems have been studied for: air provision at building central zone, air provision at building downstream zone, and air suction at building leeward wall. Airflow rate and airflow distribution inside the building have been assessed and compared to those observed before integrating the catcher. It has been concluded that catcher integration with the domed and vaulted roofs has a positive effect on the observed natural ventilation performance, despite the fact that inflow rate provided by the catcher is relatively small (about 12% of the total inflow rate).

The positive effect of integrating the catcher with the examined domed roofs can be summarised as follows:

- When the catcher is utilised for air provision, natural ventilation conditions in both upstream and downstream parts of the building have been improved. In the case of 0^o and 90^o wind directions, this is because the catcher increases both outflow rate through the dome, and outflow rate through wall openings. This is generally true for both square and rectangular building forms. In the case of 45^o wind direction, catcher utilisation mainly affects airflow rates through wall openings due to the resulting curved air movement, which improves internal airflow distribution.
- When the catcher is utilised for air suction, outflow rate through the dome has ceased and outflow rate through wall openings has increased. This allows more air to penetrate the downstream wing of the building, and improves airflow distribution there. This is most significant in the case of rectangular building form and 90^o wind direction due to the weak suction acting over the dome.

In the case of vaulted roofs, wind catcher has been utilised for air provision at the downstream zone of the building. The positive effect of integrating the catcher with the examined vaulted roofs can be summarised as follows:

- In the case of 0^o wind direction, catcher effect is similar to what has been observed in the domed roofs. However, the difference observed between square and rectangular forms is more significant. Outflow rate through the vault in the square form has increased by 60%, compared to 20% in the domed roofs, and by 30% in the rectangular form, compared to 23% in the domed roofs. The observed sheltering effect of the catcher has increased the efficiency of the vaulted roofs in air suction, since it reduces inflow rate through the large inlets of the vault. Thus, the observed increase in outflow rates through wall openings is higher in the square building form, which resulted in a better internal airflow distribution.
- In the case of 45^o wind direction, the observed internal airflow pattern is similar to the one observed in the case of utilising the catcher with the dome. However, the improvement observed here is less because the higher net outflow rate through the vault has weakened the observed curved air movement.
- In the case of 90^o wind direction, outflow rate through the vault openings has been reduced, which is the opposite of what has been observed in the domed roofs. Thus larger increase in outflow rate through wall openings has been observed. This improves internal airflow distribution more significantly in the rectangular building form, which possesses a deep plan.

Generally, wind catcher has been found to balance suction forces acting on building roof and walls. It has been concluded that utilising the architectural traditional elements of curved roofs and wind catchers for natural ventilation is an effective ventilation strategy. Thus, many systems and features can be proposed and optimised in order to reform internal airflow paths, especially under the undesired conditions of deep building plans or low reference wind velocities. In order to give the obtained results ‘more value’ in the practical side, Chapter 9 will assess the resulting thermal comfort conditions after utilising the studied natural ventilation system.

CHAPTER 9 : THERMAL COMFORT IN BUILDINGS INCORPORATING CURVED ROOFS AND WIND CATCHER

Introduction

This chapter aims to assess the effect of utilising the examined curved roofs, integrated with wind catchers, for natural ventilation on human thermal comfort. In Chapter 2 of this study, the relationship between natural ventilation and thermal comfort has been discussed. It was concluded that thermal comfort is highly, but not solely, dependant on natural ventilation. In the case of wind-induced natural ventilation studies, air velocity is the main parameter that is under investigation. Therefore, this chapter will focus on the effect of the resulting internal air velocities, as recorded in some selected Fluent cases from Chapters 6 to 8, on occupants' thermal comfort.

Tropical Summer Index (TSI) is the tool that has been used here to assess human thermal comfort. It is possible using this index to observe the change in the percentage of people feeling thermally comfortable as a response to the change in internal air velocity. This air velocity is measured before and after the utilisation of the dome and wind-catcher. It is important here to mention that this study is aimed to be a complimentary one of the main CFD study carried out in Chapters 5 to 8. Therefore, and due to the limitation of the study size, this chapter will tackle this issue briefly and leave the door open for a further investigation. As a direct implication, TSI has been found to be an appropriate thermal comfort model, and has been used here.

9.1 A brief recall of the effect of air velocity on thermal comfort

The effect of air velocity on thermal comfort has been discussed in details in Section 2.7.4 of this study. As a main fundamental, air movement encourages heat loss from the human body to the ambient environment in order to improve thermal comfort, especially in hot climates. In general, increasing air velocities enhances heat loss by evaporation over the skin surface because drier ambient air replaces saturated air near the skin. When outdoor air temperature is less than the indoor one, increasing air velocities also enhances heat loss by convection. If the outdoor daytime temperature is higher than the comfort limit, then the use of night-time ventilation can be useful for increasing heat loss by convection and radiation, since night-time ventilation reduces the Mean Radiant Temperature of the space.

9.2 Tropical Summer Index

It is not an easy task to predict human thermal comfort. This is because it tries to measure some aspects related to human sensation. However, many methods have been developed, with the consideration of some assumptions in order to simplify the problem. This is why there are always some differences in the outputs of these models. One of these models is the Tropical Summer Index (TSI). This model has been found to be an appropriate one for this study, since it has been developed considering the hot climate conditions.

Similarly to the other thermal comfort assessment methods, TSI is based on the theoretical background introduced in Section 2.7 of this study. Sharma and Ali (1986) have developed this index considering the hot-dry and warm-humid conditions. This has been carried out depending on a three-year field study in India followed by intensive numerical analysis. TSI has also been validated and compared to several existing thermal comfort indices and a good agreement has been observed. Four environmental parameters were observed during the field study: dry-bulb temperature (20–40^{o}C), wet-bulb temperature (13–30^{o}C), globe temperature (19–43^{o}C), and air velocity (0–2 m/s).

According to Sharma and Ali (1986, p.17), TSI is defined as "the air/globe temperature of still air at 50% RH, which produces the same overall thermal sensation as the environment under investigation". It is possible in this index to use a simple equation, which correlates the different interacting factors, in order to estimate human thermal comfort conditions. This equation is:

$$S = 0.067t_w + 0.162t_g - 0.449V^{1/2} - 1.917 \qquad \textbf{(9.1)}$$

Where, S is the index value (^oC), t_g is the global temperature (^oC), t_w is the wet-bulb temperature (^oC), and V is air speed (m/s).

In this equation, the globe temperature mainly accounts for the effect of air temperature and the radiant heat. However, Sharma and Ali mentioned that it is possible, instead, to consider air temperature. This is because their study showed that air temperature is almost equally well correlated with the thermal sensation as the globe temperature. This conclusion is most valid in the case of buildings that have high thermal mass because of the high thermal capacity of building materials. This conclusion facilitates the use of the index, since the measurement of air temperature is easier and more practical than the globe temperature.

The above-mentioned equation has been used to construct the following psychrometric chart. This chart is more practical, and it facilitates studying the effect of any specific environmental factor on human thermal comfort, keeping the other factors at assumed fixed values. Knowing the index value, it is possible to directly find out the percentage of people feeling comfortable using the attached normal-distribution curve. Then, the value of the index can be corrected, to consider air velocity using the table attached to the chart.

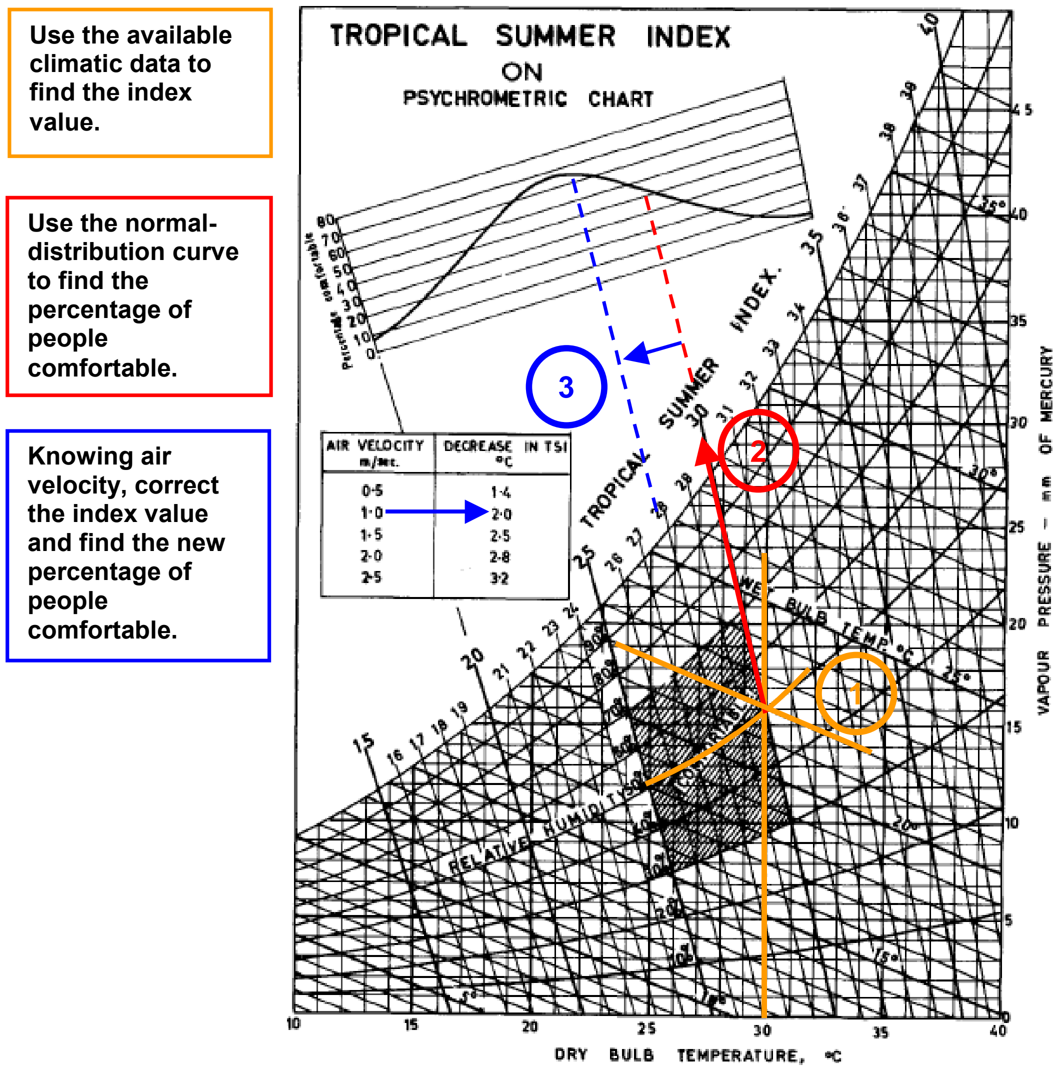

Figure 9.1: Tropical Summer Index (TSI) on a psychrometric chart

9.3 Estimation of internal air velocity

This study focuses on wind-induced natural ventilation. Therefore, the environmental variable related to thermal comfort assessment here is air velocity. Many approaches can be distinguished in the relevant studies here. For example, some studies suggest the method of selecting some well-distributed points in building interior and recording air velocities at these points. In some other studies, internal air velocity is averaged and, possibly, divided by the reference air velocity in order to reduce the velocity value. However, and to some extent, there is a lack of accuracy in both methods. This is because any selected points will not comprehensively represent the entire space under investigation. Also, the averaged air velocity for the whole space does not consider the significance of some local increases or decreases of air velocity values.

Therefore, the method adopted here includes the advantage of both methods and utilises the abilities of Fluent 5 software. In this method, plane 1, which passes horizontally through the building at windows level, has been divided into nine sub-planes. For each sub-plane, Fluent has been used to compute the average internal velocity. In this regard, two options are available: the facet average velocity and the area-weighted average. The second one has been adopted, which considers the frequency of occurrence, in addition to the velocity magnitude, in the estimation of the average air velocity. Figure 9.2 shows the method adopted in dividing plane 1 into the above-mentioned nine planes.

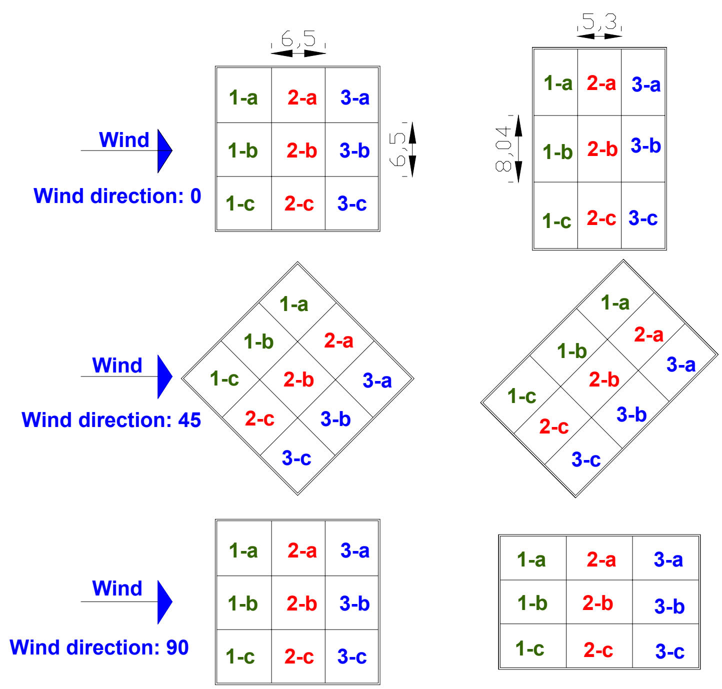

Figure 9.2: Method adopted in dividing Plane 1 into nine sub-planes for thermal comfort assessment

It is not intended here to repeat the comparison held in Chapters 6 to 8 between natural ventilation performance of the different building configurations tested. Therefore, some cases that have resulted in an improved natural ventilation performance after the utilisation of curved roofs and wind catchers have been selected, as illustrated in Figure 9.3.

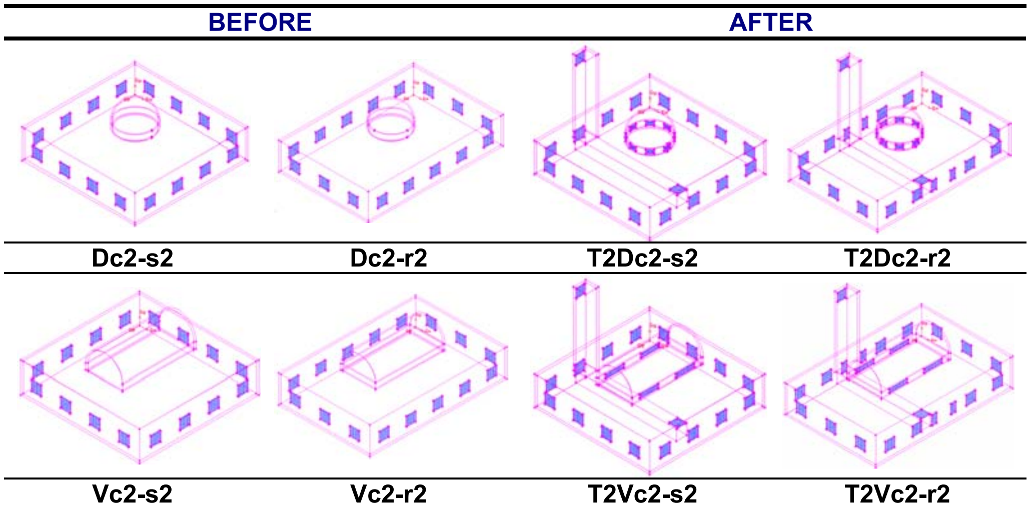

Figure 9.3: Different building configurations tested in the thermal comfort study, illustrated in the 0^o wind direction

Results obtained are presented in Figures 9.4 and 9.5, and are available numerically in Appendix D.1. It has been observed that the improvement in the average air velocity is generally insignificant in the case of 1 m/s reference wind velocity (only an increase of 0.1 m/s in the best case). This is true for both domed and vaulted roofs, as can be noticed in Tables D.1.1 & D.1.2 in Appendix D.1. This is because increasing the average air velocity is not easy in the case of low reference wind velocities. This means that achieving a higher internal air velocity requires an optimisation of the studied natural ventilation system, which might lead to more improvement. Unfortunately, this is out of the scope of this study. However, some ideas are:

- To adjust the height, inlet opening area, and possibly the number of wind catchers used.
- To adjust the ratio between roof openings area and building plan area.
- To use different cross ventilation strategies at wall openings, such as opposite ventilation strategies with more opening area at the leeward façade to maximise the internal air velocity.

In the case of the higher reference wind velocity, i.e. 3 m/s, the observed increase at average wind velocity is more significant. The different reasons behind this increase in the different cases tested have been discussed in Chapters 6 to 8. In a glance, some key points are:

- In the windward zone of the building, air velocity is induced due to suction forces acting over the curved roofs.
- In the leeward zone of the building, air velocity is induced due to air provided by the wind catcher.
- In the literal zones of the building, air velocity value depends on the internal airflow behaviour. For example, if airflow movement is more centralised due to the resulting airflow path between the roof and catcher openings, then internal airflow in the literal zones may be reduced, and vice versa.

Results obtained show that average internal air velocity has recorded more increase and in the case of square plan form and for both curved roofs tested, i.e. domed and vaulted. This is more significant at 0^o and 90^o wind directions, where the increase has mainly occurred in the central zones 1-b, 2-b, and 3-b, as a direct effect of utilising the curved roofs and wind catchers. This is also true, but less significant, in the case of 45^o wind direction. In addition, air velocity distribution in this wind direction is unsymmetrical around building central zone. Generally, zone ‘c’ enjoyed higher value of air velocity, compared to zones ‘a’ and ‘b’. As explained in Section 8.2.3 (B), this is due to the resulting anticlockwise curved air movement inside the building, which speed up airflow at zone ‘c’. This is because wind catcher is attached to one windward face of the building, which causes imbalance between airflow movement between building windward and leeward faces.

In the rectangular cases, i.e. some improvements have generally been observed in the central and leeward zones, zone 2 and 3. The improvement is more significant in the middle of zone 3, i.e. zone 3-b. This indicates that the resulting airflow movement between the catcher and the leeward wall openings is stronger than airflow movement between the catcher and the roof openings, which is justified by the smaller depth of the building, compared to the square cases. These results show the effect of both curved roofs integrated with the catcher in encouraging air movement in the deep-plan configurations tested.

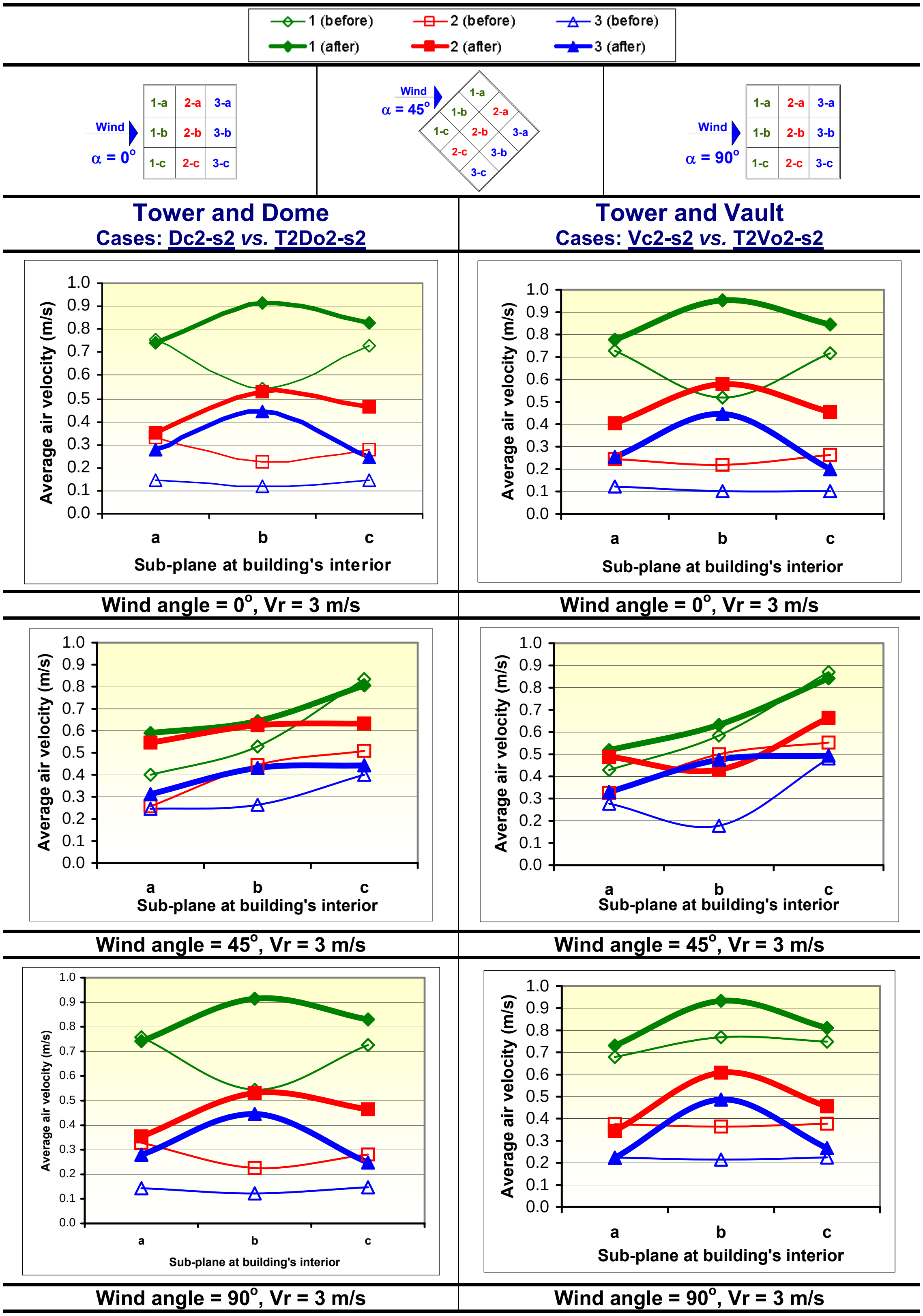

Figure 9.4: Average air velocity (for the different sub-planes at square cases interiors) before and after the utilisation of curved roofs and catcher

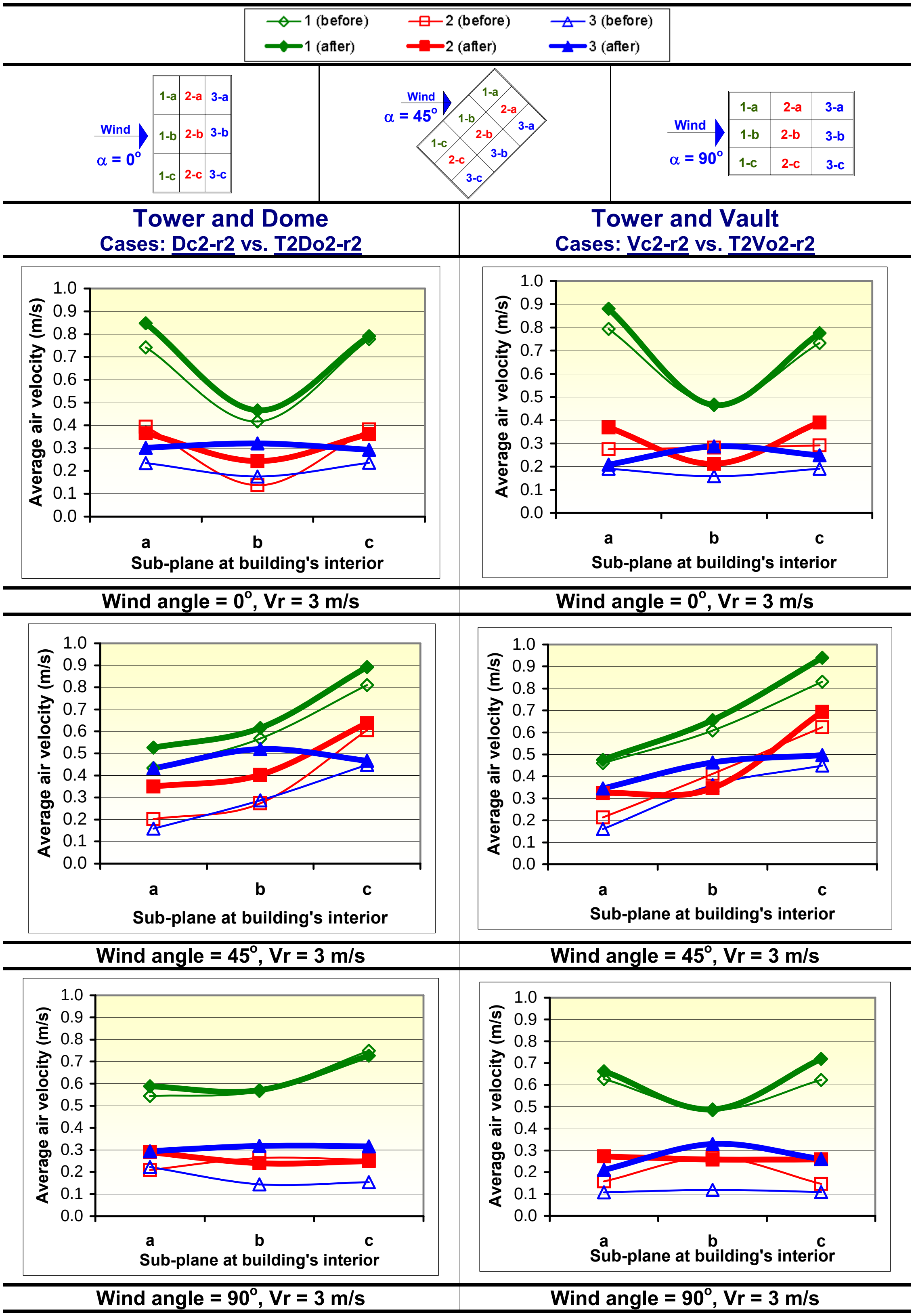

Figure 9.5: Average air velocity (for the different sub-planes at rectangular cases interiors) before and after the utilisation of curved roofs and catcher

9.4 Thermal comfort assessment

Knowing the average internal velocity, it is possible to carry out the thermal comfort assessment. With an exception of internal air velocity, all other variables in the thermal comfort index, TSI, will be assumed fixed. In order to predict percentage of people feeling comfortable, or on the opposite Percentage of People Dissatisfied (PPD), the psychrometric chart depicted in Figure 9.1 has been used as has been explained in Section 9.2. In order to deal with the small values of indoor air velocity observed in this study, the table attached to the TSI chart has been interpolated as follows:

Table 9.1: The effect of air velocity on Tropical Summer Index value

Air velocity (m/s)	Decrease in TSI (°C)
0.1	0.34
0.2	0.66
0.3	0.94
0.4	1.18
0.5	1.40
0.6	1.58
0.7	1.74
0.8	1.86
0.9	1.94
1.0	2.00

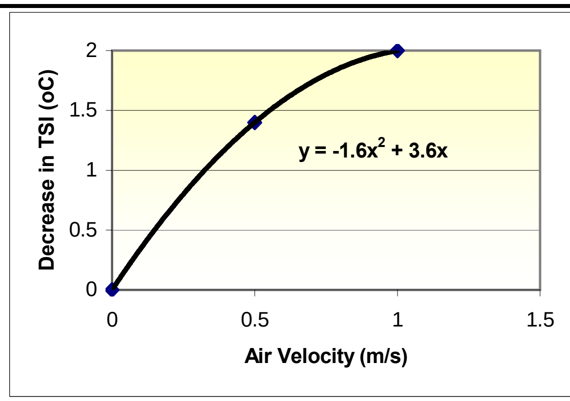

In general, thermal comfort is more sensitive to air temperature. Szokolay (2004) mentioned that air temperature is the main environmental factor that determines convective heat dissipation. Therefore, the difference between relative humidity values tested here is assumed larger than the one of the air temperature, as explained below. To determine the climatic values that will be tested, some observations on TSI psychrometric chart and some rules of thumb are used.

The recommended RH is between 40 – 70% depending on the values of the other climatic factors affecting thermal comfort (McMullan, 2002). Therefore, two value of RH will be assumed: 30% to represent a relatively low humidity, and 70% to represent a relatively high humidity. At these RH values, thermal comfort zone occurs when air temperature is less than about 30°C (29°C when RH is 70% and 31°C when RH is 30%). Therefore, two air temperature values will be assumed: 30

and 35°C. Also, it can be noticed in the TSI psychrometric chart that increasing air velocity can positively affect thermal comfort in such high values of air temperature and humidity. This could be noticed in the normal distribution curve attached to the TSI psychrometric chart. Therefore, to carry out the thermal comfort assessment, the following climatic conditions are assumed:

a. T_{db} = 30 °C, RH = 30%.
b. T_{db} = 35 °C, RH = 30%.
c. T_{db} = 30 °C, RH = 70%.
d. T_{db} = 35 °C, RH = 70%.

Results obtained from this assessment are summarised in Table 9.2, which shows the effect of utilising curved roofs integrated with wind catchers on thermal comfort performance under various climatic conditions and plan shapes. In this table, percentages of people feeling thermally comfortable are averaged for the whole building. The detailed results for the nine zones of building interiors, as indicated in Figure 9.2, are listed in Tables D.2.1 to D.2.4 in Appendix D.2.

Table 9.2: Difference in percentage of people feeling comfortable after the utilisation of curved roofs and wind catchers for natural ventilation under various climatic conditions and for a reference wind velocity of 3 m/s.

Case		Wind angle	Average difference in percentage of people feeling thermally comfortable (%)			
			T_{db} = 30 °C, RH = 30%	T_{db} = 35 °C, RH = 30%	T_{db} = 30 °C, RH = 70%	T_{db} = 35 °C, RH = 70%
Tower & Dome	Square	0°	+2.3	+3.1	+5.2	+0.9
		45°	+1.1	+2.3	+3.4	+0.7
		90°	+2.3	+3.1	+5.2	+1.0
	Rectangular	0°	+1.1	+1.6	+2.0	+0.2
		45°	+1.1	+1.9	+3.7	+0.4
		90°	+0.9	+0.9	+1.2	+0.1
Tower & Vault	Square	0°	+3.2	+4.3	+6.7	+1.3
		45°	+0.7	+1.3	+2.2	+0.2
		90°	+0.2	+2.0	+2.3	+0.1
	Rectangular	0°	+0.9	+0.7	+1.6	+0.3
		45°	+0.7	+1.3	+2.1	+0.1
		90°	+1.9	+1.8	+2.4	+0.3

9.5 Discussion

Results obtained in this study are numerically listed in Appendix D.2. In general, square building cases, possessing deeper plans, have resulted in more improvement, compared to rectangular cases, after the utilisation of curved roofs and wind catchers for natural ventilation. However, this improvement, wherever recorded, is dependant on the outdoor climatic conditions. Generally, air movement has more effect on improving thermal comfort under low air temperature, i.e. 30^{o}C compared to 35^{o}C, and when relative humidity is higher, i.e. 70% compared to 30%. It has been found that the best improvement has been recorded when the combination of the climatic factors leads to a TSI value between 29 and 33^{o}C. In this zone, TSI psychrometric chart shows that a reduction of 1^{o}C at TSI increases the percentage of comfortable people by 10%.

However, not all the climatic conditions tested have reduced TSI value to fall within the above-mentioned range. This means that increasing the internal air velocity does not always guarantee a better thermal comfort in all cases, as can be noticed in Figure 9.6. For example, the case of low air relative humidity and air temperature, 30% and 30^{o}C respectively, resulted in a slight overall average improvement. This is because the TSI value matches the peak of the normal distribution curve, which presents percentage of people feeling thermally comfortable. This practically means that majority of occupants feel comfortable and that there is no need to increase air velocity.

Also, the case of higher relative humidity and temperature, 70% and 35^{o}C respectively, resulted in a slight overall average improvement. This is because the TSI value matches the bottom of the normal distribution curve, where the curve is nearly flat. This practically means that there is a need to reduce air temperature or humidity more than the need for increasing air velocity. This also indicated that under such conditions, natural ventilation is more useful at night-time to help reducing surface temperature and therefore reducing air temperature.

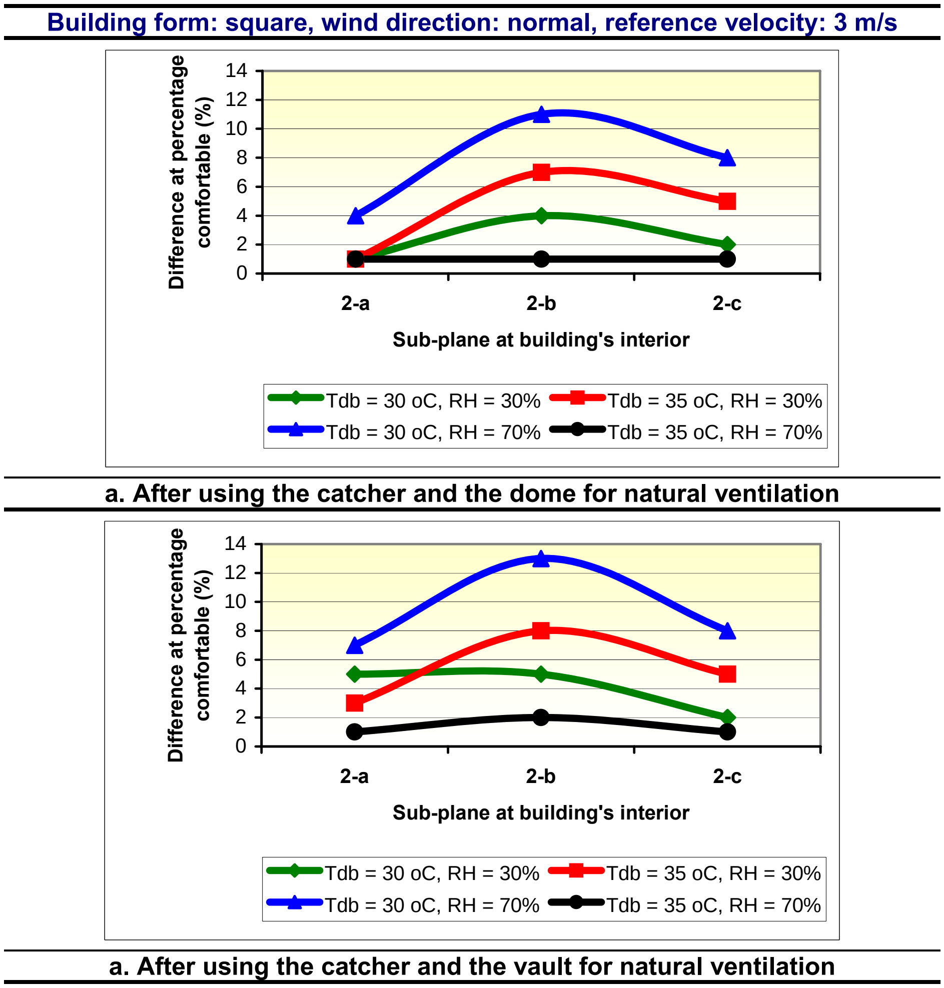

Figure 9.6: Increasing internal air velocity, due to the utilisation of curved roofs and wind catchers, does not guarantee a better thermal comfort at all climatic conditions

The other two cases, T_{db} = 35 ^{o}C, RH = 30% and T_{db} = 30 ^{o}C, RH = 70%, have presented a better improvement, especially the latter one. In the case of relative humidity of 30% and air temperature of 35^{o}C, percentage of people feeling thermally comfortable has been reduced to 20% and less. In this case, the role of increasing air velocity became more important to support the convective heat transfer. This is why the overall average improvement percentage has increased up to 3% in the tower and dome case and up to 4% in the tower and vault.

In the case of relative humidity of 70% and air temperature of 30^{o}C, the highest value of thermal comfort improvement has been recorded due to increasing air velocity. This is more significant in the square cases, where the overall average improvement is about 5% in the case of tower and dome, and about 7% in the case of tower and vault. Some local improvements have reached 11% in the case of tower and dome, and 13% in the case of tower and vault, as listed in Table D.2.3 in Appendix D.2. This is supported by the fact that in hot and humid climates, higher ventilation rates are useful to increase the bodily evaporative heat transfer, in addition to the convective one, and thus improve thermal comfort conditions.

Although the overall improvement in thermal comfort in many of the cases tested, especially the rectangular ones, seems to be low, some local improvements are quite significant, as mentioned above. This is because air velocity is only one factor among many other factors that affect thermal comfort, as reviewed in Sections 2.7 and 9.1. However, and for the cases that require more improvement, this indicates the need for optimising the current studied system, as indicated in Section 9.3, to ensure a better airflow distribution and a higher internal air velocity. However, and in all cases, increasing internal air velocity should not cause discomfort due to the undesired draught. Szokolay (2004) mentioned that, and according to some studies, under overheated conditions, internal air velocity up to 2 m/s can be acceptable.

9.6 Conclusions

This study has assessed human thermal comfort before and after the utilisation of dome and tower for natural ventilation. A variety of climatic conditions have been considered, as well as a range of buildings configurations. It has been found that thermal comfort is sensitive to increasing air velocity in different levels, depending on the climatic conditions and building design. A higher reference wind velocity has caused more thermal comfort improvement, given that the undesirable draughts should be avoided.

However, the role of both air temperature and relative humidity has been found to be crucial. This means that increasing the internal air velocity does not guarantee a better thermal comfort in all cases. For example, improvement percentage has been found to be higher when air has a relative humidity of 70%, compared to 30%, and an air temperature of 30^{o}C, compared to 35^{o}C. On the opposite, increasing air velocity has been found to have a limited effect when both air relative humidity and temperature are high.

Many local improvements at buildings interiors have been found to be significant, given that wind velocity is not the only factor that affects thermal comfort. However, the overall improvement at majority of cases tested indicates the need for a further improvement. This, on one hand, can be achieved through an optimisation study of the current studied system to ensure a better design of the curved roof and the tower. On the other hand, a thermal analysis study is required as well to investigate the effect of other factors that are expected, in addition to air velocity, to improve thermal comfort conditions. This can be, for example, the role of building materials, night-time ventilation, and building surroundings.

CHAPTER 10 : CONCLUSIONS AND RECOMMENDATIONS

Introduction

In addition to the conclusions presented at the end of each individual chapter, this chapter presents the main findings of this study, including some design guidelines. This is followed by relevant recommendations for future research, and concluded by a summary, presenting the novel contribution of this study.

10.1 Conclusions

10.1.1 Natural ventilation in buildings

Natural ventilation has been used for passive cooling in buildings for centuries. Natural ventilation usage and modelling have been reviewed at the beginning of this study. The main findings are:

- Natural ventilation is a sustainable passive cooling strategy that has many advantages, compared to the mechanical strategy.
- It has two main objectives: provision of the required air quantity and quality.
- It has many strategies, which increase its applicability to different building types and climatic conditions.
- Natural ventilation has a direct effect on thermal comfort. It affects different heat transfer mechanisms between human body and its ambient environment. This mostly occurs in the form of sensible heat, by convection and radiation, and the form of latent heat, by evaporation of moisture on the skin.
- It has many modelling techniques. These techniques have been improved in the last few years. Thus, the wind environment around buildings has become better understood.
- The use of CFD modelling has been found to be an appropriate technique for this architectural and parametric study.

10.1.2 Re-introduction of the use of traditional architectural elements for natural ventilation

In recent decades, the environmental problems associated with the extensive use of energy in buildings have increased the need for design that is energy efficient. One way of achieving this target is to re-introduce the use of traditional architectural elements and passive systems, which include many experiences in improving the quality of buildings indoor environment. This includes the use of curved roofs and wind catchers for natural ventilation in the Middle East, which is the concern of this study. This can be achieved by employing the existing elements, so that they will have an environmental role in the building.

There are opportunities for as well as limitations to such a re-introduction. For example, minarets and church towers can be re-introduced as wind catchers. As religious buildings usually possess large spans, curved roof can be used to cover the main hall. Thus, it is possible to implement the ventilation system in this study by employing both curved roofs and towers for natural ventilation. On the other hand, it is possible to use this type of ventilation system in contemporary design, as illustrated in Figures 4.1 and 4.8 in Chapter 4. Examples on different types of buildings, like residential, commercial, and educational buildings, have been presented in this thesis. Nevertheless, there are some design limitations to be considered. For example, the use of curved roofs in multi-storey buildings can only benefit the top floor. Also, in the case of multi-zone buildings, partitions used between the different zones restrict the continuity of airflow paths between the catcher and the curved roof.

Generally, it has been found that:

- These elements have a great potential for natural ventilation, and have been used for this purpose in many examples of vernacular architecture.
- These elements possess great architectural importance due to their historical value. Thus, it is possible also to benefit from this symbolism in increasing public environmental awareness, in addition to passive cooling and energy saving.
- Utilisation of these traditional elements for natural ventilation, individually and in combination, still requires more systematic investigation. This can be achieved keeping these elements within the frame of their historical reference.

10.1.3 Natural ventilation modelling using CFD

It has been proved in this study that the use of CFD is an effective and reliable approach. This is due to:

- Its reliability; CFD simulation has been compared with the Network mathematical model for airflow rate estimation in buildings. The CFD software used was Fluent 5.5. The implemented pressure coefficients data in the Network mathematical model are those recommended by Liddament (1986). Results obtained showed good agreement.
- Its accuracy, where at all the cases tested, and according to the Law of Mass Conservation, the summation of inflow and outflow rates through the different elements of the buildings was zero.
- Its applicability, especially in parametric studies. Variation of different parameters can be relatively done shorter time, compared to physical models.

10.1.4 Utilisation of dome for natural ventilation

Dome utilisation for natural ventilation in buildings has been assessed considering different parameters. This included: square and rectangular building plans, three different building floor areas of 225, 400, and 625 m^2, three wind directions of 0^o, 45^o, and 90^o, and two reference wind velocities of 1 and 3 m/s. Results of ventilation rates obtained from Fluent 5.5 software have been analysed in two ways: airflow rate through the dome and wall openings, and airflow distribution at the occupied level of the building (at 1.7 m above the ground). This has been done using contours of air velocity magnitudes, where area of different velocity zones has been estimated as a percentage of the building total area.

In general, utilisation of dome, with openings in its base, has been found to improve natural ventilation performance. Suction force acting over and around the dome induces inflow rate through the building windward facades, especially in the case of oblique wind direction. However, this has not guaranteed a significant improvement in air distribution inside the occupied level of the space since air is attracted to leave the building directly through the dome before it penetrates the downstream zone of the building. It has also been observed that airflow has the same behaviour in the case of both low and high reference wind velocities, but with different values. This similarity has been found true as well in the case of using the vault and the catcher.

The main conclusions of the Dome Study are listed below, including some relevant design guidelines:

A. In the case of 0^o wind direction

- The use of dome with rectangular building is more efficient than an equivalent square one, especially for small building areas, as outflow rate is inversely proportional to the area. This is because net outflow rate through the dome is higher by about 35%, due to the shorter distance between the dome and building windward sharp edge, over which airflow separation occurs. Thus, higher suction forces act on the dome, which also generates a strong air vortex before the dome inlet. This reduces the dome inflow rate and increases its potential for air suction. However, it is possible to increase outflow rate through the dome in the square building form if the dome inlet is closed. For example, this increase is 13% for case Do2-s2.
- This suction induces more inflow rate through the building windward face. However, this increase is relatively low (about 2%). The effect of this suction is more pronounced in attracting some air to leave through the dome instead of wall openings. Thus, outflow rate through wall openings has been reduced by about 15%. However, this generally does not have a significant effect on internal airflow distribution, especially for a building downstream zone. For example, area of still air zone is about 21%, compared to about 30% in the square cases. This is due to the fact that air movement mainly occurs in the high level of building interior.
- Although dome performance in suction is better in the rectangular building form, it seems that this does not cause a significant difference between rectangular and square forms, in terms of airflow rate observed through wall openings. This is because opening area of the dome is only about 10% of wall openings area. Thus reducing wall openings area for the advantage of the dome is expected to improve the performance of the studied system. This is typically the situation when the building is wind-sheltered.

B. In the case of 45^o wind direction

- The use of dome with either square or rectangular plan form has the same advantage. This is because net outflow rate observed is nearly the same for both building forms. This is because airflow separation occurs here over both building windward edges. In the rectangular cases, this results in an equivalent suction force to the one observed in the normal wind direction. In the square cases, suction force here is higher, compared to the normal wind direction. However, the effectiveness of this high outflow rate is reduced by the high inflow rate observed, due to the absence of air vortex in front of dome inlet. Thus, closing this inlet is more critical here, as it increases net outflow rate. For example, this increase is about 30% for both square and rectangular forms (cases Do2-s2 and Do2-r2). This means that the dome has more potential for air suction in the case of oblique wind.

- The same effect of the dome on airflow rates through wall openings is true here as well, given that there is some sort of balance between the increase in inflow rate and the reduction of outflow rate (about 6.5%). This is because areas of inlet and outlet opening are equivalent.
- Compared to the normal wind direction, a better internal airflow distribution has been observed. For example, area of the still-air zone in case Do2-s2 is 11%, compared to 37% in the normal wind direction. This is because the oblique wind direction has facilitated the use of opposite ventilation, and limited the effect of the literal wall openings in attracting airflow before it penetrates the space. Utilisation of the dome has caused slight improvement in general. However, in the cases that have the largest depth, 5H in the square case, and 4H in the rectangular one, where H is building height and equals 5 m, utilisation of the dome has caused a slight reverse effect. This is because part of the airflow leaves through dome openings instead of wall outlets.

C. In the case of 90^o wind direction

- The use of dome with square building form is more efficient than an equivalent rectangular one, especially for small building areas. Outflow and inflow rates through dome and wall openings in the square cases show the same behaviour presented in the normal wind direction. This is because square cases are symmetrical around both their axes. Concerning rectangular building form, the large depth of the building in this orientation reduces suction forces acting over the dome. Thus, net outflow rate in the rectangular configurations presented fewer values compared to the square configurations (less by about 30%).

- Cross ventilation between wall openings is not as efficient as the square form. This is because of the large building depth and the relatively shorter windward building face, which can accommodate less inlet area.
- The still-air zone in the downstream wing is significantly high (about 40%). Dome utilisation has only caused a slight improvement. The reversed airflow acting on the rectangular building leeward face has contributed to improving the internal airflow distribution, specifically in the leeward zone.

10.1.5 Utilisation of vault for natural ventilation

Vault utilisation for natural ventilation in buildings has also been assessed considering different parameters. This included:

- Square and rectangular building forms, with a fixed plan area of 400 m^2.
- Three areas of the vault, starting from a square vault that has the same plan area of dome configuration Do2.
- Three wind angles (0^o, 45^o, and 90^o), and two wind velocities (1 and 3 m/s).

Vault openings are also located in its base. They are equally divided between the vault windward and leeward faces. It has been generally concluded that there are many similarities between domed and vaulted roofs, in terms of their natural ventilation performance. From an aerodynamic standpoint, this is due to the suction force generated when air passes through their curved face. However, a comparison held between dome configuration Do2 and its equivalent vault configuration Vo1 has revealed some differences. The main conclusions of the Vault Study are listed below, including some relevant design guidelines:

A. In the case of 0^o wind direction

- The use of vault with rectangular building form is more efficient than an equivalent square one. The large inlet area, compared to the dome, made the vault configuration tested more sensitive to changing building depth. For example, net outflow rate through the vault in case Vo2-r2 is higher than case Vo2-s2 by more than 200%. This is justified in the same way explained in the Dome Study. The interesting finding here is that outflow rate through the vault is always higher than inflow rate, despite equal opening areas located at both windward and leeward faces of the vault.

- By comparing two equivalent dome and vault configurations, it has been found that the dome is more efficient for air suction, especially in the case of square building form. Net outflow rate for dome outlet unit area is higher by 65% in the square cases. Closing the vault inlet has significantly improved its performance by about 100%, and reduced the difference in net outflow rate between it and the domed roof to only 12%. However, closing the vault inlet has no effect in the rectangular case, as inflow rate through the vault is zero.
- Increasing the plan area of the vault results in higher inflow and outflow rates through vault openings. This occurs linearly due to the openings area uniform increase when vault plan area increases. Generally, suction force acting on the vault has resulted in a similar behaviour to the one observed in the Dome Study, in terms of airflow rates through wall openings and internal airflow distribution. However, airflow rates observed are less here.

B. In the case of 45^{o} wind direction

- The use of vault with either square or rectangular plan form has the same advantage, as explained in the Dome Study. By comparing the equivalent dome and vault configurations, it has been concluded that the use of either roof shape has nearly the same advantage. However, the use of the vault is more efficient after closing its inlet. This has increased its net outflow rate to be higher than the dome by 40% for both square and rectangular cases.
- Utilisation of the vault affects airflow rates through wall openings in the same way explained in the case of the dome. This is also true for the observed internal airflow distribution. However, airflow rates observed are less here.

C. In the case of 90^{o} wind direction

- The use of vault with rectangular building form is more effective, as it improves ventilation conditions in the leeward zone by the resulting reversed airflow. However, vault performance here in suction is much higher, compared to the previous wind directions. This is because all of its openings are acting as outlets. By comparing the equivalent dome and vault configurations, the use of the vault has been found more effective. Net outflow rate recorded through the vault is higher by 25% and 55% than the one recorded through the dome for square and rectangular cases, respectively. After closing the roof inlet, namely for dome, difference in net outflow rate has been reduced. Net outflow rate recorded through the vault is now higher by 10% and 35% than the one recorded through the dome for square and rectangular cases, respectively.

- The high suction observed here highly affects airflow rates through building walls, especially when the vault area is higher. For example, inflow rate in case V3-s2 has increased by 11%, and outflow rate has reduced by 30%. Thus, a significant improvement in airflow distribution has been observed. For example, area of the still air zone in the rectangular cases has been reduced by about 15%, compared to about 5% in the dome study.

10.1.6 Integration of wind catchers and curved roofs

In general, utilisation of curved roofs, with openings provided at their base, for wind-induced natural ventilation has been found to be useful. Curved roofs always increase inflow rate through building windward(s), and reduce outflow rate through wall openings, because this roof attracts this airflow to leave through it instead of the wall. However, this vertical air movement does not secure an acceptable internal air distribution. Thus it has been suggested in Section 4.1 of this study that the unique architectural relationship between curved roofs and towers can be invested for natural ventilation. This means that curved roofs, which are effective in air suction, can be integrated with wind catchers, which are effective in air supply or suction, in order to encourage air movement in the downstream wing of buildings.

Thus, catcher integration with domed and vaulted roofs for natural ventilation in buildings has been assessed considering different parameters. These included:

- Square and rectangular building forms, with a fixed plan area of 400 m^2.
- Three systems of the catcher: air provision at building centre, air provision at building downstream zone, and air suction at building leeward wall.
- Three wind angles (0^o, 45^o, and 90^o), and two wind velocities (1 and 3 m/s).

It has been observed that both low and high wind velocities examined have generally recorded the same behaviour, but with a higher rate in the case of the higher wind speed. Generally, this study shows the advantage of utilising the catcher for the improvement of natural ventilation performance, in terms of airflow rates and internal airflow distribution. This effect is expected to be even more apparent in the case of the building being sheltered. This is summarised generally as follows:

- It encourages suction ventilation through the curved roof openings.
- It encourages suction ventilation through leeward wall openings.
- It improves airflow distribution, especially in the downstream zone.

A. Integration of wind catcher and domed roofs

- In the case of 0^o wind direction, utilisation of the catcher for air provision has been found to be more useful in the square cases, and utilising it for air suction has been found to be more useful in the rectangular cases. Utilisation of the catcher for air provision increases outflow rate through the dome by about 20%, and through walls openings by about 15% in the square cases and 10% in the rectangular ones. This is because catcher shading effect reduces inflow rate through the dome, in addition to the additional amount of air provided by the catcher itself. This has redistributed airflow inside the building and caused a significant improvement in internal airflow distribution, mainly in the square configurations, where the area of the still-air zone has been reduced by 12% and 24%, respectively for the fist two wind-catcher systems. Utilising the catcher as a wind chimney has reduced outflow rate through the dome by about 28% in the square form, and 23% in the rectangular one. The catcher attracts this air, as a slight effect has been recorded at airflow rates through walls openings. Thus, a significant improvement in internal airflow distribution has been observed, mainly in the rectangular configuration due to its smaller depth.
- In the case of 45^o wind direction, utilisation of the catcher for air provision has been found to be more effective. In this case, a dramatic change in internal airflow behaviour has been observed, due to the observed curved air movement. This occurs due to the imbalance caused by both building windward faces after placing the catcher at one of them. This causes significant improvement in internal airflow distribution.
- In the case of 90^o wind direction, airflow behaviour in the square cases shows the same behaviour presented and discussed in the case of normal wind direction. This is because square cases are symmetrical around both their axes. Regarding the rectangular ones, utilisation of the catcher as a wind chimney has been found more useful than utilising it as a wind catcher. Suction forces acting over the dome are originally weak. Thus, utilising the catcher as a wind chimney significantly reduces outflow rate through the dome by 55%. Thus, more air is

induced by suction forces acting on the catcher to penetrate the deep plan more easily, which reduces area of the still-air zone by 19%.

B. Integration of wind catcher and vaulted roofs

This study was limited to the second wind-catcher system, where catcher provides air to the downstream zone. This system has improved internal airflow distribution in most of the cases tested. It was also limited to the second vaulted roof configuration, due to the similarity observed between the different vaulted roofs tested. In all cases, utilisation of the vault has been found to be useful for internal airflow distribution. Results obtained lead to the following conclusions and design guidelines:

- In the case of 0^o wind direction, utilisation of the catcher has resulted in the same behaviour explained in the dome case. This has caused a significant improvement in internal airflow distribution, mainly in the square configuration, where still-air zone area has been reduced by 25%.
- In the case of 45^o wind direction, utilisation of the catcher with the square building form has resulted in the same behaviour explained in the dome case, given that the internal curved air motion is weaker. This is because net outflow rate through the vault is higher here by about 12%. Thus, internal airflow distribution has been improved, but less than the case of integrating the catcher with the dome. Net outflow rate is higher in the rectangular case by about 33%, which prevents the occurrence of curved air motion. Thus, internal airflow distribution has been improved, but more than the case of integrating the catcher with the dome. This is due to the relatively elongated geometry of the vault, which eliminates the still-air bubble that always occurs in the top downstream corner of rectangular cases in this wind direction.
- In the case of 90^o wind direction, utilisation of the catcher reduces net outflow rate through the vault by 13% for the square case, and 6% for the rectangular one. Thus, large amount of air is returned to the occupied level of the building, so that it leaves through walls openings. Thus, outflow rate through these openings increased by about 25%, which also improves internal airflow distribution.

Tables 10.1 to 10.4 summarise, in a practical manner, the main findings of the different CFD modelling studies carried out in this research.

Table 10.1: Summary of the Dome Study

	Wind angle	Square cases	Examples* and illustrations**	Rectangular cases	Examples* and illustrations**
				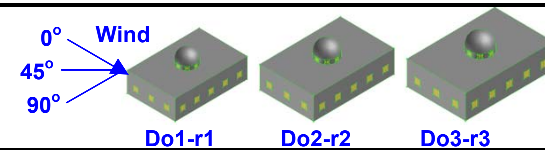	
Airflow rate	**0°**	Dome induces more inflow, and attracts large amount of outflow to leave through it instead of the walls. This is in inverse proportion to floor area.	Inflow: +1.6%. Outflow: -14%.	Similar to the square cases. However, dome is more effective here because it is subjected to a higher suction (net outflow rate through the dome is higher by 35%).	Inflow: +2.6%. Outflow: -15%.
	45°	Dome is subjected to a higher suction here, especially when its inlet is closed.	Inflow: +6%. Outflow: -7%.	Suction acting on the dome is equivalent to that observed in normal wind direction.	Inflow: +6%. Outflow: -7%.
	90°	The same as explained at 0° wind direction (the building is symmetrical).	---	The deep plan limited the role of the dome in inducing more inflow.	Inflow: +0.5%. Outflow: -14%.
Internal airflow distribution	**0°**	A slight improvement in building upstream and central zones. Still-air zone area is less by 6%. No improvement has been observed at 6H*6H floor area.	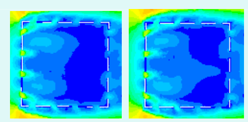	Similar to the square cases. In the small area, change in airflow (from horizontal to diagonal) prevents any improvement.	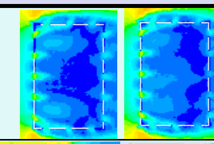
	45°	Dome effect is limited here, because of the strong air movement between walls openings, caused by cross ventilation.	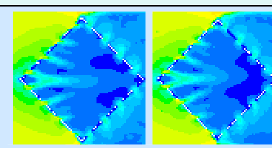	Similar to the square cases, but with unsymmetrical airflow pattern.	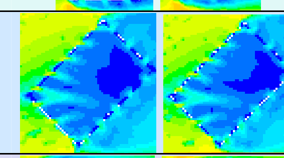
	90°	The same as explained at 0° wind direction (the building is symmetrical).	---	The reversed flow causes an additional slight improvement in the leeward zone. Still-air zone area is less by 5%.	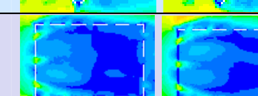

Building form: square, and rectangular (1:1.5 aspect ratio), height, H = 5 m, plan area: 4H*4H = (225m^2), 5H*5H = (400m^2), & 6H*6H = (625m^2), porosity: 10% of floor area (16 opening), dome form: hemispherical, dome plan area: 7.5% of floor area, dome porosity: 13% of its plan area (8 openings at its base).

* Difference between airflow through the walls, averaged for the three cases (originally measured in (l/s)/m^2 of floor unit area at 3 m/s reference wind speed (before & after utilising the dome). ** Presented by velocity contours for Do2-s2, and Do2-r2 (before & after utilising the dome).

Table 10.2: Summary of the Vault Study

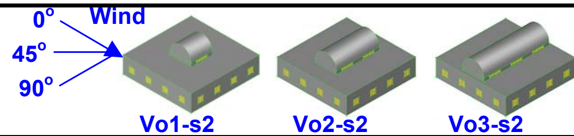				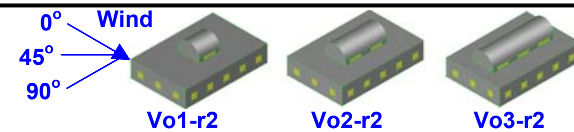	
	Wind angle	**Square cases**	**Examples* and illustrations****	**Rectangular cases**	**Examples* and illustrations****
Airflow rate	**0°**	Vault induces some inflow, and attracts some outflow to leave through it instead of the walls, proportionally to its plan area. The use of the dome is more effective.	Inflow: +0.8%. Outflow: -5.9%.	Vault is more effective with this form, because of the shorter distance between it and the windward sharp edge. However, the use of the dome is still more effective.	Inflow: +1.2%. Outflow: -8.7%.
	45°	To benefit from the higher suction here, it is essential to close vault inlet(s), which makes it more effective than the dome.	Inflow: +4%. Outflow: -4%.	Similar to the square form.	Inflow: +5%. Outflow: -5.4%.
	90°	Maximum suction. All vault openings are outlets. It is more effective than the dome.	Inflow: +6.4%. Outflow: -27%.	Similar to the square form, but with more airflow increase.	Inflow: +8%. Outflow: -30%.
Internal airflow distribution	**0°**	A slight improvement in building upstream and central zones. Still-air zone area is less by 5%.	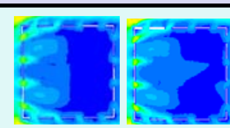	Similar to the square cases.	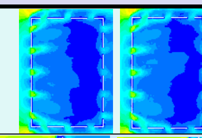
	45°	Similarly to the dome, vault effect is limited here, because of the strong air movement between walls openings.	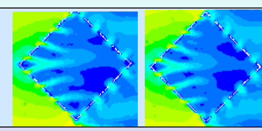	Similar to the square cases.	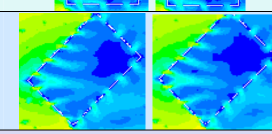
	90°	Improved in the upstream and central zones, but on the account of the downstream one. Still-air zone area is more by 7%.	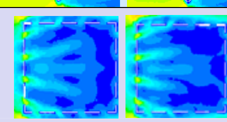	The reversed airflow at the leeward zone facilitates air penetration of the leeward zone. Still-air zone area is less by 14%.	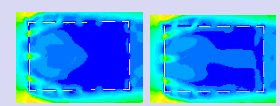

Building form: square, and rectangular (1:1.5 aspect ratio), height, H = 5 m, plan area: 5H*5H = 400m^2, porosity: 10% of floor area (16 opening), vault form: semicircular, vault plan area: 7.5%, 15%, 22.5% of floor area, vault porosity: 13% of its plan area (2, 4, and 6 openings at its base).

* Difference between airflow through the walls, averaged for the three cases (originally measured in (l/s)/m^2 of floor unit area at 3 m/s reference wind speed (before & after utilising the vault). ** Presented by velocity contours for Do2-s2, and Do2-r2 (before & after utilising the vault).

Table 10.3: Summary of the Tower and Dome Study

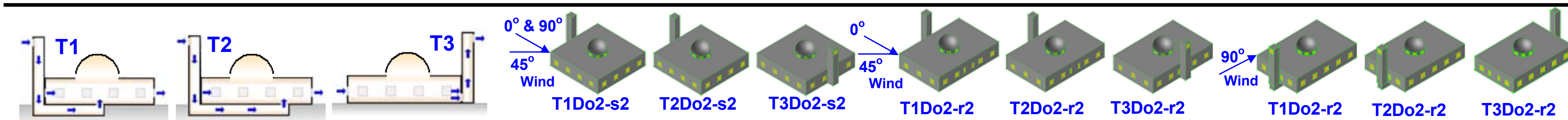

	Wind angle	Square cases	Examples* and illustrations**	Rectangular cases	Examples* and illustrations**
Airflow rate	0°	Utilisation of the catcher for air provision (T1 & T2) is more useful, as it increases airflow rates through dome and walls openings.	Outflow (T2, dome): +20%. Outflow (T2, walls): +15%.	Utilisation of the catcher for air suction (T3) is more useful, because of the smaller plan depth.	Outflow (T3, dome): -23%. Outflow (T3, walls): -0.2%.
	45°	As explained above.	Outflow (T1, dome): -2.7%. Outflow (T1, walls): +6.3%.	Similar to the square cases.	Outflow (T1, dome): +7.5%. Outflow (T1, walls): +8%.
	90°	The same as explained at 0° wind direction (the building is symmetrical).	---	Utilisation of the catcher for air suction (T3) is more useful, because of the weak suction acting on the dome.	Outflow (T3, dome): -55%. Outflow (T3, walls): +2%.
Internal airflow distribution	0°	Air provided by the catcher, especially in T2, significantly improves internal flow distribution, as still-air zone area has been reduced by 22%.	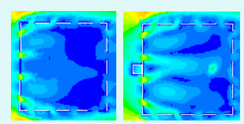	The catcher attracts more air to the leeward zone, which reduces still-air zone area by 18%.	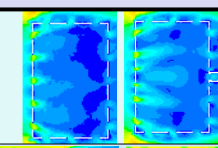
	45°	The resulting internal curved air motion significantly improves air distribution, especially in T1 (illustrated), where still-air zone area is less by 9%.	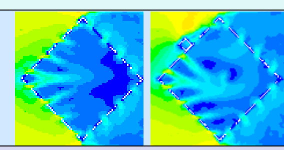	Similar to the square cases, but without the air being reversed to the literal face. Still-air zone area is less by 12% in both T1 (illustrated) & T2.	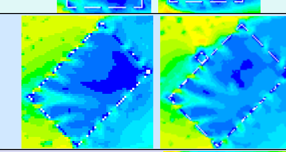
	90°	The same as explained at 0° wind direction (the building is symmetrical).	---	Still-air zone area has been reduced by 19%.	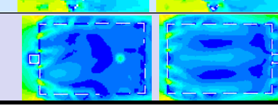

Building form: square, & rectangular (1:1.5 aspect ratio), building height, H = 5 m, plan area: 5H*5H, porosity: 10% of floor area, dome form: hemispherical, dome plan area: 7.5% of floor area, dome porosity: 13% of its plan area, tower form: square, tower area: 1.2% of floor area, tower height: 2.5H.

* Difference between airflow through the dome and the walls for the indicated wind-catcher system (originally measured in (l/s)/m^2 of floor unit area at 3 m/s reference wind speed (before & after utilising the tower). ** Presented by velocity contours for the relevant cases (before & after utilising the tower).

Table 10.4: Summary of the Tower and Vault Study

		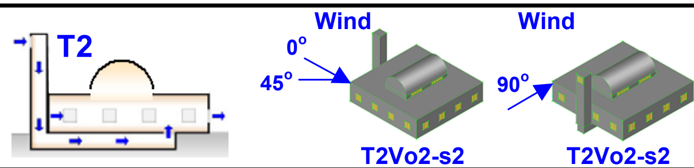		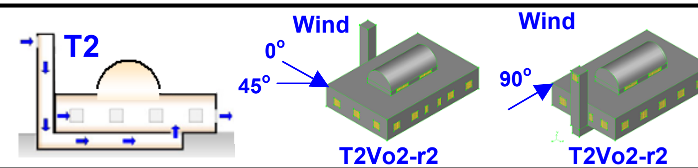	
	Wind angle	**Square cases**	**Examples* and illustrations****	**Rectangular cases**	**Examples* and illustrations****
Airflow rate	**0°**	Higher flow rates through the vault and walls openings, which improves ventilation conditions in the building.	Outflow (vault): +28%. Outflow (walls): +8%.	Similar to the square case. However, air provided by the catcher mainly increases outflow through the vault.	Outflow (vault): +60%. Outflow (walls): +1.7%.
	45°	Similar to the normal wind direction, but less significant	Outflow (vault): +16%. Outflow (walls): +1.5%.	Similar to the normal wind, but with more increase in airflow rate through the walls.	Outflow (vault): +35%. Outflow (walls): +5%.
	90°	Airflow provided by the catcher supports the role of walls openings in suction.	Outflow (vault): -13%. Outflow (walls): +26%.	Similar to the square case.	Outflow (vault): -6%. Outflow (walls): +27%.
Internal airflow distribution	**0°**	Significant improvement, as area of still-air zone has been reduced by 25%.	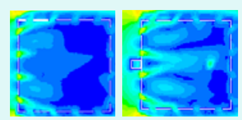	Less significant than the square case. Area of still-air zone has been reduced by 5%. Air provided by the catcher mainly leaves through the vault.	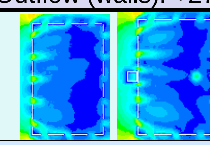
	45°	The resulting internal curved air motion improves air distribution, where still-air zone area is less by 6%.	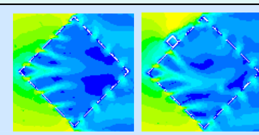	The higher suction on the vault prevents the curved air motion, but causes more improvement, compared to the square form. Still-air zone area is less by 18%.	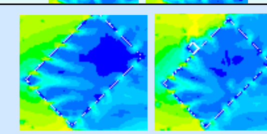
	90°	The large air amount returned to the occupied level improves air distribution, where still-air zone area is less by 19%.	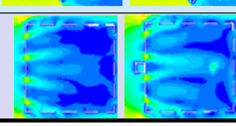	Similar to the square case, but less significant. Still-air zone area is less by 13%.	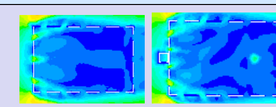

<u>Building form</u>: square, and rectangular (1:1.5 aspect ratio), <u>building height</u>, H = 5 m, <u>plan area</u>: 5H*5H = 400m^2, <u>wall porosity</u>: 10% of floor area, <u>vault form</u>: semicircular, <u>vault plan area</u>: 15% of floor area, <u>vault porosity</u>: 13% of its plan area, <u>tower form</u>: square, <u>tower area</u>: 1.2% of floor area, <u>tower height</u>: 2.5H.

* Difference between airflow through the vault and the walls for T2 wind-catcher system (originally measured in (l/s)/m^2 of floor unit area at 3 m/s reference wind speed (before & after utilising the tower). ** Presented by velocity contours for T2Vo2-s2, and T2Vo2-r2 (before & after utilising the tower).

10.1.7 Thermal comfort improvement

The ultimate aim of using natural ventilation in buildings is to improve human thermal comfort conditions. Thus, this study has carried out a thermal comfort assessment before and after utilising the studied natural ventilation system. To carry out this assessment, a reasonable variety of climatic conditions have been considered. This includes two values of a relatively high air temperature, 30^o and 35^{o}C, and two values of air relative humidity, 30% and 70%, to represent hot arid and hot humid climates. Average internal air velocity has been recorded on the building plan at a height of 1.7 m. This plan has been divided into nine zones, having the same area, in order to account for any local improvement in air velocity. Then, thermal comfort assessment has been carried out using the Tropical Summer Index, TSI, which estimates percentage of people feeling satisfied, PPS.

In general, it has been found that:

- Thermal comfort is sensitive to increasing air velocity, depending on the local climatic conditions. Improvement recorded in PPS has been found to be higher when air has a relative humidity of 70%, compared with 30%, and an air temperature of 30^{o}C, compared with 35^{o}C. When both air temperature and relative humidity are high, increasing air velocity has limited effect.
- The studied system has been found to be useful in improving thermal comfort. This is true and consistent for both domed and vaulted roofs. This is more pronounced in the higher reference wind velocity, 3 m/s. The improvement observed as an average for the whole building is limited. However, many local improvements are significant, as PPS has increased by about 10%.
- In the low reference wind velocity, less improvement has been always recorded in average air velocity. However, it cannot be ignored. This is because any increase in air velocity can be influential on thermal comfort achievement. For example, ASHRAE Fundamentals, (see: Bahadori, 1985), stated that building occupants seated in sedentary condition and wearing light-weight clothing, feel thermally comfortable under the following climatic conditions of dry-bulb temperature, relative humidity and air velocity, respectively: 27.5^{o}C, 20%, and 0.2m/s; or 28.2 ^{o}C, 60%, and 1.5m/s.

- This indicates the need for other passive cooling strategies to enhance the role of air velocity, which is one factor amongst many factors affecting thermal comfort. This also indicates the need for optimising the studied natural ventilation system to ensure more improvement, as discussed in Section 10.7.5.

10.1.8 Limitations of the results

It has been concluded in this study that the parameters affecting natural ventilation application in buildings are numerous. CIBSE (1988, p. B3-12) summarized these parameters in the following statement: "exposure, terrain, height above the ground level, building shape, and wall/wind orientation all influence the rate of airflow into the building". These parameters can be grouped in three categories:

- o Climatic parameters: this includes wind speed and direction.
- o Geometrical parameters: this includes building shape, roof shape, etc.
- o Urban parameters: this includes sheltering effect of adjacent objects.

It was intended to carry out this investigation through a parametric approach, as introduced in Section 1.4, so that the study will not be too individual. Nevertheless, it was a necessity to reduce parameter variety, depending on some assumptions, in order to keep the study within its proposed size. This surely reduces its applicability. However, it was possible to conclude many design guidelines and useful observations, as has been discussed in the previous sections. These results are subjected to the following limits, which are discussed in detail in Sections 6.1, 6.2, 7.1, and 8.1:

- The chosen area range, buildings forms, and porosity.
- Geometries and porosity of domed and vaulted roofs.
- Shape and height of the catcher.
- Wind angles and velocity range chosen.
- Wind velocity profile chosen, given that buildings are not wind-shaded.

The main concern was to observe the effect of specific parameters on airflow behaviour and natural ventilation performance in order to introduce effective ventilation strategies in buildings. The parameters that were restricted in this study are put forward for fellow researchers as recommendations for further research. This collaborative methodology allows the investigation of such complicated research topics with many interacting parameters. These recommendations are discussed below.

10.2 Recommendations for future work

10.2.1 Effect of site planning

Buildings usually exist in urban sites, and are surrounded by other buildings with different heights. Thus, it is important to simulate the sheltering effect of these adjacent buildings on the studied natural ventilation system. For example, Yaghobi (1991) concluded in his study on natural ventilation performance of wind towers that wind towers are more effective in reducing building internal air temperature when they are shaded. However, this study has considered the effect of the site in the modelled ‘city’ wind velocity profile, as explained in Section 5.2.1. This is because simulating the site has been found to be beyond the available mesh size in Fluent 5.5. In order to cope with this limitation, some ideas are:

- To reduce air velocity value to an assumed value, usually very low, and up to the sheltering building height. This idea has been implemented by Shao *et al.* (1993) using Fluent 4 software, and has shown reasonable findings. Wind velocity has been reduced from its reference value of 5 m/s to 0.5m/s. However, no clear guidelines to specify this value have been mentioned.
- To use other CFD programs, like Airpak (Goverdhan, 2005), which are specially developed for building applications.
- To simulate the site physically in wind tunnels. In such case, the size of the urban context is critical and limited by the size of the wind tunnel.

10.2.2 Thermal behaviour of the studied ventilation system

This study has revealed the great benefit of utilising curved roofs and wind catchers for natural ventilation in buildings. However, the issue of environmental sustainability in buildings has to be tackled comprehensively considering its different aspects. Although this study did not analyse the thermal behaviour of the studied architectural elements, it is expected that this behaviour will affect their natural ventilation performance by stack effect. Elseragy (2003) has done his relevant study within the same research group, and concluded that curved roofs geometry has a great effect on their thermal performance, as reviewed in Section 4.3.2. Thus, it is required to link both studies in a way that considers the effect of this thermal performance in natural ventilation application, like utilisation of the stack effect, and how it affects the height of the curved roof and wind catcher, the effect of building materials on utilising night-time ventilation strategy, and shading effect of building surroundings.

10.2.3 Investigation of other geometries

This study has focused on the general use of both curved roofs and wind catchers as a natural ventilation strategy. Thus, simple and abstract building configurations have been modelled. These included: simple sharp-edged main building volume, hemispherical domes, semi cylindrical vaults, and square wind catchers. However, other interesting geometries are recommended for further investigation. This includes:

- Building shapes other than sharp-edged, such as curved-edged buildings.
- Integration of curved roofs and other roof shapes, like pitched roofs.
- Other geometries of the dome, like onion dome, saucer dome, half domes, and combined domes. This is in addition to dome relation with the main volume. For example, increasing dome height, with respect to the span, is expected to increase the drop in air pressure around dome base. The opposite scenario is expected in shallow domes, where the drop in air pressure increases at dome apex.
- Other geometries of the vault, like groin vault, annular vaults, pointed vaults, and half or segmental vaults.
- Other geometries of the catcher, like cylindrical catchers. Also to study the optimum tilt of catcher roof. In some historical examples, the roof of the catcher tilts forward in order to facilitate wind catching. This is because the use of a flat roof may obstruct wind catching by the existence of an air vortex in the internal corner between the flat roof and the tower walls.
- Different combinations of the studied elements, like the use of the dome, vault, and catcher all together.
- Implementation of some technologies, like the use of the sliding domes, air distribution systems, etc.

10.2.4 Indoor air quality assessment

The objective of any natural ventilation system is to provide the required quantity and quality of air. This study has focused on the objective, since examining both of them is out of its scope. Provision of the required air quality requires an analysis of the way in which the targeted building is used. This leads to prediction of contaminant concentrations in air, and to decide on the required ventilation strategies and airflow rates to remove them. This is usually done depending on the recommendations of natural ventilation manuals and local building regulations. Nowadays, it is common practice to study Indoor Air Quality using CFD applications. One relevant side here is to study smoke behaviour in the case of fire to ensure that the studied ventilation system meets safety requirements.

10.2.5 Optimisation of the studied ventilation system

As concluded from Chapter 9 of this study, the studied system has resulted in many cases to an acceptable thermal comfort improvement, depending on the observed increase at local wind velocities inside the building. However, insignificant thermal comfort improvement has also been observed in many cases. This indicates the importance of optimising the studied ventilation system, in terms of the detailed design of the studied curved roofs and wind catchers. This includes: height of the catcher, relationship between plan-depth and roof geometry, and porosity of the different architectural elements used. It is required also to specify some critical points in which airflow tends to change its behaviour. For example, the critical plan depth in which airflow changes its direction to diagonal instead of horizontal. This should be done in a way that increases the potential of the studied system for increasing internal air velocity at all building zones, and, thus, improving thermal comfort conditions.

10.2.6 Structural requirements of the studied ventilation system

In fact, natural ventilation applications in buildings should account for the structural needs. For example, increasing suction forces acting over the curved roofs tested in this study was a desired parameter. This occurs, for example, when wind approaches the main building volume at an angle of 45^o. This is due to the intense vortices generated at the top corner of the windward face. According to Sachs (1978), pressure coefficient value here may reach -3.0 or more. Such suction force may be desired for natural ventilation, but at the same time can damage the roof, depending on the structural system and materials used. Thus, it is recommended to study the structural implications of the studied natural ventilation system.

10.3 Summary

It is believed that this study has introduced many innovative ideas and contributions to knowledge. It is believed that this has been fulfilled within the frame of the main aims and objectives stated earlier in Chapter 1. These findings have been discussed in the first section of this chapter. It is worth mentioning here that more than 175 cases have been modelled in this study, with a total file size of about 18 GB. In general, prediction of airflow in naturally ventilated buildings is very useful to improve indoor environment conditions. Natural ventilation performance has been assessed in terms of airflow rate and internal airflow distribution.

It has also been observed that there is always a conflict between different airflow driving forces. Implementation of Law of Mass Conservation and the use of Fluent 5.5 modelling techniques have helped understanding this conflict, and utilise it for natural ventilation improvement in buildings. It has been found that curved roofs and wind catchers offer a high potential for improving natural ventilation and thermal comfort conditions in buildings. The combination of both curved roofs and wind catchers in one ventilation system has been found to improve airflow rates and distribution inside buildings. This is because:

- The use of roof-level openings at domed and vaulted roofs increases suction forces acting on these roofs. This improves natural ventilation performance in the upstream and central zones of the building, but does not guarantee that for the downstream one.
- The use of wind catchers, for air provision or suction, can effectively improve and balance the roles of curved roofs and walls openings in ventilation. This improves natural ventilation performance in the downstream zone of the building. This could be noticed as a reduction in the still-air zone, and as an increase in the other velocity zones in the building.

BIBLIOGRAPHY

Al-Koheji, M., 2003. *Application of porous ceramics and wind-catchers for direct and indirect evaporative cooling in buildings*. Ph.D. thesis, University of Nottingham.

Allard, F., ed., 1998. *Natural ventilation in buildings: a design handbook*. London: James & James Ltd.

Allard, F., and Alvarez, S., 1998. Fundamentals of natural ventilation. *In*: Allard, F., ed. *Natural ventilation in buildings: a design handbook*. London: James & James Ltd., 1998, p. 9-62.

Al-Qahtani, T. H., 2000. *An improved design of wind towers for wind induced natural ventilation*. Ph.D. thesis, University of Bath.

Alvarez, S., Sanchez, F., and Molina, J. L., 1998. Air flow pattern at courtyard. *In*: Maldonado, E. and Yannas, S, ed. *Proceedings of PLEA 98, Lisbon, Portugal, June 1998.* London: James and James Ltd, p. 503-506.

ArchNet, [no date]. *ArchNet Digital Library* [online]. Available at: <http://archnet.org/library/sites> [Accessed 21 October 2004].

ASHRAE, 1997. *ASHRAE Handbook: Fundamentals*. S.I. ed. Atlanta, Ga.: American Society of Heating Refrigerating and Air Conditioning Engineering.

Athienitis, A. K., and Santamouris, M., 2002. *Thermal analysis and design of passive solar buildings*. London: James & James Ltd.

Awbi, H., 1994. Design considerations for naturally ventilate buildings. *Renewable Energy*, 5(2), 1081-1090.

Awbi, H., 2003. *Ventilation of buildings*. 2nd ed. London: Spon Press.

Badran, A. A., 2002. Performance of cool towers under various climates in Jordan. *Energy and Buildings*, 35, 1031-1035.

Bahadori, M., 1985. An improved design of wind towers for natural ventilation and passive cooling. *Solar Energy*, 35(2), 119-129.

Bahadori, M., 1994. Viability of wind towers in achieving summer comfort in the hot arid regions. *Renewable Energy*, 5(2), 879-892.

Bahadori, M., and Haghighat, F., 1985. Passive cooling in hot arid regions in developing countries by employing domed roofs and reducing the temperature of internal spaces. *Building and Environment*, 20(2), 103-113.

Bain, D., Baker, P., and Rowat, M., 1971. *Wind tunnels: an aid to engineering structure design*. Cranfield : British Hydromechanics Research Association.

Baskaran, A., and Kashef, A., 1996. Investigation of air flow around buildings using Computational Fluid Dynamics techniques. *Engineering Structures,* 18(11), 861-873.

Bensalem, R., 1991. *Wind-driven natural ventilation in courtyard and atrium-type buildings*. Ph.D. thesis, University of Sheffield.

BICEPS module, 1997. *Ventilation: energy efficiency and indoor air quality illustrations*'. Watford: Building Research Establishment.

BRE, 1994. *Natural ventilation in non-domestic buildings*. BRE Digest 399. Garston: Building Research Establishment.

BSI, 1991. BS 5925: *Code of practice for ventilation principles and designing for natural ventilation*. London: British Standards Institution.

BSI, 2005. BS EN ISO 7730: *Ergonomics of the thermal environment – Analytical determination and interpretation of thermal comfort using calculation of the PMV and PPD indices and local thermal comfort criteria*. London: British Standards Institution.

Chand, I., Sharma, V. K., and Krishak, N. V., 1990. Studies on the design and performance of wind catchers. *Architectural Science Review*, 33, 93-96.

Charles, K., Reardon, J. T., and Magee, R. J., 2005. *Indoor air quality and thermal comfort in open-plan offices* [online]. Available at: <http://irc.nrc-cnrc.gc.ca/pubs/ctus/64_e.html> [Accessed 5 February 2006].

Chow, W. K., 2004. Wind-induced indoor-air flow in a high-rise building adjacent to a vertical wall. *Applied Energy*, 77, 225-234.

CIBSE, 1988. *CIBSE Guide*. Vol. A. and B. 5th ed. London: the Chartered Institution of Building Services Engineers.

CIBSE, 1997. *Natural ventilation in non-domestic buildings*. Application manual AM10. London: the Chartered Institution of Building Services Engineers.

CIBSE, 1998. *Energy efficiency in buildings*. London: the Chartered Institution of Building Services Engineers.

Cohen, R. R., 1997. Environmental criteria for naturally ventilated buildings. *In*: Clements-Croome, D., ed. *Naturally ventilated buildings: building for the senses, economy and society*. London: E & FN Spon, 1997, p. 105-122.

Commonwealth of Australia, 2004. *Technical Manual* [online]. Available at: <http://www.greenhouse.gov.au/yourhome/technical/fs15_e.htm> [Accessed 12 June 2005].

Dalgliesh, W. A., and Schriever, W. R., 1965. *Wind pressures and suctions on roofs* [online]. Available at: <http://irc.nrc-cnrc.gc.ca/pubs/cbd/cbd068_e.html> [Accessed 11 October 2005].

Davenport, A. G., 1982. The interaction of wind and structures. *In*: Plate, E., ed. *Engineering meteorology*. Oxford: Elsevier Scientific Publishing, 1982, p. 527-572.

Deru, M., and Burns, P., 2003. *Infiltration and natural ventilation model for whole building energy simulation of residential buildings* [online]. Available at: <http://www.nrel.gov/docs/fy03osti/33698.pdf> [Accessed 19 Jane 2005].

Edwards, B., and Hyett, P., 2001. *Rough guide to sustainability*, London: RIBA Publications.

El-Sawi, A. M., 1999. Mosque as an Islamic institution between constants and variables. *In*: Eben Saleh, M. and Alkokani, A., eds. *Proceedings of the symposium on mosque architecture, Vol. 5: The planning and design criteria of mosque architecture, Riyadh, 30 January - 3 February, 1999.* Riyadh: King Saud University, p. 1-30.

Elnokaly, A. M., 2004. *Airflow behaviour around tensile fabric membrane skins in hot arid regions*. Ph.D. thesis, University of Nottingham.

Elseragy, A. A., 2003. *Architectural and solar potential of curved and flat roofs in hot arid regions*. Ph.D. thesis, University of Nottingham.

Energy Efficiency Best Practice Programme, 1998. *Natural ventilation in non-domestic buildings - a guide for designers, developers and owners*. Good practice guide 237. London: the Chartered Institution of Building Services Engineers.

Escrig, F., 1998. *Towers and domes*. Southampton: Computational Mechanics Publications.

Farija, G. M., 1997. *Wind induced natural ventilation for wind tower houses in maritime-desert climates with special reference to Bahrain*. Ph.D. thesis. University of Reading.

Fathy, H., 1973. *Architecture for the poor*. Chicago: University of Chicago.

Fathy, H., 1986. *Natural energy and vernacular architecture: principles and examples with reference to hot arid climates*. Chicago: United Nations University and the University of Chicago.

Fearnley, C. J., 2002. *The R. Buckminster Fuller FAQ* [online]. Available at: <http://www.cjfearnley.com/fuller-faq-4.html> [Accessed 18 January 2005].

Fluent Inc., 1988. *Gambit 1.3 program help menu*.

Fluent Inc., 1998. *Fluent 5.5 program help menu*.

Fluent Inc., 2004. *Flow modelling for heating, ventilation, air conditioning and refrigeration* [online]. Available at: <http://www.fluent.com/solutions/hvac/index.htm> [Accessed 28 September 2004].

Fluent Inc., 2006. *Airpak* [online]. Available at: <http://airpak.fluent.com> [Accessed 3 March 2005].

Fordham, M., 2000. Natural ventilation. *Renewable Energy*, 19, 17-37.

Franchini, S., *et al.*, 2005. A parametric, experimental analysis of conical vortices on curved roofs of low-rise buildings. *Journal of Wind Engineering and Industrial Aerodynamics,* 93(8), 639-650.

Goulding, J. R., Lewis, J. O., and Steemers, T. C, 1992. *Energy in architecture: the European passive solar handbook*. London: Batsford Limited.

Goverdhan, C.A., (cag@fluent.co.in) 2005. *RE: Fluent for the built environment*. 3 March. Email to: Omar Asfour (laxosa@nottingham.ac.uk).

Graça, G., *et al.*, 2002. Simulation of wind-driven ventilative cooling systems for an apartment building in Beijing and Shanghai. *Energy and Buildings*, 34, 1-11.

Gympel, J., 1996. *The story of architecture from antiquity to the present*. Köln: Könemann.

Hallet, S., 1980. *Traditional architecture in Afghanistan*. New York: Garland STPM Press.

Holod, R., and Khan, H., 1997. *The contemporary mosque: architects, clients and designs since 1950s*. New York: Rizzoli International Publications, Inc.

Ismail, A. B., 1996. *Wind-driven natural ventilation in high-rise office buildings with special reference to the hot-humid climate of Malaysia*. Ph.D. thesis, University of Wales.

Jones, P. J., 1992. Computational Fluid Dynamics for building air flow prediction - current status and capabilities. *Building and Environment*, 27(3), 321-338.

Jones, P. J., 1997. Natural ventilation: prediction, measurement and design. *In*: Clements-Croome, D. ed., 1997. *Naturally ventilated buildings: building for the senses, economy and society*. London: E & FN Spon. p. 139-150

Karakatsani, C., Bahadori, M. N., and Vickery, B. J., 1986. Evaluation of pressure coefficients and estimation of airflow rates in buildings employing wind towers. *Solar Energy,* 37(5), 363-374.

Kindamgen, J., Krauss, G., and Depecker, P., 1997. Effects of roof shapes on wind-induced air motion inside buildings. *Building and Environment*, 32(1), 1-11.

Liddament, M. W., 1986. *Air infiltration calculation techniques - an application guide. Bracknell*, Coventry: The Air Infiltration and Ventilation Centre.

Liddament, M. W., 1996. *A guide to energy efficient ventilation*. Coventry: Air Infiltration and Ventilation Centre.

Lighthill, M., F.R.S., and Silverleaf, A., 1971. *Discussion on architectural aerodynamics*. London: The Royal Society.

Lund Institute of Technology, 2004. *Double skin façades* [online]. Available at: < http://www2.ebd.lth.se/avd%20ebd/main/personal/Harris> [Accessed 15 September 2006].

Maghrabi, A. A., 2000. *Airflow characteristics of modulated louvered windows with reference to the rowshan of Jeddah, Saudi Arabia*. Ph.D. thesis, University of Sheffield.

Marsh, A., 1998a. *Efficient design: human comfort* [online]. Available at: <http://www.squ1.com/comfort/> [Accessed 15 September 2004].

Marsh, A., 1998b. *Climate classification* [online]. Available at: <http://www.squ1.com/site.html> [Accessed 30 May 2005].

Marsh, A., 2006. *PMV Tool* [online]. Available at: <http://www.squ1.com/downloads> [Accessed 14 September 2006].

Meroney, R. N., 1982. Turbulent diffusion near buildings. *In*: Plate, E., ed. *Engineering meteorology*. Oxford: Elsevier Scientific Publishing, 1982, p. 481-525.

McMullan, R., 2002. *Environmental science in building*. 5th ed. Basingstoke: Palgrave.

Monodraught, 2003. *Windcatcher: natural ventilation systems*. Buckinghamshire: Monodraught.

Moore, F., 1993. *Environmental control systems: heating cooling lighting*. New York: McGraw-Hill, Inc.

National Physical Laboratory, 2002. *Good practice guidance note: buoyancy correction and air density measurement* [online]. Available at: <http://www.npl.co.uk/mass/guidance/buoycornote.pdf> [Accessed 11 July 2004].

Oakley, G., 2002. *A combined daylighting passive stack ventilation and solar heating system*. Ph.D. thesis, University of Nottingham.

Oke, T. R., 1988. Street design and urban canopy layer climate. *Energy and Buildings*, 11(1-3), 103-113.

Penwarden, A. D., 1973. Acceptable wind speeds in towns. *Building Science*, 8(3), 259-267.

Penwarden, A. D., and Wise, A. F., 1975. *Wind environment around buildings*. London: H.M.S.O.

Plate, E. J., ed., 1982. *Engineering meteorology*. Oxford : Elsevier Scientific.

Priolo, C. F., 1998. Design guidelines and technical solutions. *In*: Allard, F., ed. *Natural ventilation in buildings: a design handbook*. London: James & James Ltd., 1998, p. 195-252.

Queiroz, T., and Bastos, L., 1998. Integration of natural ventilation systems and factory building's architectural elements, related with thermal comfort and indoor environment air quality. *In*: Maldonado, E. and Yannas, S, ed. *Proceedings of PLEA 98, Lisbon, Portugal, June 1998.* London: James and James Ltd, p. 475-478.

Rahman, S. A., Ahmed, A. Z., and Ahmed, S., 2004. A passive ventilation system for energy efficiency in tropical buildings. *In*: *Proceedings of the 3rd SET Conference on sustainable energy technologies*, *Nottingham, 28-20 June 2004* [CD-ROM]. Nottingham: University of Nottingham.

Riazuddin, S.R., 1994. Recognition of passive cooling techniques. *Renewable Energy,* 5(2), 1143-1146.

Risø National Laboratory, 2006. Wind atlases of the world [online]. Available at: <http://www.windatlas.dk/World/Index.htm> [Accessed 14 September 2006].

Robertson, *et al.*, 2002. Wind pressures on permeably and impermeably-clad structures. *Journal of Wind Engineering and Industrial Aerodynamics,* 90(4/5), 461-474.

Roth, L. M., 1998. *Understanding architecture its elements, history and meaning*. London: Herbert Press.

Runsheng, T., Meir, I. A., and Etzion, Y., 2003. Thermal behaviour of buildings with curved roofs as compared with flat roofs. *Solar Energy*, 74, 273-286.

Sachs, P., 1978. *Wind forces in engineering*. 2nd ed. Oxford: Pergamon.

Sami, V., 2003. *Applying Computational Fluid Dynamics to analyze natural ventilation and human comfort in buildings* [online]. Available at: <http://www.sbse.org/awards/docs/2003/sami1.pdf> [Accessed 17 March 2005].

Santamouris, M., 1998. Prediction methods. *In*: Allard, F., ed. *Natural ventilation in buildings: a design handbook*. London: James & James Ltd. p. 63-158.

Santamouris, M., and Asimakopoulos, D., eds, 1996. *Passive cooling of buildings*. London: James & James Ltd.

Schriever, W. R., 1976. *Ground-level winds around tall buildings* [online]. Available at: <http://irc.nrc-cnrc.gc.ca/cbd/cbd174e.html> [Accessed 1 October 2004].

Scruton, C., 1981. *An introduction to wind effects on structures*. Oxford: Oxford University Press for the Design Council, the British Standards Institution, and the Council of Engineering Institutions.

Shao L., Walker R. R., and Woolliscroft, M., 1993. Natural ventilation via courtyards: the application of CFD. *In*: *Proceedings of the 14th AIVC Conference: Energy impact of ventilation and air infiltration*, *Copenhagen, 21-23 September 1993*. London: BRE, p. 393-403.

Sharma, M., and Ali, S., 1986. Tropical Summer Index - a study of thermal comfort of Indian subjects. *Building and Environment*, 21(1), 11-24.

Sharples, S., and Bensalem, R., 2001. Airflow in courtyard and atrium buildings in the urban environment: a wind tunnel study. *Solar Energy*, 70(3), 237-244.

Smith, P. F., 2001. *Architecture in a climate of change*. Oxford: Architectural Press.

Soliman, B. F., 1976. *A study of the wind pressure forces acting on groups of buildings*. Ph.D. thesis, University of Sheffield.

Stangroom, P., 2004. *CFD modeling of wind flow over terrain*. Ph.D. thesis, The University of Nottingham.

Statham, H. H., 1927. *A short critical history of Architecture.* London: Batsford Ltd.

Steele, J., 1997. An architecture for people the complete works of Hassan Fathy. London: Thomas and Hudson Ltd.

Szokolay, S. V., 2004. *Introduction to architectural science: the basis of sustainable design*. Oxford : Architectural Press.

The World of Wind Atlases, 2004. Available at: <http://www.windatlas.dk/World/Index.htm> [Accessed 21 January 2004].

Thomas, R, ed., 1999. *Environmental design an introduction for architects and engineers*. 2nd ed. London: E & FN Spon.

Troen, I., 1989. *European Wind Atlas*. Roskilde: Riso National Laboratory.

University of Basel, 2001. *Wind tunnel experiments* [online]. Available at: <http://pages.unibas.ch/geo/mcr/Projects/BUBBLE/textpages/md_windtunnel.en.htm> [Accessed 15 September 2006].

Walker R. R., Shao L., and Woolliscroft, M., 1993. Natural ventilation via courtyards: theory and measurement. *In*: *Proceedings of the 14th AIVC Conference: Energy impact of ventilation and air infiltration*, *Copenhagen, 21-23 September, 1993*. London: BRE, p. 235-250.

Weatherbase website, 2005. Available at: <http://www.weatherbase.com> [Accessed 11 December 2004].

Wikipedia, 2006a. *Reynolds Number* [online]. Available at: <http://en.wikipedia.org/wiki/Reynolds_number> [Accessed 18 January 2005].

Wikipedia, 2006b. *Köppen climate classification* [online]. Available at: <http://en.wikipedia.org/wiki/K%C3%B6ppen_climate_classification_scheme> [Accessed 10 December 2004].

Wikipedia, 2006c. *Venturi Effect* [online]. Available at: <http://en.wikipedia.org/wiki/Venturi_effect> [Accessed 15 January 2006].

Yaghobi, M. A., 1991. Air Flow Patterns Around Domed Roof Buildings. *Renewable Energy,* 1(3/4), 345-350.

Yaghobi, M. A., Sabzervari, A., and Golneshan, A. A., 1991. Wind towers: measurement and performance. *Solar Energy,* 47(2), 97-106.

Yaghoubi, M. A., Sabzevari A., and Golneshan A., 1991. Wind towers: measurements and performance. *Solar Energy*, 47(2), 97-106.

Ziegert, S., 1997. *Investigation into the relationship between natural ventilation, room depth and comfort using CFD*. MSc dissertation, University of Leeds.

Zöld, A., ed., [no date]. *Ecobuild: electronic teaching package* [online]. Available at: <http://www.egt.bme.hu/ecobuild/pcool/f0602006.htm> [Accessed 17 September 2004].

APPENDICES

Appendix A: Airflow rates recorded in the Dome Study, (Chapter 6)

Appendix B: Airflow rates recorded in the Vault Study, (Chapter 7)

Appendix C: Airflow rates recorded in the Tower & Dome, and Tower & Vault Studies, (Chapter 8)

Appendix D: Thermal comfort calculations, (Chapter 9)

Appendix A: Airflow rates recorded in the Dome Study, (Chapter 6)

A.1: CAD illustrations for the cases modelled in Chapter 6

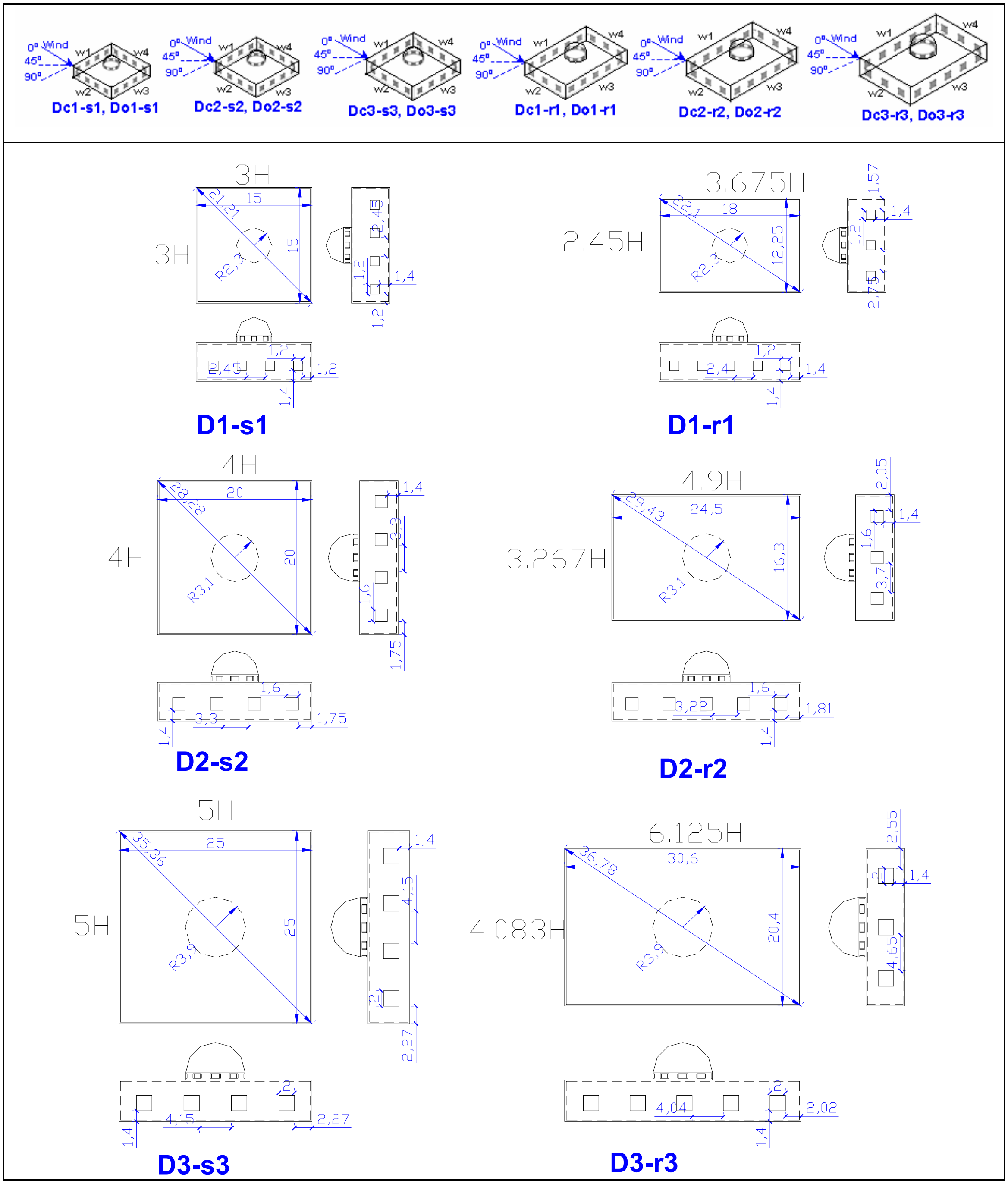

A.2: Mass airflow rates in the case of closed dome openings. Average values presents volumetric airflow rate for building plan-area unit, (sections 6.5 and 6.6 of the study)

Table A.2.1: Airflow rates of building configuration Dc1-s1

Opening no.	Mass flow rate (kg/s)					
	α = 0° 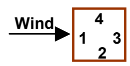		α = 45° 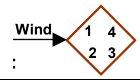		α = 90° 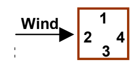	
	Vr =1 m/s	Vr =3 m/s	Vr =1 m/s	Vr =3 m/s	Vr =1 m/s	Vr=3 m/s
w1-o1	1.20	3.60	0.46	1.39	-0.29	-0.85
w1-o2	1.28	3.83	0.63	1.91	-0.49	-1.47
w1-o3	1.25	3.76	0.78	2.34	-0.55	-1.67
w1-o4	1.18	3.53	0.95	2.85	-0.77	-2.32
Total (kg/s)	**4.90**	**14.71**	**2.82**	**8.48**	**-2.10**	**-6.31**
Total (l/s)/m2	**17.80**	**53.39**	**10.24**	**30.75**	**-7.61**	**-22.91**
w2-o1	-0.79	-2.37	0.96	2.87	1.20	3.60
w2-o2	-0.53	-1.58	0.76	2.29	1.28	3.83
w2-o3	-0.44	-1.31	0.61	1.83	1.25	3.76
w2-o4	-0.29	-0.87	0.42	1.26	1.18	3.53
Total (kg/s)	**-2.04**	**-6.13**	**2.75**	**8.25**	**4.90**	**14.71**
Total (l/s)/m2	**-7.40**	**-22.25**	**9.98**	**29.94**	**17.80**	**53.39**
w3-o1	-0.26	-0.78	-0.88	-2.64	-0.79	-2.37
w3-o2	-0.10	-0.29	-0.74	-2.21	-0.53	-1.58
w3-o3	-0.13	-0.38	-0.69	-2.08	-0.44	-1.31
w3-o4	-0.28	-0.82	-0.65	-1.96	-0.29	-0.87
Total (kg/s)	**-0.77**	**-2.27**	**-2.96**	**-8.89**	**-2.04**	**-6.13**
Total (l/s)/m2	**-2.78**	**-8.23**	**-10.74**	**-32.27**	**-7.40**	**-22.25**
w4-o1	-0.29	-0.85	-0.60	-1.81	-0.26	-0.78
w4-o2	-0.49	-1.47	-0.58	-1.74	-0.10	-0.29
w4-o3	-0.55	-1.67	-0.65	-1.94	-0.13	-0.38
w4-o4	-0.77	-2.32	-0.78	-2.35	-0.28	-0.82
Total (kg/s)	**-2.10**	**-6.31**	**-2.61**	**-7.83**	**-0.77**	**-2.27**
Total (l/s)/m2	**-7.61**	**-22.91**	**-9.49**	**-28.42**	**-2.78**	**-8.23**

Table A.2.2: Airflow rates of building configuration Dc2-s2

Opening no.	Mass flow rate (kg/s)					
	α = 0° 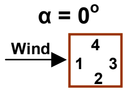		α = 45° 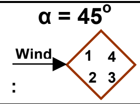		α = 90° 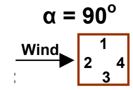	
	Vr =1 m/s	Vr =3 m/s	Vr =1 m/s	Vr =3 m/s	Vr =1 m/s	Vr =3 m/s
w1-o1	2.12	6.35	0.78	2.34	-0.45	-1.34
w1-o2	2.22	6.66	1.12	3.36	-0.52	-1.56
w1-o3	2.23	6.69	1.41	4.21	-0.77	-2.32
w1-o4	2.16	6.47	1.68	5.05	-1.35	-4.06
Total (kg/s)	**8.72**	**26.17**	**4.99**	**14.97**	**-3.09**	**-9.27**
Total (l/s)/m2	**17.80**	**53.42**	**10.18**	**30.54**	**-6.30**	**-18.93**
w2-o1	-1.23	-3.69	1.72	5.17	2.12	6.35

w2-o2	-0.80	-2.41	1.39	4.18	2.22	6.66
w2-o3	-0.57	-1.69	1.15	3.44	2.23	6.69
w2-o4	-0.52	-1.56	0.82	2.46	2.16	6.47
Total (kg/s)	**-3.11**	**-9.35**	**5.08**	**15.25**	**8.72**	**26.17**
Total (l/s)/m2	**-6.35**	**-19.07**	**10.37**	**31.13**	**17.80**	**53.42**
w3-o1	-0.76	-2.27	-1.33	-3.96	-1.23	-3.69
w3-o2	-0.56	-1.66	-1.31	-3.94	-0.80	-2.41
w3-o3	-0.51	-1.52	-1.22	-3.66	-0.57	-1.69
w3-o4	-0.71	-2.10	-1.09	-3.27	-0.52	-1.56
Total (kg/s)	**-2.52**	**-7.55**	**-4.94**	**-14.84**	**-3.11**	**-9.35**
Total (l/s)/m2	**-5.15**	**-15.41**	**-10.09**	**-30.29**	**-6.35**	**-19.07**
w4-o1	-0.45	-1.34	-1.13	-3.40	-0.76	-2.27
w4-o2	-0.52	-1.56	-1.22	-3.67	-0.56	-1.66
w4-o3	-0.77	-2.32	-1.32	-3.96	-0.51	-1.52
w4-o4	-1.35	-4.06	-1.45	-4.34	-0.71	-2.10
Total (kg/s)	**-3.09**	**-9.27**	**-5.13**	**-15.38**	**-2.52**	**-7.55**
Total (l/s)/m2	**-6.30**	**-18.93**	**-10.46**	**-31.38**	**-5.15**	**-15.41**

Table A.2.3: Airflow rates of building configuration Dc3-s3

Opening no.	**Mass flow rate (kg/s)**					
	α = 0° 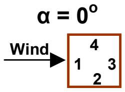		**α = 45°** 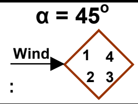		**α = 90°** 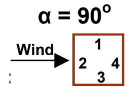	
	Vr =1 m/s	**Vr =3 m/s**	**Vr =1 m/s**	**Vr =3 m/s**	**Vr =1 m/s**	**Vr =3 m/s**
w1-o1	3.42	10.27	1.30	3.91	-0.77	-2.28
w1-o2	3.49	10.47	1.82	5.46	-0.73	-2.20
w1-o3	3.51	10.52	2.28	6.85	-1.11	-3.34
w1-o4	3.40	10.18	2.74	8.24	-1.88	-5.68
Total (kg/s)	**13.82**	**41.45**	**8.15**	**24.45**	**-4.49**	**-13.50**
Total (l/s)/m2	**18.05**	**54.14**	**10.64**	**31.94**	**-5.87**	**-17.64**
w2-o1	-1.96	-5.91	2.76	8.27	3.42	10.27
w2-o2	-1.00	-3.02	2.23	6.70	3.49	10.47
w2-o3	-0.73	-2.19	1.81	5.42	3.51	10.52
w2-o4	-0.76	-2.25	1.27	3.80	3.40	10.18
Total (kg/s)	**-4.45**	**-13.38**	**8.06**	**24.19**	**13.82**	**41.45**
Total (l/s)/m2	**-5.81**	**-17.47**	**10.53**	**31.60**	**18.05**	**54.14**
w3-o1	-1.24	-3.71	-2.20	-6.61	-1.96	-5.91
w3-o2	-1.18	-3.51	-2.13	-6.40	-1.00	-3.02
w3-o3	-1.23	-3.69	-2.06	-6.18	-0.73	-2.19
w3-o4	-1.22	-3.66	-1.80	-5.41	-0.76	-2.25
Total (kg/s)	**-4.87**	**-14.57**	**-8.19**	**-24.60**	**-4.45**	**-13.38**
Total (l/s)/m2	**-6.36**	**-19.03**	**-10.70**	**-32.13**	**-5.81**	**-17.47**
w4-o1	-0.77	-2.28	-1.76	-5.28	-1.24	-3.71
w4-o2	-0.73	-2.20	-2.00	-6.00	-1.18	-3.51
w4-o3	-1.11	-3.34	-2.08	-6.23	-1.23	-3.69
w4-o4	-1.88	-5.68	-2.18	-6.54	-1.22	-3.66
Total (kg/s)	**-4.49**	**-13.50**	**-8.02**	**-24.05**	**-4.87**	**-14.57**
Total (l/s)/m2	**-5.87**	**-17.64**	**-10.47**	**-31.41**	**-6.36**	**-19.03**

Table A.2.4: Airflow rates of building configuration Dc1-r1

Opening no.	Mass flow rate (kg/s)					
	α = 0° 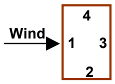		α = 45° 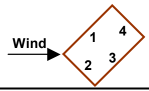		α = 90° 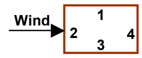	
	Vr=1 m/s	Vr=3 m/s	Vr=1 m/s	Vr=3 m/s	Vr=1 m/s	Vr=3 m/s
w1-o1	1.13	3.39	0.47	1.40	-0.08	-0.24
w1-o2	1.22	3.66	0.62	1.87	-0.23	-0.69
w1-o3	1.23	3.69	0.72	2.15	-0.31	-0.92
w1-o4	1.21	3.64	0.84	2.51	-0.48	-1.45
w1-o5	1.11	3.35	0.99	2.98	-0.66	-1.99
Total (kg/s)	**5.90**	**17.73**	**3.64**	**10.92**	**-1.77**	**-5.30**
Total (l/s)/m2	**21.41**	**64.31**	**13.20**	**39.63**	**-6.41**	**-19.22**
w2-o1	-0.85	-2.57	0.90	2.69	1.19	3.56
w2-o2	-0.59	-1.77	0.69	2.08	1.22	3.66
w2-o3	-0.45	-1.36	0.45	1.35	1.19	3.58
Total (kg/s)	**-1.89**	**-5.70**	**2.04**	**6.12**	**3.60**	**10.80**
Total (l/s)/m2	**-6.85**	**-20.68**	**7.40**	**22.21**	**13.06**	**39.17**
w3-o1	-0.43	-1.29	-0.96	-2.88	-0.65	-1.94
w3-o2	-0.37	-1.10	-0.78	-2.33	-0.47	-1.41
w3-o3	-0.41	-1.22	-0.78	-2.34	-0.36	-1.09
w3-o4	-0.41	-1.23	-0.67	-2.01	-0.14	-0.42
w3-o5	-0.46	-1.37	-0.60	-1.81	-0.03	-0.08
Total (kg/s)	**-2.08**	**-6.21**	**-3.78**	**-11.36**	**-1.64**	**-4.94**
Total (l/s)/m2	**-7.55**	**-22.54**	**-13.73**	**-41.22**	**-5.97**	**-17.93**
w4-o1	-0.51	-1.53	-0.59	-1.76	-0.17	-0.50
w4-o2	-0.55	-1.65	-0.63	-1.90	0.18	0.55
w4-o3	-0.87	-2.64	-0.68	-2.03	-0.20	-0.60
Total (kg/s)	**-1.93**	**-5.81**	**-1.89**	**-5.68**	**-0.19**	**-0.56**
Total (l/s)/m2	**-7.01**	**-21.09**	**-6.87**	**-20.62**	**-0.68**	**-2.02**

Table A.2.5: Airflow rates of building configuration Dc2-r2

Opening no.	Mass flow rate (kg/s)					
	α = 0° 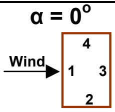		α = 45° 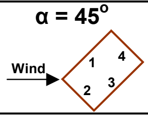		α = 90° 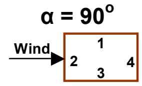	
	Vr =1 m/s	Vr =3 m/s	Vr =1 m/s	Vr =3 m/s	Vr =1 m/s	Vr =3 m/s
w1-o1	2.04	6.11	0.83	2.48	-0.10	-0.29
w1-o2	2.16	6.50	1.11	3.32	-0.18	-0.55
w1-o3	2.17	6.52	1.29	3.86	-0.35	-1.06
w1-o4	2.15	6.45	1.51	4.53	-0.71	-2.13
w1-o5	2.01	6.04	1.75	5.26	-1.09	-3.27
Total (kg/s)	**10.53**	**31.60**	**6.48**	**19.45**	**-2.43**	**-7.30**
Total (l/s)/m2	**21.48**	**64.50**	**13.23**	**39.70**	**-4.96**	**-14.89**
w2-o1	-1.35	-4.05	1.62	4.86	2.15	6.43
w2-o2	-0.95	-2.85	1.30	3.91	2.19	6.57
w2-o3	-0.75	-2.24	0.85	2.55	2.16	6.48
Total (kg/s)	**-3.04**	**-9.15**	**3.77**	**11.33**	**6.49**	**19.48**
Total (l/s)/m2	**-6.21**	**-18.68**	**7.70**	**23.11**	**13.25**	**39.76**
w3-o1	-0.86	-2.56	-1.68	-5.04	-1.16	-3.50
w3-o2	-0.87	-2.63	-1.49	-4.48	-0.69	-2.07

w3-o3	-0.87	-2.62	-1.38	-4.15	-0.38	-1.15
w3-o4	-0.88	-2.64	-1.16	-3.48	-0.30	-0.90
w3-o5	-0.90	-2.70	-1.08	-3.26	-0.24	-0.72
Total (kg/s)	**-4.38**	**-13.14**	**-6.80**	**-20.41**	**-2.78**	**-8.35**
Total (l/s)/m2	**-8.94**	**-26.82**	**-13.87**	**-41.64**	**-5.67**	**-17.04**
w4-o1	-0.77	-2.30	-1.08	-3.26	-0.65	-1.95
w4-o2	-0.94	-2.82	-1.15	-3.44	-0.08	-0.20
w4-o3	-1.39	-4.19	-1.22	-3.68	-0.56	-1.70
Total (kg/s)	**-3.10**	**-9.31**	**-3.46**	**-10.37**	**-1.29**	**-3.84**
Total (l/s)/m2	**-6.33**	**-19.00**	**-7.06**	**-21.17**	**-2.63**	**-7.84**

Table A.2.6: Airflow rates of building configuration Dc3-r3

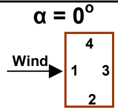

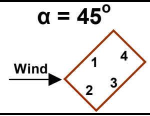

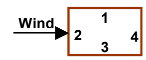

Opening no.	**Mass flow rate (kg/s)**					
	α = 0°		**α = 45°**		**α = 90°**	
	Vr =1 m/s	**Vr =3 m/s**	**Vr =1 m/s**	**Vr =3 m/s**	**Vr =1 m/s**	**Vr =3 m/s**
w1-o1	3.22	9.65	1.28	3.86	-0.29	-0.87
w1-o2	3.41	10.22	1.67	5.01	-0.32	-0.94
w1-o3	3.38	10.14	1.96	5.87	-0.45	-1.37
w1-o4	3.36	10.09	2.35	7.04	-0.87	-2.62
w1-o5	3.25	9.76	2.78	8.35	-1.69	-5.09
Total (kg/s)	**16.61**	**49.86**	**10.04**	**30.13**	**-3.62**	**-10.89**
Total (l/s)/m2	**21.70**	**65.12**	**13.11**	**39.35**	**-4.73**	**-14.22**
w2-o1	-2.10	-6.30	2.60	7.79	3.46	10.38
w2-o2	-1.33	-4.01	2.02	6.07	3.42	10.26
w2-o3	-1.09	-3.26	1.38	4.14	3.42	10.26
Total (kg/s)	**-4.52**	**-13.57**	**6.00**	**18.00**	**10.30**	**30.90**
Total (l/s)/m2	**-5.90**	**-17.73**	**7.83**	**23.51**	**13.46**	**40.36**
w3-o1	-1.42	-4.26	-2.36	-7.08	-1.55	-4.65
w3-o2	-1.58	-4.75	-2.33	-7.01	-0.84	-2.55
w3-o3	-1.53	-4.60	-2.17	-6.52	-0.56	-1.68
w3-o4	-1.63	-4.87	-1.84	-5.54	-0.45	-1.35
w3-o5	-1.47	-4.40	-1.74	-5.25	-0.38	-1.11
Total (kg/s)	**-7.63**	**-22.88**	**-10.45**	**-31.39**	**-3.77**	**-11.34**
Total (l/s)/m2	**-9.97**	**-29.89**	**-13.64**	**-41.00**	**-4.92**	**-14.81**
w4-o1	-1.20	-3.58	-1.84	-5.51	-1.11	-3.33
w4-o2	-1.24	-3.73	-1.77	-5.30	-0.55	-1.59
w4-o3	-2.03	-6.09	-1.97	-5.92	-1.25	-3.76
Total (kg/s)	**-4.47**	**-13.40**	**-5.59**	**-16.73**	**-2.91**	**-8.67**
Total (l/s)/m2	**-5.83**	**-17.50**	**-7.30**	**-21.85**	**-3.81**	**-11.33**

A.3: Mass airflow rates in the case of opened dome openings. Average values presents volumetric airflow rate for building plan-area unit, (sections 6.5 and 6.6 of the study):

Table A.3.1: Airflow rates of building configuration Do1-s1

Opening no.	**Mass flow rate (kg/s)**

	α = 0° 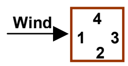		α = 45° 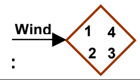		α = 90° 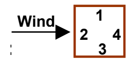	
	Vr =1 m/s	Vr =3 m/s	Vr =1 m/s	Vr =3 m/s	Vr =1 m/s	Vr =3 m/s
w1-o1	1.22	3.66	0.49	1.47	-0.17	-0.49
w1-o2	1.29	3.86	0.66	1.99	-0.35	-1.05
w1-o3	1.30	3.90	0.81	2.43	-0.60	-1.80
w1-o4	1.21	3.62	0.97	2.90	-0.76	-2.30
Total (kg/s)	**5.01**	**15.03**	**2.93**	**8.80**	**-1.88**	**-5.65**
Total (l/s)/m2	**18.18**	**54.54**	**10.64**	**31.92**	**-6.82**	**-20.49**
w2-o1	-0.76	-2.27	0.99	2.97	1.22	3.66
w2-o2	-0.53	-1.61	0.82	2.47	1.29	3.86
w2-o3	-0.32	-0.95	0.67	2.01	1.30	3.90
w2-o4	-0.17	-0.49	0.50	1.49	1.21	3.62
Total (kg/s)	**-1.78**	**-5.33**	**2.98**	**8.95**	**5.01**	**15.03**
Total (l/s)/m2	**-6.44**	**-19.33**	**10.83**	**32.46**	**18.18**	**54.54**
w3-o1	-0.24	-0.72	-0.78	-2.34	-0.76	-2.27
w3-o2	0.08	0.26	-0.62	-1.85	-0.53	-1.61
w3-o3	-0.05	0.17	-0.53	-1.58	-0.32	-0.95
w3-o4	-0.28	-0.86	-0.51	-1.54	-0.17	-0.49
Total (kg/s)	**-0.49**	**-1.15**	**-2.43**	**-7.31**	**-1.78**	**-5.33**
Total (l/s)/m2	**-1.80**	**-4.19**	**-8.83**	**-26.53**	**-6.44**	**-19.33**
w4-o1	-0.17	-0.49	-0.52	-1.56	-0.24	-0.72
w4-o2	-0.35	-1.05	-0.57	-1.70	0.08	0.26
w4-o3	-0.60	-1.80	-0.66	-1.99	-0.05	0.17
w4-o4	-0.76	-2.30	-0.82	-2.44	-0.28	-0.86
Total (kg/s)	**-1.88**	**-5.65**	**-2.57**	**-7.68**	**-0.49**	**-1.15**
Total (l/s)/m2	**-6.82**	**-20.49**	**-9.32**	**-27.88**	**-1.80**	**-4.19**
d-o1	0.01	0.03	-0.03	-0.09	-0.16	-0.47
d-o2	-0.10	-0.30	0.36	1.07	-0.10	-0.29
d-o3	-0.15	-0.46	-0.03	-0.09	0.01	0.03
d-o4	-0.16	-0.49	-0.25	-0.74	-0.10	-0.30
d-o5	-0.15	-0.44	-0.25	-0.76	-0.15	-0.46
d-o6	-0.17	-0.50	-0.21	-0.63	-0.16	-0.49
d-o7	-0.16	-0.47	-0.26	-0.77	-0.15	-0.44
d-o8	-0.10	-0.29	-0.24	-0.73	-0.17	-0.50
Total in. (kg/s)	**0.01**	**0.03**	**0.36**	**1.07**	**0.01**	**0.03**
Total in. (l/s)/m2	**0.05**	**0.13**	**1.29**	**3.87**	**0.05**	**0.13**
Total out. (kg/s)	**-0.98**	**-2.94**	**-1.27**	**-3.82**	**-0.98**	**-2.94**
Total (l/s)/m2	**-3.55**	**-10.66**	**-4.61**	**-13.84**	**-3.55**	**-10.66**

Table A.3.2: Airflow rates of building configuration Do2-s2

Opening no.	Mass flow rate (kg/s)					
	α = 0° 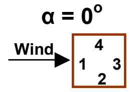		α = 45° 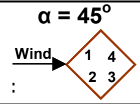		α = 90° 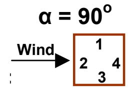	
	Vr =1 m/s	Vr =3 m/s	Vr =1 m/s	Vr =3 m/s	Vr =1 m/s	Vr =3 m/s
w1-o1	2.15	6.45	0.88	2.62	-0.35	-1.04
w1-o2	2.26	6.79	1.22	3.65	-0.39	-1.17
w1-o3	2.26	6.79	1.45	4.35	-0.79	-2.38
w1-o4	2.17	6.51	1.75	5.27	-1.20	-3.60

Total (kg/s)	**8.84**	**26.54**	**5.30**	**15.89**	**-2.72**	**-8.18**
Total (l/s)/m2	**18.05**	**54.15**	**10.81**	**32.43**	**-5.55**	**-16.70**
w2-o1	-1.18	-3.57	1.80	5.39	2.15	6.45
w2-o2	-0.81	-2.45	1.48	4.44	2.26	6.79
w2-o3	-0.45	-1.34	1.23	3.69	2.26	6.79
w2-o4	-0.33	-0.99	0.92	2.76	2.17	6.51
Total (kg/s)	**-2.77**	**-8.34**	**5.43**	**16.28**	**8.84**	**26.54**
Total (l/s)/m2	**-5.66**	**-17.03**	**11.07**	**33.23**	**18.05**	**54.15**
w3-o1	-0.65	-1.96	-1.29	-3.86	-1.18	-3.57
w3-o2	-0.36	-1.05	-1.13	-3.39	-0.81	-2.45
w3-o3	-0.35	-1.04	-1.10	-3.31	-0.45	-1.34
w3-o4	-0.68	-2.04	-0.99	-2.96	-0.33	-0.99
Total (kg/s)	**-2.04**	**-6.09**	**-4.51**	**-13.51**	**-2.77**	**-8.34**
Total (l/s)/m2	**-4.17**	**-12.44**	**-9.20**	**-27.58**	**-5.66**	**-17.03**
w4-o1	-0.35	-1.04	-1.04	-3.13	-0.65	-1.96
w4-o2	-0.39	-1.17	-1.19	-3.57	-0.36	-1.05
w4-o3	-0.79	-2.38	-1.25	-3.75	-0.35	-1.04
w4-o4	-1.20	-3.60	-1.40	-4.20	-0.68	-2.04
Total (kg/s)	**-2.72**	**-8.18**	**-4.88**	**-14.65**	**-2.04**	**-6.09**
Total (l/s)/m2	**-5.55**	**-16.70**	**-9.96**	**-29.91**	**-4.17**	**-12.44**
d-o1	0.08	0.24	-0.07	-0.22	-0.23	-0.67
d-o2	-0.12	-0.35	0.50	1.50	-0.14	-0.41
d-o3	-0.22	-0.65	-0.08	-0.25	0.08	0.24
d-o4	-0.25	-0.75	-0.33	-1.00	-0.12	-0.35
d-o5	-0.20	-0.61	-0.36	-1.07	-0.22	-0.65
d-o6	-0.24	-0.71	-0.31	-0.93	-0.25	-0.75
d-o7	-0.23	-0.67	-0.36	-1.09	-0.20	-0.61
d-o8	-0.14	-0.41	-0.31	-0.94	-0.24	-0.71
Total in. (kg/s)	**0.08**	**0.24**	**0.5**	**1.5**	**0.08**	**0.24**
Total in. (l/s)/m2	**0.16**	**0.49**	**1.02**	**3.06**	**0.16**	**0.49**
Total out. (kg/s)	**-1.39**	**-4.42**	**-1.83**	**-5.50**	**-1.39**	**-4.42**
Total (l/s)/m2	**-2.84**	**-8.49**	**-3.74**	**-11.23**	**-2.84**	**-8.49**

Table A.3.3: Airflow rates of building configuration Do3-s3

Opening no.	**Mass flow rate (kg/s)**					
	α = 0° 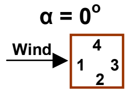		**α = 45°** 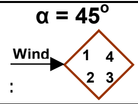		**α = 90°** 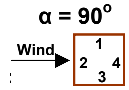	
	Vr = 1 m/s	**Vr = 3 m/s**	**Vr = 1 m/s**	**Vr =3 m/s**	**Vr =1 m/s**	**Vr =3 m/s**
w1-o1	3.47	10.42	1.41	4.22	-0.58	-1.73
w1-o2	3.55	10.66	1.97	5.90	-0.58	-1.75
w1-o3	3.55	10.67	2.37	7.13	-0.97	-2.92
w1-o4	3.42	10.24	2.87	8.60	-1.87	-5.65
Total (kg/s)	**14.00**	**41.99**	**8.61**	**25.85**	**-4.01**	**-12.05**
Total (l/s)/m2	**18.28**	**54.85**	**11.25**	**33.76**	**-5.24**	**-15.74**
w2-o1	-1.92	-5.79	2.86	8.58	3.47	10.42
w2-o2	-0.93	-2.81	2.33	6.98	3.55	10.66
w2-o3	-0.52	-1.55	1.92	5.77	3.55	10.67
w2-o4	-0.49	-1.46	1.35	4.06	3.42	10.24
Total (kg/s)	**-3.86**	**-11.62**	**8.46**	**25.39**	**14.00**	**41.99**
Total (l/s)/m2	**-5.05**	**-15.17**	**11.05**	**33.16**	**18.28**	**54.85**

w3-o1	-1.19	-3.56	-2.22	-6.66	-1.92	-5.79
w3-o2	-1.00	-2.98	-2.07	-6.20	-0.93	-2.81
w3-o3	-1.03	-3.07	-1.88	-5.63	-0.52	-1.55
w3-o4	-1.21	-3.63	-1.68	-5.06	-0.49	-1.46
Total (kg/s)	**-4.43**	**-13.25**	**-7.85**	**-23.56**	**-3.86**	**-11.62**
Total (l/s)/m2	**-5.79**	**-17.30**	**-10.25**	**-30.77**	**-5.05**	**-15.17**
w4-o1	-0.58	-1.73	-1.59	-4.78	-1.19	-3.56
w4-o2	-0.58	-1.75	-1.78	-5.34	-1.00	-2.98
w4-o3	-0.97	-2.92	-1.94	-5.81	-1.03	-3.07
w4-o4	-1.87	-5.65	-2.18	-6.52	-1.21	-3.63
Total (kg/s)	**-4.01**	**-12.05**	**-7.48**	**-22.45**	**-4.43**	**-13.25**
Total (l/s)/m2	**-5.24**	**-15.74**	**-9.77**	**-29.32**	**-5.79**	**-17.30**
d-o1	0.12	0.36	-0.16	-0.48	-0.29	-0.86
d-o2	-0.17	-0.51	0.64	1.93	-0.19	-0.58
d-o3	-0.30	-0.90	-0.16	-0.47	0.12	0.36
d-o4	-0.33	-0.99	-0.44	-1.30	-0.17	-0.51
d-o5	-0.21	-0.61	-0.45	-1.36	-0.30	-0.90
d-o6	-0.33	-0.98	-0.31	-0.93	-0.33	-0.99
d-o7	-0.29	-0.86	-0.44	-1.33	-0.21	-0.61
d-o8	-0.19	-0.58	-0.43	-1.29	-0.33	-0.98
Total in. (kg/s)	**0.12**	**0.36**	**0.64**	**1.93**	**0.12**	**0.36**
Total in. (l/s)/m2	**0.16**	**0.47**	**0.84**	**2.52**	**0.16**	**0.47**
Total out. (kg/s)	**-1.81**	**-5.43**	**-2.39**	**-7.16**	**-1.81**	**-5.43**
Total (l/s)/m2	**-2.37**	**-7.10**	**-3.12**	**-9.36**	**-2.37**	**-7.10**

Table A.3.4: Airflow rates of building configuration Do1-r1

Opening no.	Mass flow rate (kg/s)					
	α = 0° 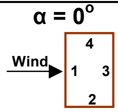		α = 45° 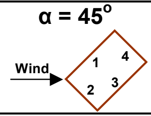		α = 90° 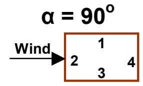	
	Vr = 1 m/s	Vr = 3 m/s	Vr = 1 m/s	Vr = 3 m/s	Vr = 1 m/s	Vr = 3 m/s
w1-o1	1.16	3.48	0.51	1.52	0.01	0.05
w1-o2	1.26	3.77	0.67	2.00	-0.12	-0.37
w1-o3	1.26	3.79	0.77	2.30	-0.27	-0.81
w1-o4	1.24	3.71	0.88	2.63	-0.48	-1.44
w1-o5	1.15	3.45	1.05	3.16	-0.62	-1.86
Total (kg/s)	**6.07**	**18.21**	**3.87**	**11.61**	**-1.48**	**-4.43**
Total (l/s)/m2	**22.01**	**66.06**	**14.03**	**42.12**	**-5.36**	**-16.07**
w2-o1	-0.82	-2.48	0.93	2.77	1.18	3.54
w2-o2	-0.47	-1.41	0.75	2.26	1.25	3.74
w2-o3	-0.40	-1.20	0.48	1.44	1.19	3.56
Total (kg/s)	**-1.70**	**-5.09**	**2.16**	**6.47**	**3.61**	**10.84**
Total (l/s)/m2	**-6.15**	**-18.48**	**7.83**	**23.49**	**13.11**	**39.31**
w3-o1	-0.35	-1.05	-0.90	-2.69	-0.64	-1.94
w3-o2	-0.29	-0.88	-0.72	-2.16	-0.46	-1.37
w3-o3	-0.21	-0.62	-0.73	-2.18	-0.29	-0.89
w3-o4	-0.26	-0.78	-0.60	-1.81	-0.15	-0.44
w3-o5	-0.35	-1.04	-0.52	-1.55	-0.01	-0.03
Total (kg/s)	**-1.46**	**-4.37**	**-3.46**	**-10.39**	**-1.56**	**-4.68**
Total (l/s)/m2	**-5.30**	**-15.84**	**-12.56**	**-37.71**	**-5.64**	**-16.98**
w4-o1	-0.40	-1.22	-0.53	-1.58	-0.10	-0.28

w4-o2	-0.44	-1.33	-0.50	-1.49	0.22	0.67
w4-o3	-0.76	-2.28	-0.65	-1.94	-0.09	-0.25
Total (kg/s)	**-1.60**	**-4.82**	**-1.67**	**-5.01**	**0.04**	**0.14**
Total (l/s)/m2	**-5.81**	**-17.51**	**-6.07**	**-18.18**	**0.15**	**0.50**
d-o1	-0.11	-0.33	-0.07	-0.20	-0.14	-0.42
d-o2	-0.14	-0.43	0.33	1.00	-0.05	-0.14
d-o3	-0.17	-0.49	0.01	0.04	0.13	0.37
d-o4	-0.19	-0.56	-0.23	-0.68	-0.02	-0.08
d-o5	-0.18	-0.54	-0.25	-0.76	-0.13	-0.39
d-o6	-0.19	-0.57	-0.21	-0.63	-0.14	-0.42
d-o7	-0.18	-0.55	-0.26	-0.78	-0.13	-0.38
d-o8	-0.15	-0.45	-0.23	-0.68	-0.14	-0.41
Total in. (kg/s)	**0.00**	**0.00**	**0.34**	**1.04**	**0.13**	**0.37**
Total in. (l/s)/m2	**0.00**	**0.00**	**1.23**	**3.77**	**0.47**	**1.34**
Total out. (kg/s)	**-1.31**	**-3.92**	**-1.24**	**-3.72**	**-0.75**	**-2.24**
Total (l/s)/m2	**-4.74**	**-14.23**	**-4.50**	**-13.51**	**-2.71**	**-8.12**

Table A.3.5: Airflow rates of building configuration Do2-r2

Opening no.	**Mass flow rate (kg/s)**					
	α = 0° 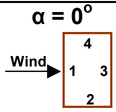		**α = 45°** 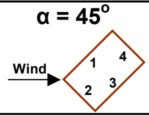		**α = 90°** 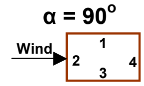	
	Vr =1 m/s	**Vr = 3 m/s**	**Vr = 1 m/s**	**Vr = 3 m/s**	**Vr = 1 m/s**	**Vr = 3 m/s**
w1-o1	2.10	6.30	0.94	2.82	-0.02	-0.04
w1-o2	2.20	6.62	1.19	3.57	-0.08	-0.25
w1-o3	2.23	6.70	1.38	4.14	-0.27	-0.80
w1-o4	2.21	6.62	1.56	4.69	-0.76	-2.32
w1-o5	2.10	6.30	1.83	5.49	-1.08	-3.26
Total (kg/s)	**10.84**	**32.53**	**6.90**	**20.71**	**-2.21**	**-6.66**
Total (l/s)/m2	**22.13**	**66.40**	**14.08**	**42.26**	**-4.51**	**-13.59**
w2-o1	-1.28	-3.87	1.71	5.13	2.16	6.49
w2-o2	-0.80	-2.42	1.32	3.95	2.20	6.59
w2-o3	-0.52	-1.53	0.92	2.75	2.18	6.53
Total (kg/s)	**-2.60**	**-7.82**	**3.94**	**11.84**	**6.54**	**19.61**
Total (l/s)/m2	**-5.31**	**-15.96**	**8.05**	**24.16**	**13.34**	**40.03**
w3-o1	-0.84	-2.52	-1.61	-4.82	-1.07	-3.23
w3-o2	-0.66	-1.99	-1.43	-4.30	-0.77	-2.34
w3-o3	-0.59	-1.78	-1.35	-4.04	-0.33	-1.00
w3-o4	-0.70	-2.08	-1.06	-3.20	-0.17	-0.52
w3-o5	-0.85	-2.56	-0.95	-2.84	-0.09	-0.27
Total (kg/s)	**-3.64**	**-10.92**	**-6.40**	**-19.21**	**-2.45**	**-7.36**
Total (l/s)/m2	**-7.44**	**-22.29**	**-13.06**	**-39.20**	**-5.00**	**-15.01**
w4-o1	-0.56	-1.66	-1.02	-3.05	-0.62	-1.85
w4-o2	-0.98	-2.93	-1.00	-2.99	0.14	0.45
w4-o3	-1.29	-3.89	-1.17	-3.51	-0.46	-1.35
Total (kg/s)	**-2.83**	**-8.48**	**-3.19**	**-9.56**	**-0.93**	**-2.75**
Total (l/s)/m2	**-5.77**	**-17.32**	**-6.51**	**-19.50**	**-1.89**	**-5.62**
d-o1	-0.08	-0.25	-0.12	-0.37	-0.20	-0.60
d-o2	-0.19	-0.57	0.46	1.39	-0.04	-0.12
d-o3	-0.23	-0.69	0.04	0.12	0.12	0.35
d-o4	-0.27	-0.80	-0.33	-0.98	-0.06	-0.19

d-o5	-0.27	-0.81	-0.35	-1.05	-0.20	-0.59
d-o6	-0.29	-0.86	-0.26	-0.79	-0.21	-0.62
d-o7	-0.25	-0.74	-0.36	-1.08	-0.16	-0.49
d-o8	-0.19	-0.57	-0.34	-1.02	-0.20	-0.58
Total in. (kg/s)	**0.00**	**0.00**	**0.50**	**1.51**	**0.12**	**0.35**
Total in. (l/s)/m2	**0.00**	**0.00**	**1.02**	**3.08**	**0.24**	**0.71**
Total out. (kg/s)	**-1.77**	**-5.31**	**-1.76**	**-5.29**	**-1.07**	**-3.20**
Total out. (l/s)/m2	**-3.61**	**-10.83**	**-3.59**	**-10.80**	**-2.18**	**-6.52**

Table A.3.6: Airflow rates of building configuration Do3-r3

Opening no.	Mass flow rate (kg/s)					
	α = 0° 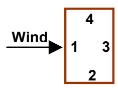		α = 45° 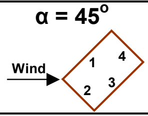		α = 90° 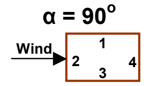	
	Vr=1 m/s	Vr=3 m/s	Vr=1 m/s	Vr=3 m/s	Vr=1 m/s	Vr=3 m/s
w1-o1	3.29	9.87	1.45	4.35	-0.22	-0.63
w1-o2	3.43	10.31	1.79	5.38	-0.25	-0.70
w1-o3	3.46	10.39	2.09	6.25	-0.37	-1.03
w1-o4	3.42	10.25	2.44	7.34	-0.79	-2.41
w1-o5	3.35	10.05	2.88	8.63	-1.63	-5.02
Total (kg/s)	**16.95**	**50.87**	**10.65**	**31.95**	**-3.25**	**-9.80**
Total (l/s)/m2	**22.14**	**66.44**	**13.91**	**41.74**	**-4.25**	**-12.80**
w2-o1	-1.80	-5.42	2.69	8.07	3.43	10.25
w2-o2	-1.14	-3.43	2.13	6.41	3.40	10.25
w2-o3	-0.92	-2.75	1.47	4.40	3.47	10.43
Total (kg/s)	**-3.86**	**-11.60**	**6.29**	**18.88**	**10.29**	**30.93**
Total (l/s)/m2	**-5.04**	**-15.15**	**8.22**	**24.65**	**13.44**	**40.39**
w3-o1	-1.45	-4.35	-2.35	-7.05	-1.52	-4.45
w3-o2	-1.38	-4.13	-2.29	-6.89	-0.72	-2.27
w3-o3	-1.23	-3.69	-2.13	-6.40	-0.36	-1.12
w3-o4	-1.38	-4.14	-1.75	-5.25	-0.24	-0.72
w3-o5	-1.50	-4.49	-1.54	-4.63	-0.24	-0.74
Total (kg/s)	**-6.94**	**-20.80**	**-10.06**	**-30.22**	**-3.07**	**-9.31**
Total (l/s)/m2	**-9.06**	**-27.16**	**-13.14**	**-39.47**	**-4.02**	**-12.16**
w4-o1	-0.85	-2.55	-1.59	-4.78	-1.21	-3.71
w4-o2	-1.01	-3.03	-1.79	-5.34	-0.37	-1.05
w4-o3	-1.94	-5.83	-1.89	-5.67	-1.10	-3.25
Total (kg/s)	**-3.80**	**-11.41**	**-5.27**	**-15.79**	**-2.68**	**-8.01**
Total (l/s)/m2	**-4.97**	**-14.90**	**-6.88**	**-20.63**	**-3.50**	**-10.46**
d-o1	-0.10	-0.31	-0.16	-0.48	-0.26	-0.75
d-o2	-0.23	-0.68	0.59	1.77	-0.10	-0.30
d-o3	-0.35	-1.06	-0.07	-0.21	0.19	0.59
d-o4	-0.38	-1.14	-0.43	-1.28	-0.12	-0.38
d-o5	-0.33	-0.99	-0.48	-1.43	-0.29	-0.90
d-o6	-0.39	-1.17	-0.20	-0.61	-0.26	-0.79
d-o7	-0.35	-1.06	-0.46	-1.37	-0.18	-0.51
d-o8	-0.22	-0.65	-0.40	-1.20	-0.26	-0.77
Total in. (kg/s)	**0.00**	**0.00**	**0.59**	**1.77**	**0.19**	**0.59**
Total in. (l/s)/m2	**0.00**	**0.00**	**0.77**	**2.31**	**0.25**	**0.77**
Total out. (kg/s)	**-2.35**	**-7.07**	**-2.20**	**-6.59**	**-1.48**	**-4.40**
Total out. (l/s)/m2	**-3.07**	**-9.23**	**-2.87**	**-8.60**	**-1.93**	**-5.75**

Appendix B: Airflow rates recorded in the Vault Study, (Chapter 7)

B.1: CAD illustrations for the cases modelled in Chapter 7

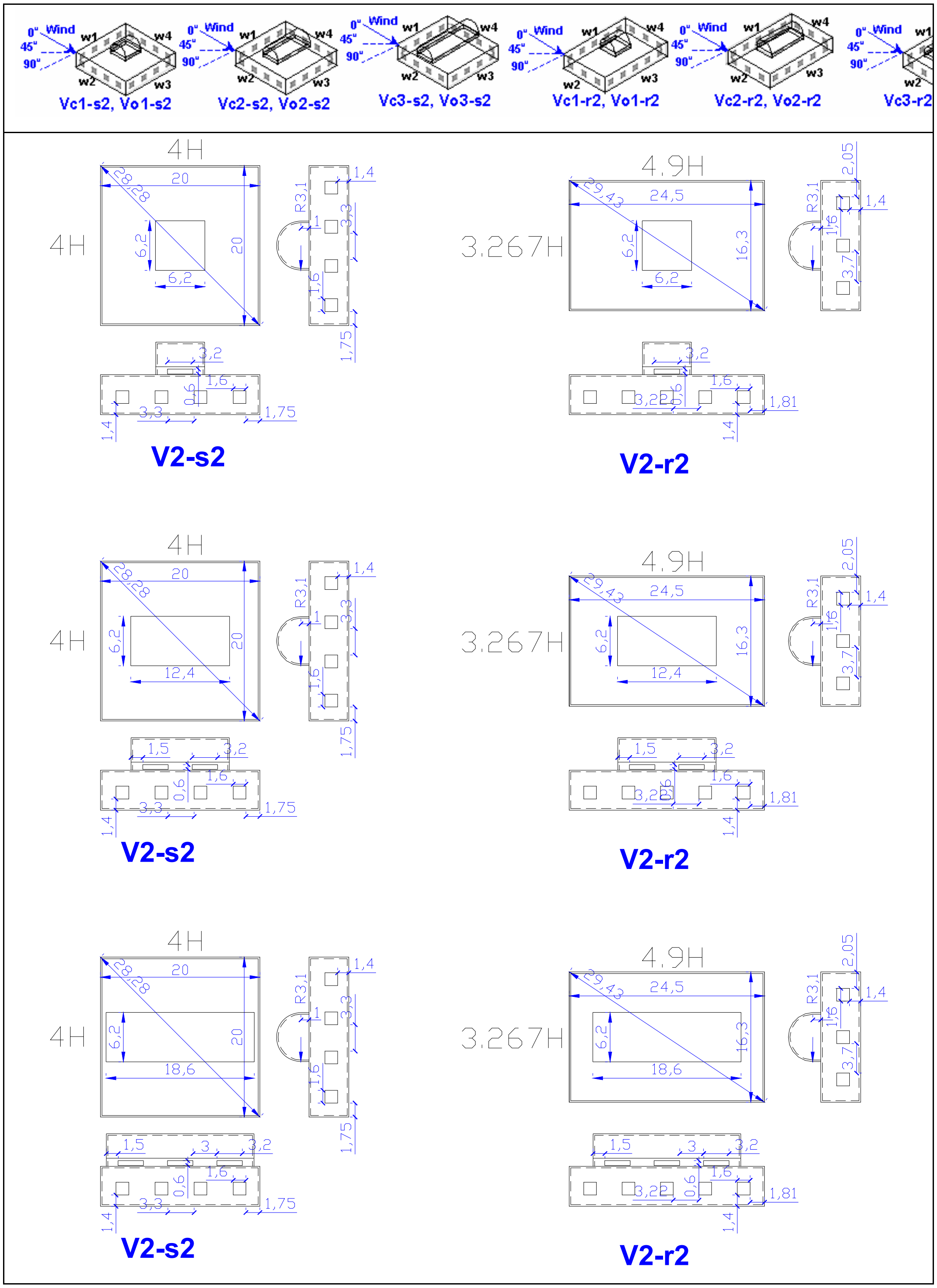

B.2: Mass airflow rates in the case of closed vault openings. Average values presents volumetric airflow rate for building plan-area unit, (sections 7.3 and 7.4 of the study)

Table B.2.1: Airflow rates of building configurations, Vr =3 m/s
Vc1-s2 and Vc1-r2

Opening no.	Mass flow rate (kg/s) α = 0°	α = 45°	α = 90°	Opening no.	α = 0°	α = 45°	α = 90°
	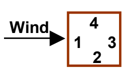	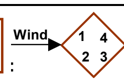	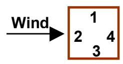		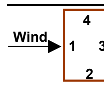	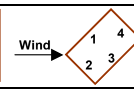	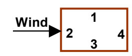
w1-o1	6.41	2.38	-1.34	w1-o1	6.14	2.19	-0.51
w1-o2	6.69	3.44	-1.69	w1-o2	6.51	3.22	-0.87
w1-o3	6.76	4.18	-2.44	w1-o3	6.55	3.80	-1.13
w1-o4	6.43	5.12	-3.62	w1-o4	6.47	4.48	-2.37
Total (kg/s)	**26.29**	**15.11**	**-9.08**	w1-o5	6.11	5.32	-3.22
Total (l/s)/m2	**53.65**	**30.84**	**-18.53**	Total (kg/s)	**31.78**	**19.01**	**-8.11**
w2-o1	-3.61	5.11	6.39	Total (l/s)/m2	**64.86**	**38.80**	**-16.55**
w2-o2	-2.43	4.19	6.71	w2-o1	-4.10	4.89	6.45
w2-o3	-1.93	3.35	6.67	w2-o2	-3.01	3.81	6.53
w2-o4	-1.74	2.24	6.34	w2-o3	-2.11	2.49	6.46
Total (kg/s)	**-9.70**	**14.90**	**26.10**	Total (kg/s)	**-9.21**	**11.19**	**19.44**
Total (l/s)/m2	**-19.80**	**30.41**	**53.27**	Total (l/s)/m2	**-18.80**	**22.84**	**39.67**
w3-o1	-2.16	-3.89	-3.89	w3-o1	-2.68	-4.59	-3.13
w3-o2	-1.75	-3.91	-2.34	w3-o2	-2.62	-4.18	-2.23
w3-o3	-1.66	-3.71	-1.75	w3-o3	-2.63	-4.11	-1.35
w3-o4	-1.97	-3.67	-1.55	w3-o4	-2.57	-3.33	-1.07
Total (kg/s)	**-7.54**	**-15.19**	**-9.53**	w3-o5	-2.81	-3.26	-0.69
Total (l/s)/m2	**-15.39**	**-31.00**	**-19.45**	Total (kg/s)	**-13.31**	**-19.47**	**-8.47**
w4-o1	-1.31	-3.58	-2.08	Total (l/s)/m2	**-27.16**	**-39.73**	**-17.29**
w4-o2	-1.58	-3.52	-1.78	w4-o1	-2.25	-3.34	-1.48
w4-o3	-2.44	-3.79	-1.68	w4-o2	-3.13	-3.70	-0.21
w4-o4	-3.72	-3.94	-1.97	w4-o3	-3.88	-3.70	-1.17
Total (kg/s)	**-9.04**	**-14.83**	**-7.50**	Total (kg/s)	**-9.26**	**-10.73**	**-2.86**
Total (l/s)/m2	**-18.45**	**-30.27**	**-15.31**	Total (l/s)/m2	**-18.90**	**-21.90**	**-5.84**

Table B.2.2: Airflow rates of building configurations, Vr =1 m/s
Vc2-s2 and Vc2-r2

Opening no.	Mass flow rate (kg/s) α = 0°	α = 45°	α = 90°	Opening no.	α = 0°	α = 45°	α = 90°
	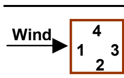	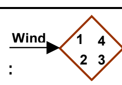	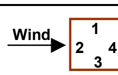		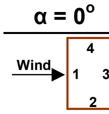	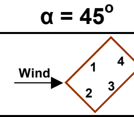	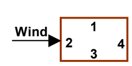
w1-o1	2.18	0.85	-0.45	w1-o1	2.06	0.75	-0.15
w1-o2	2.27	1.20	-0.60	w1-o2	2.19	1.11	-0.33
w1-o3	2.26	1.47	-1.01	w1-o3	2.21	1.30	-0.43
w1-o4	2.17	1.74	-1.17	w1-o4	2.17	1.49	-0.87
Total (kg/s)	**8.88**	**5.27**	**-3.23**	w1-o5	2.03	1.80	-1.06
Total (l/s)/m2	**18.12**	**10.76**	**-6.59**	Total (kg/s)	**10.67**	**6.46**	**-2.85**
w2-o1	-1.20	1.75	2.15	Total (l/s)/m2	**21.78**	**13.18**	**-5.82**

w2-o2	-0.82	1.42	2.29	w2-o1	-1.40	1.64	2.17
w2-o3	-0.66	1.13	2.27	w2-o2	-1.03	1.24	2.21
w2-o4	-0.56	0.78	2.12	w2-o3	-0.76	0.80	2.16
Total (kg/s)	**-3.24**	**5.08**	**8.83**	**Total (kg/s)**	**-3.20**	**3.68**	**6.54**
Total (l/s)/m2	**-6.61**	**10.37**	**18.02**	**Total (l/s)/m2**	**-6.53**	**7.51**	**13.35**
w3-o1	-0.60	-1.41	-1.37	w3-o1	-0.92	-1.46	-1.11
w3-o2	-0.60	-1.40	-0.80	w3-o2	-0.84	-1.38	-0.88
w3-o3	-0.60	-1.30	-0.61	w3-o3	-0.84	-1.31	-0.45
w3-o4	-0.63	-1.32	-0.46	w3-o4	-0.79	-1.22	-0.30
Total (kg/s)	**-2.43**	**-5.43**	**-3.24**	w3-o5	-0.95	-1.18	-0.16
Total (l/s)/m2	**-4.96**	**-11.08**	**-6.61**	**Total (kg/s)**	**-4.33**	**-6.55**	**-2.89**
w4-o1	-0.52	-1.19	-0.68	**Total (l/s)/m2**	**-8.84**	**-13.37**	**-5.90**
w4-o2	-0.58	-1.15	-0.46	w4-o1	-0.77	-1.11	-0.29
w4-o3	-0.88	-1.27	-0.49	w4-o2	-0.98	-1.21	-0.20
w4-o4	-1.23	-1.31	-0.72	w4-o3	-1.39	-1.27	-0.31
Total (kg/s)	**-3.22**	**-4.92**	**-2.35**	**Total (kg/s)**	**-3.14**	**-3.59**	**-0.81**
Total (l/s)/m2	**-6.57**	**-10.04**	**-4.80**	**Total (l/s)/m2**	**-6.41**	**-7.33**	**-1.65**

Table B.2.3: Airflow rates of building configurations, Vr =3 m/s
Vc2-s2 and Vc2-r2

Opening no.	Mass flow rate (kg/s)						
	α = 0°	α = 45°	α = 90°	Opening no.	α = 0°	α = 45°	α = 90°
	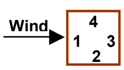	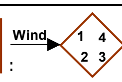	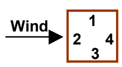		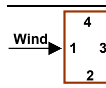	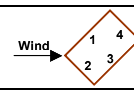	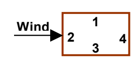
w1-o1	6.53	2.56	-1.34	w1-o1	6.18	2.26	-0.44
w1-o2	6.82	3.61	-1.81	w1-o2	6.55	3.34	-1.02
w1-o3	6.79	4.42	-3.04	w1-o3	6.68	3.90	-1.32
w1-o4	6.52	5.22	-3.50	w1-o4	6.54	4.47	-2.66
Total (kg/s)	**26.66**	**15.81**	**-9.69**	w1-o5	6.11	5.40	-3.18
Total (l/s)/m2	**54.41**	**32.27**	**-19.78**	**Total (kg/s)**	**32.06**	**19.37**	**-8.62**
w2-o1	-3.60	5.26	6.44	**Total (l/s)/m2**	**65.43**	**39.53**	**-17.59**
w2-o2	-2.48	4.26	6.87	w2-o1	-4.16	4.93	6.50
w2-o3	-1.99	3.39	6.81	w2-o2	-3.12	3.73	6.65
w2-o4	-1.66	2.33	6.37	w2-o3	-2.28	2.40	6.49
Total (kg/s)	**-9.73**	**15.24**	**26.48**	**Total (kg/s)**	**-9.56**	**11.05**	**19.64**
Total (l/s)/m2	**-19.86**	**31.10**	**54.04**	**Total (l/s)/m2**	**-19.51**	**22.55**	**40.08**
w3-o1	-1.80	-4.24	-4.12	w3-o1	-2.83	-4.38	-3.32
w3-o2	-1.78	-4.22	-2.41	w3-o2	-2.43	-4.14	-2.65
w3-o3	-1.79	-3.90	-1.83	w3-o3	-2.40	-3.94	-1.34
w3-o4	-1.91	-3.96	-1.41	w3-o4	-2.45	-3.66	-0.90
Total (kg/s)	**-7.28**	**-16.32**	**-9.77**	w3-o5	-2.86	-3.53	-0.46
Total (l/s)/m2	**-14.86**	**-33.31**	**-19.94**	**Total (kg/s)**	**-12.98**	**-19.66**	**-8.68**
w4-o1	-1.56	-3.57	-2.02	**Total (l/s)/m2**	**-26.49**	**-40.12**	**-17.71**
w4-o2	-1.74	-3.46	-1.37	w4-o1	-2.36	-3.33	-0.86
w4-o3	-2.65	-3.79	-1.48	w4-o2	-2.95	-3.62	-0.52
w4-o4	-3.70	-3.91	-2.15	w4-o3	-4.21	-3.81	-0.96
Total (kg/s)	**-9.65**	**-14.73**	**-7.02**	**Total (kg/s)**	**-9.53**	**-10.77**	**-2.34**
Total (l/s)/m2	**-19.69**	**-30.06**	**-14.33**	**Total (l/s)/m2**	**-19.45**	**-21.98**	**-4.78**

Table B.2.4: Airflow rates of building configurations, Vr =3 m/s
Vc3-s2 and Vc3-r2

Opening no.	Mass flow rate (kg/s) α = 0°	α = 45°	α = 90°	Opening no.	α = 0°	α = 45°	α = 90°
	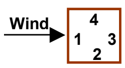	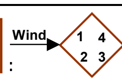	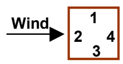		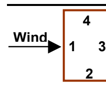	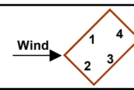	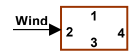
w1-o1	6.56	2.68	-1.31	w1-o1	6.23	2.30	-0.57
w1-o2	6.89	3.75	-1.61	w1-o2	6.79	3.47	-1.11
w1-o3	6.94	4.54	-2.99	w1-o3	6.82	3.97	-1.60
w1-o4	6.49	5.35	-3.94	w1-o4	6.74	4.62	-2.41
Total (kg/s)	**26.87**	**16.32**	**-9.84**	w1-o5	6.25	5.46	-3.61
Total (l/s)/m2	**54.84**	**33.31**	**-20.08**	Total (kg/s)	**32.82**	**19.81**	**-9.30**
w2-o1	-3.78	5.57	6.39	**Total (l/s)/m2**	**66.98**	**40.43**	**-18.98**
w2-o2	-2.41	4.46	6.94	w2-o1	-4.44	5.02	6.34
w2-o3	-2.31	3.18	6.90	w2-o2	-2.90	3.68	6.64
w2-o4	-2.15	2.06	6.33	w2-o3	-2.80	2.38	6.40
Total (kg/s)	**-10.66**	**15.28**	**26.56**	Total (kg/s)	**-10.13**	**11.07**	**19.38**
Total (l/s)/m2	**-21.76**	**31.18**	**54.20**	**Total (l/s)/m2**	**-20.67**	**22.59**	**39.55**
w3-o1	-1.68	-4.23	-4.29	w3-o1	-2.64	-4.36	-3.64
w3-o2	-1.48	-3.99	-2.63	w3-o2	-2.63	-4.17	-2.53
w3-o3	-1.37	-4.10	-1.61	w3-o3	-2.64	-4.12	-1.31
w3-o4	-1.57	-4.15	-1.31	w3-o4	-2.49	-3.87	-0.88
Total (kg/s)	**-6.10**	**-16.48**	**-9.85**	w3-o5	-2.69	-3.61	-0.49
Total (l/s)/m2	**-12.45**	**-33.63**	**-20.10**	Total (kg/s)	**-13.08**	**-20.12**	**-8.85**
w4-o1	-1.98	-3.88	-2.26	**Total (l/s)/m2**	**-26.69**	**-41.06**	**-18.06**
w4-o2	-2.13	-3.74	-1.17	w4-o1	-2.65	-3.49	-1.15
w4-o3	-2.01	-3.64	-1.11	w4-o2	-2.77	-3.59	0.52
w4-o4	-4.00	-3.86	-2.34	w4-o3	-4.20	-3.69	-0.60
Total (kg/s)	**-10.11**	**-15.12**	**-6.87**	Total (kg/s)	**-9.61**	**-10.77**	**-1.22**
Total (l/s)/m2	**-20.63**	**-30.86**	**-14.02**	**Total (l/s)/m2**	**-19.61**	**-21.98**	**-2.49**

B.3: Mass airflow rates in the case of opened vault openings. Average values presents volumetric airflow rate for building plan-area unit, (sections 7.3 and 7.4 of the study)

Table B.3.1: Airflow rates of building configurations, Vr =3 m/s
Vo1-s2 and Vo1-r2

Opening no.	Mass flow rate (kg/s) α = 0°	α = 45°	α = 90°	Opening no.	α = 0°	α = 45°	α = 90°
	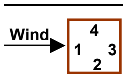	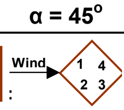	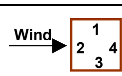		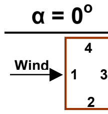	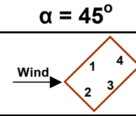	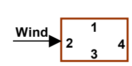
w1-o1	6.41	2.52	-0.74	w1-o1	6.21	2.42	-0.16
w1-o2	6.75	3.54	-1.17	w1-o2	6.56	3.35	-0.44
w1-o3	6.80	4.35	-2.44	w1-o3	6.64	3.95	-0.77
w1-o4	6.47	5.19	-3.65	w1-o4	6.60	4.59	-2.01
Total (kg/s)	**26.43**	**15.60**	**-7.99**	w1-o5	6.19	5.44	-3.25
Total (l/s)/m2	**53.94**	**31.84**	**-16.31**	Total (kg/s)	**32.19**	**19.75**	**-6.63**
w2-o1	-3.70	5.27	6.52	**Total (l/s)/m2**	**65.69**	**40.31**	**-13.53**
w2-o2	-2.33	4.28	6.95	w2-o1	-4.06	5.04	6.49

w2-o3	-1.73	3.57	6.81	w2-o2	-2.51	3.95	6.62
w2-o4	-1.51	2.59	6.56	w2-o3	-2.14	2.55	6.50
Total (kg/s)	**-9.27**	**15.72**	**26.84**	**Total (kg/s)**	**-8.71**	**11.54**	**19.60**
Total (l/s)/m2	**-18.92**	**32.08**	**54.78**	**Total (l/s)/m2**	**-17.78**	**23.55**	**40.00**
w3-o1	-2.03	-4.12	-3.68	w3-o1	-2.72	-4.42	-2.88
w3-o2	-1.70	-3.74	-2.11	w3-o2	-2.28	-4.14	-2.08
w3-o3	-1.54	-3.36	-1.25	w3-o3	-2.14	-3.88	-1.05
w3-o4	-2.12	-3.48	-0.92	w3-o4	-2.26	-3.19	-0.43
Total (kg/s)	**-7.38**	**-14.70**	**-7.96**	w3-o5	-2.72	-3.09	-0.15
Total (l/s)/m2	**-15.06**	**-30.00**	**-16.24**	**Total (kg/s)**	**-12.11**	**-18.72**	**-6.58**
w4-o1	-1.32	-3.36	-2.13	**Total (l/s)/m2**	**-24.71**	**-38.20**	**-13.43**
w4-o2	-1.44	-3.50	-0.61	w4-o1	-2.12	-3.19	-1.05
w4-o3	-2.29	-3.85	-0.74	w4-o2	-2.75	-3.49	0.55
w4-o4	-3.95	-3.92	-1.87	w4-o3	-3.87	-3.52	-0.95
Total (kg/s)	**-9.00**	**-14.62**	**-5.35**	**Total (kg/s)**	**-8.73**	**-10.20**	**-1.45**
Total (l/s)/m2	**-18.37**	**-29.84**	**-10.92**	**Total (l/s)/m2**	**-17.82**	**-20.82**	**-2.96**
v1-o1	0.93	1.96	-2.69	v1-o1	-0.12	1.56	-2.31
v3-o1	-1.71	-3.96	-2.84	v1-o2	-2.53	-3.93	-2.63
Total in.(kg/s)	**0.93**	**1.96**	**0.0**	**Total in.(kg/s)**	**0.00**	**1.56**	**0.00**
Total (l/s)/m2	**1.90**	**4.00**	**0.00**	**Total (l/s)/m2**	**0.00**	**3.18**	**0.00**
Total out.(kg/s)	**-1.71**	**-3.96**	**-5.54**	**Total out.(kg/s)**	**-2.65**	**-3.93**	**-4.94**
Total (l/s)/m2	**-3.49**	**-8.08**	**-11.31**	**Total (l/s)/m2**	**-5.41**	**-8.02**	**-10.08**

Table B.3.2: Airflow rates of building configurations, Vr =1 m/s Vo2-s2 and Vo2-r2

Opening no.	Mass flow rate (kg/s)						
	α = 0°	α = 45°	α = 90°	Opening no.	α = 0°	α = 45°	α = 90°
	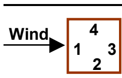	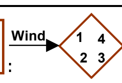	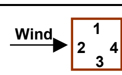		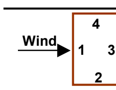	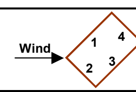	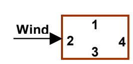
w1-o1	2.17	0.87	-0.17	w1-o1	2.07	0.80	0.05
w1-o2	2.29	1.23	-0.39	w1-o2	2.21	1.16	-0.10
w1-o3	2.29	1.51	-0.74	w1-o3	2.25	1.34	-0.29
w1-o4	2.20	1.77	-1.09	w1-o4	2.06	1.58	-0.73
Total (kg/s)	**8.95**	**5.37**	**-2.40**	w1-o5	2.21	1.88	-1.05
Total (l/s)/m2	**18.27**	**10.96**	**-4.89**	**Total (kg/s)**	**10.81**	**6.77**	**-2.12**
w2-o1	-1.13	1.79	2.21	**Total (l/s)/m2**	**22.06**	**13.82**	**-4.33**
w2-o2	-0.78	1.49	2.35	w2-o1	-1.30	1.70	2.16
w2-o3	-0.58	1.18	2.35	w2-o2	-0.85	1.31	2.23
w2-o4	-0.43	0.85	2.20	w2-o3	-0.66	0.86	2.18
Total (kg/s)	**-2.91**	**5.32**	**9.10**	**Total (kg/s)**	**-2.82**	**3.87**	**6.57**
Total (l/s)/m2	**-5.93**	**10.85**	**18.58**	**Total (l/s)/m2**	**-5.75**	**7.91**	**13.42**
w3-o1	-0.56	-1.31	-1.25	w3-o1	-0.86	-1.46	-1.09
w3-o2	-0.46	-1.28	-0.73	w3-o2	-0.69	-1.32	-0.67
w3-o3	-0.49	-1.22	-0.32	w3-o3	-0.67	-1.24	-0.34
w3-o4	-0.56	-1.26	-0.16	w3-o4	-0.75	-1.14	-0.12
Total (kg/s)	**-2.07**	**-5.08**	**-2.45**	w3-o5	-0.91	-1.08	0.04
Total (l/s)/m2	**-4.22**	**-10.37**	**-5.00**	**Total (kg/s)**	**-3.88**	**-6.24**	**-2.18**
w4-o1	-0.49	-1.15	-0.58	**Total (l/s)/m2**	**-7.93**	**-12.74**	**-4.44**
w4-o2	-0.57	-1.13	0.07	w4-o1	-0.74	-1.02	0.05
w4-o3	-0.77	-1.22	0.12	w4-o2	-0.92	-1.09	0.19
w4-o4	-1.23	-1.26	-0.53	w4-o3	-1.36	-1.16	0.13

Total (kg/s)	**-3.07**	**-4.76**	**-0.92**	**Total (kg/s)**	**-3.03**	**-3.27**	**0.37**
Total (l/s)/m2	**-6.26**	**-9.71**	**-1.88**	**Total (l/s)/m2**	**-6.18**	**-6.68**	**0.76**
v1-o1	0.16	0.27	-0.66	**v1-o1**	0.22	0.24	-0.63
v1-o2	0.31	1.04	-0.98	**v1-o2**	0.20	0.79	-0.71
v3-o1	-0.68	-1.28	-1.07	**v3-o1**	-0.76	-1.26	-0.71
v3-o2	-0.69	-0.88	-0.63	**v3-o2**	-0.74	-0.90	-0.60
Total in.(kg/s)	**0.47**	**1.31**	**0.00**	**Total in.(kg/s)**	**0.42**	**1.03**	**0.00**
Total (l/s)/m2	**0.95**	**2.68**	**0.00**	**Total (l/s)/m2**	**0.85**	**2.09**	**0.00**
Total out.(kg/s)	**-1.37**	**-2.16**	**-3.33**	**Total out.(kg/s)**	**-1.50**	**-2.16**	**-2.65**
Total (l/s)/m2	**-2.79**	**-4.42**	**-6.81**	**Total (l/s)/m2**	**-3.05**	**-4.40**	**-5.40**

Table B.3.3: Airflow rates of building configurations, Vr =3 m/s Vo2-s2 and Vo2-r2

Opening no.	Mass flow rate (kg/s) α = 0°	α = 45°	α = 90°	Opening no.	α = 0°	α = 45°	α = 90°
w1-o1	6.51	2.62	-0.54	**w1-o1**	6.21	2.42	0.16
w1-o2	6.88	3.68	-1.21	**w1-o2**	6.65	3.48	-0.30
w1-o3	6.88	4.52	-2.22	**w1-o3**	6.75	4.02	-0.88
w1-o4	6.59	5.31	-3.27	**w1-o4**	6.20	4.73	-2.22
Total (kg/s)	**26.86**	**16.13**	**-7.24**	**w1-o5**	6.64	5.66	-3.14
Total (l/s)/m2	**54.82**	**32.92**	**-14.78**	**Total (kg/s)**	**32.45**	**20.31**	**-6.38**
w2-o1	-3.39	5.38	6.61	**Total (l/s)/m2**	**66.22**	**41.45**	**-13.02**
w2-o2	-2.33	4.46	7.04	**w2-o1**	-3.91	5.11	6.50
w2-o3	-1.74	3.57	7.02	**w2-o2**	-2.57	3.93	6.72
w2-o4	-1.28	2.56	6.60	**w2-o3**	-1.97	2.59	6.54
Total (kg/s)	**-8.74**	**15.96**	**27.28**	**Total (kg/s)**	**-8.45**	**11.63**	**19.76**
Total (l/s)/m2	**-17.84**	**32.57**	**55.67**	**Total (l/s)/m2**	**-17.24**	**23.73**	**40.33**
w3-o1	-1.68	-3.94	-3.75	**w3-o1**	-2.57	-4.38	-3.27
w3-o2	-1.37	-3.83	-2.16	**w3-o2**	-2.08	-3.97	-2.03
w3-o3	-1.45	-3.68	-0.97	**w3-o3**	-1.96	-3.71	-1.03
w3-o4	-1.67	-3.80	-0.50	**w3-o4**	-2.27	-3.42	-0.35
Total (kg/s)	**-6.16**	**-15.25**	**-7.39**	**w3-o5**	-2.74	-3.23	0.13
Total (l/s)/m2	**-12.57**	**-31.12**	**-15.08**	**Total (kg/s)**	**-11.62**	**-18.71**	**-6.56**
w4-o1	-1.48	-3.47	-1.75	**Total (l/s)/m2**	**-23.71**	**-38.18**	**-13.39**
w4-o2	-1.72	-3.37	0.27	**w4-o1**	-2.22	-3.07	0.14
w4-o3	-2.32	-3.65	0.37	**w4-o2**	-2.78	-3.26	0.58
w4-o4	-3.71	-3.78	-1.52	**w4-o3**	-4.09	-3.47	0.39
Total (kg/s)	**-9.23**	**-14.27**	**-2.64**	**Total (kg/s)**	**-9.08**	**-9.81**	**1.11**
Total (l/s)/m2	**-18.84**	**-29.12**	**-5.39**	**Total (l/s)/m2**	**-18.53**	**-20.02**	**2.27**
v1-o1	0.46	0.80	-1.95	**v1-o1**	0.64	0.70	-1.87
v1-o2	0.91	3.12	-2.95	**v1-o2**	0.55	2.36	-2.13
v3-o1	-2.04	-3.83	-3.17	**v3-o1**	-2.27	-3.78	-2.13
v3-o2	-2.07	-2.66	-1.94	**v3-o2**	-2.22	-2.70	-1.80
Total in.(kg/s)	**1.37**	**3.92**	**0.00**	**Total in.(kg/s)**	**1.19**	**3.06**	**0.00**
Total (l/s)/m2	**2.80**	**8.00**	**0.00**	**Total (l/s)/m2**	**2.43**	**6.24**	**0.00**
Total out.(kg/s)	**-4.11**	**-6.49**	**-10.01**	**Total out.(kg/s)**	**-4.48**	**-6.48**	**-7.93**
Total (l/s)/m2	**-8.39**	**-13.24**	**-20.43**	**Total (l/s)/m2**	**-9.14**	**-13.22**	**-16.18**

Table B.3.4: Airflow rates of building configurations, Vr =3 m/s
Vo3-s2 and Vo3-r2

Opening no.	Mass flow rate (kg/s)						
	α = 0°	α = 45°	α = 90°	Opening no.	α = 0°	α = 45°	α = 90°
w1-o1	6.65	2.84	-0.51	**w1-o1**	6.35	2.62	0.36
w1-o2	6.96	3.88	-1.22	**w1-o2**	6.81	3.61	0.00
w1-o3	7.01	4.68	-2.52	**w1-o3**	6.88	4.23	-0.90
w1-o4	6.59	5.51	-3.64	**w1-o4**	6.80	4.89	-2.18
Total (kg/s)	**27.20**	**16.91**	**-7.89**	**w1-o5**	6.35	5.66	-3.35
Total (l/s)/m2	**55.51**	**34.51**	**-16.10**	**Total (kg/s)**	**33.19**	**21.01**	**-6.06**
w2-o1	-3.74	5.68	6.68	**Total (l/s)/m2**	**67.73**	**42.88**	**-12.37**
w2-o2	-2.08	4.65	7.18	**w2-o1**	-4.04	5.27	6.55
w2-o3	-1.98	3.47	7.19	**w2-o2**	-2.69	3.97	6.78
w2-o4	-1.76	2.27	6.63	**w2-o3**	-2.52	2.63	6.53
Total (kg/s)	**-9.56**	**16.08**	**27.67**	**Total (kg/s)**	**-9.25**	**11.87**	**19.86**
Total (l/s)/m2	**-19.51**	**32.82**	**56.47**	**Total (l/s)/m2**	**-18.88**	**24.22**	**40.53**
w3-o1	-1.48	-3.95	-4.13	**w3-o1**	-2.47	-4.13	-3.67
w3-o2	-1.31	-3.82	-2.18	**w3-o2**	-2.24	-3.66	-2.11
w3-o3	-1.46	-3.86	-1.12	**w3-o3**	-1.74	-4.00	-0.62
w3-o4	-1.70	-3.95	-0.64	**w3-o4**	-2.23	-3.66	-0.07
Total (kg/s)	**-5.96**	**-15.58**	**-8.06**	**w3-o5**	-2.53	-3.46	0.31
Total (l/s)/m2	**-12.16**	**-31.80**	**-16.45**	**Total (kg/s)**	**-11.21**	**-18.90**	**-6.15**
w4-o1	-1.89	-3.53	-1.36	**Total (l/s)/m2**	**-22.88**	**-38.57**	**-12.55**
w4-o2	-2.05	-3.51	0.88	**w4-o1**	-2.40	-3.26	0.28
w4-o3	-2.00	-3.61	0.92	**w4-o2**	-2.76	-3.24	1.31
w4-o4	-3.87	-3.85	-1.33	**w4-o3**	-3.95	-3.78	0.26
Total (kg/s)	**-9.82**	**-14.50**	**-0.90**	**Total (kg/s)**	**-9.11**	**-10.27**	**1.85**
Total (l/s)/m2	**-20.04**	**-29.59**	**-1.84**	**Total (l/s)/m2**	**-18.59**	**-20.96**	**3.78**
v1-o1	1.35	0.60	-0.62	**v1-o1**	0.51	0.66	-0.57
v1-o2	1.57	2.18	-1.53	**v1-o2**	1.07	1.72	-1.57
v1-o1	1.35	3.64	-3.04	**v1-o1**	1.56	3.19	-2.45
v3-o1	-2.11	-4.44	-3.05	**v3-o1**	-2.18	-3.87	-2.27
v3-o2	-1.97	-2.57	-1.83	**v3-o2**	-2.47	-3.09	-1.79
v3-o3	-2.07	-2.31	-0.74	**v3-o3**	-2.11	-2.33	-0.84
Total in.(kg/s)	**4.27**	**6.42**	**0.00**	**Total in.(kg/s)**	**3.14**	**5.57**	**0.00**
Total (l/s)/m2	**8.71**	**13.10**	**0.00**	**Total (l/s)/m2**	**6.41**	**11.37**	**0.00**
Total out.(kg/s)	**-6.14**	**-9.32**	**-10.82**	**Total out.(kg/s)**	**-6.76**	**-9.28**	**-9.49**
Total (l/s)/m2	**-12.53**	**-19.02**	**-22.08**	**Total (l/s)/m2**	**-13.80**	**-18.94**	**-19.37**

Appendix C: Airflow rates recorded in the Tower & Dome, and Tower & Vault Studies, (Chapter 8)

C.1: CAD illustrations for the cases modelled in Chapter 8 (three-dimensional illustrations are depicted in section C.3)

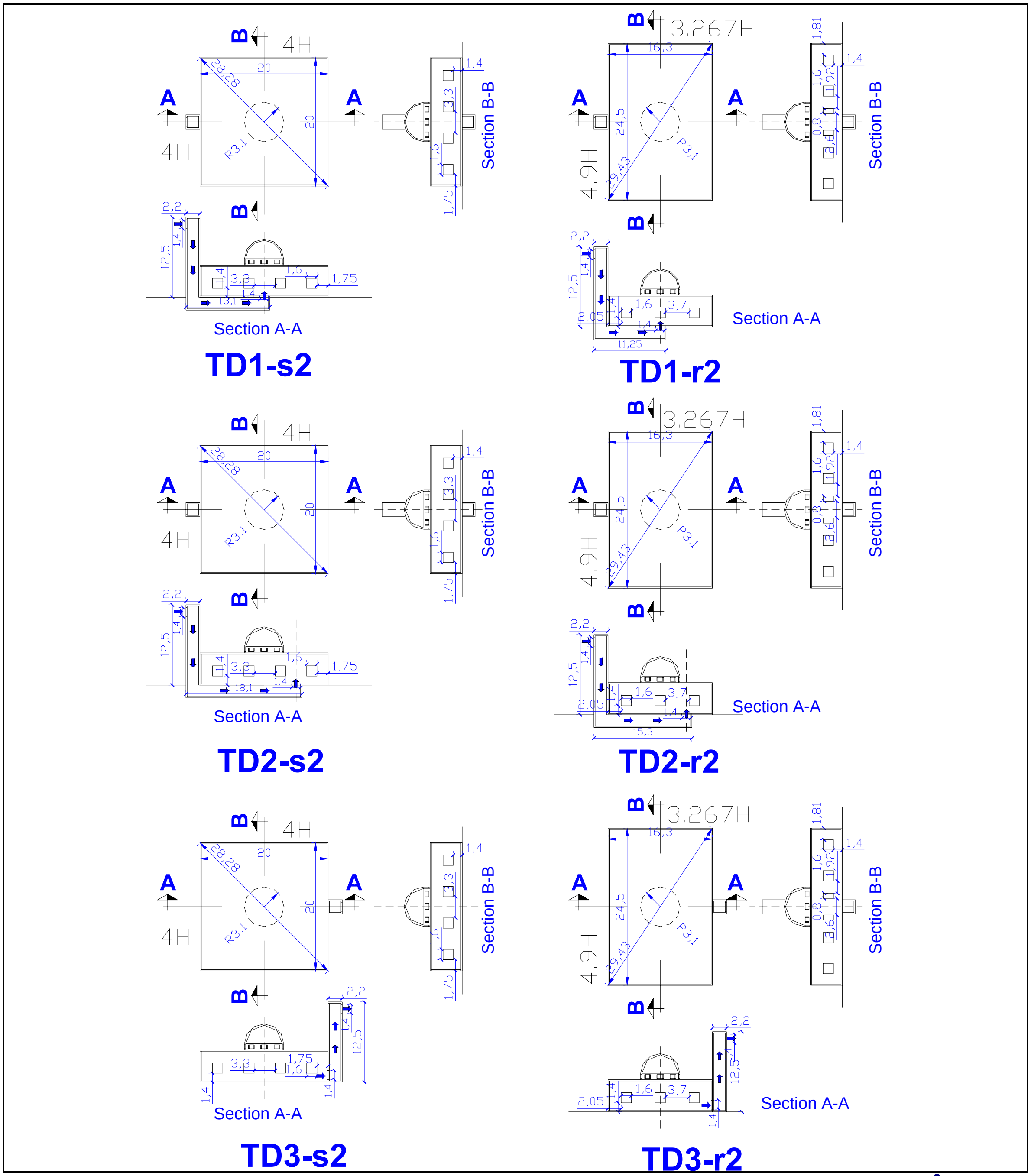

Figure C.1.1: Cases modelled in the Tower and Dome study (cases are shown at 0° wind direction)

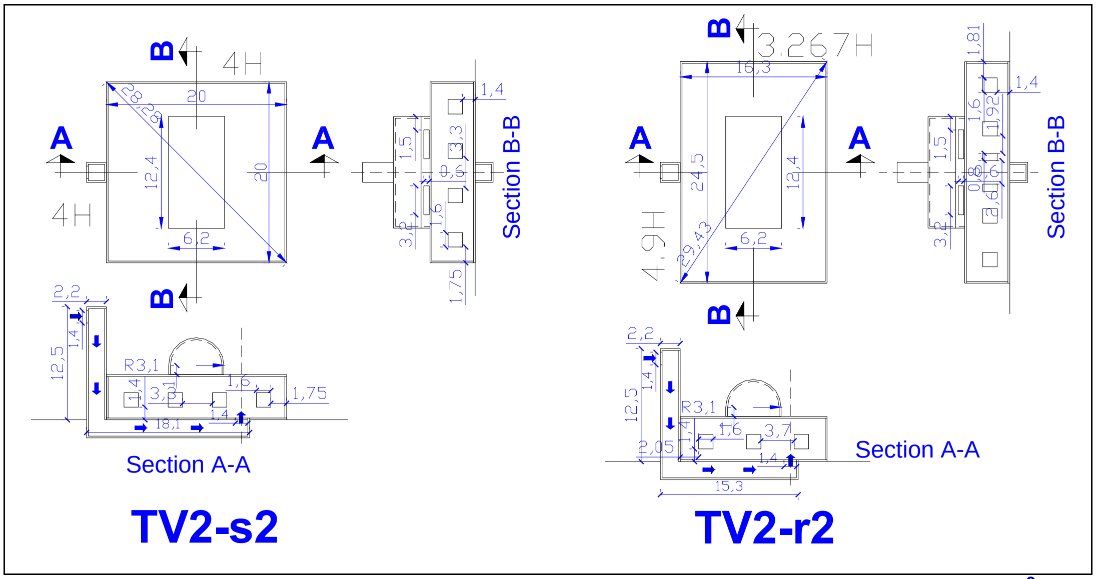

Figure C.1.2: Cases modelled in the Tower and Vault study (cases are shown at 0° wind direction)

C.2: Mass and volumetric airflow rates for Tower and Dome, and Tower and Vault studies, averaged for building plan-area unit, (sections 8.2.2, 8.2.3, 8.3.2, and 8.3.3 of the study)

Table C.2.1: Airflow rates of building configuration Ts1

Opening no.	Mass flow rate (kg/s)					
	α = 0°		α = 45°		α = 90°	
	Vr=1 m/s	Vr=3 m/s	Vr=1 m/s	Vr=3 m/s	Vr=1 m/s	Vr=3 m/s
Wall openings						
w1-o1	2.17	6.51	1.26	3.79	-0.45	-1.27
w1-o2	2.35	7.06	-0.64	-1.93	-0.73	-2.27
w1-o3	2.31	6.97	2.05	6.17	-0.79	-2.40
w1-o4	2.17	6.51	1.98	5.93	-1.35	-4.09
Total (kg/s)	**9.00**	**27.04**	**4.65**	**13.95**	**-3.32**	**-10.04**
Total (l/s)/m2	**18.37**	**55.18**	**9.49**	**28.48**	**-6.78**	**-20.48**
w2-o1	-1.26	-3.77	1.68	5.04	2.17	6.51
w2-o2	-0.98	-2.97	1.42	4.26	2.35	7.06
w2-o3	-0.74	-2.21	1.17	3.50	2.31	6.97
w2-o4	-0.39	-1.12	0.84	2.52	2.17	6.51
Total (kg/s)	**-3.38**	**-10.08**	**5.11**	**15.33**	**9.00**	**27.04**
Total (l/s)/m2	**-6.89**	**-20.57**	**10.42**	**31.28**	**18.37**	**55.18**
w3-o1	-0.65	-1.92	-1.36	-4.07	-1.26	-3.77
w3-o2	-0.36	-1.08	-1.33	-4.00	-0.98	-2.97
w3-o3	-0.41	-1.17	-1.20	-3.60	-0.74	-2.21
w3-o4	-0.58	-1.81	-1.07	-3.22	-0.39	-1.12
Total (kg/s)	**-2.01**	**-5.97**	**-4.97**	**-14.89**	**-3.38**	**-10.08**

Total (l/s)/m2	**-4.10**	**-12.19**	**-10.14**	**-30.39**	**-6.89**	**-20.57**
w4-o1	-0.45	-1.27	-1.16	-3.50	-0.65	-1.92
w4-o2	-0.73	-2.27	-1.07	-3.23	-0.36	-1.08
w4-o3	-0.79	-2.40	-0.86	-2.56	-0.41	-1.17
w4-o4	-1.35	-4.09	-1.27	-3.84	-0.58	-1.81
Total (kg/s)	**-3.32**	**-10.04**	**-4.36**	**-13.13**	**-2.01**	**-5.97**
Total (l/s)/m2	**-6.78**	**-20.48**	**-8.90**	**-26.79**	**-4.10**	**-12.19**
			Dome openings			
d-o1	-0.21	-0.62	-0.10	-0.28	-0.20	-0.61
d-o2	-0.22	-0.65	0.53	1.61	-0.20	-0.60
d-o3	-0.20	-0.59	-0.09	-0.28	-0.21	-0.62
d-o4	-0.21	-0.65	-0.35	-1.05	-0.22	-0.65
d-o5	-0.21	-0.62	-0.36	-1.09	-0.20	-0.59
d-o6	-0.22	-0.68	-0.28	-0.84	-0.21	-0.65
d-o7	-0.20	-0.61	-0.30	-0.89	-0.21	-0.62
d-o8	-0.20	-0.60	-0.31	-0.92	-0.22	-0.68
Total in. (kg/s)	**0.00**	**0.00**	**0.53**	**1.61**	**0.00**	**0.00**
Total in. (l/s)/m2	**0.00**	**0.00**	**1.08**	**3.29**	**0.00**	**0.00**
Total out. (kg/s)	**-1.66**	**-5.03**	**-1.79**	**-5.35**	**-1.66**	**-5.03**
Total out. (l/s)/m2	**-3.38**	**-10.26**	**-3.65**	**-10.92**	**-3.38**	**-10.26**
			Tower openings			
t-ot	1.36	4.08	0.83	2.48	1.36	4.08
t-ob	-1.36	-4.08	-0.83	-2.48	-1.36	-4.08
Total in. (l/s)/m2	**2.77**	**8.32**	**1.68**	**5.06**	**2.77**	**8.32**
Total out. (l/s)/m2	**-2.77**	**-8.32**	**-1.68**	**-5.06**	**-2.77**	**-8.32**

Table C.2.2: Airflow rates of building configuration Ts2

Opening no.	**Mass flow rate (kg/s)**					
	α = 0° 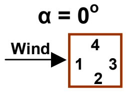		**α = 45°** 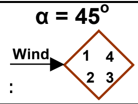		**α = 90°** 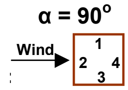	
	Vr=1 m/s	**Vr=3 m/s**	**Vr=1 m/s**	**Vr=3 m/s**	**Vr=1 m/s**	**Vr=3 m/s**
			Wall openings			
w1-o1	2.13	6.38	1.20	3.60	-0.49	-1.47
w1-o2	2.29	6.88	-0.61	-1.81	-0.66	-2.00
w1-o3	2.31	6.93	2.06	6.17	-0.85	-2.55
w1-o4	2.14	6.41	1.96	5.88	-1.38	-4.14
Total (kg/s)	**8.87**	**26.60**	**4.61**	**13.84**	**-3.39**	**-10.16**
Total (l/s)/m2	**18.10**	**54.29**	**9.41**	**28.25**	**-6.91**	**-20.74**
w2-o1	-1.29	-3.89	1.71	5.12	2.13	6.38
w2-o2	-0.89	-2.67	1.41	4.21	2.29	6.88
w2-o3	-0.61	-1.87	1.17	3.52	2.31	6.93
w2-o4	-0.41	-1.20	0.83	2.50	2.14	6.41
Total (kg/s)	**-3.20**	**-9.63**	**5.12**	**15.34**	**8.87**	**26.60**
Total (l/s)/m2	**-6.53**	**-19.65**	**10.44**	**31.31**	**18.10**	**54.29**
w3-o1	-0.52	-1.55	-1.35	-4.07	-1.29	-3.89
w3-o2	-0.45	-1.34	-1.34	-4.03	-0.89	-2.67
w3-o3	-0.59	-1.80	-1.22	-3.67	-0.61	-1.87
w3-o4	-0.49	-1.43	-1.07	-3.21	-0.41	-1.20
Total (kg/s)	**-2.05**	**-6.13**	**-4.99**	**-14.98**	**-3.20**	**-9.63**
Total (l/s)/m2	**-4.18**	**-12.50**	**-10.19**	**-30.57**	**-6.53**	**-19.65**

w4-o1	-0.49	-1.47	-1.09	-3.26	-0.52	-1.55
w4-o2	-0.66	-2.00	-1.14	-3.43	-0.45	-1.34
w4-o3	-0.85	-2.55	-0.85	-2.53	-0.59	-1.80
w4-o4	-1.38	-4.14	-1.14	-3.41	-0.49	-1.43
Total (kg/s)	**-3.39**	**-10.16**	**-4.21**	**-12.64**	**-2.05**	**-6.13**
Total (l/s)/m2	**-6.91**	**-20.74**	**-8.59**	**-25.79**	**-4.18**	**-12.50**
			Dome openings			
d-o1	-0.20	-0.59	-0.13	-0.39	-0.19	-0.56
d-o2	-0.22	-0.66	0.49	1.46	-0.19	-0.57
d-o3	-0.18	-0.54	-0.07	-0.20	-0.20	-0.59
d-o4	-0.19	-0.57	-0.36	-1.08	-0.22	-0.66
d-o5	-0.19	-0.59	-0.37	-1.12	-0.18	-0.54
d-o6	-0.22	-0.66	-0.29	-0.85	-0.19	-0.57
d-o7	-0.19	-0.56	-0.30	-0.90	-0.19	-0.59
d-o8	-0.19	-0.57	-0.30	-0.88	-0.22	-0.66
Total in. (kg/s)	**0.00**	**0.00**	**0.49**	**1.46**	**0.00**	**0.00**
Total in. (l/s)/m2	**0.00**	**0.00**	**1.00**	**2.98**	**0.00**	**0.00**
Total out. (kg/s)	**-1.58**	**-4.75**	**-1.81**	**-5.42**	**-1.58**	**-4.75**
Total out. (l/s)/m2	**-3.23**	**-9.69**	**-3.69**	**-11.06**	**-3.23**	**-9.69**
			Tower openings			
t-ot	1.35	4.06	0.80	2.40	1.35	4.06
t-ob	-1.35	-4.06	-0.80	-2.40	-1.35	-4.06
Total in. (l/s)/m2	**2.75**	**8.29**	**1.63**	**4.89**	**2.75**	**8.29**
Total out. (l/s)/m2	**-2.75**	**-8.29**	**-1.63**	**-4.89**	**-2.75**	**-8.29**

Table C.2.3: Airflow rates of building configuration Ts3

Opening no.	**Mass flow rate (kg/s)**					
	α = 0° 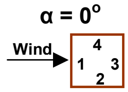		**α = 45°** 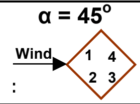		**α = 90°** 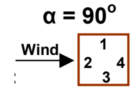	
	Vr=1 m/s	**Vr=3 m/s**	**Vr=1 m/s**	**Vr=3 m/s**	**Vr=1 m/s**	**Vr=3 m/s**
			Wall openings			
w1-o1	2.18	6.55	0.89	2.67	-0.19	-0.56
w1-o2	2.28	6.84	1.25	3.75	-0.27	-0.80
w1-o3	2.29	6.88	1.52	4.56	-0.63	-1.89
w1-o4	2.20	6.60	1.81	5.44	-1.14	-3.45
Total (kg/s)	**8.96**	**26.87**	**5.47**	**16.43**	**-2.23**	**-6.70**
Total (l/s)/m2	**18.28**	**54.83**	**11.17**	**33.53**	**-4.55**	**-13.67**
w2-o1	-1.15	-3.46	1.89	5.67	2.18	6.55
w2-o2	-0.69	-2.06	1.57	4.72	2.28	6.84
w2-o3	-0.38	-1.15	1.34	4.03	2.29	6.88
w2-o4	-0.24	-0.71	0.99	2.97	2.20	6.60
Total (kg/s)	**-2.45**	**-7.38**	**5.79**	**17.38**	**8.96**	**26.87**
Total (l/s)/m2	**-5.00**	**-15.06**	**11.82**	**35.48**	**18.28**	**54.83**
w3-o1	-0.74	-2.22	-1.33	-3.99	-1.15	-3.46
w3-o2	-0.62	-1.85	-1.28	-3.85	-0.69	-2.06
w3-o3	-0.57	-1.69	-1.03	-3.10	-0.38	-1.15
w3-o4	-0.77	-2.32	-1.08	-3.24	-0.24	-0.71
Total (kg/s)	**-2.71**	**-8.07**	**-4.72**	**-14.17**	**-2.45**	**-7.38**
Total (l/s)/m2	**-5.52**	**-16.47**	**-9.64**	**-28.93**	**-5.00**	**-15.06**
w4-o1	-0.19	-0.56	-1.08	-3.23	-0.74	-2.22

w4-o2	-0.27	-0.80	-1.19	-3.58	-0.62	-1.85
w4-o3	-0.63	-1.89	-1.35	-4.05	-0.57	-1.69
w4-o4	-1.14	-3.45	-1.45	-4.33	-0.77	-2.32
Total (kg/s)	**-2.23**	**-6.70**	**-5.06**	**-15.18**	**-2.71**	**-8.07**
Total (l/s)/m2	**-4.55**	**-13.67**	**-10.32**	**-30.99**	**-5.52**	**-16.47**
			Dome openings			
d-o1	0.01	0.04	-0.05	-0.15	-0.16	-0.48
d-o2	-0.11	-0.32	0.50	1.50	-0.09	-0.27
d-o3	-0.18	-0.55	0.00	0.00	0.01	0.04
d-o4	-0.17	-0.51	-0.23	-0.69	-0.11	-0.32
d-o5	-0.11	-0.34	-0.24	-0.73	-0.18	-0.55
d-o6	-0.17	-0.51	-0.19	-0.56	-0.17	-0.51
d-o7	-0.16	-0.48	-0.27	-0.81	-0.11	-0.34
d-o8	-0.09	-0.27	-0.31	-0.95	-0.17	-0.51
Total in. (kg/s)	**0.01**	**0.04**	**0.50**	**1.50**	**0.01**	**0.04**
Total in. (l/s)/m2	**0.02**	**0.08**	**1.02**	**3.06**	**0.02**	**0.08**
Total out. (kg/s)	**-0.99**	**-2.98**	**-1.29**	**-3.89**	**-0.99**	**-2.98**
Total out. (l/s)/m2	**-2.02**	**-6.08**	**-2.63**	**-7.94**	**-2.02**	**-6.08**
			Tower openings			
t-ot	-0.59	-1.78	-0.69	-2.07	-0.59	-1.78
t-ob	0.59	1.78	0.69	2.07	0.59	1.78
Total in. (l/s)/m2	**1.21**	**3.63**	**1.41**	**4.23**	**1.21**	**3.63**
Total out. (l/s)/m2	**-1.21**	**-3.63**	**-1.41**	**-4.23**	**-1.21**	**-3.63**

Table C.2.4: Airflow rates of building configuration Tr1

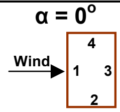

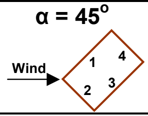

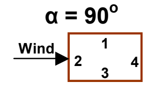

Opening no.	**Mass flow rate (kg/s)**						
	α = 0°		**α = 45°**		**Opening no.**	**α = 90°**	
	Vr=1 m/s	**Vr=3 m/s**	**Vr=1 m/s**	**Vr=3 m/s**		**Vr=1 m/s**	**Vr=3 m/s**
			Wall openings				
w1-o1	2.07	6.21	1.01	3.04	**w1-o1**	-0.08	-0.24
w1-o2	2.25	6.77	1.61	4.84	**w1-o2**	-0.27	-0.83
w1-o3-a	1.06	3.17	-0.45	-1.37	**w1-o3**	-0.57	-1.69
w1-o3-b	1.06	3.17	1.07	3.22	**w1-o4**	-0.84	-2.53
w1-o4	2.26	6.78	1.79	5.37	**w1-o5**	-1.30	-3.94
w1-o5	2.08	6.25	1.89	5.68	**Total (kg/s)**	**-3.06**	**-9.23**
Total (kg/s)	**10.78**	**32.35**	**6.93**	**20.78**	**Total (l/s)/m2**	**-6.24**	**-18.83**
Total (l/s)/m2	**21.99**	**66.02**	**14.13**	**42.40**	**w2-o1**	2.16	6.48
w2-o1	-1.26	-3.77	1.62	4.87	**w2-o2-a**	1.04	3.12
w2-o2	-0.98	-2.95	1.24	3.73	**w2-o2-b**	1.05	3.14
w2-o3	-0.71	-2.08	0.80	2.40	**w2-o3**	2.18	6.55
Total (kg/s)	**-2.95**	**-8.80**	**3.67**	**11.00**	**Total (kg/s)**	**6.43**	**19.29**
Total (l/s)/m2	**-6.03**	**-17.97**	**7.48**	**22.45**	**Total (l/s)/m2**	**13.12**	**39.36**
w3-o1	-0.88	-2.63	-1.73	-5.19	**w3-o1**	-1.21	-3.61
w3-o2	-0.73	-2.15	-1.56	-4.67	**w3-o2**	-0.91	-2.75
w3-o3-a	-0.31	-0.92	-0.72	-2.17	**w3-o3**	-0.59	-1.78
w3-o3-b	-0.31	-0.92	-0.64	-1.91	**w3-o4**	-0.26	-0.75
w3-o4	-0.72	-2.22	-1.11	-3.33	**w3-o5**	-0.02	-0.05
w3-o5	-0.88	-2.64	-0.96	-2.87	**Total (kg/s)**	**-2.99**	**-8.95**
Total (kg/s)	**-3.83**	**-11.47**	**-6.72**	**-20.14**	**Total (l/s)/m2**	**-6.11**	**-18.27**

Total (l/s)/m2	-7.82	-23.41	-13.71	-41.11	w4-o1	-0.36	-1.09
w4-o1	-0.82	-2.50	-1.02	-3.06	w4-o2-a	0.11	0.35
w4-o2	-0.94	-2.84	-0.86	-2.59	w4-o2-b	0.10	0.31
w4-o3	-1.39	-4.20	-1.28	-3.86	w4-o3	-0.24	-0.67
Total (kg/s)	**-3.15**	**-9.54**	**-3.17**	**-9.51**	**Total (kg/s)**	**-0.38**	**-1.10**
Total (l/s)/m2	**-6.42**	**-19.47**	**-6.46**	**-19.41**	**Total (l/s)/m2**	**-0.77**	**-2.25**
				Dome openings			
d-o1	-0.27	-0.80	-0.22	-0.67	d-o1	-0.18	-0.55
d-o2	-0.29	-0.88	0.38	1.15	d-o2	-0.16	-0.49
d-o3	-0.28	-0.84	-0.01	-0.03	d-o3	-0.13	-0.39
d-o4	-0.26	-0.78	-0.35	-1.05	d-o4	-0.14	-0.44
d-o5	-0.25	-0.74	-0.37	-1.10	d-o5	-0.16	-0.49
d-o6	-0.27	-0.81	-0.29	-0.86	d-o6	-0.18	-0.53
d-o7	-0.28	-0.82	-0.32	-0.97	d-o7	-0.18	-0.55
d-o8	-0.29	-0.87	-0.34	-1.01	d-o8	-0.18	-0.55
Total in. (kg/s)	**0.00**	**0.00**	**0.38**	**1.15**	**Total in. (kg/s)**	**0.00**	**0.00**
Total in. (l/s)/m2	**0.00**	**0.00**	**0.78**	**2.35**	**Total in. (l/s)/m2**	**0.00**	**0.00**
Total out. (kg/s)	**-2.18**	**-6.55**	**-1.90**	**-5.69**	**Total out. (kg/s)**	**-1.32**	**-3.98**
Total out. (l/s)/m2	**-4.45**	**-13.36**	**-3.88**	**-11.61**	**Total out. (l/s)/m2**	**-2.70**	**-8.12**
				Tower openings			
t-ot	1.34	4.01	0.81	2.42	t-ot	1.32	3.97
t-ob	-1.34	-4.01	-0.81	-2.42	t-ob	-1.32	-3.97
Total in. (l/s)/m2	**2.73**	**8.19**	**1.64**	**4.93**	**Total in. (l/s)/m2**	**2.70**	**8.11**
Total out. (l/s)/m2	**-2.73**	**-8.19**	**-1.64**	**-4.93**	**Total out. (l/s)/m2**	**-2.70**	**-8.11**

Table C.2.5: Airflow rates of building configuration Tr2

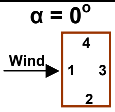

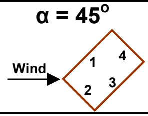

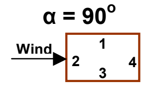

Opening no.	Mass flow rate (kg/s) α = 0°		α = 45°		Opening no.	α = 90°	
	Vr=1 m/s	Vr=3 m/s	Vr=1 m/s	Vr=3 m/s		Vr=1 m/s	Vr=3 m/s
				Wall openings			
w1-o1	2.07	6.20	1.02	3.07	w1-o1	-0.15	-0.43
w1-o2	2.27	6.81	1.60	4.80	w1-o2	-0.27	-0.79
w1-o3-a	1.07	3.21	-0.47	-1.42	w1-o3	-0.53	-1.58
w1-o3-b	1.07	3.20	1.06	3.17	w1-o4	-0.95	-2.86
w1-o4	2.27	6.83	1.83	5.48	w1-o5	-1.19	-3.57
w1-o5	2.08	6.25	1.88	5.64	**Total (kg/s)**	**-3.08**	**-9.23**
Total (kg/s)	**10.82**	**32.50**	**6.91**	**20.74**	**Total (l/s)/m2**	**-6.28**	**-18.84**
Total (l/s)/m2	**22.09**	**66.33**	**14.11**	**42.34**	w2-o1	2.17	6.49
w2-o1	-1.43	-4.34	1.63	4.89	w2-o2-a	1.04	3.13
w2-o2	-0.92	-2.76	1.24	3.70	w2-o2-b	1.04	3.12
w2-o3	-0.71	-2.10	0.78	2.34	w2-o3	2.13	6.38
Total (kg/s)	**-3.06**	**-9.20**	**3.64**	**10.93**	**Total (kg/s)**	**6.37**	**19.12**
Total (l/s)/m2	**-6.24**	**-18.78**	**7.43**	**22.30**	**Total (l/s)/m2**	**13.01**	**39.92**
w3-o1	-0.81	-2.40	-1.65	-4.95	w3-o1	-1.22	-3.66
w3-o2	-0.82	-2.46	-1.54	-4.63	w3-o2	-0.73	-2.20
w3-o3-a	-0.33	-0.98	-0.74	-2.22	w3-o3	-0.54	-1.64
w3-o3-b	-0.32	-0.97	-0.68	-2.03	w3-o4	-0.28	-0.83
w3-o4	-0.78	-2.34	-1.16	-3.49	w3-o5	-0.16	-0.49

w3-o5	-0.84	-2.53	-1.00	-3.01	**Total (kg/s)**	**-2.94**	**-8.82**
Total (kg/s)	**-3.90**	**-11.68**	**-6.77**	**-20.34**	**Total (l/s)/m2**	**-5.99**	**-18.0**
Total (l/s)/m2	**-7.95**	**-23.83**	**-13.82**	**-41.50**	**w4-o1**	-0.19	-0.59
w4-o1	-0.85	-2.54	-1.07	-3.21	**w4-o2-a**	0.01	0.04
w4-o2	-0.86	-2.58	-0.88	-2.65	**w4-o2-b**	0.00	0.00
w4-o3	-1.33	-4.01	-1.17	-3.49	**w4-o3**	-0.25	-0.74
Total (kg/s)	**-3.04**	**-9.14**	**-3.12**	**-9.35**	**Total (kg/s)**	**-0.44**	**-1.28**
Total (l/s)/m2	**-6.20**	**-18.65**	**-6.37**	**-19.07**	**Total (l/s)/m2**	**-0.89**	**-2.61**
				Dome openings			
d-o1	-0.28	-0.85	-0.21	-0.63	**d-o1**	-0.18	-0.54
d-o2	-0.30	-0.90	0.38	1.14	**d-o2**	-0.15	-0.47
d-o3	-0.27	-0.80	-0.01	-0.02	**d-o3**	-0.11	-0.34
d-o4	-0.25	-0.74	-0.34	-1.01	**d-o4**	-0.13	-0.40
d-o5	-0.23	-0.70	-0.38	-1.15	**d-o5**	-0.17	-0.52
d-o6	-0.25	-0.76	-0.28	-0.84	**d-o6**	-0.17	-0.51
d-o7	-0.27	-0.82	-0.32	-0.96	**d-o7**	-0.14	-0.42
d-o8	-0.30	-0.90	-0.33	-1.00	**d-o8**	-0.17	-0.51
Total in. (kg/s)	**0.00**	**0.00**	**0.38**	**1.14**	**Total in. (kg/s)**	**0.00**	**0.00**
Total in. (l/s)/m2	**0.00**	**0.00**	**0.78**	**2.33**	**Total in. (l/s)/m2**	**0.00**	**0.00**
Total out. (kg/s)	**-2.16**	**-6.47**	**-1.87**	**-5.60**	**Total out. (kg/s)**	**-1.22**	**-3.70**
Total out. (l/s)/m2	**-4.40**	**-13.21**	**-3.82**	**-11.43**	**Total out. (l/s)/m2**	**-2.49**	**-7.55**
				Tower openings			
t-ot	1.33	3.99	0.82	2.47	**t-ot**	1.30	3.91
t-ob	-1.33	-3.99	-0.82	-2.47	**t-ob**	-1.30	-3.91
Total in. (l/s)/m2	**2.71**	**8.14**	**1.68**	**5.04**	**Total in. (l/s)/m2**	**2.65**	**7.98**
Total out. (l/s)/m2	**-2.71**	**-8.14**	**-1.68**	**-5.04**	**Total out. (l/s)/m2**	**-2.65**	**-7.98**

Table C.2.6: Airflow rates of building configuration Tr3

Opening no.	**Mass flow rate (kg/s)**						
	α = 0° 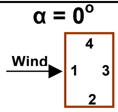		**α = 45°** 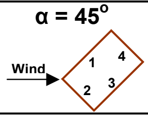		**Opening no.**	**α = 90°** 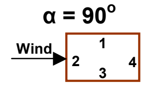	
	Vr=1 m/s	**Vr=3 m/s**	**Vr=1 m/s**	**Vr=3 m/s**		**Vr=1 m/s**	**Vr=3 m/s**
				Wall openings			
w1-o1	2.13	6.39	0.99	2.96	**w1-o1**	0.01	0.04
w1-o2	2.26	6.78	1.27	3.83	**w1-o2**	-0.01	-0.06
w1-o3-a	1.13	3.40	0.63	1.89	**w1-o3**	-0.10	-0.30
w1-o3-b	1.14	3.41	0.76	2.29	**w1-o4**	-0.67	-2.02
w1-o4	2.23	6.68	1.61	4.84	**w1-o5**	-1.10	-3.32
w1-o5	2.13	6.39	1.90	5.70	**Total (kg/s)**	**-1.88**	**-5.66**
Total (kg/s)	**11.01**	**33.04**	**5.19**	**15.57**	**Total (l/s)/m2**	**-3.84**	**-11.55**
Total (l/s)/m2	**22.48**	**67.44**	**10.59**	**31.78**	**w2-o1**	2.16	6.46
w2-o1	-1.24	-3.71	1.77	5.30	**w2-o2-a**	1.10	3.31
w2-o2	-0.79	-2.37	1.41	4.23	**w2-o2-b**	1.10	3.31
w2-o3	-0.50	-1.50	0.95	2.86	**w2-o3**	2.17	6.48
Total (kg/s)	**-2.52**	**-7.59**	**4.13**	**12.39**	**Total (kg/s)**	**6.53**	**19.56**
Total (l/s)/m2	**-5.15**	**-15.48**	**8.42**	**25.28**	**Total (l/s)/m2**	**13.32**	**39.92**
w3-o1	-0.84	-2.56	-1.69	-5.08	**w3-o1**	-1.01	-3.07
w3-o2	-0.68	-2.03	-1.46	-4.39	**w3-o2**	-0.73	-2.18
w3-o3-a	-0.26	-0.77	-0.70	-2.11	**w3-o3**	-0.15	-0.44

w3-o3-b	-0.34	-1.02	-0.62	-1.86	**w3-o4**	0.06	0.18
w3-o4	-0.77	-2.28	-1.21	-3.64	**w3-o5**	0.09	0.27
w3-o5	-0.93	-2.82	-0.97	-2.90	**Total (kg/s)**	**-1.75**	**-5.24**
Total (kg/s)	**-3.83**	**-11.49**	**-6.65**	**-19.98**	**Total (l/s)/m2**	**-3.56**	**-10.70**
Total (l/s)/m2	**-7.82**	**-23.44**	**-13.58**	**-40.77**	**w4-o1**	-0.68	-2.03
w4-o1	-0.63	-1.84	-0.85	-2.54	**w4-o2-a**	-0.21	-0.62
w4-o2	-0.81	-2.44	-1.03	-3.09	**w4-o2-b**	-0.30	-0.88
w4-o3	-1.29	-3.81	-1.26	-3.76	**w4-o3**	-0.74	-2.21
Total (kg/s)	**-2.73**	**-8.09**	**-3.13**	**-9.38**	**Total (kg/s)**	**-1.93**	**-5.73**
Total (l/s)/m2	**-5.57**	**-16.52**	**-6.39**	**-19.15**	**Total (l/s)/m2**	**-3.93**	**-11.69**
				Dome openings			
d-o1	0.04	0.11	-0.12	-0.37	**d-o1**	-0.14	-0.41
d-o2	-0.14	-0.44	0.48	1.45	**d-o2**	-0.04	-0.14
d-o3	-0.21	-0.64	0.08	0.25	**d-o3**	0.17	0.51
d-o4	-0.21	-0.64	-0.27	-0.81	**d-o4**	-0.02	-0.05
d-o5	-0.14	-0.42	-0.19	-0.57	**d-o5**	-0.13	-0.38
d-o6	-0.22	-0.67	-0.06	-0.17	**d-o6**	-0.09	-0.26
d-o7	-0.23	-0.69	-0.28	-0.84	**d-o7**	-0.08	-0.22
d-o8	-0.20	-0.60	-0.30	-0.91	**d-o8**	-0.11	-0.33
Total in. (kg/s)	**0.04**	**0.11**	**0.56**	**1.70**	**Total in. (kg/s)**	**0.17**	**0.51**
Total in. (l/s)/m2	**0.08**	**0.22**	**1.14**	**3.47**	**Total in. (l/s)/m2**	**0.35**	**1.04**
Total out. (kg/s)	**-1.34**	**-4.09**	**-1.22**	**-3.68**	**Total out. (kg/s)**	**-0.60**	**-1.78**
Total out. (l/s)/m2	**-2.73**	**-8.35**	**-2.49**	**-7.51**	**Total out. (l/s)/m2**	**-1.22**	**-3.63**
				Tower openings			
t-ot	-0.64	-1.90	-0.85	-2.55	**t-ot**	-0.55	-1.66
t-ob	0.64	1.90	0.85	2.55	**t-ob**	0.55	1.66
Total in. (l/s)/m2	**1.30**	**3.88**	**1.73**	**5.20**	**Total in. (l/s)/m2**	**1.13**	**3.38**
Total out. (l/s)/m2	**-1.30**	**-3.88**	**-1.73**	**-5.20**	**Total out. (l/s)/m2**	**-1.13**	**-3.38**

Table C.2.7: Airflow rates of building configuration T2Vo2-s2

Opening no.	**Mass flow rate (kg/s)**					
	α = 0° 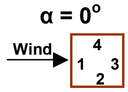		**α = 45°** 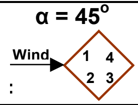		**α = 90°** 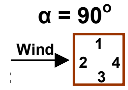	
	Vr=1 m/s	**Vr=3 m/s**	**Vr=1 m/s**	**Vr=3 m/s**	**Vr=1 m/s**	**Vr=3 m/s**
			Wall openings			
w1-o1	2.14	6.41	1.26	3.81	-0.34	-0.99
w1-o2	2.35	7.06	-0.52	-1.61	-0.49	-1.45
w1-o3	2.38	7.13	2.09	6.28	-0.74	-2.25
w1-o4	2.16	6.49	2.03	6.10	-1.39	-4.19
Total (kg/s)	**9.03**	**27.09**	**4.86**	**14.58**	**-2.61**	**-8.89**
Total (l/s)/m2	**18.43**	**55.30**	**9.92**	**29.76**	**-5.34**	**-18.14**
w2-o1	-1.29	-3.89	1.77	5.31	2.16	6.48
w2-o2	-0.76	-2.28	1.49	4.49	2.35	7.06
w2-o3	-0.61	-1.83	1.18	3.53	2.36	7.08
w2-o4	-0.54	-1.60	0.84	2.55	2.15	6.46
Total (kg/s)	**-3.20**	**-9.60**	**5.28**	**15.88**	**9.02**	**27.08**
Total (l/s)/m2	**-6.54**	**-19.59**	**10.78**	**32.40**	**18.41**	**55.27**
w3-o1	-0.46	-1.36	-1.43	-4.29	-1.38	-4.12
w3-o2	-0.43	-1.31	-1.33	-4.00	-0.78	-2.34
w3-o3	-0.64	-1.88	-1.24	-3.72	-0.58	-1.77

w3-o4	-0.56	-1.71	-1.23	-3.67	-0.47	-1.44
Total (kg/s)	**-2.10**	**-6.26**	**-5.23**	**-15.68**	**-3.20**	**-9.67**
Total (l/s)/m2	**-4.28**	**-12.78**	**-10.67**	**-32.01**	**-6.54**	**-19.73**
w4-o1	-0.65	-1.94	-1.12	-3.37	-0.49	-1.48
w4-o2	-0.64	-1.96	-1.01	-2.99	-0.12	-0.39
w4-o3	-0.68	-2.06	-0.83	-2.53	-0.30	-0.81
w4-o4	-1.40	-4.22	-1.28	-3.82	-0.43	-1.32
Total (kg/s)	**-3.37**	**-10.17**	**-4.25**	**-12.72**	**-1.35**	**-4.00**
Total (l/s)/m2	**-6.87**	**-20.76**	**-8.67**	**-25.95**	**-2.75**	**-8.15**
			Vault openings			
v1-o1	0.06	0.16	-0.25	-0.78	-0.61	-1.81
v1-o2	-0.60	-1.80	1.02	3.06	-0.81	-2.42
v3-o1	-0.56	-1.67	-1.47	-4.41	-0.81	-2.45
v3-o2	-0.61	-1.80	-0.78	-2.36	-0.66	-1.95
Total in. (kg/s)	**0.06**	**0.16**	**1.02**	**3.06**	**0.00**	**0.00**
Total in. (l/s)/m2	**0.12**	**0.33**	**2.08**	**6.24**	**0.00**	**0.00**
Total out. (kg/s)	**-1.76**	**-5.27**	**-2.50**	**-7.55**	**-2.88**	**-8.64**
Total out. (l/s)/m2	**-3.59**	**-10.76**	**-5.10**	**-15.41**	**-5.88**	**-17.63**
			Tower openings			
t-ot	1.35	4.04	0.81	2.43	1.37	4.11
t-ob	-1.35	-4.04	-0.81	-2.43	-1.37	-4.11
Total in. (l/s)/m2	**2.76**	**8.24**	**1.65**	**4.96**	**2.80**	**8.39**
Total out. (l/s)/m2	**-2.76**	**-8.24**	**-1.65**	**-4.96**	**-2.80**	**-8.39**

Table C.2.8: Airflow rates of building configuration T2Vo2-r2

Opening no.	Mass flow rate (kg/s)						
	α = 0° 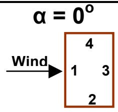		α = 45° 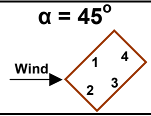		Opening no.	α = 90° 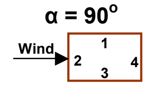	
	Vr=1 m/s	Vr=3 m/s	Vr=1 m/s	Vr=3 m/s		Vr=1 m/s	Vr=3 m/s
			Wall openings				
w1-o1	2.08	6.25	1.05	3.17	w1-o1	-0.06	-0.18
w1-o2	2.29	6.86	1.57	4.73	w1-o2	-0.23	-0.68
w1-o3-a	1.08	3.26	-0.42	-1.26	w1-o3	-0.48	-1.44
w1-o3-b	1.08	3.25	1.10	3.29	w1-o4	-0.86	-2.61
w1-o4	2.31	6.94	1.87	5.61	w1-o5	-1.19	-3.59
w1-o5	2.10	6.29	1.98	5.93	Total (kg/s)	**-2.82**	**-8.50**
Total (kg/s)	**10.93**	**32.85**	**7.15**	**21.47**	**Total (l/s)/m2**	**-5.76**	**-17.35**
Total (l/s)/m2	**22.31**	**67.04**	**14.60**	**43.81**	w2-o1	2.19	6.57
w2-o1	-1.36	-4.09	1.69	5.06	w2-o2-a	1.05	3.16
w2-o2	-0.91	-2.72	1.31	3.92	w2-o2-b	1.06	3.18
w2-o3	-0.73	-2.20	0.84	2.54	w2-o3	2.18	6.53
Total (kg/s)	**-2.99**	**-9.02**	**3.83**	**11.51**	Total (kg/s)	**6.48**	**19.44**
Total (l/s)/m2	**-6.10**	**-18.41**	**7.82**	**23.49**	**Total (l/s)/m2**	**13.22**	**39.67**
w3-o1	-0.91	-2.73	-1.56	-4.69	w3-o1	-1.24	-3.74
w3-o2	-0.76	-2.29	-1.39	-4.16	w3-o2	-0.88	-2.64
w3-o3-a	-0.27	-0.82	-0.64	-1.93	w3-o3	-0.38	-1.12
w3-o3-b	-0.29	-0.87	-0.60	-1.81	w3-o4	-0.15	-0.46
w3-o4	-0.86	-2.37	-1.13	-3.40	w3-o5	-0.04	-0.13
w3-o5	-0.78	-2.61	-1.06	-3.20	Total (kg/s)	**-2.68**	**-8.08**
Total (kg/s)	**-3.88**	**-11.69**	**-6.40**	**-19.20**	**Total (l/s)/m2**	**-5.47**	**-16.49**

Total (l/s)/m2	**-7.92**	**-23.86**	**-13.06**	**-39.18**	**w4-o1**	0.03	0.09
w4-o1	-0.80	-2.38	-1.04	-3.11	**w4-o2-a**	0.12	0.37
w4-o2	-0.86	-2.62	-0.91	-2.74	**w4-o2-b**	0.14	0.44
w4-o3	-1.32	-3.94	-1.22	-3.65	**w4-o3**	-0.09	-0.26
Total (kg/s)	**-2.98**	**-8.94**	**-3.17**	**-9.50**	**Total (kg/s)**	**0.20**	**0.63**
Total (l/s)/m2	**-6.08**	**-18.24**	**-6.47**	**-19.39**	**Total (l/s)/m2**	**0.41**	**1.29**
				Vault openings			
v1-o1	-0.67	-2.06	-0.58	-1.75	**d-o1**	-0.38	-1.15
v1-o2	-0.38	-1.14	0.68	2.02	**d-o2**	-0.78	-2.37
v3-o1	-0.67	-2.02	-1.42	-4.25	**d-o3**	-0.77	-2.30
v3-o2	-0.68	-1.99	-0.92	-2.74	**d-o4**	-0.55	-1.65
Total in. (kg/s)	**0.00**	**0.00**	**0.68**	**2.02**	**Total in. (kg/s)**	**0.00**	**0.00**
Total in. (l/s)/m2	**0.00**	**0.00**	**1.39**	**4.12**	**Total in. (l/s)/m2**	**0.00**	**0.00**
Total out. (kg/s)	**-2.41**	**-7.21**	**-2.91**	**-8.74**	**Total out. (kg/s)**	**-2.49**	**-7.46**
Total out. (l/s)/m2	**-4.92**	**-14.71**	**-5.94**	**-17.84**	**Total out. (l/s)/m2**	**-5.08**	**-15.22**
				Tower openings			
t-ot	1.33	4.02	0.81	2.44	**t-ot**	1.32	3.97
t-ob	-1.33	-4.02	-0.81	-2.44	**t-ob**	-1.32	-3.97
Total in. (l/s)/m2	**2.71**	**8.20**	**1.65**	**4.98**	**Total in. (l/s)/m2**	**2.69**	**8.10**
Total out. (l/s)/m2	**-2.71**	**-8.20**	**-1.65**	**-4.98**	**Total out. (l/s)/m2**	**-2.69**	**-8.10**

C.3: Average volumetric airflow rate through wall openings at reference wind speed of 1 m/s, (sections 8.2.3 and 8.3.3 of the study)

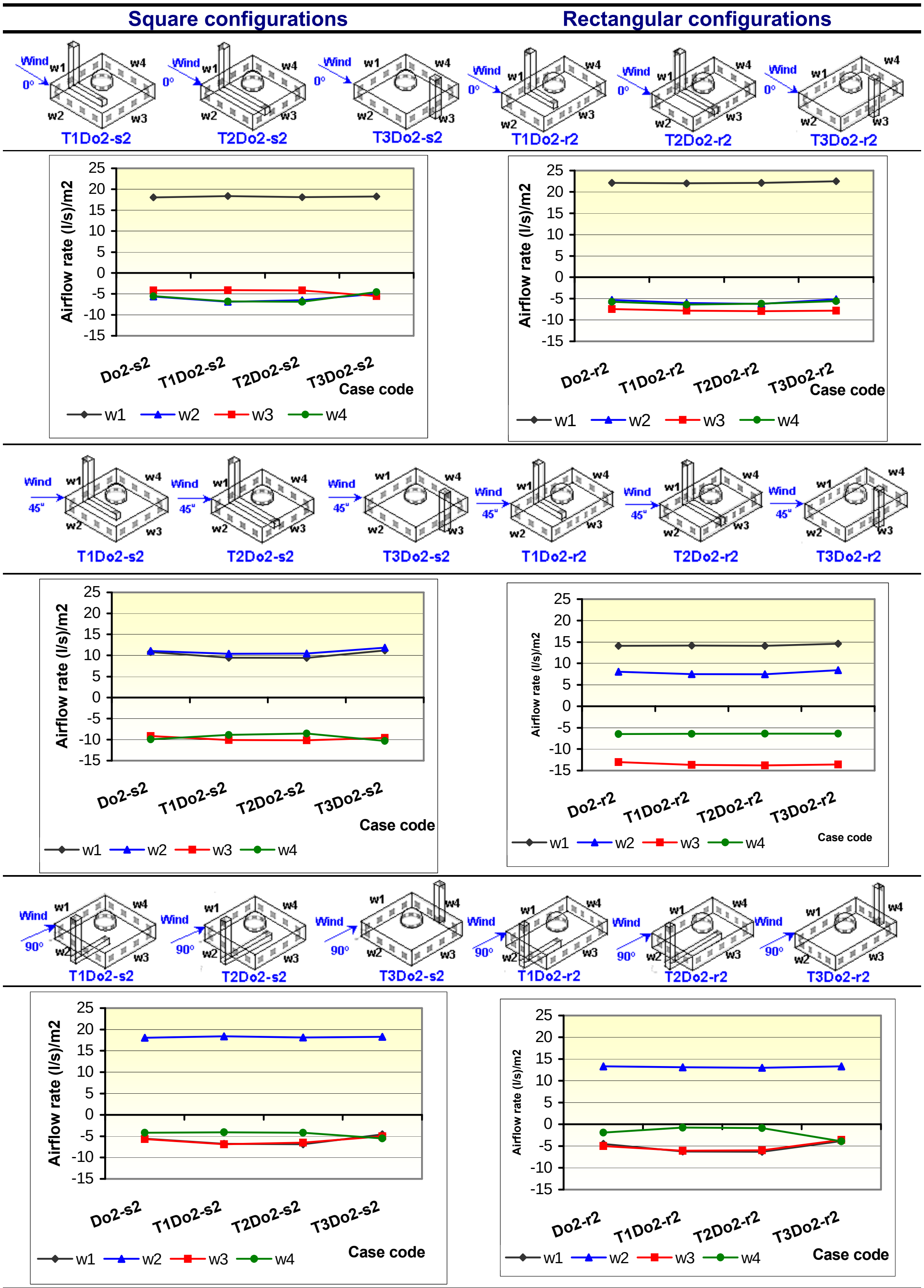

* Positive sign for inflow and negative one for outflow rate.

Figure C.3.1: Average volumetric airflow rate through wall openings recorded in the Tower and Dome Study at reference wind speed of 1 m/s

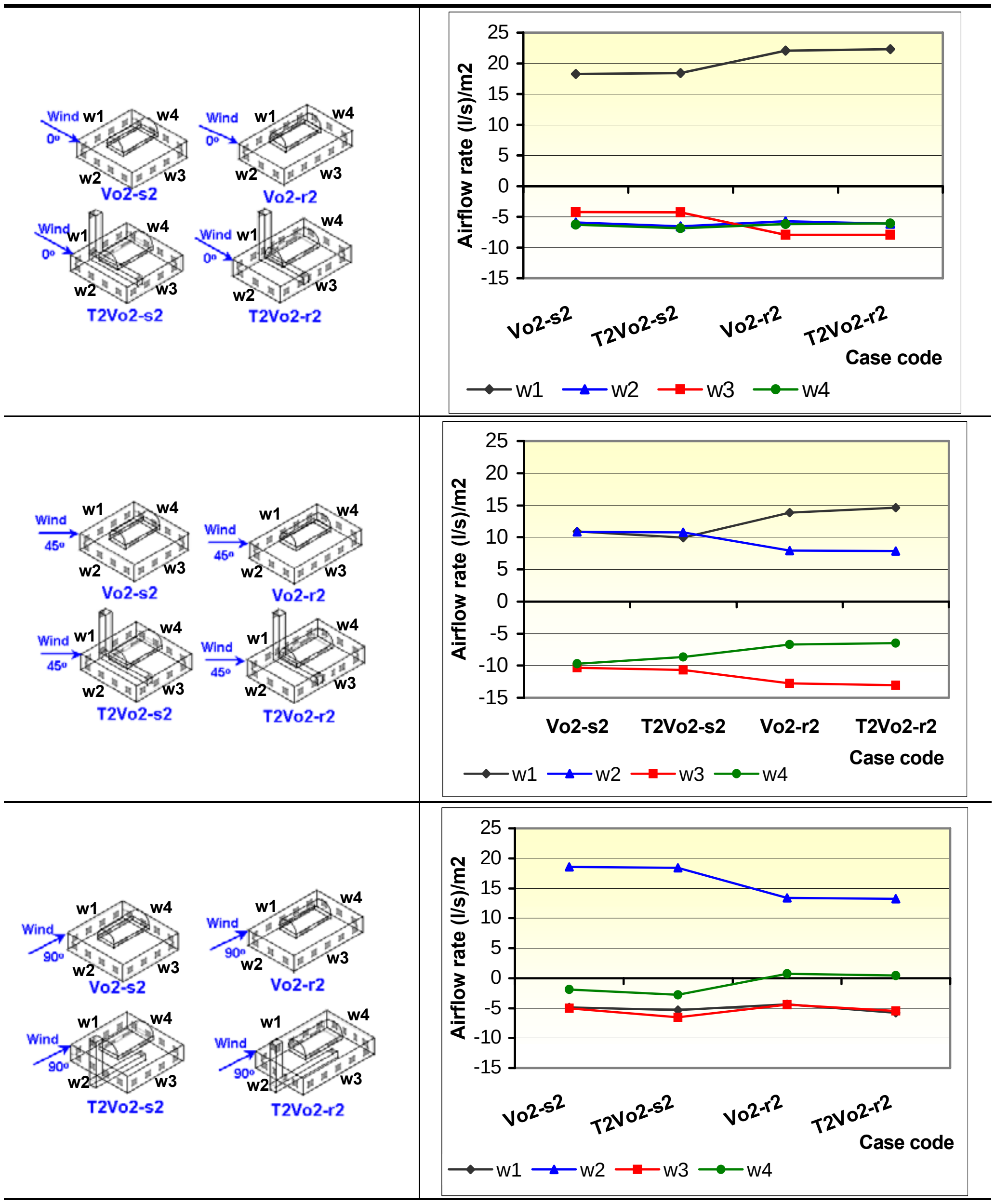

* Positive sign for inflow and negative one for outflow rate.

Figure C.3.2: Average volumetric airflow rate through wall openings recorded in the Tower and Vault Study at reference wind speed of 3 m/s

Appendix D: Thermal comfort calculations, (Chapter 9)

D.1: Area-weighted average air velocity, (Section 9.3 of the study)

Table D.1.1: Area-weighted average air velocity in the case of the selected square cases and 1 m/s reference wind velocity

Illustration	Zone	$Vi_{(av.)}$, (Vr = 1 m/s) TOWER & DOME		TOWER & VAULT	
		Before Dc2	After T2Do2	Before Vc2	After T2Vo2
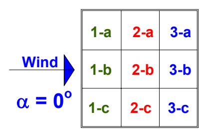	1-a	0.25	0.25	0.24	0.25
	1-b	0.18	0.31	0.17	0.31
	1-c	0.24	0.27	0.24	0.28
	2-a	0.10	0.12	0.08	0.13
	2-b	0.07	0.18	0.07	0.18
	2-c	0.09	0.15	0.09	0.15
	3-a	0.05	0.09	0.04	0.09
	3-b	0.04	0.14	0.03	0.15
	3-c	0.05	0.08	0.03	0.07
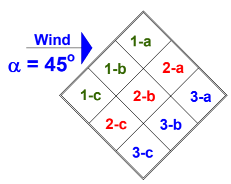	1-a	0.14	0.19	0.14	0.17
	1-b	0.18	0.21	0.19	0.21
	1-c	0.28	0.27	0.29	0.28
	2-a	0.08	0.18	0.11	0.16
	2-b	0.15	0.20	0.17	0.16
	2-c	0.17	0.21	0.19	0.22
	3-a	0.08	0.11	0.09	0.11
	3-b	0.09	0.15	0.06	0.15
	3-c	0.13	0.15	0.16	0.16
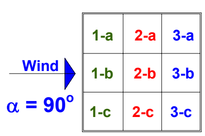	1-a	0.25	0.25	0.23	0.25
	1-b	0.18	0.31	0.26	0.31
	1-c	0.24	0.27	0.25	0.27
	2-a	0.10	0.12	0.13	0.11
	2-b	0.07	0.18	0.12	0.19
	2-c	0.09	0.15	0.13	0.15
	3-a	0.05	0.09	0.07	0.07
	3-b	0.04	0.14	0.07	0.16
	3-c	0.05	0.08	0.08	0.09

Table D.1.2: Area-weighted average air velocity in the case of the selected rectangular cases and 1 m/s reference wind velocity

Illustration	Zone	$Vi_{(av.)}$, (Vr = 1 m/s) TOWER & DOME		TOWER & VAULT	
		Before Dc2	After T2Do2	Before Vc2	After T2Vo2
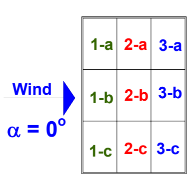	1-a	0.24	0.28	0.25	0.29
	1-b	0.14	0.15	0.15	0.16
	1-c	0.26	0.27	0.26	0.26
	2-a	0.13	0.12	0.10	0.12
	2-b	0.05	0.08	0.07	0.08
	2-c	0.13	0.12	0.12	0.13
	3-a	0.08	0.10	0.08	0.08
	3-b	0.06	0.11	0.05	0.09
	3-c	0.08	0.09	0.06	0.08

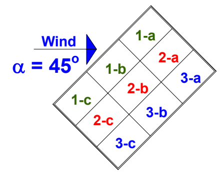	1-a	0.14	0.18	0.15	0.16
	1-b	0.19	0.21	0.20	0.21
	1-c	0.27	0.29	0.28	0.31
	2-a	0.07	0.12	0.07	0.11
	2-b	0.09	0.14	0.13	0.12
	2-c	0.20	0.21	0.21	0.23
	3-a	0.05	0.14	0.05	0.11
	3-b	0.10	0.18	0.12	0.15
	3-c	0.15	0.16	0.15	0.17
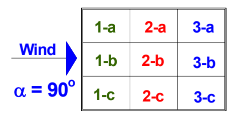	1-a	0.19	0.20	0.21	0.22
	1-b	0.19	0.18	0.16	0.16
	1-c	0.25	0.24	0.21	0.24
	2-a	0.07	0.10	0.05	0.09
	2-b	0.09	0.08	0.09	0.09
	2-c	0.08	0.09	0.05	0.09
	3-a	0.07	0.10	0.04	0.07
	3-b	0.05	0.10	0.04	0.11
	3-c	0.05	0.10	0.03	0.09

Table D.1.3: Area-weighted average air velocity in the case of the selected square cases and 3 m/s reference wind velocity

Illustration	Zone	$Vi_{(av.)}$, (Vr = 3 m/s)			
		TOWER & DOME		TOWER & VAULT	
		Before Dc2	After T2Do2	Before Vc2	After T2Vo2
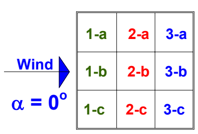	1-a	0.76	0.74	0.73	0.78
	1-b	0.54	0.91	0.52	0.95
	1-c	0.73	0.83	0.72	0.85
	2-a	0.33	0.35	0.24	0.40
	2-b	0.23	0.53	0.22	0.58
	2-c	0.28	0.46	0.26	0.45
	3-a	0.14	0.28	0.12	0.25
	3-b	0.12	0.44	0.10	0.45
	3-c	0.15	0.25	0.10	0.20
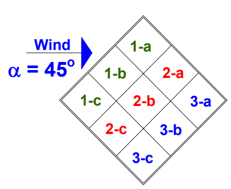	1-a	0.40	0.59	0.43	0.52
	1-b	0.53	0.64	0.58	0.63
	1-c	0.84	0.81	0.87	0.84
	2-a	0.26	0.55	0.33	0.49
	2-b	0.45	0.63	0.50	0.43
	2-c	0.51	0.63	0.55	0.66
	3-a	0.25	0.31	0.28	0.33
	3-b	0.26	0.43	0.18	0.47
	3-c	0.40	0.44	0.48	0.49
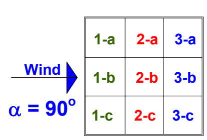	1-a	0.76	0.74	0.68	0.73
	1-b	0.54	0.91	0.77	0.93
	1-c	0.73	0.83	0.75	0.81
	2-a	0.33	0.35	0.38	0.34
	2-b	0.23	0.53	0.36	0.61
	2-c	0.28	0.46	0.38	0.46
	3-a	0.14	0.28	0.22	0.22
	3-b	0.12	0.44	0.21	0.49
	3-c	0.15	0.25	0.22	0.27

Table D.1.4: Area-weighted average air velocity in the case of the selected rectangular cases and 3 m/s reference wind velocity

Illustration	Zone	$Vi_{(av.)}$, (Vr = 3 m/s) TOWER & DOME Before Dc2	TOWER & DOME After T2Do2	TOWER & VAULT Before Vc2	TOWER & VAULT After T2Vo2
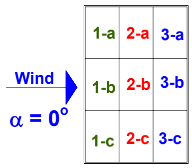	1-a	0.74	0.85	0.79	0.88
	1-b	0.42	0.47	0.47	0.47
	1-c	0.78	0.79	0.73	0.78
	2-a	0.39	0.37	0.28	0.37
	2-b	0.14	0.24	0.28	0.21
	2-c	0.38	0.36	0.29	0.39
	3-a	0.23	0.30	0.19	0.21
	3-b	0.18	0.32	0.16	0.29
	3-c	0.24	0.29	0.19	0.25
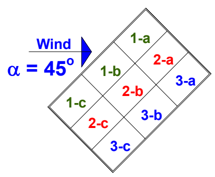	1-a	0.43	0.53	0.46	0.48
	1-b	0.57	0.62	0.61	0.66
	1-c	0.81	0.89	0.83	0.94
	2-a	0.20	0.35	0.21	0.32
	2-b	0.27	0.40	0.41	0.35
	2-c	0.60	0.64	0.62	0.69
	3-a	0.16	0.43	0.16	0.35
	3-b	0.29	0.52	0.36	0.46
	3-c	0.45	0.47	0.45	0.50
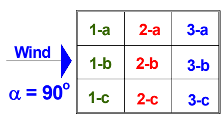	1-a	0.54	0.59	0.63	0.66
	1-b	0.57	0.57	0.48	0.49
	1-c	0.75	0.73	0.62	0.72
	2-a	0.21	0.29	0.16	0.27
	2-b	0.26	0.24	0.27	0.26
	2-c	0.26	0.25	0.15	0.26
	3-a	0.22	0.29	0.11	0.21
	3-b	0.14	0.32	0.12	0.33
	3-c	0.15	0.32	0.11	0.26

D.2: Percentage of people feeling thermally comfortable (PPS), (section 9.4)

Table D.2.1: PPS before and after the utilisation of curved roofs and wind catcher, where: T_{db} = 30 °C, RH = 30%, Vr = 3 m/s

Cases	Zones	TOWER & DOME						TOWER & VAULT					
		Before Dc2		After T2Do2		Diff. (%)		Before Vc2		After T2Vo2		Diff. (%)	
		TSI	PPS	TSI	PPS			TSI	PPS	TSI	PPS		
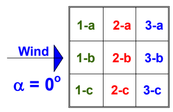	1-a	27.1	65	27.3	65	0	Average = 2.3 %	27.3	65	27.1	65	0	Average = 3.2 %
	1-b	27.5	64	27.0	65	+1		27.5	64	26.9	66	+2	
	1-c	27.3	65	27.1	65	0		27.3	65	27.0	65	0	
	2-a	28.1	62	27.8	63	+1		28.2	60	27.1	65	+5	
	2-b	28.3	60	27.5	64	+4		28.2	60	27.4	65	+5	
	2-c	28.1	62	27.5	64	+2		28.1	62	27.5	64	+2	
	3-a	28.6	57	28.1	62	+5		28.6	57	28.1	62	+5	
	3-b	28.6	57	27.8	63	+6		28.6	57	27.5	64	+7	
	3-c	28.2	60	28.0	62	+2		28.6	57	28.2	60	+3	
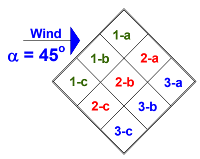	1-a	27.8	63	27.4	65	+2	Average = 1.0 %	27.1	65	27.5	64	-1	Average = 0.7 %
	1-b	27.5	64	27.4	65	+1		27.4	65	27.4	65	0	
	1-c	27.1	65	27.1	65	0		27.0	65	27.1	65	0	
	2-a	28.1	62	27.4	65	+3		28.1	62	27.5	64	+2	
	2-b	27.8	63	27.4	65	+2		27.5	64	27.1	65	+1	
	2-c	27.5	64	27.4	65	+1		27.4	65	27.3	65	0	
	3-a	28.1	62	28.1	62	0		28.1	62	28.1	62	0	
	3-b	28.1	62	27.8	63	+1		28.2	60	27.5	64	+4	
	3-c	27.8	63	27.8	63	0		27.5	64	27.5	64	0	
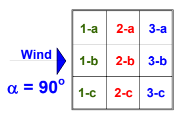	1-a	27.1	65	27.3	65	0	Average = 2.3 %	27.3	65	27.3	65	0	Average = 0.2 %
	1-b	27.5	64	27.0	65	+1		27.1	65	27.0	65	0	
	1-c	27.3	65	27.1	65	0		27.1	65	27.1	65	0	
	2-a	28.1	62	27.8	63	+1		27.1	65	28.1	62	-3	
	2-b	28.3	60	27.5	64	+4		27.1	65	27.4	65	0	
	2-c	28.1	62	27.5	64	+2		27.1	65	27.5	64	-1	
	3-a	28.6	57	28.1	62	+5		28.2	60	28.2	60	0	
	3-b	28.6	57	27.8	63	+6		28.2	60	27.5	64	+4	
	3-c	28.2	60	28.0	62	+2		28.2	60	28.1	62	+2	
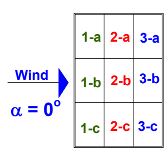	1-a	27.3	65	27.0	65	0	Average = 1.1 %	27.1	65	27.0	65	0	Average = 0.9 %
	1-b	27.8	63	27.5	64	+1		27.5	64	27.5	64	0	
	1-c	27.1	65	27.1	65	0		27.3	65	27.1	65	0	
	2-a	27.8	63	27.8	63	0		28.1	62	27.1	65	+3	
	2-b	28.6	57	28.3	60	+3		28.1	62	28.2	60	-2	
	2-c	27.8	63	27.8	63	0		28.1	62	27.1	65	+3	
	3-a	28.3	60	28.1	62	+2		28.2	60	28.2	60	0	
	3-b	28.3	60	28.1	62	+2		28.2	60	28.1	62	+2	
	3-c	28.3	60	28.1	62	+2		28.2	60	28.1	62	+2	
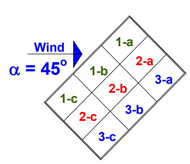	1-a	27.8	63	27.5	64	+1	Average = 1.1 %	27.5	64	27.5	64	0	Average = 0.7 %
	1-b	27.4	65	27.4	65	0		27.4	65	27.3	65	0	
	1-c	27.1	65	27.0	65	0		27.1	65	27.0	65	0	
	2-a	28.3	60	27.8	63	+3		28.2	60	28.1	62	+2	
	2-b	28.1	62	27.8	63	+1		27.1	65	27.1	65	0	
	2-c	27.4	65	27.4	65	0		27.4	65	27.3	65	0	
	3-a	28.3	60	27.8	63	+3		28.2	60	27.1	65	+5	
	3-b	28.1	62	27.5	64	+2		27.1	65	27.5	64	-1	
	3-c	27.5	64	27.5	64	+0		27.5	64	27.5	64	0	
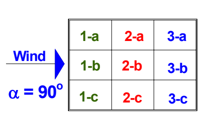	1-a	27.5	64	27.4	65	+1	Average = 0.9 %	27.4	65	27.3	65	0	Average = 1.9 %
	1-b	27.4	65	27.4	65	0		27.5	64	27.5	64	0	
	1-c	27.1	65	27.3	65	0		27.4	65	27.3	65	0	
	2-a	28.3	60	28.1	62	+2		28.2	60	28.1	62	+2	
	2-b	28.1	62	28.3	60	-2		28.1	62	28.1	62	0	
	2-c	28.1	62	28.3	60	-2		28.2	60	28.1	62	+2	
	3-a	28.3	60	28.1	62	+2		28.6	57	28.2	60	+3	
	3-b	28.6	57	28.1	62	+5		28.6	57	28.1	62	+5	
	3-c	28.3	60	28.1	62	+2		28.6	57	28.1	62	+5	

Table D.2.2: PPS before and after the utilisation of curved roofs and wind catcher, where: T_{db} = 35 °C, RH = 30%, Vr = 3 m/s

Cases	Zones	TOWER & DOME						TOWER & VAULT					
		Before Dc2		After T2Do2		Diff. (%)		Before Vc2		After T2Vo2		Diff. (%)	
		TSI	PPS	TSI	PPS			TSI	PPS	TSI	PPS		
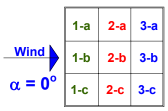	1-a	32.0	20	32.2	19	-1	Average = 3.1 %	32.2	19	32.0	20	+1	Average = 4.3 %
	1-b	32.4	17	31.9	21	+4		32.4	17	31.8	22	+5	
	1-c	32.2	19	32.0	20	+1		32.2	19	31.9	21	+2	
	2-a	33.0	12	32.7	13	+1		33.2	10	32.7	13	+3	
	2-b	33.2	10	32.4	17	+7		33.2	10	32.3	18	+8	
	2-c	33.0	12	32.4	17	+5		33.0	12	32.4	17	+5	
	3-a	33.5	8	33.0	12	+4		33.5	8	33.0	12	+4	
	3-b	33.5	8	32.7	13	+5		33.5	8	32.4	17	+9	
	3-c	33.2	10	33.0	12	+2		33.5	8	33.2	10	+2	
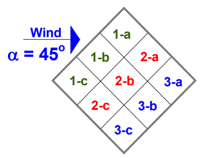	1-a	32.7	13	32.3	18	+5	Average = 2.3 %	32.7	13	32.4	17	+4	Average = 1.3 %
	1-b	32.4	17	32.3	18	+1		32.3	18	32.3	18	0	
	1-c	32.0	20	32.0	20	0		31.9	21	32.0	20	-1	
	2-a	33.0	12	32.3	18	+6		33.0	12	32.4	17	+5	
	2-b	32.7	13	32.3	18	+5		32.4	17	32.7	13	-4	
	2-c	32.4	17	32.3	18	+1		32.3	18	32.2	19	+1	
	3-a	33.2	10	33.0	12	+2		33.0	12	33.0	12	0	
	3-b	33.0	12	32.7	13	+1		33.2	10	32.4	17	+7	
	3-c	32.7	13	32.7	13	0		32.4	17	32.4	17	0	
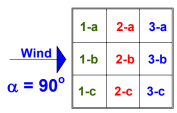	1-a	32.0	20	32.2	19	-1	Average = 3.1 %	32.2	19	32.2	19	0	Average = 2.0 %
	1-b	32.4	17	31.9	21	+4		32.0	20	31.9	21	+1	
	1-c	32.2	19	32.0	20	+1		32.0	20	32.0	20	0	
	2-a	33.0	12	32.7	13	+1		32.7	13	33.0	12	-1	
	2-b	33.2	10	32.4	17	+7		32.7	13	32.3	18	+5	
	2-c	33.0	12	32.4	17	+5		32.7	13	32.4	17	+4	
	3-a	33.5	8	33.0	12	+4		33.2	10	33.2	10	0	
	3-b	33.5	8	32.7	13	+5		33.2	10	32.4	17	+7	
	3-c	33.2	10	33.0	12	+2		33.2	10	33.0	12	+2	
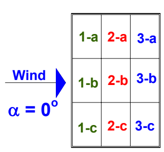	1-a	32.2	19	31.9	21	+2	Average = 1.6 %	32.0	20	31.9	21	+1	Average = 0.7 %
	1-b	32.7	13	32.4	17	+4		32.4	17	32.4	17	0	
	1-c	32.0	20	32.0	20	0		32.2	19	32.0	20	+1	
	2-a	32.7	13	32.7	13	0		33.0	12	32.7	13	+1	
	2-b	33.5	8	33.2	10	+2		33.0	12	33.2	10	-2	
	2-c	32.7	13	32.7	13	0		33.0	12	32.7	13	+1	
	3-a	33.2	10	33.0	12	+2		33.2	10	33.2	10	0	
	3-b	33.2	10	33.0	12	+2		33.2	10	33.0	12	+2	
	3-c	33.2	10	33.0	12	+2		33.2	10	33.0	12	+2	
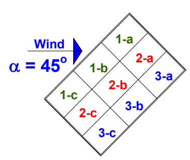	1-a	32.7	13	32.4	17	+4	Average = 1.9 %	32.4	17	32.4	17	0	Average = 1.3 %
	1-b	32.3	18	32.3	18	0		32.3	18	32.2	19	+1	
	1-c	32.0	20	31.9	21	+1		32.0	20	31.9	21	+1	
	2-a	33.2	10	32.7	13	+3		33.2	10	33.0	12	+2	
	2-b	33.0	12	32.7	13	+1		32.7	13	32.7	13	0	
	2-c	32.3	18	32.3	18	0		32.3	18	32.2	19	+1	
	3-a	33.2	10	32.7	13	+3		33.2	10	32.7	13	+3	
	3-b	33.0	12	32.4	17	+5		32.7	13	32.4	17	+4	
	3-c	32.4	17	32.4	17	0		32.4	17	32.4	17	0	
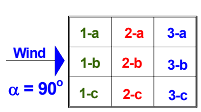	1-a	32.4	17	32.3	18	+1	Average = 0.9 %	32.3	18	32.2	19	+1	Average = 1.8 %
	1-b	32.3	18	32.3	18	0		32.4	17	32.4	17	0	
	1-c	32.0	20	32.2	19	-1		32.3	18	32.2	19	+1	
	2-a	33.2	10	33.0	12	+2		33.2	10	33.0	12	+2	
	2-b	33.0	12	33.2	10	-2		33.0	12	33.0	12	0	
	2-c	33.0	12	33.0	12	0		33.2	10	33.0	12	+2	
	3-a	33.2	10	33.0	12	+2		33.5	8	33.2	10	+2	
	3-b	33.5	8	33.0	12	+4		33.5	8	33.0	12	+4	
	3-c	33.2	10	33.0	12	+2		33.5	8	33.0	12	+4	

Table D.2.3: PPS before and after the utilisation of curved roofs and wind catcher, where: T_{db} = 30 °C, RH = 70%, Vr = 3 m/s

Cases	Zones	TOWER & DOME						TOWER & VAULT					
		Before Dc2		After T2Do2		Diff. (%)		Before Vc2		After T2Vo2		Diff. (%)	
		TSI	PPS	TSI	PPS			TSI	PPS	TSI	PPS		
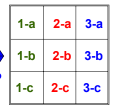 Wind α = 0°	1-a	29.2	**52**	29.4	**50**	**-2**	**Average = 5.2 %**	29.4	**50**	29.2	**52**	**+2**	**Average = 6.7 %**
	1-b	29.6	**46**	29.1	**53**	**+7**		29.6	**46**	29.0	**53**	**+7**	
	1-c	29.4	**50**	29.2	**52**	**+2**		29.4	**50**	29.1	**53**	**+3**	
	2-a	30.2	**38**	29.9	**42**	**+4**		30.4	**35**	29.9	**42**	**+7**	
	2-b	30.4	**35**	29.6	**46**	**+11**		30.4	**35**	29.5	**48**	**+13**	
	2-c	30.2	**38**	29.6	**46**	**+8**		30.2	**38**	29.6	**46**	**+8**	
	3-a	30.7	**33**	30.2	**38**	**+5**		30.7	**33**	30.2	**38**	**+5**	
	3-b	30.7	**33**	29.9	**42**	**+9**		30.7	**33**	29.6	**46**	**+13**	
	3-c	30.4	**35**	30.2	**38**	**+3**		30.7	**33**	30.4	**35**	**+2**	
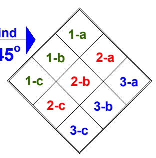 Wind α = 45°	1-a	29.9	**42**	29.5	**48**	**+6**	**Average = 3.7 %**	29.9	**42**	29.6	**46**	**+4**	**Average = 2.2 %**
	1-b	29.6	**46**	29.5	**48**	**+2**		29.5	**48**	29.5	**48**	**0**	
	1-c	29.2	**52**	29.2	**52**	**0**		29.1	**53**	29.2	**52**	**-1**	
	2-a	30.2	**38**	29.5	**48**	**+10**		30.2	**38**	29.6	**46**	**+8**	
	2-b	29.9	**42**	29.5	**48**	**+6**		29.6	**46**	29.9	**42**	**-4**	
	2-c	29.6	**46**	29.5	**48**	**+2**		29.5	**48**	29.4	**50**	**+2**	
	3-a	30.4	**35**	30.2	**38**	**+3**		30.2	**38**	30.2	**38**	**0**	
	3-b	30.2	**38**	29.9	**42**	**+4**		30.4	**35**	29.6	**46**	**+11**	
	3-c	29.9	**42**	29.9	**42**	**0**		29.6	**46**	29.6	**46**	**0**	
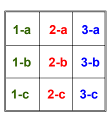 Wind α = 90°	1-a	29.2	**52**	29.4	**50**	**-2**	**Average = 5.2 %**	29.4	**50**	29.4	**50**	**0**	**Average = 2.3 %**
	1-b	29.6	**46**	29.1	**53**	**+7**		29.2	**52**	29.1	**53**	**+1**	
	1-c	29.4	**50**	29.2	**52**	**+2**		29.2	**52**	29.2	**52**	**0**	
	2-a	30.2	**38**	29.9	**42**	**+4**		29.9	**42**	30.2	**38**	**-4**	
	2-b	30.4	**35**	29.6	**46**	**+11**		29.9	**42**	29.5	**48**	**+6**	
	2-c	30.2	**38**	29.6	**46**	**+8**		29.9	**42**	29.6	**46**	**+4**	
	3-a	30.7	**33**	30.2	**38**	**+5**		30.4	**35**	30.4	**35**	**0**	
	3-b	30.7	**33**	29.9	**42**	**+9**		30.4	**35**	29.6	**46**	**+11**	
	3-c	30.4	**35**	30.2	**38**	**+3**		30.4	**35**	30.2	**38**	**+3**	
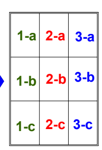 Wind α = 0°	1-a	29.4	**50**	29.1	**53**	**+3**	**Average = 2.0 %**	29.2	**52**	29.1	**53**	**+1**	**Average = 1.6 %**
	1-b	29.9	**42**	29.6	**46**	**+4**		29.6	**46**	29.6	**46**	**0**	
	1-c	29.2	**52**	29.2	**52**	**0**		29.4	**50**	29.2	**52**	**+2**	
	2-a	29.9	**42**	29.9	**42**	**0**		30.2	**38**	29.9	**42**	**+4**	
	2-b	30.7	**33**	30.4	**35**	**+2**		30.2	**38**	30.4	**35**	**-3**	
	2-c	29.9	**42**	29.9	**42**	**0**		30.2	**38**	29.9	**42**	**+4**	
	3-a	30.4	**35**	30.2	**38**	**+3**		30.4	**35**	30.4	**35**	**0**	
	3-b	30.4	**35**	30.2	**38**	**+3**		30.4	**35**	30.2	**38**	**+3**	
	3-c	30.4	**35**	30.2	**38**	**+3**		30.4	**35**	30.2	**38**	**+3**	
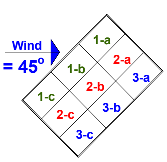 Wind α = 45°	1-a	29.9	**42**	29.6	**46**	**+4**	**Average = 3.4 %**	29.6	**46**	29.6	**46**	**0**	**Average = 2.1 %**
	1-b	29.5	**48**	29.5	**48**	**0**		29.5	**48**	29.4	**50**	**+2**	
	1-c	29.2	**52**	29.1	**53**	**+1**		29.2	**52**	29.1	**53**	**+1**	
	2-a	30.4	**35**	29.9	**42**	**+7**		30.4	**35**	30.2	**38**	**+3**	
	2-b	30.2	**38**	29.9	**42**	**+4**		29.9	**42**	29.9	**42**	**0**	
	2-c	29.5	**48**	29.5	**48**	**0**		29.5	**48**	29.4	**50**	**+2**	
	3-a	30.4	**35**	29.9	**42**	**+7**		30.4	**35**	29.9	**42**	**+7**	
	3-b	30.2	**38**	29.6	**46**	**+8**		29.9	**42**	29.6	**46**	**+4**	
	3-c	29.6	**46**	29.6	**46**	**+0**		29.6	**46**	29.6	**46**	**0**	
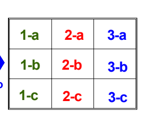 Wind α = 90°	1-a	29.6	**46**	29.5	**48**	**+2**	**Average = 1.2 %**	29.5	**48**	29.4	**50**	**+2**	**Average = 2.4 %**
	1-b	29.5	**48**	29.5	**48**	**0**		29.6	**46**	29.6	**46**	**0**	
	1-c	29.2	**52**	29.4	**50**	**-2**		29.5	**48**	29.4	**50**	**+2**	
	2-a	30.4	**35**	30.2	**38**	**+3**		30.4	**35**	30.2	**38**	**+3**	
	2-b	30.2	**38**	30.4	**35**	**-3**		30.2	**38**	30.2	**38**	**0**	
	2-c	30.2	**38**	30.2	**38**	**0**		30.4	**35**	30.2	**38**	**+3**	
	3-a	30.4	**35**	30.2	**38**	**+3**		30.7	**33**	30.4	**35**	**+2**	
	3-b	30.7	**33**	30.2	**38**	**+5**		30.7	**33**	30.2	**38**	**+5**	
	3-c	30.4	**35**	30.2	**38**	**+3**		30.7	**33**	30.2	**38**	**+5**	

Table D.2.4: PPS before and after the utilisation of curved roofs and wind catcher, where: T_{db} = 35 °C, RH = 70%, Vr = 3 m/s

Illustration	Zone	TOWER & DOME						TOWER & VAULT					
		Before Dc2		After T2Do2		Diff. (%)		Before Vc2		After T2Vo2		Diff. (%)	
		TSI	PPS	TSI	PPS			TSI	PPS	TSI	PPS		
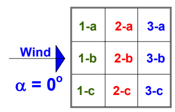	1-a	34.4	4	34.6	3	-1	Average = 0.9 %	34.6	3	34.4	4	+1	Average = 1.3 %
	1-b	34.8	2	34.3	4	+2		34.8	2	34.2	4	+2	
	1-c	34.6	3	34.4	4	+1		34.6	3	34.3	4	+1	
	2-a	35.4	1	35.1	2	+1		35.6	1	35.1	2	+1	
	2-b	35.6	1	34.8	2	+1		35.6	1	34.7	3	+2	
	2-c	35.4	1	34.8	2	+1		35.4	1	34.8	2	+1	
	3-a	35.9	0	35.4	1	+1		35.9	0	35.4	1	+1	
	3-b	35.9	0	35.1	2	+2		35.9	0	34.8	2	+2	
	3-c	35.6	1	35.4	1	0		35.9	0	35.6	1	+1	
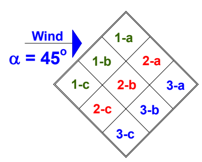	1-a	35.1	2	34.7	3	+1	Average = 0.7 %	35.1	2	34.8	2	0	Average = 0.2 %
	1-b	34.8	2	34.7	3	+1		34.7	3	34.7	3	0	
	1-c	34.4	4	34.4	4	0		34.3	4	34.4	4	0	
	2-a	35.4	1	34.8	2	+1		35.4	1	34.8	2	+1	
	2-b	35.1	2	34.7	3	+1		34.8	2	35.1	2	0	
	2-c	34.8	2	34.7	3	+1		34.7	3	34.6	3	0	
	3-a	35.6	1	35.4	1	0		35.4	1	35.4	1	0	
	3-b	35.4	1	35.1	2	+1		35.6	1	34.8	2	+1	
	3-c	35.1	2	35.1	2	0		34.8	2	34.8	2	0	
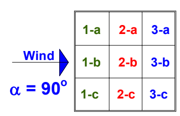	1-a	34.4	4	34.6	3	-1	Average = 0.9 %	34.6	3	34.6	3	0	Average = 0.1 %
	1-b	34.8	2	34.3	4	+2		34.4	4	34.3	4	0	
	1-c	34.6	3	34.4	4	+1		34.4	4	34.4	4	0	
	2-a	35.4	1	35.1	2	+1		35.1	2	35.4	1	-1	
	2-b	35.6	1	34.8	2	+1		35.1	2	34.7	3	+1	
	2-c	35.4	1	34.8	2	+1		35.1	2	34.8	2	0	
	3-a	35.9	0	35.4	1	+1		35.6	1	35.6	1	0	
	3-b	35.9	0	35.1	2	+2		35.6	1	34.8	2	+1	
	3-c	35.6	1	35.4	1	0		35.6	1	35.4	1	0	
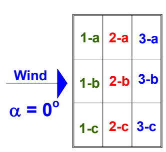	1-a	34.6	3	34.3	4	+1	Average = 0.2 %	34.4	4	34.3	4	0	Average = 0.3 %
	1-b	35.1	2	34.8	2	0		34.8	2	34.8	2	0	
	1-c	34.4	4	34.4	4	0		34.6	3	34.4	4	+1	
	2-a	35.1	2	35.1	2	0		35.4	1	35.1	2	+1	
	2-b	35.9	0	35.6	1	+1		35.4	1	35.6	1	0	
	2-c	35.1	2	35.1	2	0		35.4	1	35.1	2	+1	
	3-a	35.6	1	35.4	1	0		35.6	1	35.6	1	0	
	3-b	35.6	1	35.4	1	0		35.6	1	35.4	1	0	
	3-c	35.6	1	35.4	1	0		35.6	1	35.4	1	0	
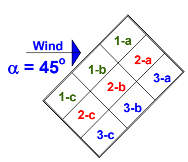	1-a	35.1	2	34.8	2	0	Average = 0.4 %	34.8	2	34.8	2	0	Average = 0.1 %
	1-b	34.7	3	34.7	3	0		34.7	3	34.6	3	0	
	1-c	34.4	4	34.3	4	0		34.4	4	34.3	4	0	
	2-a	35.6	1	35.1	2	1		35.6	1	35.4	1	0	
	2-b	35.4	1	35.1	2	+1		35.1	2	35.1	2	0	
	2-c	34.7	3	34.7	3	0		34.7	3	34.6	3	0	
	3-a	35.6	1	35.1	2	+1		35.6	1	35.1	2	+1	
	3-b	35.4	1	34.8	2	+1		35.1	2	34.8	2	0	
	3-c	34.8	2	34.8	2	0		34.8	2	34.8	2	0	
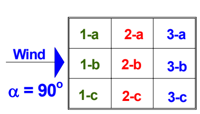	1-a	34.8	2	34.7	3	+1	Average = 0.1 %	34.7	3	34.6	3	0	Average = 0.3 %
	1-b	34.7	3	34.7	3	0		34.8	2	34.8	2	0	
	1-c	34.4	4	34.6	3	-1		34.7	3	34.6	3	0	
	2-a	35.6	1	35.4	1	0		35.6	1	35.4	1	0	
	2-b	35.4	1	35.6	1	0		35.4	1	35.4	1	0	
	2-c	35.4	1	35.4	1	0		35.6	1	35.4	1	0	
	3-a	35.6	1	35.4	1	0		35.9	0	35.6	1	+1	
	3-b	35.9	0	35.4	1	+1		35.9	0	35.4	1	+1	
	3-c	35.6	1	35.4	1	0		35.9	0	35.4	1	+1	